

Some pages of this thesis may have been removed for copyright restrictions.

If you have discovered material in AURA which is unlawful e.g. breaches copyright, (either yours or that of a third party) or any other law, including but not limited to those relating to patent, trademark, confidentiality, data protection, obscenity, defamation, libel, then please read our [Takedown Policy](#) and [contact the service](#) immediately

**DEFORMATION AND FAILURE OF WELDED STEELS USED IN
OFFSHORE CONSTRUCTIONS**

FARSHID BEHSETA

Doctor of Philosophy

THE UNIVERSITY OF ASTON IN BIRMINGHAM

DATE: JUNE 1989

This copy of thesis has been supplied on condition that anyone who consults it is understood to recognise that its copyright rests with its author and that no quotation from the thesis and no information derived from it may be published without the author's prior, written consent.

DEDICATIONS

To My Mother and Father

THE UNIVERSITY OF ASTON IN BIRMINGHAM

DEFORMATION AND FAILURE OF WELDED STEELS USED IN OFFSHORE CONSTRUCTIONS

FARSHID-BEHSETA

Doctor of Philosophy

1989.

SUMMARY

Hydrocarbons are the most commonly form of energy used to date. The activities involving exploration and exploitation of large oil and gas fields are constantly in operation and have extended to such hostile environments as the North sea. This enforces much greater demands on the materials which are used, and the need for enhancing the endurance of the existing ones which must continue parallel to the explorations.

Due to their ease in fabrications, relatively high mechanical properties and low costs, steels are the most widely favoured material for the construction of the offshore platforms. The most critical part of an offshore structures prone to failure is the welded nodal joint, particularly those which are used within the vicinity of the splash zones. This is an area of high complex stress concentrations, varying mechanical and metallurgical properties in addition to severe North sea environmental conditions.

The main area of this work has been concerned with the durability studies of this type of steel, based on the concept of the worst case analysis, consisting of combinations of welds of varying qualities, various degrees of stress concentrations and the environmental conditions of stress corrosion and hydrogen embrittlement.

The experiments have been designed to reveal significance of defects as sites of crack initiation in the welded steels and the extent to which stress corrosion and hydrogen embrittlement will limit their durability. This has been done for various heat treatments and in some experiments deformation has been forced through the welded zone of the specimens to reveal the mechanical properties of the welds themselves to provide data for finite element simulations.

A comparison of the results of these simulations with the actual deformation and fracture behaviour has been done to reveal the extent to which both mechanical and metallurgical factors control behaviour of the steels in the hostile environments of high stress, corrosion, and hydrogen embrittlement at their surface.

KEY WORDS: OFFSHORE, STEEL, WELD, DURABILITY.

ACKNOWLEDGEMENTS

I am deeply indebted to my supervisor Dr. J A Wright, for the liberal use of his time invaluable guidance, advice and sympathetic help throughout the duration of this work.

I would also like to thank the staff of the Civil and Mechanical engineering departments of Aston University for their much appreciated assistance.

Last but most of all, I owe my deepest gratitude and appreciation to my wife Julie and my two beautiful daughters Mahshid and Delara for their encouragement, support and above all being so understanding and patient during my student years.

LIST OF CONTENTS

	<u>PAGE</u>
Title page	1
Dedications	2
Thesis summary	3
Acknowledgement	4
List of contents	5
List of figures	10
List of tables	17
1. INTRODUCTION	21
2. LITERATURE REVIEW	24
2.1 Environment	24
2.2 Common offshore structures	27
2.2.1 The jacket or template	27
2.2.2 The tower	27
2.2.3 Tension leg platform (TLP)	30
2.2.4 Concrete gravity platforms	31
2.3 Construction	32
2.4 Materials requirements for offshore structures	32
2.4.1 High strength low alloy structural steels	36
2.4.2 Methods of producing HSLA steels	40
2.5 Welded tubular joints	42

2.5.1	The general effects of welding	42
2.5.2	The potential welding problem	43
2.5.3	Weldability and specifications	43
2.5.4	Welding of tubular joints (current practice)	47
2.5.5	Inspection	47
2.5.5.1	Welding quality assurance	48
2.5.5.2	Inspection of the welds	48
2.6	Durability of the steels	49
2.6.1	Splash zone	50
2.6.2	Nodal joints	51
2.6.3	Higher level of impurities	52
2.7	General corrosion of steels	53
2.7.1	Electrochemical mechanism of corrosion	53
2.7.2	Potential-pH equilibrium diagrams	54
2.7.3	Corrosion of offshore steels	56
2.8	Stress corrosion cracking (SCC)	58
2.8.1	Definition	58
2.8.2	Environmental requirements for SCC	58
2.8.3	Basic characteristics of SCC	61
2.8.4	Function of stress	61
2.8.5	The threshold stress intensity	61
2.9	Hydrogen assisted fracture	65
2.9.1	Introduction of hydrogen by electrolysis	66
2.9.2	The Hydrogen-metal interaction mechanisms	67
2.9.2.1	Internal pressure formation	68
2.9.2.2	Lattice-bond interaction	68

2.9.2.3	Dislocation interaction	70
2.10	Cyclic stressing crack propagation and fatigue effects	71
2.10.1	Crack initiation	71
2.10.2	Crack propagation	72
2.10.3	Welds	74
2.11	The finite element modelling	75
2.11.1	Introduction	75
2.11.2	Outline of the finite element process	75
2.11.2.1	Definition of the finite element mesh	76
2.11.2.2	Displacement function	77
2.11.2.3	Formulation of the stiffness equation	78
2.11.2.4	Solution of the stiffness equation	79
2.11.2.5	Determining the element strains and stresses	79
2.11.3	Non-linear materials	80
2.11.3.1	Geometric non-linearity or large displacements	80
2.11.3.2	Elastic-plastic behaviour	81
2.11.3.3	Yielding	82
2.11.4	The finite element package (PAFEC-FE)	83
2.12	The objective of the research	84
3	EXPERIMENTAL PROCEDURES	86
3.1	Material	86
3.2	Experimental matrix	86
3.3	Mechanical testing	89
3.4	Testing machine	90
3.5	Metallography and fractography	90

3.5.1	General metallographical preparation	90
3.5.2	Scanning electron microscopy (SEM)	90
3.6	Heat treatment	91
3.7	Formation of the welded joint	94
3.7.1	Sound welds	100
3.7.2	Defective welds containing gross defects	103
3.7.3	Defective welds avoiding gross defects	117
3.8	Specimens	118
3.8.1	Welded specimens	118
3.8.2	As-received specimens	119
3.9	Environmental testing	122
3.9.1	Air tests	124
3.9.2	Accelerated stress corrosion testing in sea water	124
3.9.3	Testing in sea water with hydrogen evolution	126
4.	RESULTS AND ANALYSIS OF THE RESULTS	129
4.0	Results	129
4.1	Experimental results	130
4.1.1	Tensile tests	131
4.1.2	Metallographical examinations	138
4.2	Statistical results	143
4.2.1	T-test of significance	145
4.2.2	Analysis of variance	146
4.2.3	Regression modelling	147
4.3	Finite element results	150
4.4	Analysis of the finite element results	153

5.	DISCUSSION OF THE RESULTS	163
5.1	Overview	163
5.2	Directionality of the specimen	163
5.3	Heat treatment	164
5.4	The welded joints	166
5.5	The effect of the environment	169
5.5.1	The air tests	169
5.5.2	The corrosion environment	169
5.5.3	Hydrogen evolution	171
5.6	The finite element analysis	174
5.7	Commercial implications	177
6.	CONCLUSIONS	180
7.	FUTURE WORK	184
8.	REFERENCES	187
9.	APPENDICES	196
9.1	Appendix 1 Nernst equation	197
9.2	Appendix 2 Formulating the discrete stiffness equation	198
9.3	Appendix 3 Elastic-plastic behaviour	201
9.4	Appendix 4 Plasticity solution flow diagram	203
9.5	Appendix 5 The grids printing technique	204
9.6	Appendix 6 Figures	205
9.7	Appendix 7 Tables	227
9.8	Appendix 8 Statistical analysis	230

LIST OF FIGURES

<u>FIGURE</u>	<u>TITLE</u>	<u>PAGE</u>
1.	Variation in temperature, salinity and the oxygen content of the North Sea.	26
2.	Principle of jacket or template.	28
3.	Typical tubular jacket offshore structure.	29
4.	Tension leg platform.	30
5.	Concrete gravity platform.	31
6.	Compliant system.	31
7.	Schematic illustration of a Nodal Joint.	35
8.	Reduction of area in through thickness direction as a function of S-content.	39
9.	Liquation cracking.	45
10.	Schematic illustration of lamellar tearing.	46
11.	Corrosion zones on fixed offshore steel structures.	50
12.	Marine environments: zones.	51
13.	A simplified form of the Pourbaix diagram for Iron.	55
14.	Potentiodynamic polarisation curves and expected domains of electrochemical behaviour.	60

<u>FIGURE</u>	<u>TITLE</u>	<u>PAGE</u>
15.	Relationship between initial stress intensity factor K and time to failure T_f .	62
16.	General relationship between the stress intensity factor, K_{IC} and stress corrosion crack velocity.	64
17.	Reaction steps.	67
18.	Schematic crack growth by hydrogen-lattice bond interaction.	69
19.	Fatigue crack growth rates for pre-cracked material	73
20.	Fatigue crack growth rate for rolled steel (XY) orientation	74
21.	Idealisation of two dimensional structure using triangular or quadrilateral elements.	76
22.	Three dimensional finite elements.	77
23.	Load deflection relationship.	81
24.	Stress-strain relationship.	82
25.	As received plate.	87
26.	Metallographic microstructure of as-received steel magnification X100.	92
27.	Metallographic microstructure of normalised steel magnification X100.	93
28.	Metallographic microstructure of oil quenched and tempered steel magnification X100.	93

<u>FIGURE</u>	<u>TITLE</u>	<u>PAGE</u>
29.	Metallographic microstructure of water quenched and tempered steel magnification X100.	94
30.	Preparation of the welded specimens.	95
31.	Sound weld with good manipulation pattern.	96
32.	Category (2) gross defect, lack of side wall fusion.	97
33.	Category (2) gross defect, incomplete root fusion.	97
34.	Category (2) Gross defect, macro porosity.	98
35.	Category (2) or (3) lack of root penetration.	98
36.	Category (2) or (3), microporosity.	99
37.	Category (3), addition of excessive non-metallic inclusions magnification X80.	99
38.	Increase in volume fractions of sulphide particles magnification X40.	117
39.	Increase in volume fractions of sulphide particles magnification X160.	118
40.	Diagrammatic representation of the specimen.	119
41.	Specimen.	120
42.	Printed grid on parallel length of the specimen.	121
43.	The experimental rig.	122
44.	Close-up view of an environmental test rig.	124

<u>FIGURE</u>	<u>TITLE</u>	<u>PAGE</u>
45.	Polarisation curve obtained by using the Auto-stat.	125
46.	Schematic diagram showing the arrangements for the corrosion cell.	127
47.	Stress strain curves for normalised specimens containing no weld, sound and defective welds, tested in air corrosion and hydrogen environments.	135
48.	Stress strain curves for oil quenched and tempered specimens containing no weld, sound and defective welds, tested in air corrosion and hydrogen environments.	136
49.	Stress strain curves for water quenched and tempered specimens containing no weld, sound and defective welds, tested in air corrosion and hydrogen environments.	137
50.	Fractured specimen in different environments	139
51.	Fracture characteristics of different tests in air, corrosion and hydrogen environments.	139
52.	Failure of the specimen outside the weld.	140
53.	Deformation through the weld.	140
54.	SEM details of fracture surface for tensile test specimen with a sound weld magnification X 350.	141
55.	SEM details of fracture surface for tensile test specimen with a defective weld magnification X 360.	141
56.	SEM details of fracture surface for tensile test specimen with a sound weld magnification X 2.6k.	142

<u>FIGURE</u>	<u>TITLE</u>	<u>PAGE</u>
57.	SEM details of fracture surface for tensile test specimen with a defective weld magnification X 2.6k.	142
58.	A typical graphical output from a PAFEC data file representing a deformed specimen.	150
59.	A typical PAFEC data file.	151
60.	A typical graphical output from a PAFEC data file representing the superimposed deformed specimen.	152
61.	A typical graphical output from a PAFEC data file representing an undeformed specimen.	152
62.	% Elongation for normalised specimens.	160
63.	% Elongation for oil quenched and tempered specimens.	160
64.	% Elongation for water quenched and tempered specimens.	161
65.	The boundary between different welded zones.	167
66.	The ultimate weld failure shown as a shear fracture.	167
67.	Corrosion fatigue crack data, Indicating limited diffusion of hydrogen in thick specimens o, 6 cpm open circuit, o, 6 cpm 800 mv sec. Δ 6 cpm 1200 mv .	172
68.	Stress-strain relationship for HNW1.	205
69.	Stress-strain relationship for HNW2.	205
70.	Stress-strain relationship for HNW3.	206
71.	Stress-strain relationship for HGC7.	206

<u>FIGURE</u>	<u>TITLE</u>	<u>PAGE</u>
72.	Stress-strain relationship for HGC6.	207
73.	Stress-strain relationship for HGC1.	207
74.	Stress-strain relationship for HB2.	208
75.	Stress-strain relationship for HB3.	208
76.	Stress-strain relationship for HB5.	209
77.	Stress-strain relationship for HGC5.	209
78.	Stress-strain relationship for HGC8.	210
79.	Stress-strain relationship for HGC4.	210
80.	Stress-strain relationship for HB8.	211
81.	Stress-strain relationship for HB7.	211
82.	Stress-strain relationship for HB6.	212
83.	Stress-strain relationship for ONW1.	212
84.	Stress-strain relationship for ONW2.	213
85.	Stress-strain relationship for ONW3.	213
86.	Stress-strain relationship for OG1.	214
87.	Stress-strain relationship for OG4.	214
88.	Stress-strain relationship for OG3.	215
89.	Stress-strain relationship for OB1.	215

<u>FIGURE</u>	<u>TITLE</u>	<u>PAGE</u>
90.	Stress-strain relationship for OB2.	216
91.	Stress-strain relationship for OB3.	216
92.	Stress-strain relationship for OG5.	217
93.	Stress-strain relationship for OG6.	217
94.	Stress-strain relationship for OG7.	218
95.	Stress-strain relationship for OB4.	218
96.	Stress-strain relationship for OB5.	219
97.	Stress-strain relationship for OB6.	219
98.	Stress-strain relationship for WNW1.	220
99.	Stress-strain relationship for WNW2.	220
100.	Stress-strain relationship for WNW3.	221
101.	Stress-strain relationship for GW1.	221
102.	Stress-strain relationship for GW2.	222
103.	Stress-strain relationship for GW3.	222
104.	Stress-strain relationship for BW1.	223
105.	Stress-strain relationship for BW2.	223
106.	Stress-strain relationship for BW3.	224
107.	Stress-strain relationship for transverse oriented specimen.	225
108.	Stress-strain relationship for longitudinal oriented specimen.	225
109	Diagrammatic presentation of a notched specimen	226

LIST OF TABLES

<u>TABLES</u>	<u>TITLE</u>	<u>PAGE</u>
1.	Principle areas of offshore activities.	21
2.	Major ionic constituents of sea water.	25
3.	Mechanical properties of BS4360.	34
4.	Chemical analysis of BS4360.	34
5.	Heat treatment chart.	92
6.	Controlled variables in formation of a sound weld by manual metal arc technique.	101
7.	Formation of a sound weld by metal inert gas technique.	102
8.	Weld defects, cracks.	105
9.	Weld defects, cavities.	106
10.	Weld defects, solid inclusions.	107
11.	Weld defects, incomplete fusion.	108
12.	Weld defects, incorrect shape.	109
13.	Weld defects, miscellaneous.	110
14.	Electrode type.	111
15.	Electrode angle.	112
16.	Plate geometry.	113

<u>TABLES</u>	<u>TITLE</u>	<u>PAGE</u>
17.	Variation in current and electrode size.	114
18.	Variation in power supply for manual metal arc welding.	115
19.	Effects of variation of gas flow in MIG welding.	115
20.	Miscellaneous variables.	116
21.	Number of specimens tested in different environments.	123
22.	Specimen dimensions for normalised batch.	227
23.	Specimen dimensions for oil quenched and tempered batch.	228
24.	specimen dimensions for water quenched and tempered batch.	229
25.	Specimen dimensions for as-received batch.	229
26.	General mechanical property results for normalised specimens.	132
27.	General mechanical property results for oil quenched and tempered specimens.	133
28.	General mechanical property results for water quenched and tempered specimens.	134
29.	Data file for statistical analysis	144
30.	T-test results	145
31.	Analysis of variance	147
32.	Comparison of regression results	148

<u>TABLES</u>	<u>TITLE</u>	<u>PAGE</u>
33.	Comparison of the experimental and finite element modelled results for the normalised specimens in terms of ratios.	153
34.	Comparison of the experimental and finite element modelled results for the oil quenched and tempered specimens in terms of ratios.	154
35.	Comparison of the experimental and finite element modelled results for the water quenched and tempered specimens in terms of ratios.	155
36.	Comparison of the experimental and finite element modelled results for the normalised specimens in terms of % elongations.	156
37.	Comparison of the experimental and finite element modelled results for the oil quenched and tempered specimens in terms of % elongation.	157
38.	Comparison of the experimental and finite element modelled results for the water quenched and tempered specimens in terms of % elongation.	158
39.	% Elongation for the experimental and finite element modelled results.	159
40.	Elongation of finite element modelled results as a percentage of experimental results.	159

CHAPTER ONE

INTRODUCTION

1. INTRODUCTION

Man has always been in search of convenient, cheap and accessible forms of energy. Hydrocarbons are known to have been used during the history of man-kind in many forms. Oil and gas are the most popular, economically viable and not easily replaceable forms of energy found to date. The activities involving the exploration and exploitation of new large oil and gas fields are constantly in operation, all over the world. The search for this vital element of man's life has extended into regions that are exposed to extremely severe environmental conditions such as the North sea.

Offshore oil and gas exploration started some forty five years ago in the shallow waters of the Gulf of Mexico, today there are over 10 000 offshore structures world wide⁽¹⁾, producing more than a quarter of the total of world's oil and gas production. This proportion is likely to increase in future as additional countries like China, India and Canada are expected to join the league. Table1 shows the principal areas of offshore activities around the world.

Country	% Share of Total
Saudi Arabia	17.9
United Kingdom	15.4
Mexico	12.2
USA	8.3
Venezuela	7.7
Egypt	4.0
Indonesia	4.0
Norway	4.0
Abu Dhabi	3.3
Dubai	2.7
Australia	2.6
Others	14.8

Table 1 Principal areas of offshore activities (1982-source, Scottish development agency).

As it can be seen from the table the North sea is a major offshore production area and its strategical effect on the economy of the UK is very important. Development of a new field demands massive investment in surveying and drilling. The production of the structure, pipeline, and its inspection, maintenance and repair work is a huge project, therefore possibility of failure of any kind can have a disastrous effect.

The most common type of structure that is used in the offshore industry is the fixed tubular welded space frame piled to the seabed, and it will probably continue to be so in future. The success and economical viability of any offshore platform depends essentially on the availability of suitable materials and their durability during their natural working life. This work is aimed to deal with a better understanding of parameters which are involved in a comprehensive durability studies. Areas such as crack initiation and propagation, the effect of weld quality and the importance of the environmental conditions are strongly related to comprehensive durability studies, hence they have been carefully considered in this work. Their study has been based on the principle of the worst case analysis. Finally the eventual trend in possibility of computerisation and mathematical modelling based on the finite element technique has been examined.

CHAPTER TWO

LITERATURE REVIEW

2. LITERATURE REVIEW

2.1 ENVIRONMENT

The North sea is one of the most continuously hostile marine environments in the world, with winds reaching speeds of upto 50 ms^{-1} (~ 110 mph) and waves of upto 30m in height. In addition sea water with its high concentration of salts, is one of the most corrosive of natural environments. Its biological activities has also Important consequences for structural loading and materials performance.

Water depths of upto 350ft where the deepest platform (Thistle field) is situated, have pressures of about 17 atmosphere (1.72 N/m^2) . The major ionic constituents of sea water are shown in the table 2 . The composition of the sea water, particularly the dissolved gases, and its temperature have a marked effect on material performance. Of particular interest are chloride ions concerning corrosion and corrosion fatigue.

Typical salinity is 3.5% for ocean water with little variation with depth and season⁽²⁾ (figure 1). An important factor is that in all depths because of constant mixing of surface and deeper water the water is fully saturated with oxygen (figure 1). In other seas (eg. parts of Atlantic ocean) oxygen content reduces with depths ⁽³⁾ with consequent reduction of corrosion rates.

The amount of carbon dioxide, usually present as bicarbonate or carbonate ions, can also affect corrosion rates particularly in the presence of cathodic protection since carbonate scales are formed both on the surface and within cracks ⁽⁴⁾ . In the latter case plugging of the crack can slow down crack growth rates substantially.

Temperatures in the North sea vary from about 16°C for surface regions in the late summer to 6°C in the winter (lowest temperatures are reached in March or April). Offshore structures are exposed to a range of environments varying from fully oxygenated cold sea water near the base, warmer summer conditions near the surface, splash zone conditions where structure is continually wetted and dried, and finally to the atmospheric zone which is exposed to salty air.

The parts of structure in both the splash and atmospheric zones are particularly vulnerable to corrosion because of the plentiful supply of oxygen. Finally the wave loading on offshore platforms is of particular interest in designing against fatigue. Typical waves have periods in the range 9-18 seconds, corresponding to a frequency of about 0.1 Hertz.

Major Constituents of Seawater Parts Per 1000	
Sodium	10.77
Chloride	19.37
Magnesium	1.30
Sulphate as (SO ₄)	2.71
Calcium	0.41
Potasssium	0.34
Other salts	0.20
Total Salts	35.1 Termed salinity

Table 2 Major Ionic Constituents of sea water

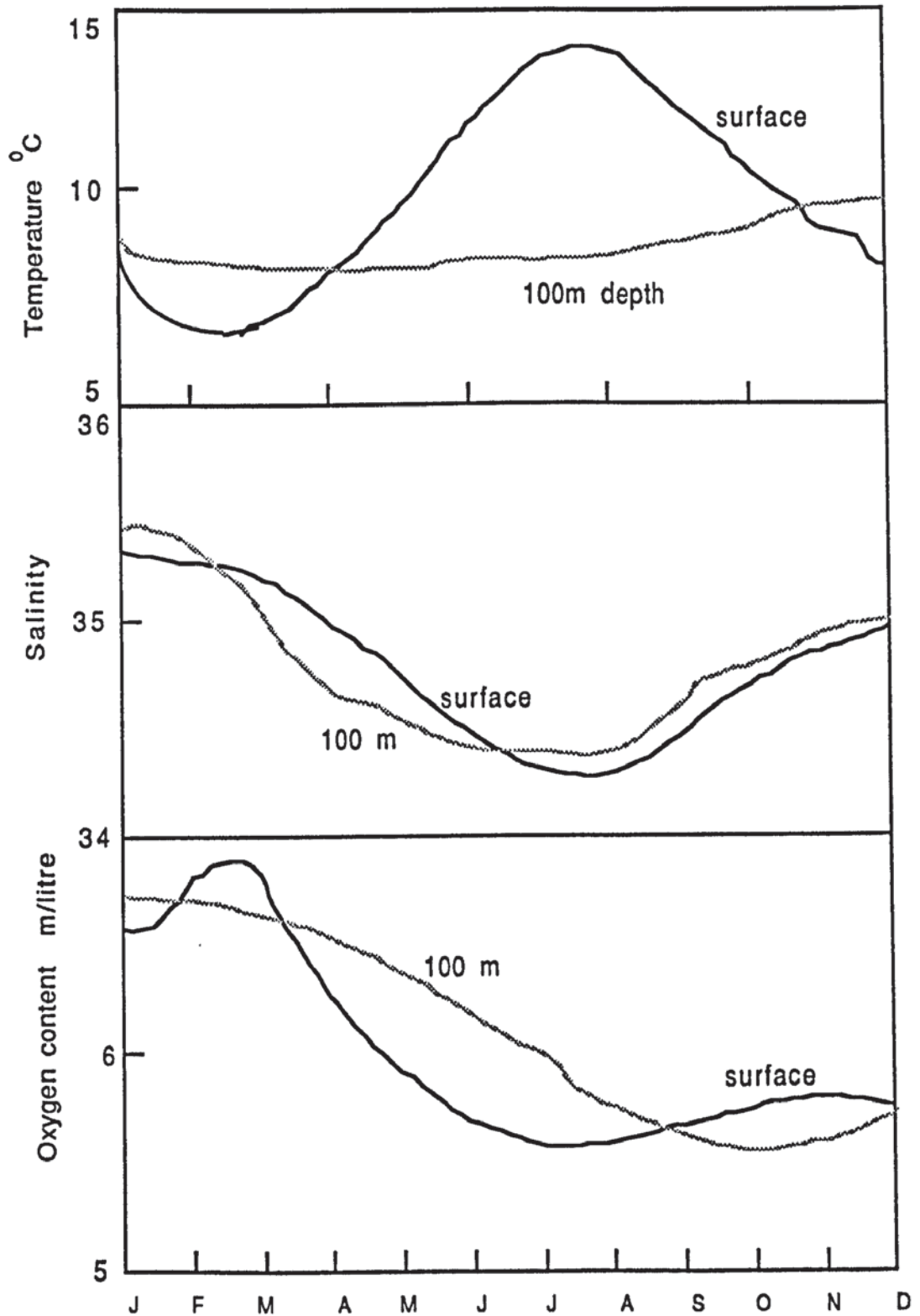


Figure 1 Variation in temperature, salinity and oxygen content of the North sea approximately 56 N, 1 E through the year, both at the surface and at a depth of 100m.

2.2 COMMON OFFSHORE STRUCTURES

The type of structure and environmental requirements inevitably are governed by the needs of a typical oil and gas installation. The following are commonly used in the industry around the world.

2.2.1 THE JACKET OR TEMPLATE

This by far represents the largest number of offshore platforms installed to date. A template or jacket is simply a space frame designed to make pile driving easier by obviating the need to provide temporary support for the piles during first driving (figure 2). This type of platform is currently being used in the shallow waters of the Gulf of Mexico. The structure is pre-fabricated at some water side facility skidded on to a flat-topped barge, and towed to a location where it is lifted into position by a derrick barge.

2.2.2 THE TOWER

The tower is an extrapolation of the jacket to deep water. Due to their size, towers are usually made self-buoyant either by enlarging several of the legs or by the use of purpose made pontoons. The completed towers have been installed in water depths of up to 250m and contain up to 40 000 tonnes of steel apiece, including deck and pilings (figure 3). However these do not represent the largest framed structures.

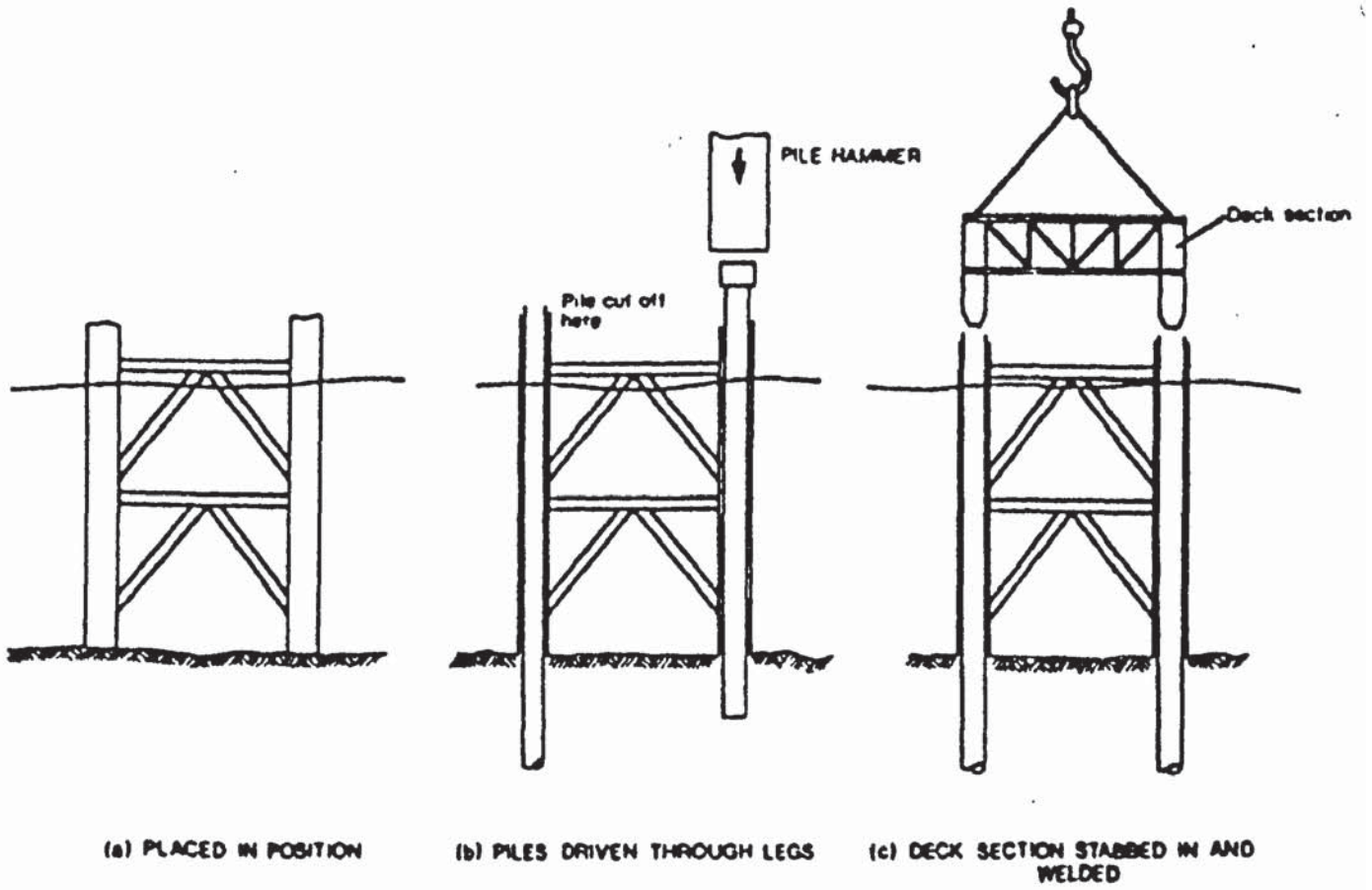


Figure 2 Principle of jacket or template



Figure 3 Typical tubular jacket offshore structure. **A** Secondary structural steel (BS4360 Grade 43D) Module walls, decking, etc; **B** Primary structural steel (BS4360 Grade 50E) Mod) jacket legs, module support, etc; and **C** special structural steel (BS4360 Grade 50E Hyzed) node joints.

2.2.3 TENSION LEG PLATFORM (TLP)

At greater water depths , although jackets may still be used, the competition from other concepts such as a TLP and guyed towers become stronger (figure 4-6). The TLP is a floating platform with a configuration resembling conventional semi-submersible units which is anchored to the sea bed with vertical tension members (figure 4). There are obvious limitations in terms of topside weight which can be utilised, and anchoring and tethering arrangements are critical.



Figure 4 Tension leg platform

2.2.4 CONCRETE GRAVITY PLATFORMS

These platforms are installed in the areas where the sea bed can support heavy loads i.e areas of heavily consolidated soils or very close to the present mud line. There are some differences between the designs built to date but the most common types comprise of a large cellular base supporting three or four concrete towers which in turn support a steel deck (figure 5).



Figure 5

Concrete gravity platform



Figure 6

Compliant system

2.3 CONSTRUCTION

The construction of fixed steel offshore structures are divided into two main phases:

- a) Fabrication
- b) Installation

In the fabrication stage the tubular joints are welded together, usually manually or by semi-automatic methods eg. Shielded metal arc welding technique. Standard procedures are available for the choice of electrodes, polarity, voltage, current, etc. precautions such as pre-heating and baking of the electrodes are necessary to ensure good weldability and fusion.

A typical template type structure is fabricated on its side in a shipyard. The completed structure is either carried on a barge (shallow waters) or for large platforms the self buoyancy techniques are used eg. flooding the dry dock and floating the structure on its sides into position, where it is set up-right by selective flooding of its legs. Once up-right it is positioned on location and landed on its bottom.

2.4 MATERIALS REQUIREMENTS FOR OFFSHORE STRUCTURES

As the shape and form of marine structures are many and varied, so are the materials of construction, but irrespective of the type of structure favoured for the future offshore installations, it appears that these will consume vast quantities of steel⁽⁵⁾. There are many advantages for the use of steel plates and tubes, in the construction of rigs and platform, and by far the greatest advantage is the relative speed in construction of tubular towers and the ease of launching and towing these.

Greater water depths, dynamic wave forces, lower temperatures and hostile environments of the North sea place stringent requirements on the steels. These steels must possess such features as adequate strength, toughness, short transverse ductility, weldability, fatigue and corrosion resistance.

Generally the weldable steels to BS4360 broadly satisfy the requirements for this application, many of the primary structural steels used conforms to grade 50D-E which has a minimum yield strength of 340 N/mm² and a Charpy V notch value of 27J at -30 °C for 50D and 27J at -50 °C for 50E (tables 3-4). The increased toughness gives greater assurance of resistance to brittle fracture .

The steels used in the construction of the jackets are of high strength low alloy structural steels commonly known as HSLA steels, which are microalloyed and delivered in the normalised condition. The strength and toughness are attained by promoting a fine grain, through the action of grain growth inhibitors such as aluminium-nitride, and niobium-carbonitride, whilst reducing the carbon content and keeping carbon equivalent (CE) < 0.43 to achieve good weldability.

Additional requirements for both toughness and through thickness ductility are imposed to ensure satisfactory performance for critical areas such as nodal joints⁽⁶⁾ (figure 7). Such welded joints are subject to high stresses in the through thickness direction and are susceptible to lamellar tearing. To reduce such risks ductilities of generally greater than 25% reduction in area have been found to be adequate. The sulphur levels are generally controlled to < 0.01 %, as this is an important requirement, with respect to the mechanical properties of the steel. A reduction in the number of and the extent of aligned inclusions, particularly MnS, play a strong role in improving the through thickness reduction in area values as well as the effect on the ductile fracture process of micro-void coalescence (7).

The design, construction and material selections of offshore structures has to comply with rules laid down by the Government (8). There are many recommended guidance notes and documents, British standard (9) and API (10) recommended practice documents are amongst some of these.

MECHANICAL PROPERTIES		SUPPLY CONDITION-NORMALISED	
Yield Stress (min.)	Ultimate Tensile Stress	Elongation (min.)	Charpy Impact Values
345 N/mm ² for sizes up to 40mm	490 N/mm ²	18%	27 J at -30 °C or 41 J at -20 °C

Table 3 Mechanical properties of BS4360

	carbon max. %	silicon max. %	manganese max. %	niobium max. %	Vanadium max. %	Sulfur max. %	Phosphorus max. %
Ladle	0.18	0.1/ 0.5	1.5	0.003/0.1	0.003/0.1	0.04	0.04
Product	0.22	0.1/ 0.55	1.6	0.003/0.1	0.003/0.1	0.05	0.05

Table 4 Chemical Analysis of BS4360

Carbon equivalent ladle less than 0.43 where

$$CE = \frac{Mn}{6} + \frac{Cr+Mo+V}{5} + \frac{Ni+Cu}{15}$$

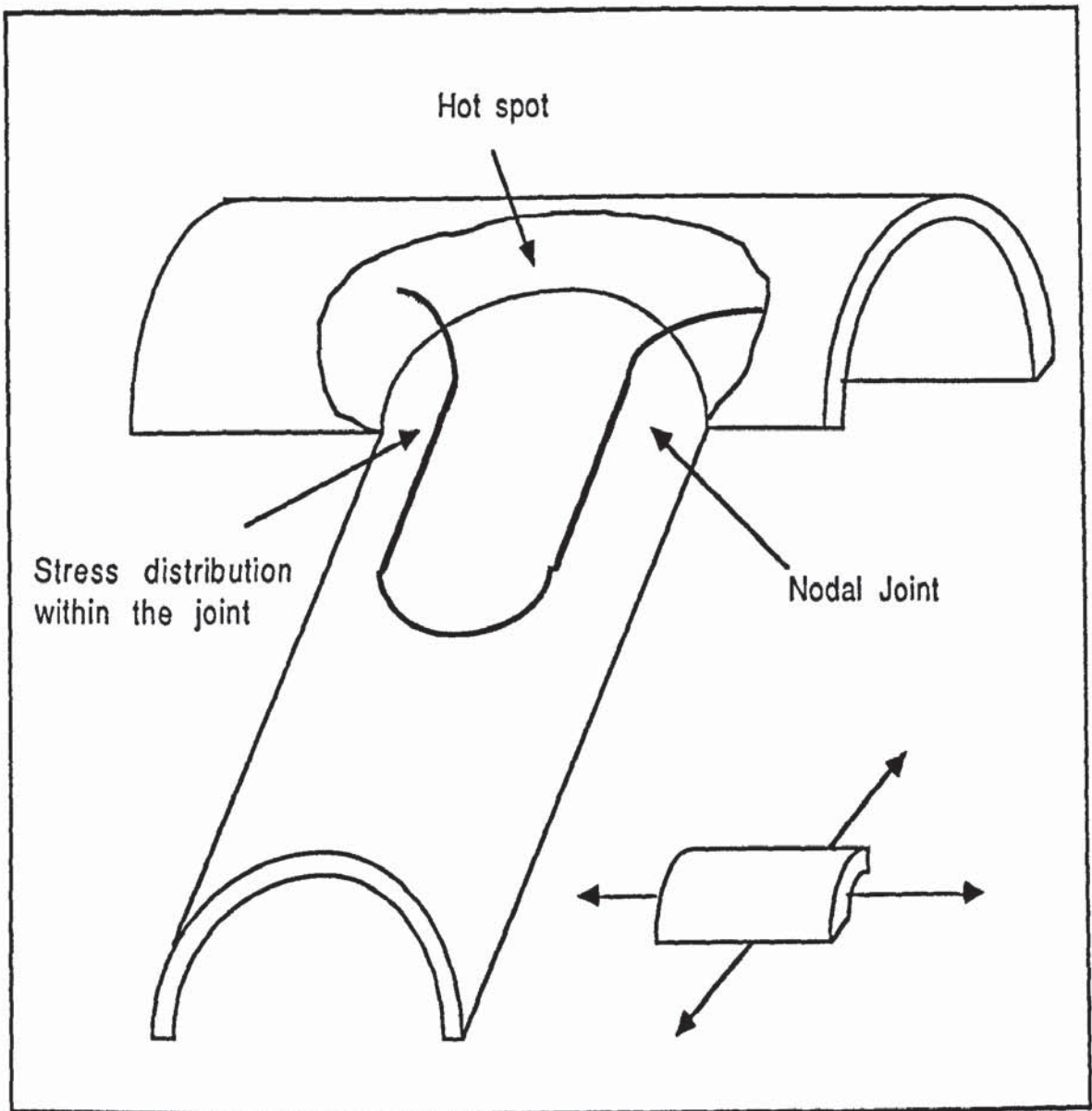


Figure 7 Schematic illustration of a Nodal Joint.

2.4.1 HIGH STRENGTH LOW ALLOY STRUCTURAL STEELS

The sixties witnessed a new class of steels. These steels are mainly used in offshore constructions, as well as line pipe materials within the oil industry (11-35), they possess such important features as;

- i) High strength
- ii) Low impact transition temperature
- iii) Good weldability
- iv) Fatigue strength
- v) Formability
- vi) Minimum cost

Their strength is due to refinement of grain size, which is refined by the addition of micro-alloying elements such as aluminium (Al), niobium (Nb), titanium (Ti) and vanadium (V), whose concentrations are usually small (less than 0.1%)(36). Aluminium and vanadium produce nitrides of limited solubilities, niobium can form carbo-nitrides Nb(C,N) or carbide NbC, and titanium forms nitrides and carbides together with vanadium.

The carbides are more stable than iron carbide, with lower solubilities in austenite, consequently, during hot working, fine precipitation of these carbides/nitrides takes place both on austenite grain boundaries and on dislocation arrays within grains. Other elements of importance to offshore steels are manganese, copper, nickel, chromium, and molybdenum, in addition to impurity elements such as oxygen, sulphur and phosphorus.

Addition of manganese to steels has a number of important effects. Addition in the range of 1.0 to 1.5 % Mn lowers the temperature at which austenite transforms to polygonal ferrite by 50 °C (37). This results in a significant ferritic grain refinement, and consequently increase in strength and toughness. Higher manganese levels promote the transformation of austenite to microstructures comprising mixed phases such as martensite-austenite, bainite, etc. Manganese contents in excess of 1.0% may cause the steel to be dirty by reacting with the silica content of the refractory lining, but this problem is usually obviated by handling the steel in high alumina or basic lined refractory vessels (38-39).

The restriction of carbon content to the range of 0.05-0.15 % for ferrite-pearlite steels is dictated by the need for weldability. The effect of higher carbon contents on increasing the amount of weld underbead cracking is well documented (40) and the coefficient of carbon in the carbon equivalent equation indicates this danger. Formability and other toughness requirements dictate relatively low carbon contents (40). The small decrease in yield strength caused by this lowering of carbon content can easily be compensated for by the use of other strengthening mechanisms.

Molybdenum kinetically suppresses ferrite transformation and therefore slightly lowers the transformation temperature. This can cause a slight reduction in grain size and hence moderate increase in strength. More significantly molybdenum suppresses the formation of pearlite. As a result, in the steels that contain high percentage of molybdenum, the austenite remaining after polygonal ferrite formation will transform to lower temperature products such as acicular ferrite, bainite and martensite-austenite (M-A) constituent.

Copper and nickel are expected to have effects on transformation behaviour similar to that of manganese, in that they may lower the transition temperature. These two elements may thus refine the grain size slightly and lead to less precipitation of carbo-nitrides in the ferrite. They may also contribute to a small solid solution hardening effect (37). Nickel seems in larger amounts to have a beneficial effect in lowering the transition temperature because of its effect on cross-slip. It has been reported (41-42) that copper in the range 0.2 to 0.3 % reduces the corrosion rate in a hydrogen sulphide environment within the pH range 4.8-5.6 (41), and hence minimises the incident of hydrogen induced cracking.

Chromium in conjunction with molybdenum is expected to alter the transformation characteristics of the steel and promote the formation of the martensite-austenite (M-A) constituent.

Sulphur, oxygen and phosphorus have a downward trend, the first two lead to the formation of non-metallic inclusions whose deleterious influence on steels are well documented (41, 42, 43). The last element is known to segregate enormously (40), thus promoting hydrogen induced cracking, possibly through the formation of hard low transformation products.

It is well known that general ductility decreases exponentially with volume fraction of second phase particles, particularly non-metallic inclusions. The major effect is when inclusions (particularly MnS), are elongated into stringers or tapes during the hot rolling process. This effect is pronounced with very plastic inclusions, the elongated planar arrays considerably impair the ductility and toughness in the transverse or through thickness directions. A recent method of combating this problem has been modification of both sulphides and oxides by addition of calcium, zirconium, or cerium (rare earths).

The modification most effective in the case of sulphides is brought about by the Ce addition, decreasing the plasticity of the inclusions with the result that they form rounded globules rather than elongated tapes or planar arrays. The transverse and through thickness ductility are greatly improved, as the material does not have an easy plane of fracture.

To illustrate the beneficial effect of low S on the reduction of area, figure 8 (96) shows the average reduction of area and the standard deviation as a function of S on high tensile steel plates having oxygen contents between 10-30 ppm. The scatter suggests that the S content may not be the only factor affecting ductility.

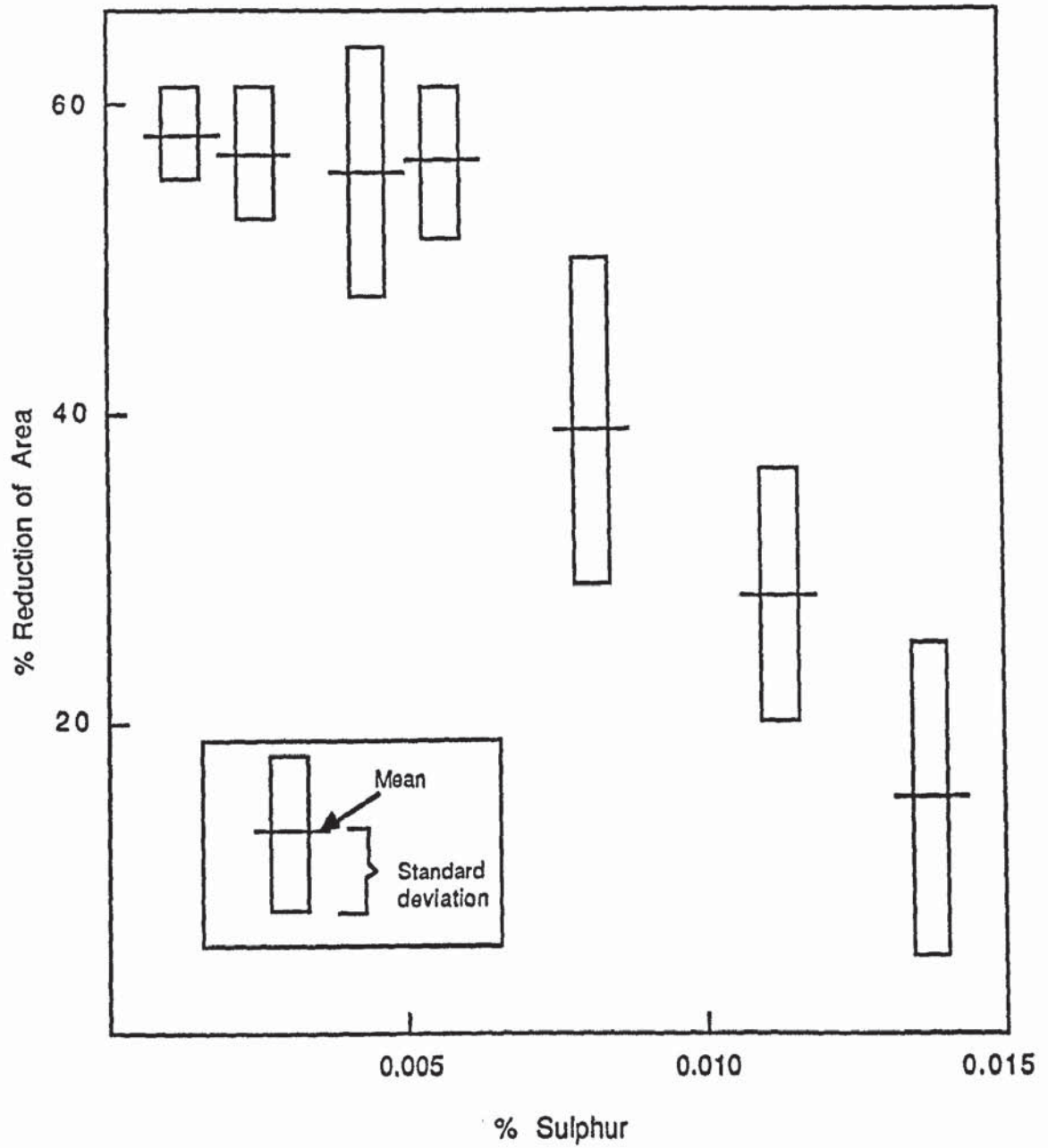


Figure 8 Reduction of Area In through thickness direction as a function of S-content.

2.4.2 METHODS OF PRODUCING HSLA STEELS

The development in production of HSLA steels in recent years has been closely associated with attempts to refine the grain size of the steel, thus producing the greatest strength and optimum toughness. Techniques which have been used are normalising after rolling, controlled rolling and / or fast cooling. Normalising after rolling has been used for many years to give a more uniform product and to improve the toughness by refining the grain size.

Controlled rolling is a thermomechanical treatment which, when carefully controlled can lead to a considerable refinement of grain size primarily by limiting austenite grain size prior to transformation. The most important phenomena in thermomechanical processing of the steel is the high nucleation and low growth rate of the ferrite. The nucleation and growth of the microalloy carbides / nitrides are also of the utmost importance, particularly for the use of controlling the recrystallisation temperature during hot working (47-48).

One of the effects of microalloying additions to HSLA is to produce the stable dispersion of particles at elevated temperatures, typically niobium carbonitrides Nb(CN), vanadium carbonitride V(CN) or titanium nitride TiN, which in turn retard recrystallisation, restrict grain growth, and produce a finer product.

The stability and solubility in austenite of various microalloyed carbides and nitrides are, however different. Nitrides are more stable than carbides, and the stability increases and solubility decreases, in the order V, Nb, Ti. Consequently, whereas the earlier generations of HSLA steels usually contained only a single microalloying addition, current steels tend to employ more than one addition in order to achieve desirable property combinations.

Niobium and to a certain extent titanium, can act as grain refining and precipitation strengthening additions⁽⁴⁹⁾, whereas vanadium is usually added to improve the yield strength. To optimise properties achieved by controlled rolling, a largely empirical understanding of solubilities of these compounds at different temperatures, their effect on recrystallisation kinetics under rolling conditions, and their precipitation strengthening effects under different mill processing conditions, have been developed.

In general terms the best combination of properties are achieved by low slab reheating temperatures, large deformations at low rolling temperatures and by rapid final cooling (50-54). The principal benefits as regards microstructure-property relationships in HSLA steels, which are derived from the accelerated cooling techniques are (55-56) ;

- i) Grain refinement of polygonal ferrite for a given austenite grain size by the virtue of inhibition of austenite grain growth before transformation.
- ii) Augmented precipitation strengthening from microalloy additions, and the lower ferrite transformation temperature range resulting in finer precipitates.
- iii) Promotion of strong, tough low-carbon bainite if the steel chemistry is appropriate.
- iv) Possibility of reducing the carbon equivalent of the steel, which is advantageous from the point of weldability, formability and toughness, without detriment to strength.
- v) Elimination of pearlite banding.

Controlled cooling can also be used to improve the properties of steels by lowering the transformation temperature to promote further ferrite grain refinement. This can be achieved by blast or water spray, but martensite or bainite formation at the surface must be avoided.

Systematic investigations (57-59) have called for careful control of the finishing rolling temperature (FRT) at above 800 °C so that accelerated cooling produces the optimum properties.

A major drawback of accelerated cooling is the maintenance of acceptable shape and flatness, the distortion arising as a result of the transformation of austenite at different points in time through the thickness. Furthermore the natural temperature difference between the edges and the centre is accentuated.

2.5 WELDED TUBULAR JOINTS

2.5.1 THE GENERAL EFFECTS OF WELDING

The large tonnages of structural steels which are consumed in the offshore industry are fabricated by welding (60). However, the potential advantages of welding can only be realised if unexpected problems can be avoided during construction and if the resulting structures have sufficient reliability during the whole of their service life. "Satisfactory weldability" depends on the choice of welding process, and the skill and control exercised during fabrication, and on service performance expected of resulting structure as well as material quality.

Most of the welding processes involve the local application of an intense heat source to produce local melting, addition of filler metal to the melted pool to produce the required weld shape and dimensions after solidification. The effects of welding are hence most apparent in the "fusion zone" and the heat affected zone (HAZ) adjacent to it.

The weld metal is essentially a small chill casting which has been cooled rapidly, its composition is derived from the parent material, whilst its metallurgical structure depends critically on the rate of cooling associated with the process and procedures. Metal adjacent to the weld is both heated and cooled extremely rapidly, so that there is a risk of change in properties, as result of phase changes, grain growth or high temperature hardening in the heat affected zones.

Local strain takes place in both heat affected zone and weld metal during the heating and cooling cycle, and this results in high tensile stresses remaining in the weld after it is cooled. These are almost as high as the yield point at the centre line of the weld in a direction parallel to it.

If there are pre-existing defects adjacent to the weld the local concentration of strain may be very considerable and the combination of the strain temperature cycles can radically affect the properties of the material locally. During the welding process there is also risk of gases concentrating in the weld pool.

Hydrogen is very difficult to avoid because hydrogen containing compounds present in fluxes, rust, grease, etc. decompose in the welding arc to atomic hydrogen, which is absorbed very quickly into the steel. Atomic hydrogen diffuses rapidly and may subsequently reduce the ductility of either the HAZ or the weld metal or both to a point which can even lead to cracking under the action of residual stresses.

2.5.2 THE POTENTIAL WELDING PROBLEM

The properties of the HAZ and the weld metal usually differ from those of the parent metal because of the differences in composition and thermal history. Welding problems can arise either through the presence of defects of technological origin, such as lack of fusion, or metallurgical origin such as weld cracking, and thus impairing the strength, ductility or toughness in welded region, or because some other important service characteristic such as corrosion behaviour, has adversely occurred to a point where useful life is shortened.

2.5.3 WELDABILITY AND SPECIFICATIONS

The parameter weldability includes strength, toughness and cracking behaviour of welded joints, in offshore structural steels. These are specified in BS4360 which deals exclusively with as-rolled steels and the classification is primarily on the basis of yield strength. The principal problem in welding these steels is hydrogen induced cracking and it is obviously a considerable advantage to the fabricator if he need take no special precautions, such as pre-heating.

The risk of hydrogen induced cracking is largely related to hardenability and for convenience a "carbon equivalent formula" based on hardenability defined as follows (BS1974):

$$\text{Carbon Equivalent} = \% \text{C} + \frac{\% \text{Mn}}{6} + \frac{\% \text{Cr} + \% \text{Mo} + \% \text{V}}{5} + \frac{\% \text{Ni} + \% \text{Cu}}{15}$$

The accuracy of the presently used carbon equivalent can be questionable when applied to very low carbon steels which are coming in use (60). Few of steels specified in BS4360 show serious liquation cracking, even when welded under high input conditions (Figure 9). The specification is broadly in line with several recent recommendations for reduced sulphur levels, in fact the majority of steels supplied to BS4360 specification, have sulphur levels well below the maximum permitted, so the actual position is better than the permitted maximum might suggest.

In offshore structures, the tubular connections and associated stiffenings at the "nodes" make particularly heavy demands on the resistance to lamellar tearing (figure 10). This demands a restriction of the inclusion content. The number of sulphide inclusions can be reduced by restricting the sulphur level. However, this alone is insufficient and must be accompanied by control of oxide inclusions. There has been controversy concerning the level of through ductility necessary to avoid lamellar tearing, even under the most severe conditions.

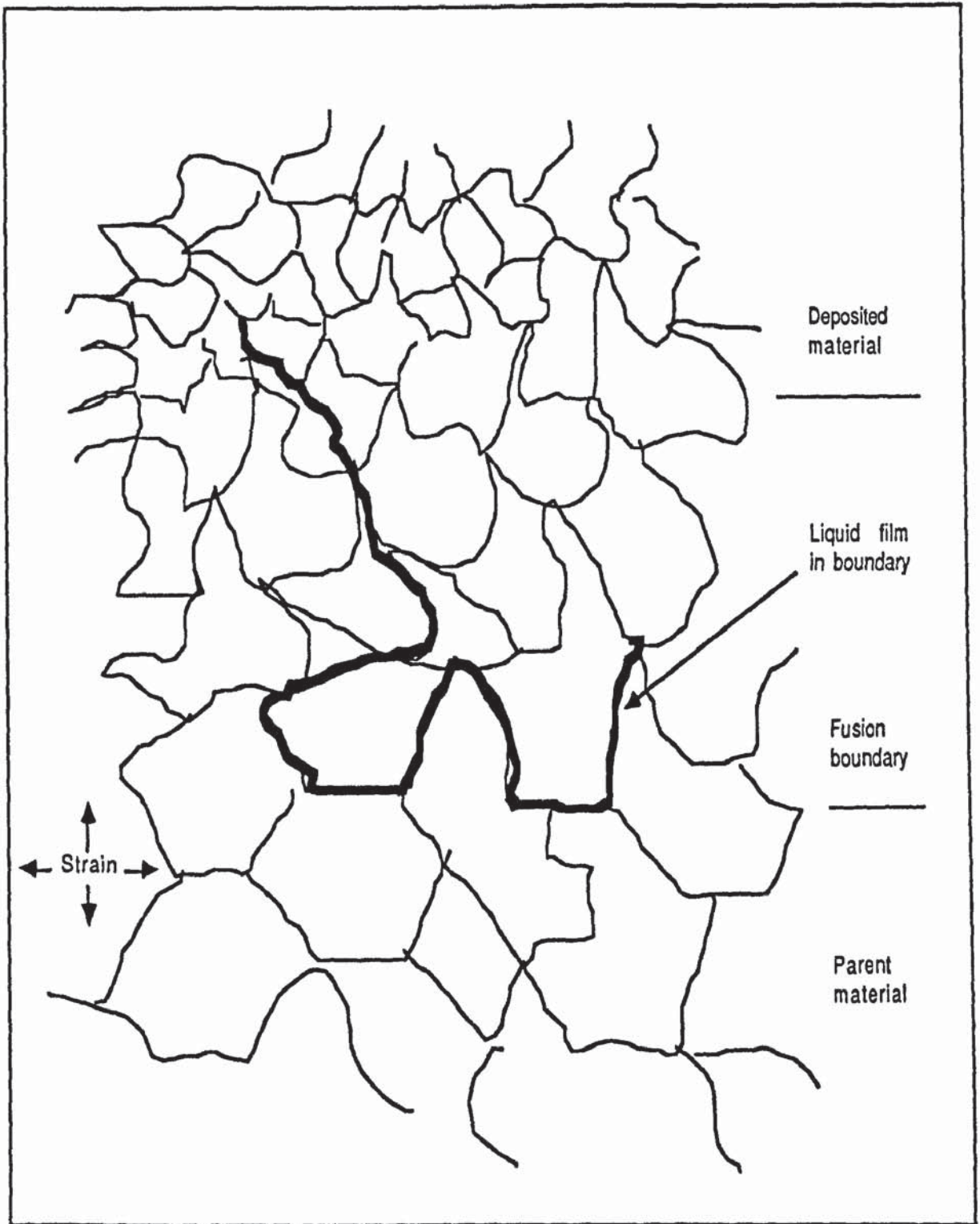


Figure 9 Liquation cracking

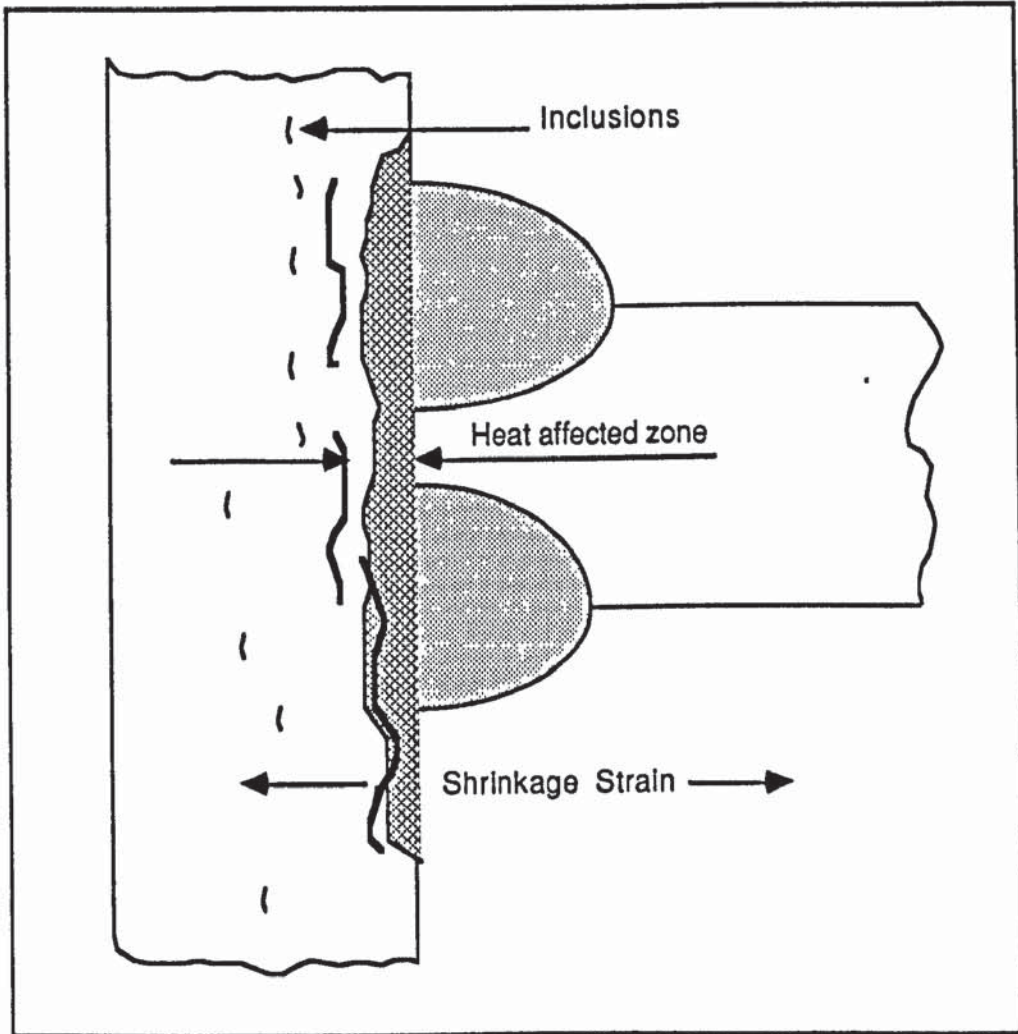


Figure 10 Schematic Illustration of lamellar tearing.

2.5.4 WELDING OF TUBULAR JOINTS (CURRENT PRACTICE)

Welding of tubular joints involves controls on how welds are made, inspections of these welds, the rejection or acceptance of weld defects and repair of defective welds. Most of the tubular joints are welded manually or by semi-automatic techniques. Preparations are made for the weld to assure weldability and fusion. The base metal is preheated and the welding rods are kept dry in special ovens (this is especially important for low hydrogen rods in humid environments) . The edge of the brace is usually prepared by grinding and cleaning the surrounding environments. Because of the accessibility majority of the root welds are made from outside of the joint only, and this requires special skill. The root pass may thus be performed by special welders, and subsequent passes to complete the weld and bring it to its required thickness by semi-skilled welders.

2.5.5. INSPECTION

As mentioned in earlier parts of this chapter, construction of fixed steel offshore structures is divided into two phases, fabrication and installation. In the fabrication phase, the primary concern is with quality assurance of the incoming material and welding of parts together. In this phase the most effective inspection scheme is to prevent the introduction of defects into a weld, rather than to find them after they occur. To this end, extensive quality tests are required for both welders and welding procedures. Inspection of welds in the complex geometries of tubular joints is difficult, and special care is needed. Also when defective welds are found it is important to find the possibility of systematic error, and inspection mainly falls into two categories;

- I) Welding quality assurance and
- II) Inspection of welds.

2.5.5.1 WELDING QUALITY ASSURANCE

These are designed to prevent defects from occurring in the first place. Since special skills are required to make one-sided full penetration groove welds, welders with this skill must be identified. There are different levels to which the welder may be qualified. These levels are set by the type of the weld (full or partial penetration, groove, butt, fillet, etc.), the position of welding (flat, horizontal, vertical, overhead, etc.), and finally the welding process, necessary to do the job.

2.5.5.2 INSPECTION OF THE WELDS

The inspection of production welds is vitally important, field inspections are of three kinds;

- i) Observation of the welding process
- ii) Visual examination of the welds and
- iii) Non-destructive examination (NDE) of the weld.

The welding process is observed to assure that qualified welders and procedures are used. Sometimes different coloured hard hats are issued to welders of different qualification levels, to make it easy to see that a qualified welder is working critical welds are watched very carefully.

Upon completion the weld is inspected visually to check its profile and see that it merges smoothly with the adjoining material without excessive undercut. Pocket gauges and magnifying glasses may be used for this purpose. A visual inspection may detect small surface cracks. For fillet welds visual examination is likely to be the only inspection, for other welds some sort of NDE is likely.

NDE for tubular joints is very difficult. This is due to complex geometry of a tubular joint and the fact that the weld is only accessible from the outside of the joint, under these conditions meaningful radiographical inspection (γ -ray or X-ray) are impossible. So the burden of NDE inspection falls upon two techniques, ultrasonic and magnetic particle. A third technique using dye penetrants is sometimes allowed when one of the above can not be performed.

Ultrasonic testing has become the most important inspection technique for tubular joints. In this test the ultrasonic echoes of flaws are measured electronically by skilled technicians. Since the interpretation of the test results are difficult especially for tubular joints, there are various recommended notes published by API, Department of Energy and various certification authorities based on the "recommended practice for ultrasonic examination of offshore structural fabrication and guidelines for qualification of ultrasonic technicians". The ultrasonic test results are best for flat plates, and least conclusive for acute angle brace to chord weld areas in K and Y joints. Because no single test is conclusive by itself, ultrasonic testing is often used in conjunction with another form of NDE testing.

For tubular joints the second major technique is magnetic particle inspection. Here an electric current is passed through the metal, creating a magnetic field, flaws in the metal alter the current flow and distort the magnetic field, this distortion can be seen in magnetic particles dusted on the surface. One draw-back to this technique is that it becomes less effective for detecting flaws the deeper the flaws are formed in the plate. Typical inspection requirements call for 100% tubular joint welds to be both ultrasonically tested and magnetic particle inspected.

In some instances dye penetrants may be used in lieu of one of the above methods, for example, when the weld is inaccessible to the testing equipment. In this method, a dye is washed over the metal and penetrates through the surface cracks. Dye left in the cracks can be detected visually. However dye penetrants cannot detect subsurface defects.

2.6 DURABILITY OF THE STEELS

A comprehensive durability study should contain the concept of worst case analysis, i.e. the performance of material at the boundary limits of stress and environmental conditions to which the material can be subjected. These boundaries in typical off shore jacket structures occur at the splash zone and the nodal joints and are aggravated by localised impurity particles. The following is a brief review of each of these cases.

2.6.1 SPLASH ZONE

Air dissolved in sea water increases the corrosion rate significantly. Dissolved air causes the metal surface areas near the sea surface to corrode more severely than surface areas at greater depths (figure 12). The splash zone extends from some distance below the mean low water line (MLW) to about 1.5-2.0 times distance above the MLW. The range depends on local conditions of tide, normal wave height, and (in cold climates) ice abrasion (figure 11).

The splash zone is the most difficult area to protect because of alternate submergence and aeration. None corrosive coverings are used, sometimes in conjunction with increased thickness of the steel members. The surfaces in the splash zone are sand blasted and painted with inorganic zinc paint, followed by epoxy, phenolic, neoprene, or vinyl coating.

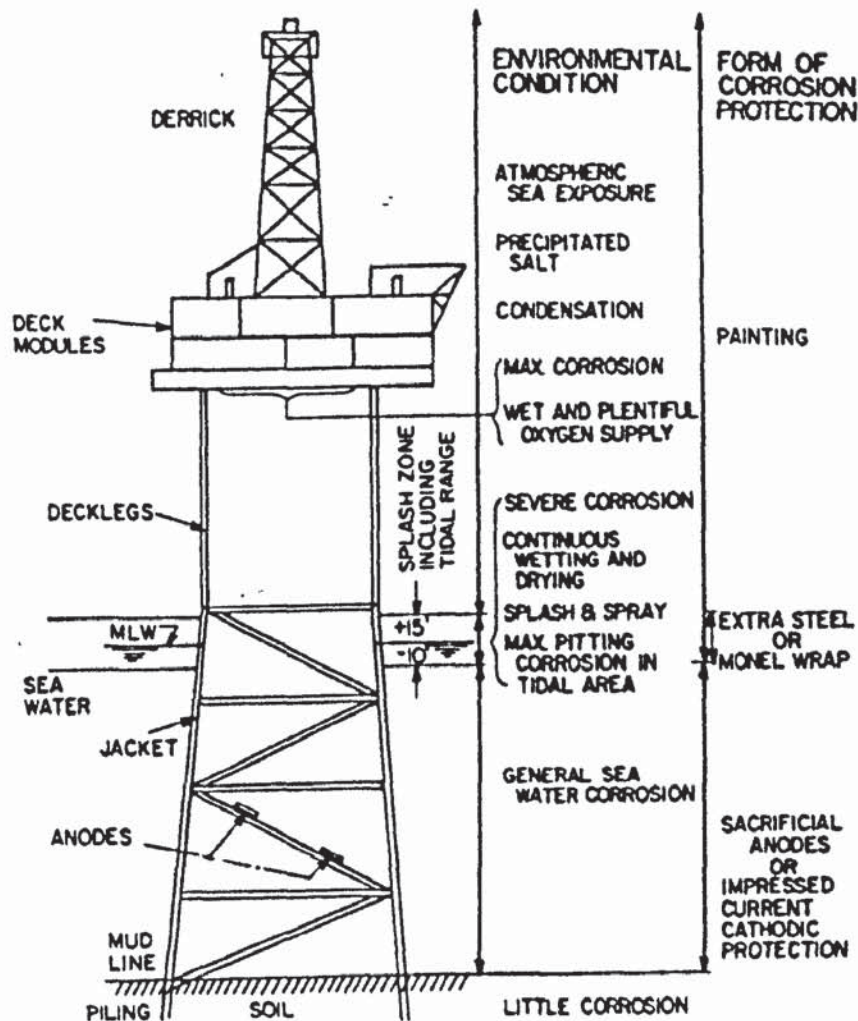


Figure 11 Corrosion zones on fixed offshore steel structures

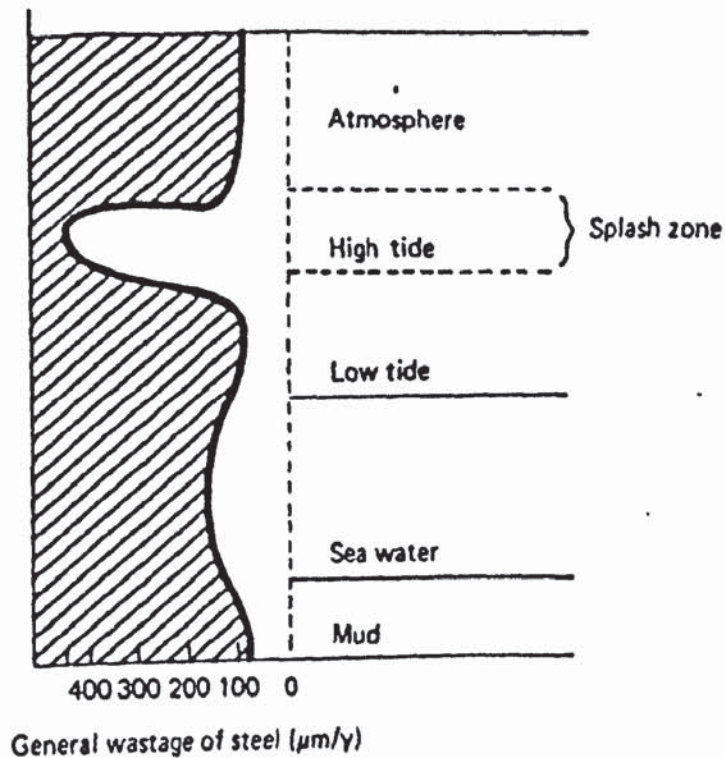


Figure 12 Marine environments: zones

Application of these coatings is rarely attempted when the humidity exceeds 85% or the temperature drops below 50 °F (= 10 °C). The purpose of the painting is to keep the sea water away from the metal surface. Moisture leaking through the coatings causes them to crack and eventually leads to peeling of the paint. Often, paint and other coatings are damaged by abrasion with objects. Where there are cracks in the paint, very rapid pitting corrosion occurs due to concentration of the corrosion process at the crack or gap.

2.6.2 NODAL JOINTS

A typical offshore structure consists of three major components; jacket, piles, and topside (deck) facilities. The jacket is the most crucial part of the entire structure, and most of the design efforts are spent on this component. The jacket consists of large diameter tubular legs framed together by a large number of smaller tubular members called braces.

The construction of these members is implemented through tubular connections joined by fusion welding, known as "Nodal joints". Technically these joints are the most sensitive parts of the structure which are subjected to high combinations of simple stresses such as tension, compression, bending or shear and thermal residual stresses which can easily occur during welding.

Since the early 1960's the stress analysis of nodal joints for offshore structures has received considerable attention, both experimentally and analytically. The problem has been studied by many investigators (61) because of its complexity and the understanding of all factors that contribute to a high durability is far from complete.

2.6.3 HIGHER LEVEL OF IMPURITIES

Studies of observed material failures in early platforms showed that the most of failures occurred in or near the welded joints, this fact led to the investigation of steel properties in the vicinity of the welds and heat affected zones (HAZ) of the material(62). The investigations of steel in failed components of platforms revealed that material contained laminations, which are planar types of discontinuities in steel plates resulting from the flattening and elongation of inclusions or voids during the rolling process (63).

In highly restrained joints within welded connections the phenomenon of lamellar tearing is the most likely possibility of the failure. Under high restraint, localised strains due to weld metal shrinkage can be several times higher than yield point strains. The cracks occurring due to lamellar tearing are caused by through-the-thickness stresses produced by weld metal shrinkage. Thus through-the-thickness ductility within these welded joints is important for the prevention of the crack initiation. The volume fraction of second phase particles is a major factor determining the degree of through-ductility the steels will possess and hence the likelihood of crack initiation (figure 8).

2.7 GENERAL CORROSION OF STEELS

Corrosion may be defined as the chemical reaction of the metal with a non-metal (or non-metals) in the surrounding environment, with the formation of compounds which are referred to as corrosion products. The degree to which this occurs will depend on the rate of corrosion reaction, which determines the extent of conversion of the metal into corrosion products after a given period of time.

Corrosion may take a variety of forms ranging from fairly uniform wastage resulting in general loss of thickness of cross section, to highly localised attacks resulting in pitting or cracking and fracture and the major part of the surface remaining unaffected.

The environment is an essential feature in determining the corrosion behaviour of metals. Chemical composition of the environment is clearly important but other factors such as degree of agitation, temperature and pressure are often of equal importance, for example, velocity can affect corrosion in a number of ways, it may remove protective corrosion products, and alter the local environment by increasing the availability of oxygen.

2.7.1 ELECTROCHEMICAL MECHANISM OF CORROSION

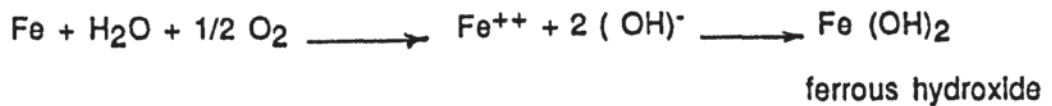
Corrosion that occurs in aqueous solutions such as sea water at ordinary temperatures is electrochemical in nature. In other words, it is a chemical reaction involving the transfer of charge (electrons) from one species to another (65-66). Exposed steels will corrode in moist atmosphere due to differences in the electrical potential on the steel surface forming anodic and cathodic sites. The metal oxidises at the anode where corrosion occurs according to;



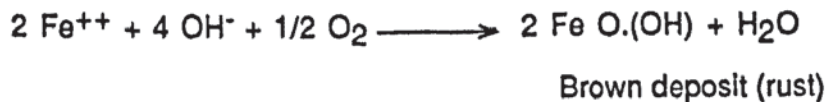
At the cathodic site the excess free electrons in the metal are consumed reducing dissolved oxygen to form OH^{-} ions or by liberation of hydrogen gas according to;



The electrons produced during this process are conducted through the metal whilst the ions formed are transported via the electrolyte (67). In natural oxygenated environments the oxygen reduction predominates so the overall reaction is;



In these solutions, ferrous hydroxide is unstable and combines further with oxygen by reaction;



2.7.2 POTENTIAL-pH EQUILIBRIUM DIAGRAMS

The term "potential" is widely used when considering corrosion reactions, particularly in relation to the electrode potentials of metals and alloys in sea water and protection of steel work by cathodic protection.

The application of thermodynamics to corrosion phenomena have been generalised by means of potential-pH plots, this diagram summarises all the different equilibria between metal, metal cations and anions and solid oxides having $E_{\text{eq.,H}}$ (subscript H indicates the potential is on the hydrogen scale) and pH as ordinates.

These are frequently called Pourbaix diagrams after professor M Pourbaix who first suggested their use. They are constructed from calculations based on the Nernst equation(see appendix 1) and solubility data for various metal compounds. The potential-pH diagram for iron is shown in figure 13 . As shown in the diagram it is possible to delineate areas in which iron, iron hydroxide, ferrous ions, etc. are thermodynamically stable. That is, these form present states of lowest free energy.

The main uses of these diagrams are;

- 1) Predicting the spontaneous directions of reactions
- 2) Estimating the composition of corrosion products and
- 3) Predicting the environmental changes which prevent or reduce the corrosion attack.

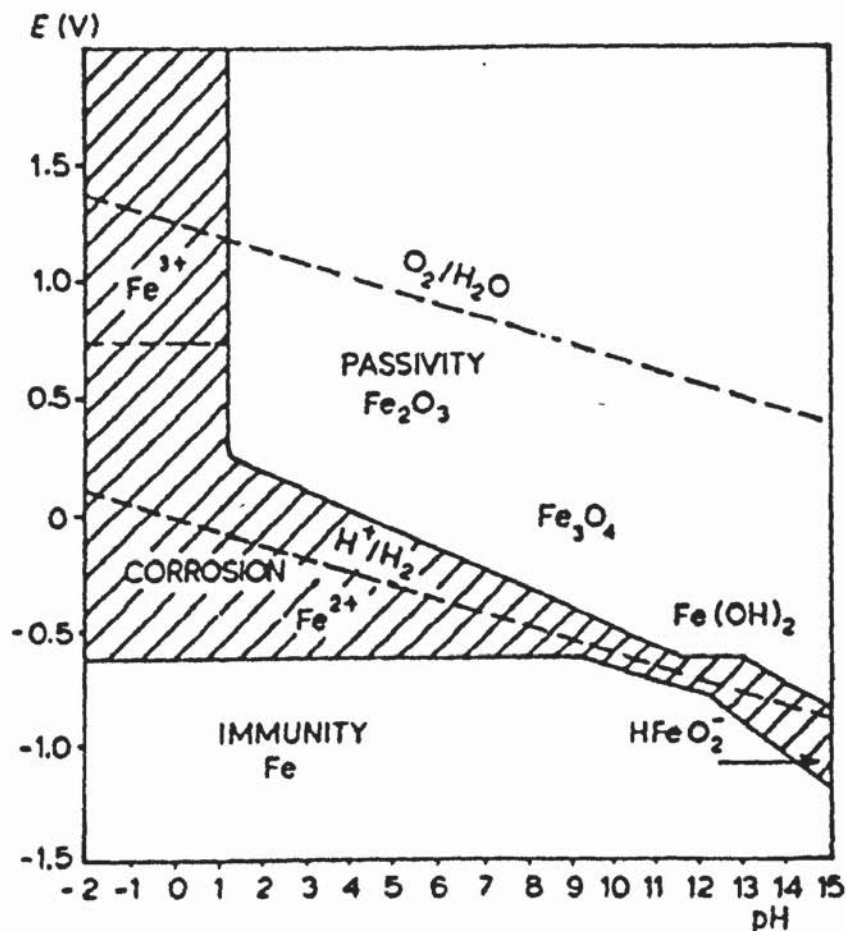


Figure 13 A simplified form of the Pourbaix diagram for Iron

2.7.3 CORROSION OF OFFSHORE STEELS

The corrosion rate in oxygenated sea water of unprotected steels as used for structural components in offshore platforms is relatively rapid (upto 0.4 mm per annum on average), With even higher or more rapid local pitting under certain conditions (68). On immersion in sea water, such steels establish a potential of about -0.65 volts (with respect to reference electrode, silver/silver chloride) known as the free corrosion potential.

Corrosion rates differ in different exposure zones as indicated in figure 12. As expected steel in the splash zone suffers the highest rate of corrosion (increased by a factor of about four on the corrosion rate of the submerged steel) because of the plentiful supply of oxygen in this region.

The submerged regions are normally protected using sacrificial anodes, an impressed current system or both, to a potential of approximately -0.85 volts with respect to the reference electrode (69). In the sacrificial anode protection system, external anodes (usually of zinc, but magnesium and aluminium are also used) are connected to the steel structure to force naturally occurring anodic areas on the steel surface to become cathodic, thus suppressing natural corrosion.

Nevertheless for a typical offshore steel platform, the total weight of sacrificial anodes could be in the region of 200 tonnes, each anode weighing typically 200 kg(69). The second type of system in use in the North sea is impressed current cathodic protection via an inert anode. Typical anode materials are a platinum coated substrate or various lead alloys which are energised at potentials of up to 25 volts, which is 100X the driving voltage of the sacrificial anode system(69) . The preferred system for the North sea platforms has been sacrificial anodes, not only because of their long history in protecting steel in a marine environment but also because of difficulties which an impressed current system has in protecting a steel jacket structure during tow-out and installation periods.

Sacrificial anodes are attached before tow-out and are therefore immediately effective. The major advantages of impressed current systems are the greater flexibility of control and less weight penalty in supporting a large number of anodes and for these reasons they are being installed on some structures.

Reduction of oxygen content in the sea-water at the cathode results in an increase in the local pH. This increased alkalinity in the solution adjacent to the surface of the cathode (the steel structure when cathodic protection is employed) can produce adverse effects on coatings such as softening or blistering of some paints and careful choice of suitable protective coatings is important. The cathodic reduction of oxygen and the increase in alkalinity can also upset the equilibrium between dissolved calcium, hydrogen, carbonate and carbon dioxide in sea water, to form insoluble calcium carbonate⁽⁶⁸⁾.

These calcareous deposits are usually beneficial by reducing the current needed to maintain cathodic protection and thereby lower the power consumption of anode materials or decrease the current requirements from an impressed current system. These deposits can also affect fatigue crack growth. Some offshore platforms are uncoated in the submerged regions and rely entirely on cathodic protection, other platforms rely on a combination of protective treatment and cathodic protection to prevent corrosion at areas where the coatings are inadequate.

In the corrosion vulnerable splash zone, cathodic protection is unsuitable because of incomplete immersion in sea water. This zone therefore, with ready access to oxygen, frequent wetting and vulnerability to mechanical damage, is the critical region from the corrosion view point. At the design stage, a generous corrosion allowance (up to 20 mm) is normally provided to limit access of sea water to the bare metal. The expected life of current protective coatings is considerably less than the life of an offshore platform, hence coatings are frequently inspected as part of the statutory certification process.

2.8 STRESS CORROSION CRACKING (S.C.C)

2.8.1 DEFINITION

"Stress corrosion cracking refers to cracking caused by simultaneous presence of tensile stress and a specific corrosive medium". Stress can either be externally applied or be internal i.e. resulting from mechanical working, rapid cooling of material from high temperature, or any other kind of residual stress. In a susceptible material and environment, cracks can grow steadily either intergranularly or transgranularly under constant stress intensity k , which is much less than K_c (69,70).

$$K = Y \times S \times \sqrt{a}$$

- K - Stress intensity factor
- Y - Constant depending on the geometrical configuration of the specimen, and includes term relating the state of stress
- S - Level of applied stress
- a - Crack or defect size

2.8.2 ENVIRONMENTAL REQUIREMENTS FOR SCC

Environmental requirements for SCC are specific in the sense that not all possible environments promote cracking. It is clear that the propagation of a stress corrosion crack requires the reactions that occur at the crack tip to proceed at a considerably faster rate than any dissolution process that may take place at the exposed surface of the metal, including the crack sides. Otherwise general corrosion or pitting will only be observed (71).

Whilst the repassivating requirements of a cracking environment are important, it is clear that the environment must also be one that permits the formation of a soluble species at the crack tip, so that dissolution and crack propagation can occur. Hence in general terms, a potent solution will need to promote a critical balance between activity and passivity.

A highly active condition will result in general corrosion or pitting, whilst a completely passive condition cannot by definition lead to stress corrosion. For the great majority of engineering alloys inactivity at exposed surfaces is the result of the presence of oxide films covering the metal surface.

Hence not surprisingly alloys of high inherent corrosion resistance, that readily develop protective films require an aggressive ion, such as halide to promote stress corrosion cracking, whilst on the other hand, to crack metals of low inherent corrosion resistance such as steels, all that may be necessary is an environment that is partially passivating.

For stress corrosion crack propagation there needs to be an active tip but relatively inactive sides otherwise pitting will take place. Inactivity in the sides of cracks is associated with the development of a surface film due to reaction with the environment which then leads to a decay in the anodic current.

A convenient way of anticipating the range of potentials in which stress corrosion cracking is likely to occur is available through potentiodynamic polarisation curves, shown in figure 14. As the film formation process is of overriding importance in determining crack propagation rates, it must also be emphasised that the nature of the film is of paramount importance as well. Passive films, usually oxides (possibly hydrated), will form at crack tips during the propagation process in competition with other possibly less protective products eg. metal salts. The final product is likely to be a complex mixture of both dependent upon the solution composition at the crack tip(72).

Aggressive ions of lower repassivation rate (\bar{r}) also make the film less protective. Cl^- ions which are abundant in sea water are of this type, and promote stress corrosion cracking. To study the influence of the aggressive species, the steels must be examined under the potentiostatic conditions. Under open circuit conditions, the

corrosion potential is likely to change upon the addition of different concentrations of a particular species and it will then become possible to distinguish the relative importance of the addition and change in potential caused by the addition (73).

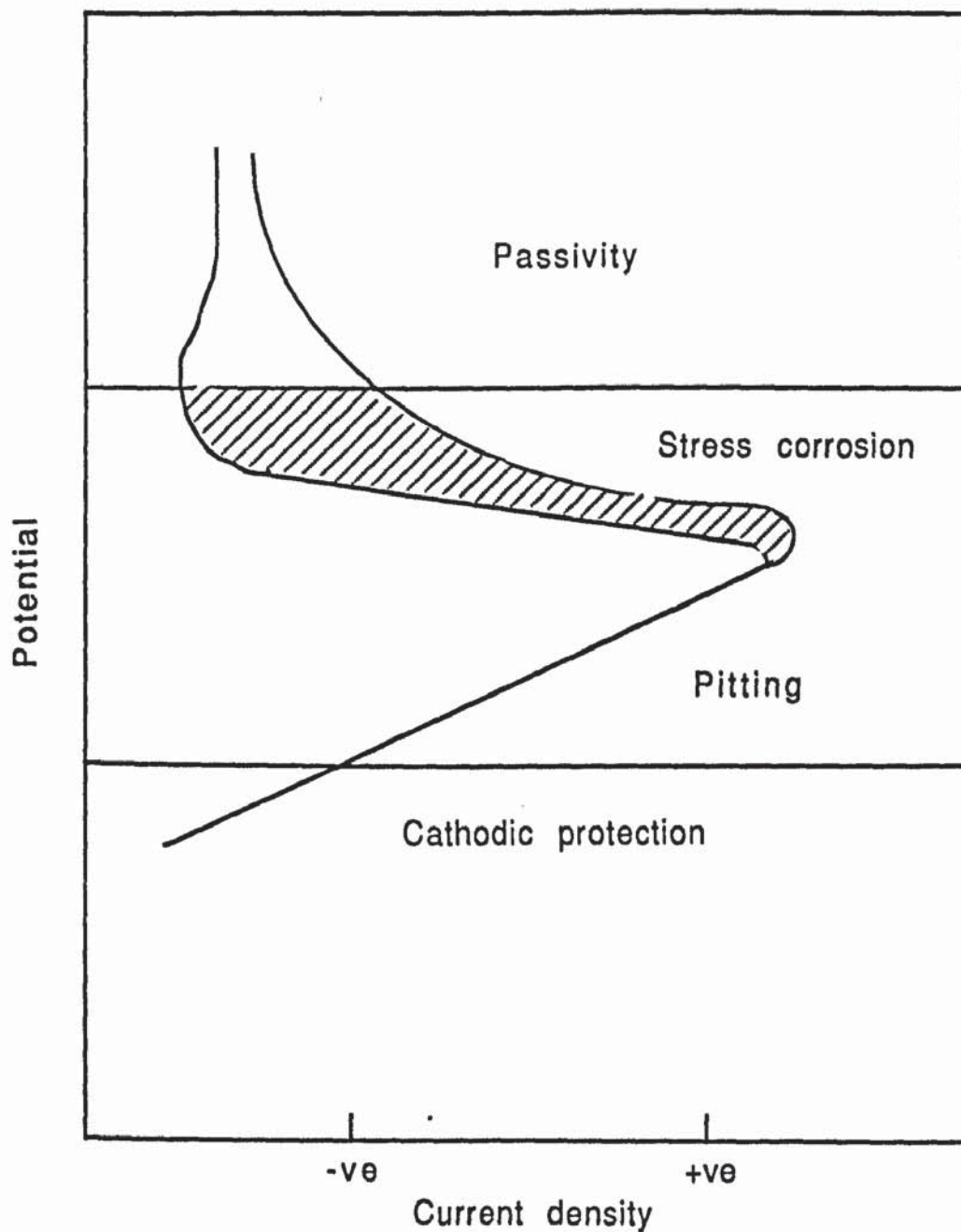


Figure 14 Potentiodynamic polarisation curves and expected domains of electrochemical behaviour.

2.8.3 BASIC CHARACTERISTICS OF SCC

Both intergranular and transgranular stress corrosion cracking (IGSCC and TGSCC), respectively occur in service, and they are essentially of equal practical importance. The mechanisms of the two forms are fundamentally different (74). In IGSCC, in most systems, cracking occurs either by the film rupture or slip dissolution model, in which crack propagates by preferential anodic dissolution at the crack tip. In contrast, TGSCC is thought to occur by environmentally induced cleavage, although the manner in which the environment induces cleavage in normally ductile alloys has not been determined. Both modes can occur in a single alloy, often in the same environment.

2.8.4 FUNCTION OF STRESS

The significance of the stress is its magnitude in relation not only to yield point of the material but also to the geometry of the crack tip, for that is what determines whether plastic strain occurs at the crack tip or not. At sufficiently high localised strain rates, stress corrosion cracking may propagate faster than the alternative failure mechanisms based on the nucleation and growth of internal cavities. If the stress were to be further increased then the localised strain rates may be so fast that there would be insufficient time for the electrochemical reactions to sensitise the material and the result would then be a failure involving ductile rupture.

2.8.5 THE THRESHOLD STRESS INTENSITY

As the crack propagates the stress intensity at the tip declines until a point is reached when the crack propagates at constant stress intensity. This is known as the threshold stress intensity for it determines the level of stress intensity below which SCC will not take place no matter how long the material is exposed to the environmental conditions (figure 15).

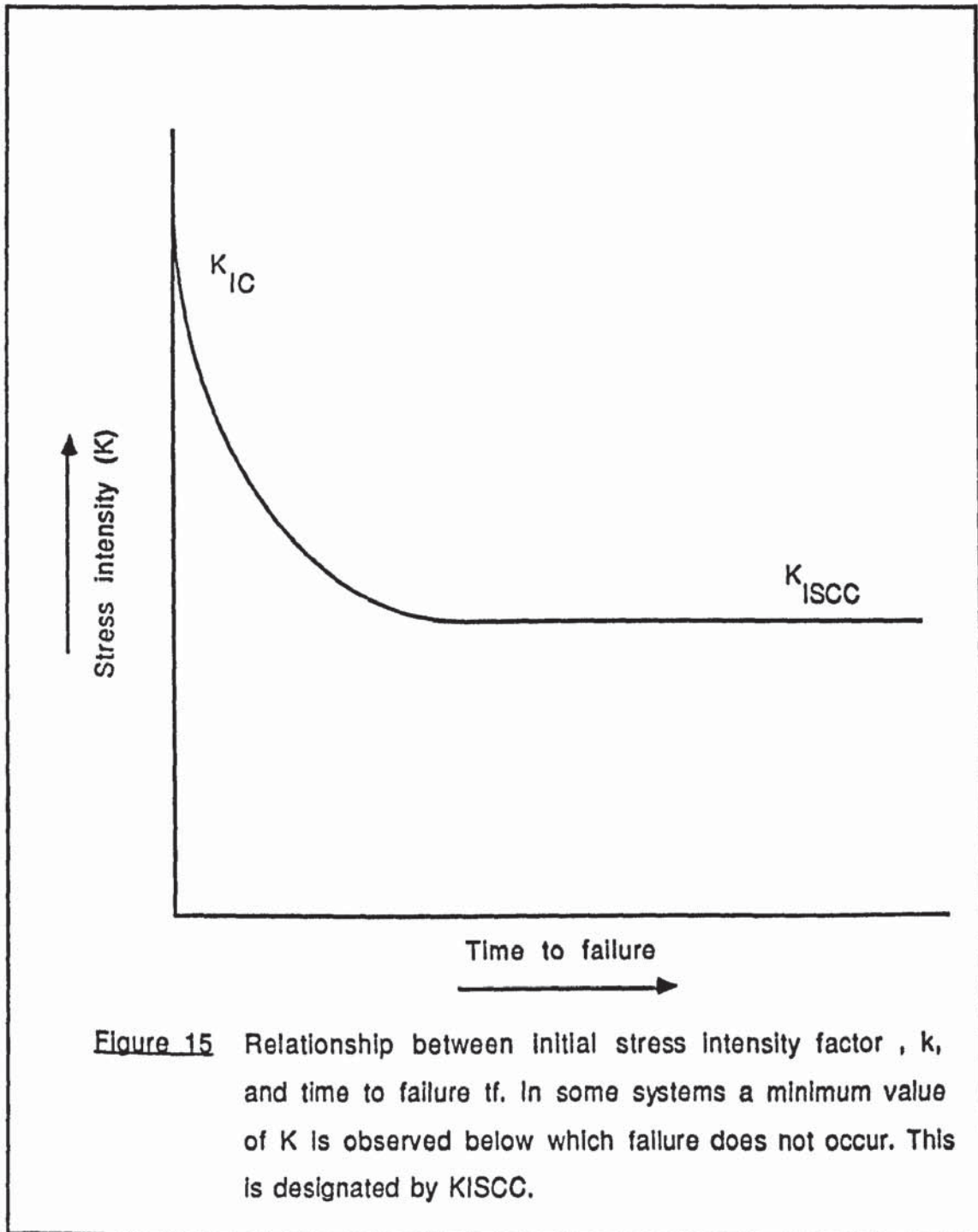


Figure 15 Relationship between initial stress intensity factor , k , and time to failure t_f . In some systems a minimum value of K is observed below which failure does not occur. This is designated by K_{ISCC} .

The velocity of stress corrosion cracking is dependent upon the value of K . The general relationship is drawn in figure 16 in which three regions of cracking is shown. It appears that there is a rapid (perhaps potential) rise in crack growth rate as K is increased. This has been termed regime I. Regime I is followed at higher stress intensities by a regime II in which velocity is insensitive to K because of the saturation of some of the transport processes.

There may be one or more steps in regime II. At still higher stress intensities there is again a K -dependent crack growth rate in a third regime III, leading to fast fracture. However from a practical point of view, regime II is the most significant and the SCC rates vary only slightly over a wide range of crack-tip stress intensities.

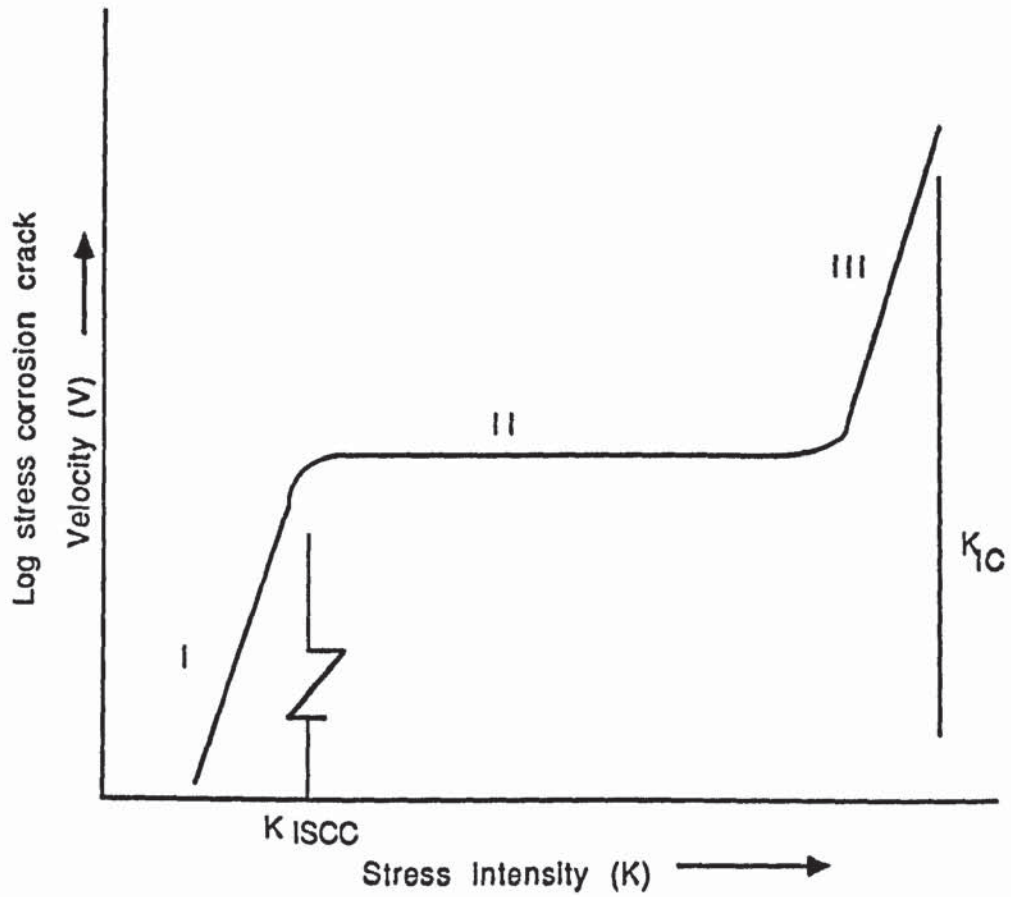


Figure 16 General relationship between the stress Intensity factor, K_{IC} and stress corrosion crack velocity. Many alloys exhibit only stage I and II.

2.9 HYDROGEN ASSISTED FRACTURE

The term hydrogen assisted fracture includes two important aspects of the fracture;

- 1) Fracture almost always occurs at lower stresses or with lower strains.
- 2) The fracture is not necessarily brittle.

The most critical aspects of the effects of hydrogen in structural materials is cracking, which is hydrogen induced or hydrogen assisted. In such processes, a crack is first nucleated and then grows until failure occurs.

The danger of this type of failure is that often the process occurs at loads well below the yield load and can even approach the design loads. Cracks can initiate below the surface of the material in the presence of internal hydrogen. Slow crack growth seems often to occur by repeated re-initiation ahead of crack tip, followed by joining up with the main crack.

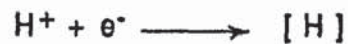
Crack initiation occurs at points where there are the triaxial tensile stresses such as the inclusion/matrix boundary, grain boundary or some other type of boundary. Consequently initiation is typically sensitive to the details of the microstructure. When hydrogen is outside the specimen at the start of the test, it is transported within the material towards the maximum triaxial stress location (s), since there the hydrogen absorption is enhanced. This transport may be by normal lattice diffusion or by dislocation transport.

Once hydrogen has been transported to the maximum stress location, a critical hydrogen concentration C_{cr} , larger than the concentration remote from such locations must be reached. When C_{cr} is attained, a crack can initiate. Once initiated, the crack can propagate in a variety of ways, i.e. intergranular cracking, interphase cracking, acceleration of normal ductile fracture process at inclusions, or by transgranular cleavage.

2.9.1 INTRODUCTION OF HYDROGEN BY ELECTROLYSIS

Hydrogen evolution is one of the major cathodic reactions in acid and alkaline solutions. The process is essentially a decomposition in which the energy required for the reaction is provided by passing an electrical current at the proper voltage through the solution. Oxygen gas is liberated at the positive electrode (anode) and hydrogen is liberated at the negative electrode (cathode).

The hydrogen evolution involves a series of steps in the reaction and it is not always clear which one is the important rate determining step. Initially hydrogen ions are converted to hydrogen atoms at the surface of cathodic steel.



Most of these atoms recombine with others and are evolved as hydrogen gas molecules.



The remainder of hydrogen ions and atoms are driven into the steel by a very high effective hydrogen pressure. Figure 17 schematically shows the reaction steps occurring for the hydrogen diffusion into the steel.

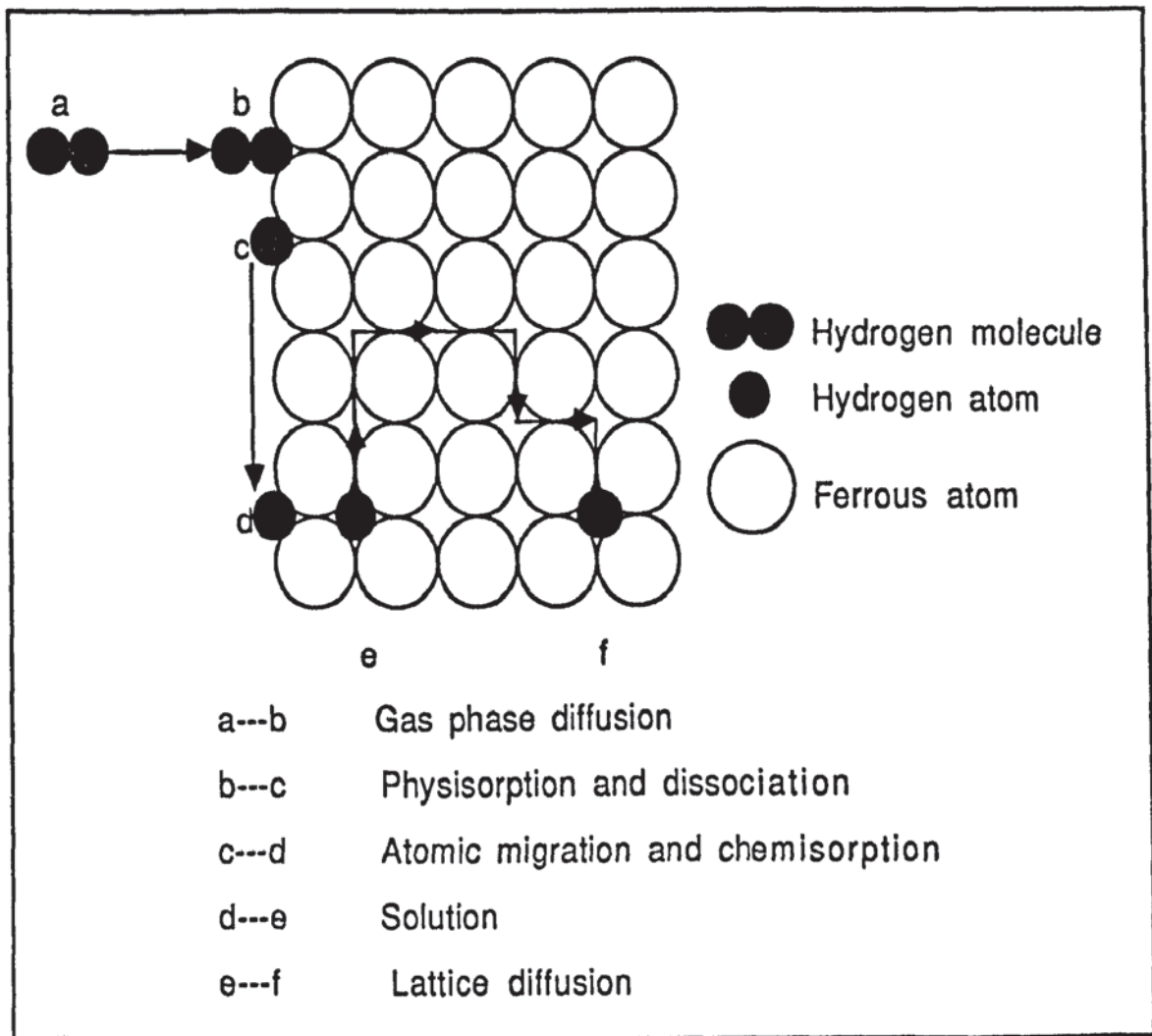


Figure 17 Reaction steps

2.9.2 THE HYDROGEN-METAL INTERACTION MECHANISM

Hydrogen Induced degradation of steels does not occur by any single degradation process, a number of hydrogen-metal interactions are possible and most probably do occur. The currently identified mechanism of hydrogen degradation can be separated into one or more of the following categories:

- 1) Internal pressure formation
- 2) Lattice-bond Interaction
- 3) Dislocation Interaction.

2.9.2.1 INTERNAL PRESSURE FORMATION

This is the oldest mechanism of hydrogen adsorption. It was first proposed by Zapffe and Sims⁽⁷⁵⁾ to explain embrittlement of the steel as the result of electrolytically charged hydrogen. Subsequent modifications have been made by Dekazinczy⁽⁷⁶⁾, Bilby and Hewitt⁽⁷⁷⁾, and Tetelman and Robertson⁽⁷⁸⁾, yielding a general mechanism of embrittlement in an alloy containing a none equilibrium supersaturated concentration of hydrogen.

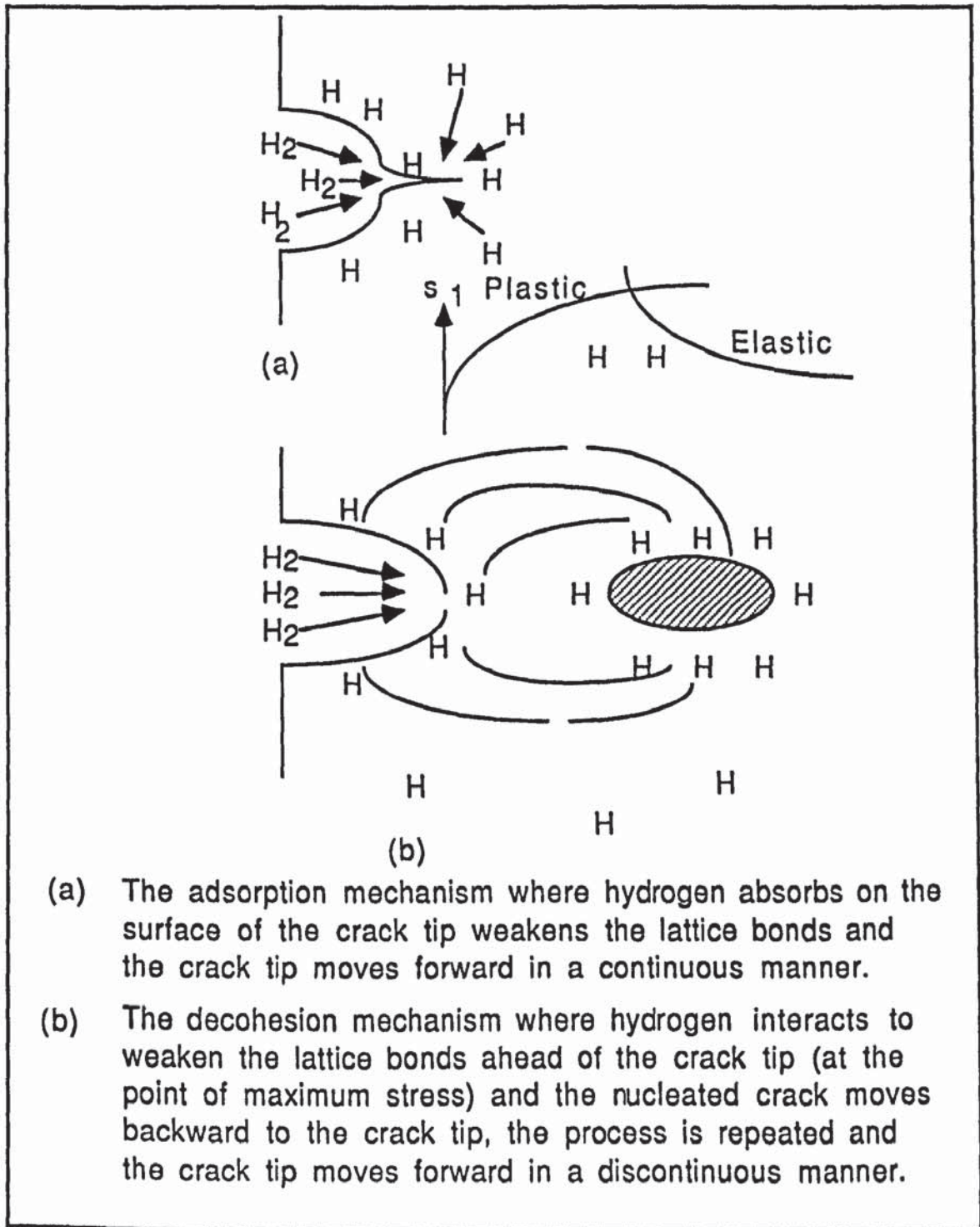
The excess hydrogen in the alloy will try to leave the alloy by forming molecular hydrogen at a surface. Hydrogen well away from an external surface will precipitate as molecular hydrogen at internal surfaces, such as the interface between an inclusion (sulphide) and the metal lattice. As the lattice hydrogen concentrations near these internal surfaces is reduced by molecular hydrogen precipitation, more hydrogen will diffuse into these regions, creating more molecular hydrogen and increasing the hydrogen pressure within this internal cavity.

The growth of the cavity will be controlled by the transport of hydrogen to the cavity. In this context, hydrogen embrittlement arises as a consequence of the development of cracks nucleated from cavities or weak interfaces containing high pressures. Also these high pressures allow cracks to propagate at lower applied stresses.

2.9.2.2 LATTICE-BOND INTERACTION

The basic idea that hydrogen can influence the bond strength of a metal lattice was first put forth by Petch and Stables⁽⁷⁹⁾ in what is sometimes termed the adsorption mechanism of embrittlement. They suggest that hydrogen when adsorbed on metal surface will lower the free energy of the surface. A lower surface free energy will result in a reduction in the work required to break the cohesive bonds across a crystallographic plane and fracture becomes easier.

Barnett and Trolano⁽⁸⁰⁾ considered a similar concept of hydrogen/lattice bond interaction well within the metal lattice will result in localised reduction in the cohesive strength of the lattice (figure 18).



- (a) The adsorption mechanism where hydrogen absorbs on the surface of the crack tip weakens the lattice bonds and the crack tip moves forward in a continuous manner.
- (b) The decohesion mechanism where hydrogen interacts to weaken the lattice bonds ahead of the crack tip (at the point of maximum stress) and the nucleated crack moves backward to the crack tip, the process is repeated and the crack tip moves forward in a discontinuous manner.

Figure 18 Schematic crack growth by hydrogen-lattice bond interaction.

This latter mechanism is sometimes termed the decohesion mechanism. In effect the adsorption and decohesion mechanism are identical and both depend on a hydrogen-induced reduction in the cohesive strength of the metal lattice. The only difference between the two is the proposed location of degradation.

2.9.2.3 DISLOCATION INTERACTION

The basis for the hydrogen dislocation interaction mechanism is the assumption that segregation of hydrogen around a dislocation can change the mobility of a dislocation. Dislocation mobility will determine the extent and character of plasticity in the steel, thereby influencing its fracture behaviour.

The idea that hydrogen will associate itself with dislocations was first proposed by Bastien and Azou (81) in the hydrogen-iron system. They proposed that because of large molal volume, it is reasonable to assume that hydrogen will interact with the dilatational stress field around a dislocation forming a hydrogen atmosphere which results in a drag force, making dislocation movement more difficult.

A mechanism involving hydrogen-enhanced plasticity has been proposed by Lynch(82). It suggests that chemisorbed hydrogen on the crack-tip surface facilitates the nucleation of dislocations. This is because atoms at a surface have fewer neighbours than atoms within the lattice, and hence, the lattice spacing will be greater at a surface than within the bulk lattice.

This "surface lattice distortion" is thought to hinder the nucleation and egress of dislocations from a surface. Since chemisorption of an active chemical species such as hydrogen will increase the number of neighbouring atoms around the surface atoms, then surface lattice distortion will be reduced and dislocation nucleation will become easier.

2.10 CYCLIC STRESSING CRACK PROPAGATION AND FATIGUE EFFECTS

In section 2.2 the environment which North sea platforms experience was described. This involves low frequency cyclic stressing coupled with strains in or around those normally experienced at the yield point. Under these conditions ordinary structural steels can suffer the initiation of cracks from cavities and other discontinuities in the body of or at the surface of the steel. On reaching a critical size, which is dependent on the nature of the crack and the change in stress intensities, the cracks are able to propagate further at a rate which depends on both the nature of the material and these imposed changes in stress intensity. Thus the fatigue life of the steel can be divided into a crack initiation and a crack propagation period.

2.10.1 CRACK INITIATION

During the first 10% of the fatigue life cyclic stressing causes slip band formation, some grain boundary decohesion, possible void coalescence and shear induced deterioration of the mechanical integrity of the steel. Some or all of these processes will take place, perhaps in a random fashion (92), until one micro crack becomes dominant. The onset of fatigue induced cracks in a ductile structural steel is generally associated with the free surface although cracks can nucleate at internal interfaces such as between sulphide particles and the matrix. The importance of free surface becomes apparent when the steels are submerged in sea water for corrosion or hydrogen absorption will occur at these places first. The additional defects that these processes give rise to i.e, vacancy clusters or gas bubbles, will help to initiate a dominant micro-crack at an earlier stage.

2.10.2 CRACK PROPAGATION

Large structures such as oil rigs will always contain some cracks that have previously been initiated or are there as a result of the steel's previous mechanical and/or thermal history eg. welds. To assess the safe life of such a structure the number of stress cycles that it can withstand before one of these cracks propagate catastrophically needs to be known.

In the steady state regime the crack growth rate is described by;

$$\frac{da}{dN} = A (\Delta K)^m$$

Where A and m are material constants and ΔK is the cyclic stress intensity.

Where the safe life $N = \int_{a_0}^{a_f} \frac{da}{A (\Delta K)^m}$

On taking logs of both sides, the plot of $\log \left(\frac{da}{dN} \right) \text{ v } \log (\Delta K)$

will give a straight line. Generally experimental curves will deviate from the linear plot when peak stress intensity levels approach K_c and also when peak stress levels are close to the threshold stress intensity (figure 19) (93).

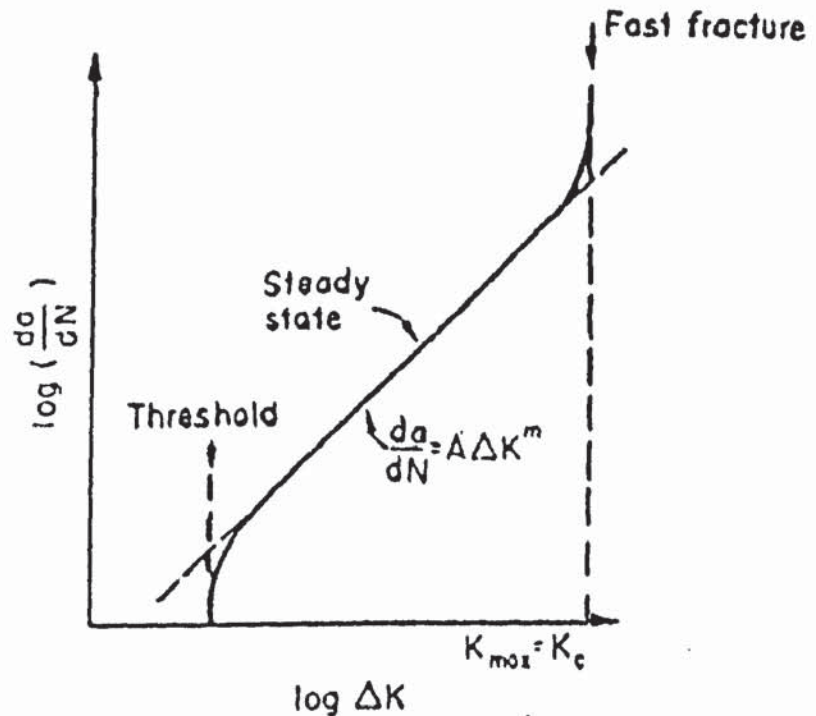


Figure 19 Fatigue crack-growth rates for pre-cracked material.

Exposure of the steels to corrosion in seawater causes a shift of the log/log plots to the left indicating a higher rate of crack propagation at similar cycle stress intensity levels. Furthermore additions of H_2S to seawater causes a further shift of the curves and also indicates a reduction of the threshold cyclic stress intensity (94)(figure 20). These results underline the sensitivity of the fatigue crack propagation rates of structural steels to both corrosion and hydrogen sulphide (H_2S) dissolved in the seawater and has implications on the safe life of the steels.

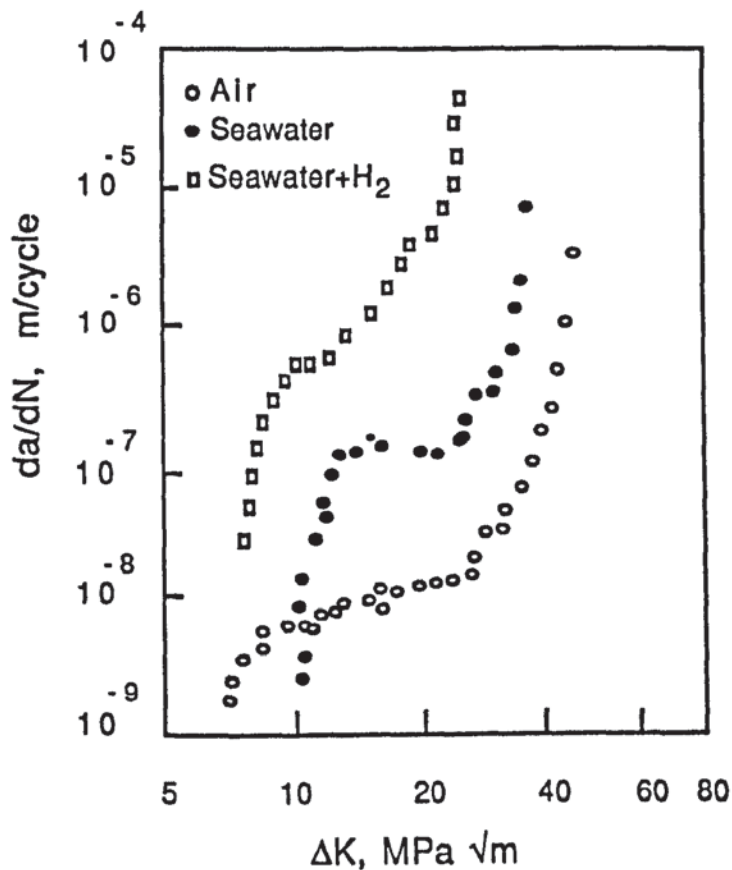


Figure 20 Fatigue crack growth rate for rolled node steel (xy) orientation

2.10.3 WELDS

Offshore structures contain many welds submerged in seawater and the fatigue of welded joints presents a further complication to the prediction of a safe life. The geometries of the weld, and its effect as a source of stress concentration, and also the possibility of weld flaws are two very significant features from the point of view of the welds' fatigue properties.

All offshore structures need to satisfy the Department of Energy Guidance Notes, the most vulnerable welds are those at the nodes of tubular joints and the guidance notes refer to "hot spots" whereby special allowance is made for the stress concentration factors associated with the joint geometry (95). The hot spot stresses can be calculated using finite element analysis.

European offshore rules also include allowance for seawater corrosion in which fatigue life is considered to be one half of that for specimens tested in air, unless they are cathodically protected, when the air value is taken. This rule appears to be a pragmatic one and more research is required before the safe life can accurately be predicted.

2.11 THE FINITE ELEMENT MODELLING

2.11.1 INTRODUCTION

The finite element method is one of the most powerful methods of analysing a structure on a computer. The finite element method is based upon a technique in which a continuum, is approximated by using an assemblage of subregions known as elements, each with a finite number of degrees of freedom.

The element behaviour is described by a set of assumed functions representing the stresses or displacements. The assumed functions are usually of polynomial form, chosen because of the ease in mathematics of manipulation of formula for calculation of stresses and strains. An acceptable representation of the overall real situation is obtained when a sufficient number of elements are used. All the calculations required to define the appropriate functional behaviour is evaluated in a piecewise manner from element to element and the total contribution is summated (84).

The advent in digital computers made in 1950's gave a new impetus to the development of this technique, using the technique of a matrix algebra to deal with problems which would otherwise be too large to tackle. This represented the beginning of the finite element method as a significant tool for complex structural analysis. It was not until the early 1960's that the stiffness finite element was formulated in terms of the principle of stationary complex problems in structural and continuum mechanics, with a very extensive literature being published on the subject (83, 84).

2.11.2 OUTLINE OF THE FINITE ELEMENT PROCESS

The application of the finite element method is classified into two phases;

- a) Studying the individual elements
- b) Assemblages of the elements.

The following section deals with the various steps involved, when the finite element method is applied to stress-strain analysis (83, 84).

2.11.2.1 DEFINITION OF THE FINITE ELEMENT MESH

The continuum is subdivided into subregions or finite elements. Elements are connected at points called *nodes*, which are numbered and referenced to a co-ordinate origin. The configured network is known as a *mesh*. The total pattern of elements representing the entire structure is called the *model*. Depending on the nature of the problem, elements can be one, two and three dimensional. In case of two dimensional problems (figure 21) the element usually takes the form of a triangle or quadrilateral. The general three dimensional solid (figure 22) may be divided-up into tetrahedra or more general shapes. Distribution of elements may be uniform but they have to be clustered around regions of high stress levels.

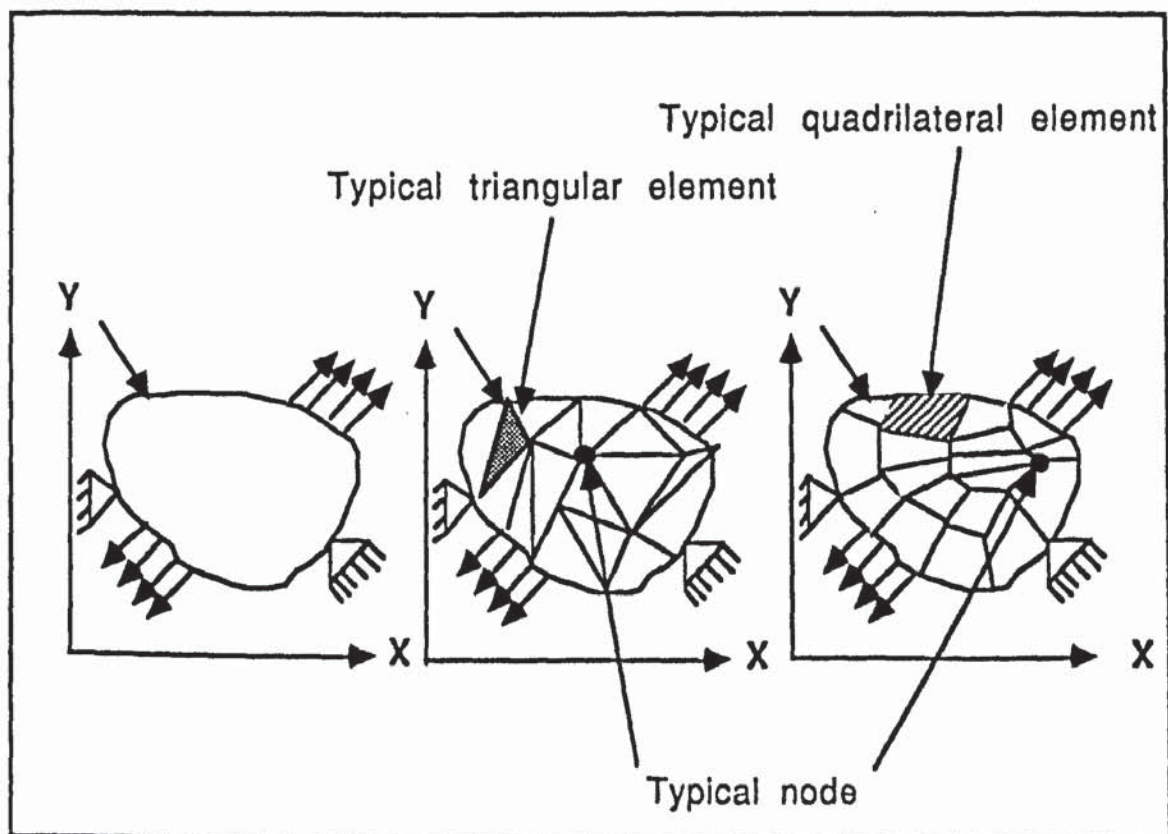


Figure 21 Idealisation of two dimensional structure

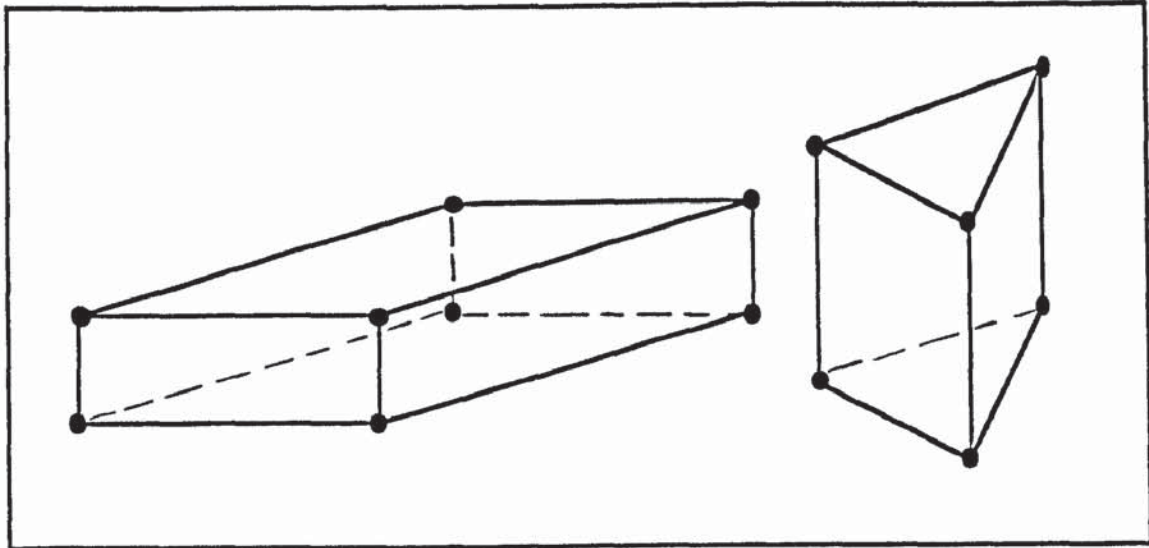


Figure 22 Three dimensional finite elements

2.11.2.2 DISPLACEMENT FUNCTION

In the finite element method the assumed element behaviour is governed by a displacement function. These functions are approximate and chosen to define the displacement field within the element in terms of nodal displacements. Polynomial series are the most widely used approximating functions in the finite element method and the degree of polynomial governs the ability of the element to approximate the true displacement field. The simplest form of the displacement of an element is a linear function, and higher order functions improve the accuracy in any particular problem (84). Usually the same form of function is used in all the discretised elements, but mixed element types are acceptable, in order to gain a more efficient approximation to the real structure. To ensure convergence to the correct result the choice of a suitable polynomial must meet the following requirements;

- i) The displacement function must be continuous within the element, and there must be compatibility between the adjacent elements. This means that the chosen approximating function does not imply openings or overlaps between elements.
- ii) Displacement pattern must be able to accommodate rigid body movements. This condition implies that all the points in the element should experience the same displacement.
- iii) The function must include the state of the constant strain. This is a necessary condition, because if the body were imagined to be divided into smaller and smaller elements, the strain state of each of the infinitesimal elements then approaches a constant.

2.11.2.3 FORMULATION OF THE STIFFNESS EQUATION

The strains at any point within the element may be expressed in terms of the element nodal displacements (Appendix 2). The strain distribution, and consequently the total potential energy of the discrete approximation to the continuum may be determined from ;

$$V = U + P = \sum_e (u_e + p_e)$$

Where u_e is the element strain energy and p_e is the potential energy of the loading on the element. The equilibrium condition $\delta v = 0$ leads to the stiffness equations;

$$[K] \{q\} = \{Q\}$$

Here $[K]$ is a stiffness matrix $\{q\}$ and $\{Q\}$ are vectors of generalised coordinates and generalised forces respectively.

2.11.2.4 SOLUTION OF THE STIFFNESS EQUATION

The solution of matrix equation $[K] \{q\} = \{Q\}$ is a standard procedure in matrix algebra. A number of equation solving routines, commonly based on Gaussian elimination or Cholesky decomposition process, are available. In order to obtain an acceptable representation of the continuum system, the number of unknowns resulting from the discretisation needs to be very large.

As a consequence, solution of these equations can only be contemplated with the aid of a high speed digital computer. The efficient solving routines take into account the symmetric, banded nature of the stiffness matrix in order to reduce the storage requirements demanded of the computer.

2.11.2.5 DETERMINING THE ELEMENT STRAINS AND STRESSES

The element strains are easily calculated from the displacement shape function using the normal strain-displacement relations once the nodal displacements have been determined. The stresses are then obtained by means of Hooke's law.

$$\{\sigma\} = [D] \{\epsilon\}$$

$\{\sigma\}$ -	Stress matrix
$[D]$ -	constant
$\{\epsilon\}$ -	strain matrix

Since the equilibrium conditions are satisfied only in some average overall manner and not point by point, the stress field is discontinuous from element to element, hence the accuracy of the stress at a particular node may be improved by taking the average of the individual element stresses at that node.

2.11.3 NON-LINEAR MATERIALS

When the following stiffness equation is written for system displacement, it is assumed that the stiffness matrix is constant during the application of loads.

$$[K] \{q\} = \{Q\}$$

This is the usual assumption of linearity and leads to straight forward evaluation of $\{q\}$ knowing $[K]$ and $\{Q\}$. However in many engineering problems the effect of non-linearity can not be neglected, and either the $[K]$ matrix or $\{Q\}$ vector or both of these are dependent upon the displacement vector $\{q\}$.

2.11.3.1 GEOMETRIC NON-LINEARITY OR LARGE DISPLACEMENTS

If a structure undergoes large displacements as a load is applied then the stiffness matrix may vary during the loading process. When the structure is subjected to a point load and the applied load is small, the structure absorbs the strain energy of deformation. However if the applied load becomes large enough to deform the structure significantly the structure needs to stretch for further deformation to take place. This means that the stiffness of the structure has increased. The relationship between load and deformation is shown in (figure 23).

From mathematical point of view a non-linearity is dealt with through an iterating technique provided that the effects of the stresses on the stiffness matrices are small. The load is divided into a series of sufficiently small increments and these are applied one at a time. After application of each load increment, the deflections caused by it are calculated using the stiffness equation $[K] \{q\} = \{Q\}$. The original co-ordinates of the nodes are then changed by the values of deflections that have been calculated. The stiffness matrix is calculated for the deformed structure and the process is repeated.

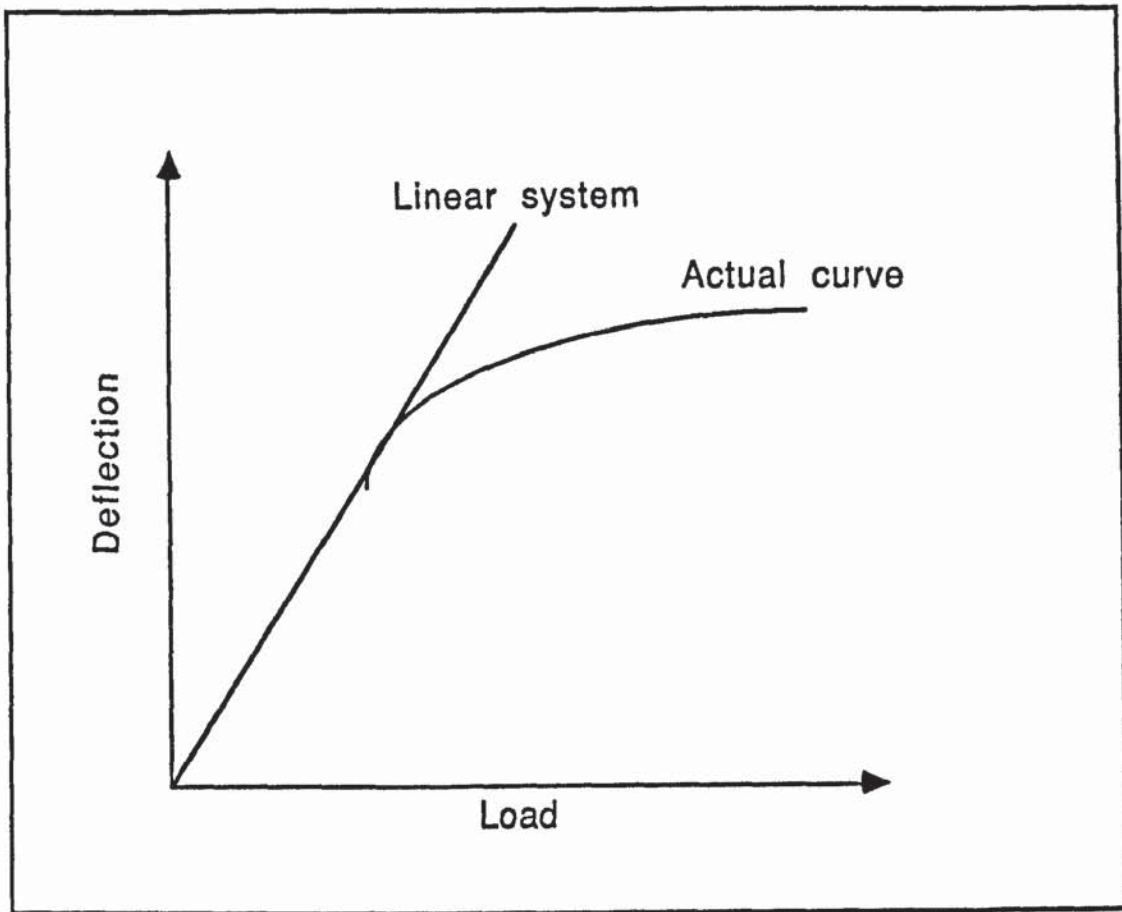


Figure 23 Load-Deflection relationships

2.11.3.2 ELASTIC-PLASTIC BEHAVIOUR

The solution of structural problems in which the strain displacement and stress-strain relationships are linear is relatively straight forward, solutions with non-linear elastic and elastic-plastic materials are more difficult, and these are obtained by using the linear solutions modified with an incremental and iterative approach.

2.11.3.3 YIELDING

The material is assumed to behave elastically before the yield according to Hooke's law. If the material is loaded beyond the yield point, additional plastic strains occur, which if the load is removed leaves a residual deformation. Often the uniaxial stress-strain curves (figure 24) will approximate to two straight lines of linear elasticity and linear strain hardening, so that the overall curve is defined by the elastic modulus, the yield stress and the plastic stress-strain gradient.

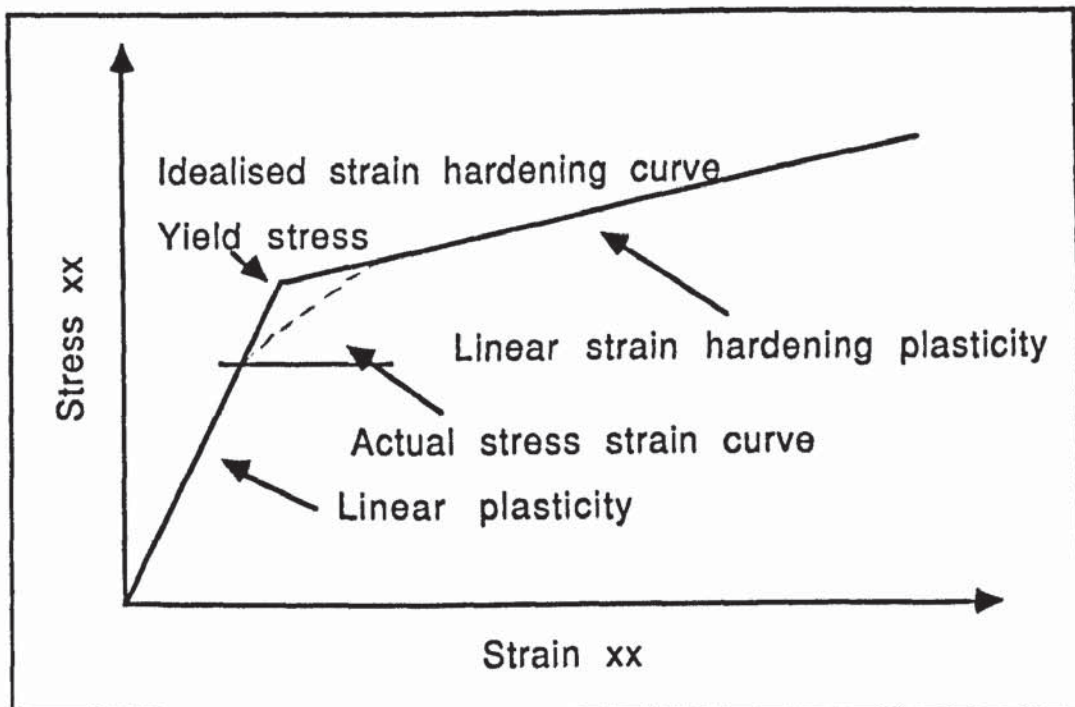


Figure 24 Stress- Strain relationship

In the iteration technique for solving plasticity problems the phenomenon of equivalent stress and equivalent strain is used, i.e stresses and strains are divided into elastic and plastic parts, and this is given by;

$$\sigma_{eq.} = \sigma_{el.} + \sigma_{pl.} \quad \text{and} \quad \epsilon_{eq.} = \epsilon_{el.} + \epsilon_{pl.}$$

When the equivalent stress becomes greater than the uniaxial yield stress, then yielding takes place, i.e. for yield condition ;

$$\sigma_{eq.} > \sigma_{yield}$$

This is the well established Von mises yield criterion. Plasticity routines are based on the incremental equations, it is normally necessary to apply the final load on the structure in load increments. These load steps are continued until the total load has been applied, or until the structure has experienced plastic collapse (For detailed method of calculation see appendix 3).

2.11.4 THE FINITE ELEMENT PACKAGE (PAFEC-FE)

PAFEC stands for automatic finite element calculations. The software has been designed so that the users may input data in a very straight forward manner. An interactive system which complements the PAFEC finite element is PIGS, which stands for PAFEC Interactive Graphic System, and it provides full display of output including mesh generation and verification with colour, shading, hidden line removal and a host of other features.

Data is input to PAFEC in a modular form, each module begins with a name, after this there will be headline giving the titles of columns which form the remainder of the module. This line is called the "control line". The end of a module is signalled by the next modules name. The complete set of modules presented at any time is terminated by the statement END . OF. DATA . which is placed after the last module.

The PAFEC finite element system, PAFEC-FE uses the finite element method to solve a wide range of engineering problems, such as the determination of stresses and displacements on various static structures. Input to PAFEC-FE comes in a form of a data file which contains a complete description of the geometry of the structure to be analysed, together with a description of the loads and restraints acting on the structure.

The PAFEC-FE data file can be created manually or using a graphics pre-processor. The PAFEC-FE system can produce graphics output files, from which plot of the structure, the displacement shape of the structure, and stress contours can be obtained.

2.12 THE OBJECTIVE OF THE RESEARCH

The main area of this work has been concerned with the durability studies of the steels used in the construction of the jackets of the offshore structures. Various studies have shown that the most critical part of the jacket which is prone to failure is the welded nodal joint, which is the area of complex stress concentrations and varying mechanical and metallurgical properties. In addition to this the severe North sea environmental conditions superimposes extra demands on the property requirements of the steels, particularly those nodal joints which are used within the vicinity of the splash zone. Taking the critical demands required in performance of the steels, the overall studies of the durability have been based on the concept of the worst case analysis, which consists of a combination of welds of varying inclusion content, various degrees of stress concentration, and the environmental conditions of stress corrosion and hydrogen embrittlement.

The experiments have been designed to reveal the significance of defects as sites of crack initiation in the welded steels and the extent to which stress corrosion and hydrogen embrittlement will limit their durability. This has been done for different heat treatments. In some experiments deformation has been forced through the welded zone of the specimens to reveal the mechanical properties of the welds themselves to provide data for finite element simulations. A comparison of the results of these simulations with the actual deformation and fracture behaviour has been done to reveal the extent to which both mechanical and metallurgical factors control behaviour of the steels in the hostile environments of high stress corrosion and hydrogen evolution at their surface.

CHAPTER 3

EXPERIMENTAL PROCEDURES

3. EXPERIMENTAL PROCEDURES

3.1 MATERIAL

The material used was commercial steel received in the form of 6 mm thick plate, in accordance with BS 4360 grade 50E. This is the quality of steel widely used for the fabrication of the nodal joints in construction of the jackets. The mechanical properties and compositional analysis of these are shown in tables 3 and 4.

3.2 EXPERIMENTAL MATRIX

The experimental matrix of the project included the following specimens made from;

- 1) As received metal machined with parallel length along the rolling direction figure 25.
- 2) As received metal machined with the parallel length perpendicular to the rolling direction figure 25.
- 3) Heat treated normalised i.e steel which is heated to 900 °C and then cooled in air figure 27.
- 4) Austenitised, quenched in water, and then tempered figure 29.
- 5) Austenitised, quenched in oil, and then tempered figure 28.
- 6) Sound weld from 3-5 of the above.
- 7) Defective weld from each of 3-5, on which the defects are invisible to the naked eye and would escape detection by the normal NDE methods.

- 8) Environmental testing of each of 3-7 under stress corrosion conditions.
- 9) Environmental testing of each of 3-7 under hydrogen evolution conditions.
- 10) Sound and defective welds containing a notch in the weld.

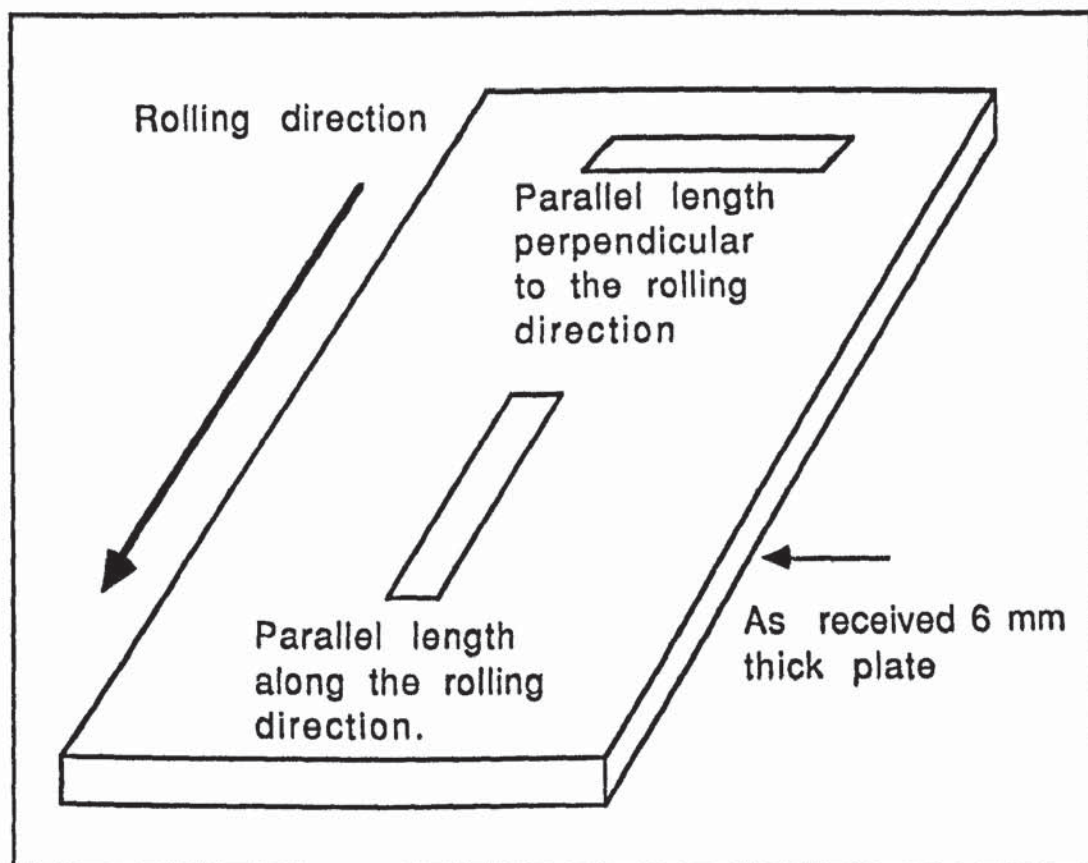


Figure 25 As received plate

Although these 10 factors were included in the experimental design, a full experimental matrix were restricted to the following;

a)	Heat treatment	Level 1 Level 2 Level 3	Normalised Quench in oil and tempered Quench in water and tempered
b)	Welding	Level 1 Level 2 Level 3	No weld Sound weld Defective weld
c)	Environment	Level 1 Level 2 Level 3	Air test Corrosion H ₂ evolution

The pattern of the full part of the experimental matrix is as follows.

<u>Heat treatment</u>	<u>Welding</u>	<u>Environment</u>
1	1	1
1	1	2
1	1	3
1	2	1
1	2	2
1	2	3
1	3	1
1	3	2
1	3	3
2	1	1
2	1	2
2	1	3
2	2	1
2	2	2
2	2	3
2	3	1
2	3	2
2	3	3
3	1	1
3	1	2
3	1	3
3	2	1
3	2	2
3	2	3
3	3	1
3	3	2
3	3	3

This involves 27 separate tests. Each specimen was cut from a longitudinal direction and no notches were machined into the gauge length. In addition other factors were examined i.e directionality and the effect of machined notches.

The directionality tests were restricted to the X-Y plane of the sheet and were only performed on plain specimens tested in air. The tests where the specimen contained machined notches were restricted to specimens containing welds, as the objective was to learn more about the mechanical properties of the weld material as opposed to the parent plate. There were 3 tests involving the directionality factor; and 12 extra tests involving notches as only normalised and oil quenching and tempering heat treatments

were involved. Thus the total number of specimens involved in the experimental design was 42.

3.3 MECHANICAL TESTING

The purpose of mechanical testing is to establish the basic properties of the steel in the control condition and then to measure the changes in strength ductility and toughness after the formation of welds and exposure to corrosive or hydrogen evolution conditions. Tensile testing of plain and composite test pieces in different environments is clearly one major way to evaluate these changes.

Tensile tests however do not provide an adequate measure of toughness and for plain specimen the Guidance notes ⁽⁸⁾ recommend Charpy V notch impact tests. However this research is concerned with the degradation of properties in the steel tubular nodal joints where the material is affected by the welding of the brace to the chord sections. Unfortunately there is no satisfactory method of conducting Charpy V notch tests on composite impact specimens as the position of the tip of the notch in relation to the macrostructure of the weld is of crucial importance in affecting the results. Secondly impact tests are high strain rate tests and the process of degradation is a slow one and this provides another important reason for the unsuitability of Charpy testing.

Another alternative method for evaluating toughness is by conducting K_{Ic} tests involving pre-fatigue cracked samples. The difficulty here is that to study the mechanical characteristics of the weld the fatigue crack would need to be introduced in a form that would give rise to valid test results i.e. of a controlled length, straight, and a controlled radius at its root. Again there is no satisfactory way of ensuring these rigorous conditions when introducing a fatigue crack into the weld structure. For all these reasons it was therefore decided to restrict the research to tensile tests for then finite element analysis can be used to interpret the macroscopic deformation of the composite test pieces.

3.4 TESTING MACHINE

The main criteria for the testing machine was a suitable loading capacity and the ability to operate at slow strain rates suitable for stress corrosion tests. These conditions were met by a Mand tensile testing machine of 10 tonnes capacity with cross-head speeds in the range of 10^{-5} mm s⁻¹ to 1 mm s⁻¹, and this machine was used for all the tests in this research.

3.5 METALLOGRAPHY AND FRACTOGRAPHY

3.5.1 GENERAL METALLOGRAPHICAL PREPARATION

All specimens for optical microscopy were mounted in conducting bakelite and ground and polished using automatic polishing equipment (LECOVAR POL. VP 50). Wet grinding was to 600 grit, followed by ultrasonic cleaning in Inhibisol. Final polishing was done using 6 µm and 1 µm diamond cloths. Etchants used were 2% and 4% Nital.

3.5.2 SCANNING ELECTRON MICROSCOPY (SEM)

A Cambridge Instruments Microscan 150 fitted with a Link System 860 energy dispersive analysis (EDA) unit was used for electron microscopy and microanalysis. Fracture surfaces of the specimens prior to examination were given a sputtered Carbon coat to prevent non-conducting particles eg. inclusions from charging up during examination. Because of the limited availability of the SEM facilities and time involved in observing an individual specimen only few selected specimens of containing sound and defective welds were examined by this technique.

3.6 HEAT TREATMENT

Plates used in the construction of the offshore structures are usually heat treated in either one of two ways;

- I) Normalised
- II) Quenched and tempered.

In normalising, plates are heated to a temperature of around 920 °C for an appropriate length of time depending on the materials thickness and dimensions, and then allowed to cool down in air.

In quenching, metal is heated to above its austenitisation temperature whilst cooling is done through a quenching media. In addition to the above, usually a post weld heat treatment is required in the welded nodal regions, to bring about a beneficial reduction in the level of residual stresses, and improvement in defect tolerance. Where a post weld heat treatment (PWHT) is specified the general temperature limitations vary. The usual temperature range is in the order of 580-620 °C, and the quenching period one hour per every 25 mm of section thickness.

The heat treatments carried out are given in table 5, subsequent metallographic examination revealed four distinct groups of microstructure and these were chosen for inclusion in the experimental matrix.

<u>Material</u>	<u>Temperature</u>	<u>Cooling time</u>	<u>Quenching media</u>
As-received	920 °C	1/2 hour	Air
As-received	920 °C	1/2 hour	Oil
As-received	920 °C	1/2 hour	Water

Table 5 Heat treatment chart

- 1) As received steel figure 26.
- 2) Normalised figure 27.
- 3) Quenched in oil and then tempered figure 28.
- 4) Quenched in water and then tempered figure 29.

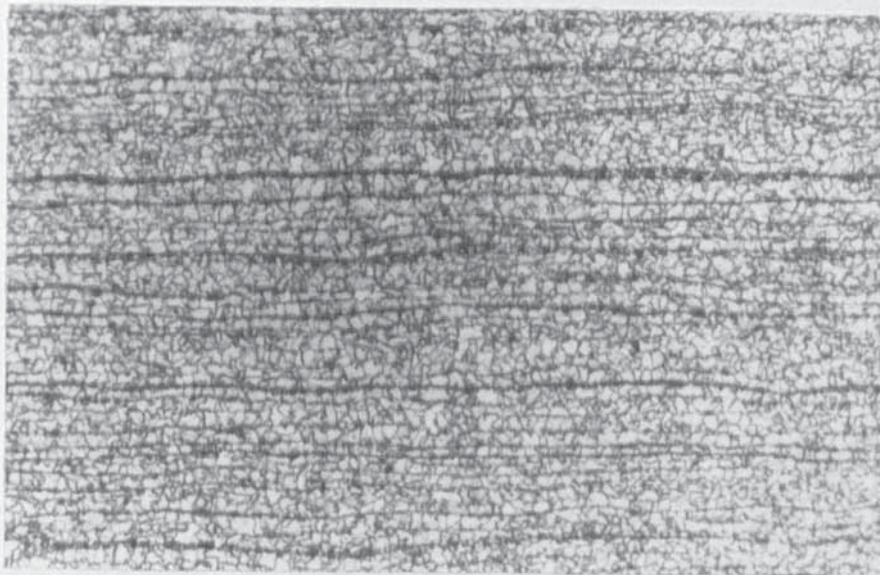


Figure 26 Metallographic microstructure of as-received steel magnification X100.

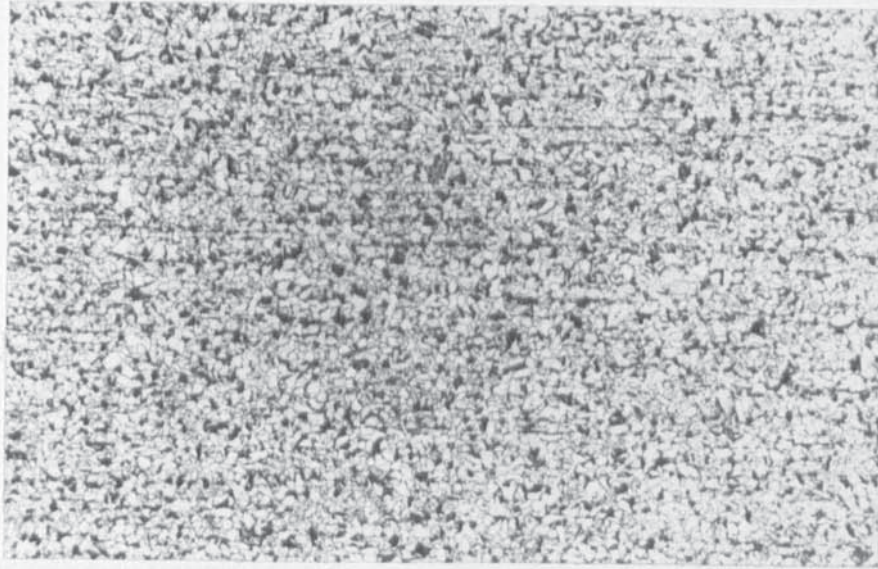


Figure 27 Metallographic microstructure of normalised steel magnification X100.

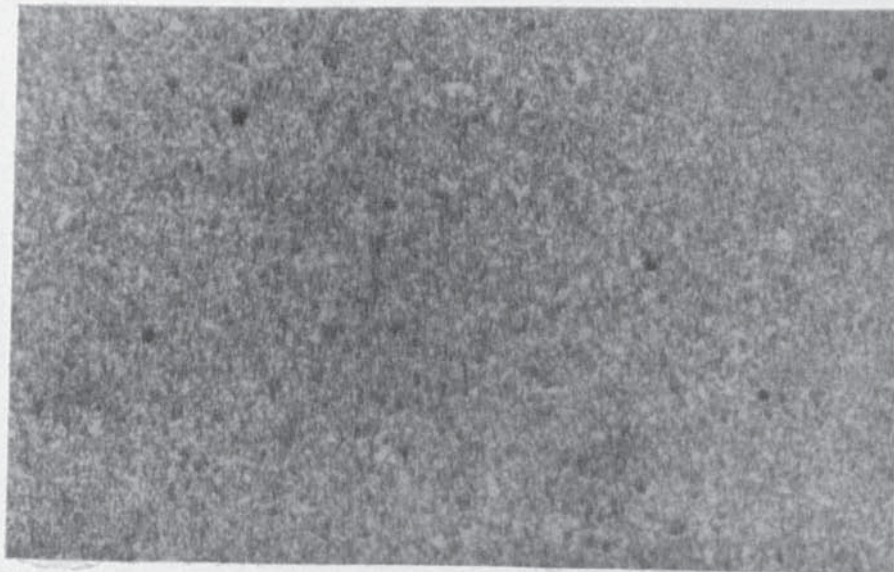


Figure 28 Metallographic microstructure of oil quenched and tempered steel magnification X100.

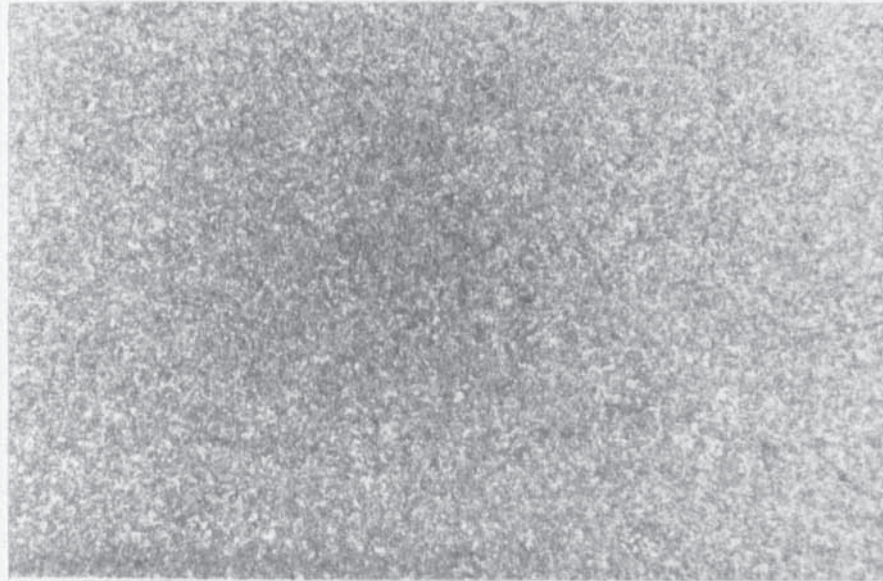


Figure 29 Metallographic microstructure of water quenched and tempered steel magnification X100.

3.7 FORMATION OF THE WELDED JOINT

Plates were cut into strips of ~ 75 X 400 mm and after the appropriate heat treatment process they were machined along one edge in preparation for butt welding (figure 30). They were then thoroughly cleaned from any contamination around the welding position, and heated in an oven to ~ 250 °C for almost 20 minutes. This is to guard against any distortion from sudden heating of the plates during welding. Finally they were welded along the 400 mm length of the plates and the weld metal was deposited in the profile (figure 30). The welding rate was chosen to ensure consistency in the weld quality for every specimen.

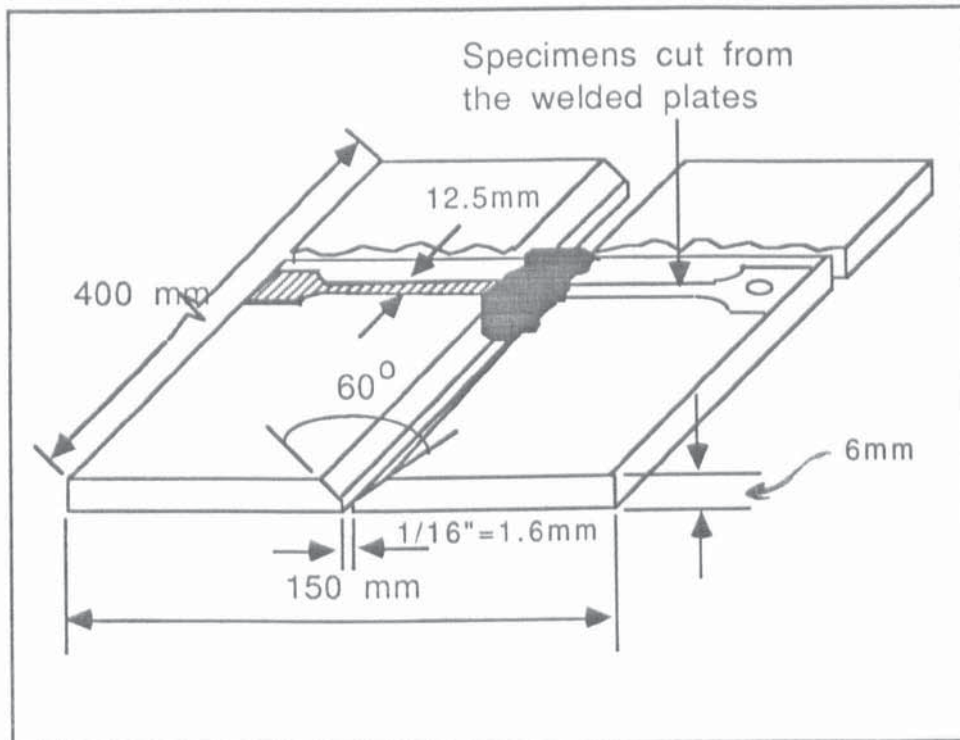


Figure 30 Preparation of the welded specimens

To simulate welds which are found in tubular joints, three different categories of weld were produced.

- 1) Sound welds.
- 2) Defective welds containing gross defects and
- 3) Defective welds, in which a deliberate change has been made to the welding conditions required for a sound weld and at the same time avoiding gross defects.

Some examples are shown in figures 32-37. The principal discontinuities found in welded joints are:

<u>Type of defects</u>	<u>Category</u>
Inadequate root penetration	2,3
Incomplete fusion	2
Undercut	3
Inclusion	3
Porosity	2 or 3
Cracking	2 or 3

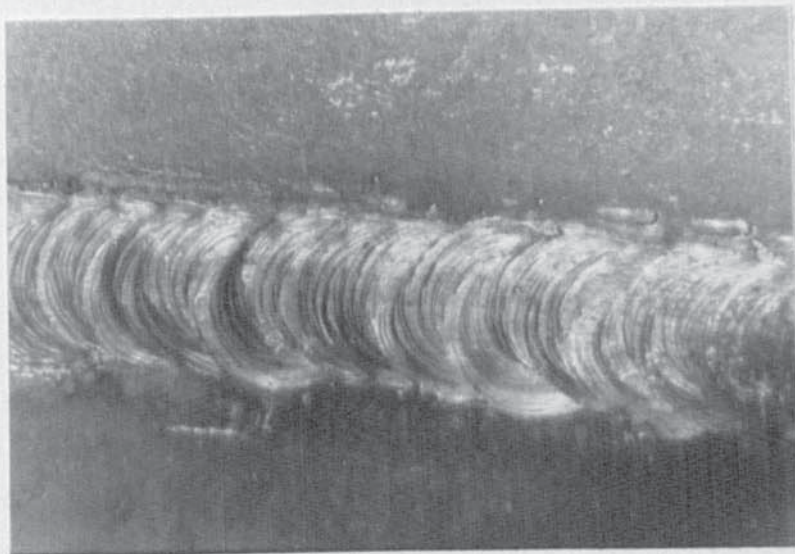


Figure 31 Sound weld with good manipulation pattern.

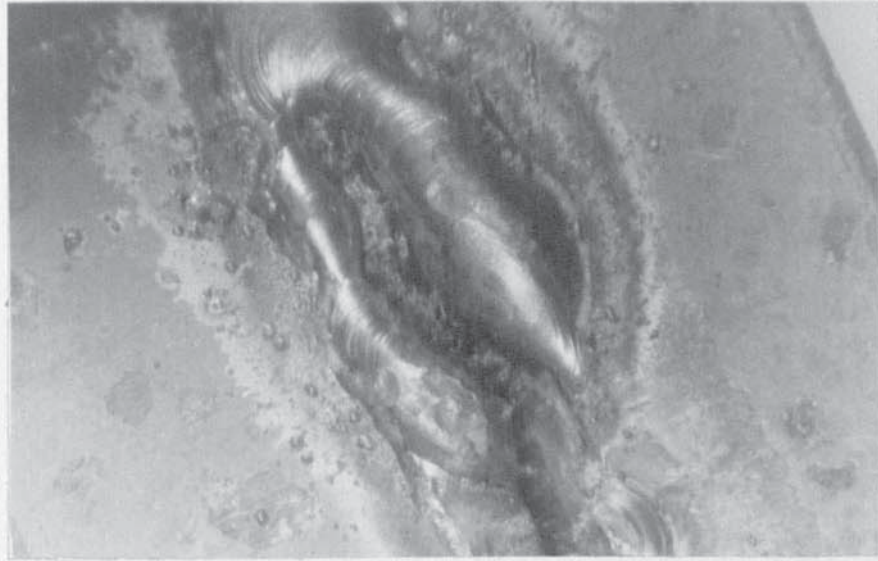


Figure 32 Category (2), gross defect lack of side wall fusion.

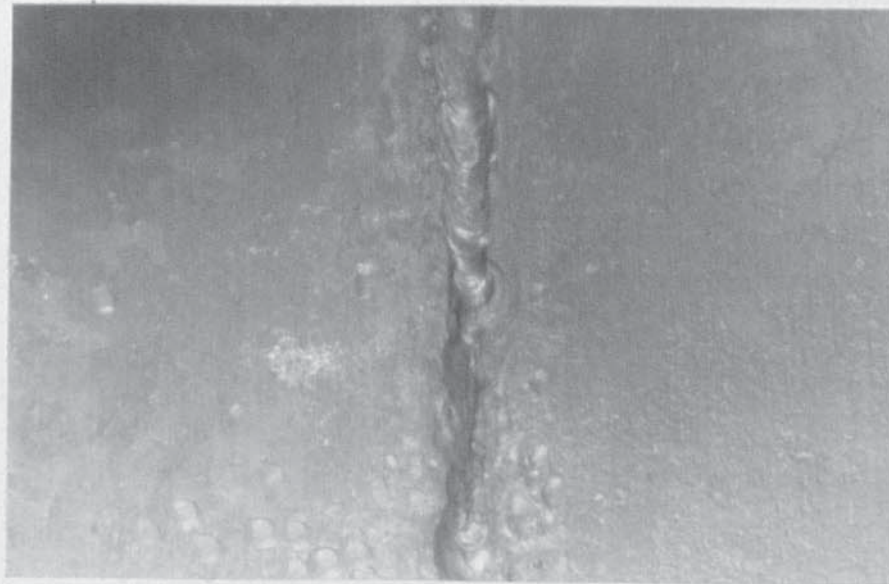


Figure 33 Category (2), gross defect incomplete root fusion

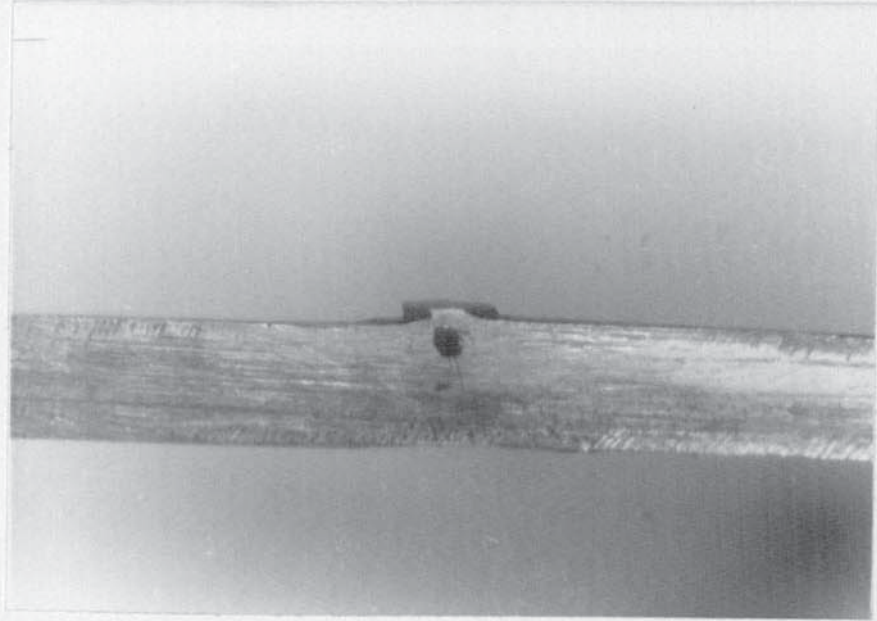


Figure 34 Category (2), gross defect macro porosity.

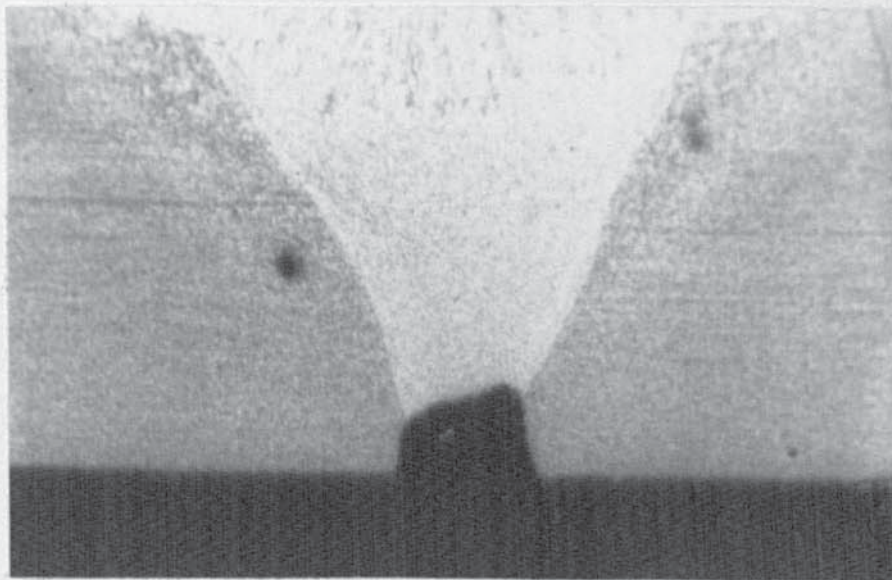


Figure 35 Category (2) or (3), lack of root penetration.

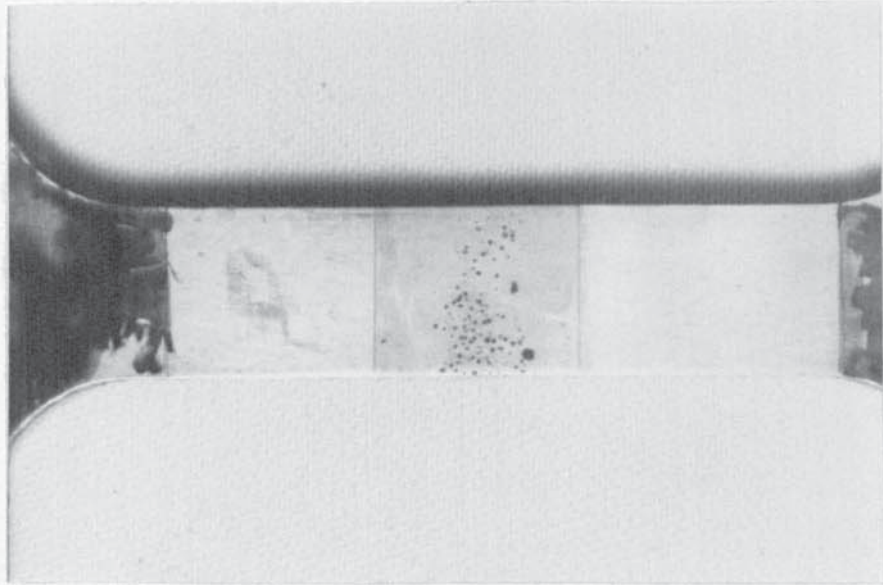


Figure 36 Category (2) or (3), micro porosity.

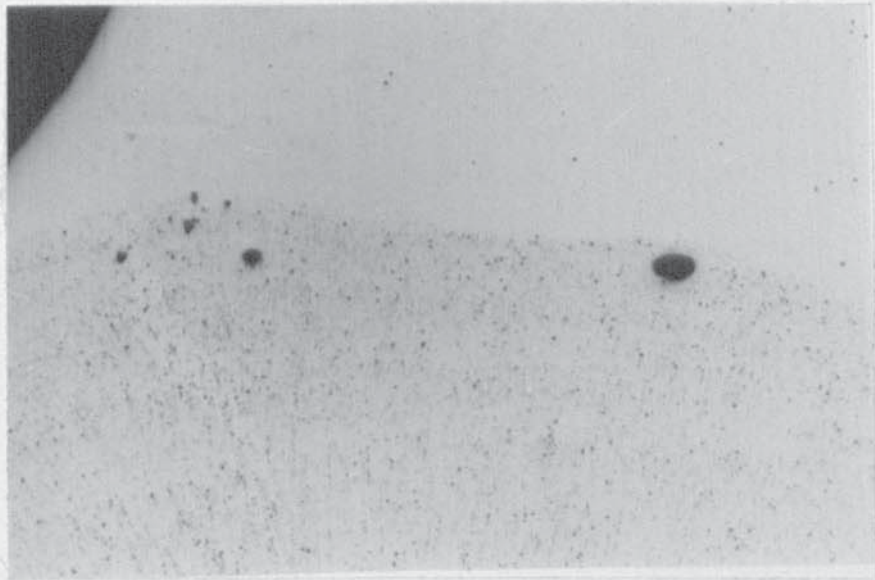


Figure 37 Category (3), addition of excessive non-metallic inclusions magnification X80.

Only category 3 defects are acceptable for stress corrosion and hydrogen embrittlement tests, because of the need to simulate credible worst case conditions that could occur in practice. The following is a list of the welding variables that were controlled in order to produce the sound and deliberately defective weldments.

- 1) Welding process
- 2) Plate geometry
- 3) Electrode type
- 4) Electrode size
- 5) Electrode current
- 6) Arc length
- 7) Travel speed of manual arc
- 8) Electrode angle i.e slope and tilt
- 9) Manipulation pattern
- 10) Additives to the weld pool and finally
- 11) Extent of interpass cleaning.

In order to produce the welds required for experimental use, three welding processes were employed:

- i) Manual metal arc and
- ii) Metal inert gas
- iii) Metal active gas

3.7.1 SOUND WELDS

For a weld to be sound it should be free from any of the defects already mentioned . The joints must possess qualities which are necessary to enable it to perform its expected function in service. For this the welded joint needs to have the required physical, mechanical and metallurgical properties . Tables 6 and 7 give a list of the welding variables that had to be controlled so that a sound weld could be obtained.

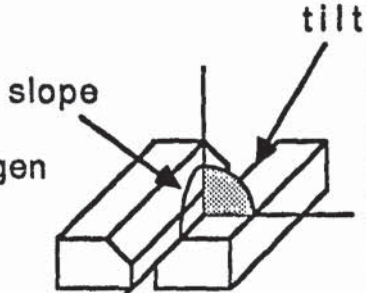
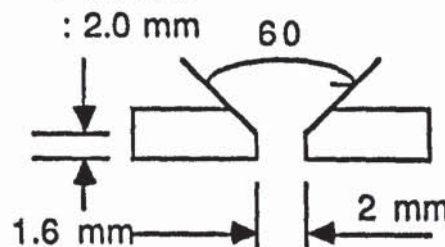
Electrode type:-	Basic low hydrogen	
Electrode angle:-	slope 60-70 tilt 90	
Electrode size:-	First run i.e root run 2.5 mm second run i.e capping run 4.0 mm	
Power:-	Direct current	
Electrode current:-	70-80 Amps for root run 150-165 Amps for capping run	
Baking electrode:-	480 °C for one hour prior to welding (to reduce hydrogen)	
Plate geometry:-	Included angle : 60 Root face : 1.6 mm Root gap : 2.0 mm	
Operational care:-	Pre heating of plates to reduce transitional distortion, Inter pass cleaning to reduce the risk of oxide and slag inclusions formation.	

Table 6 Controlled variables in formation of a sound weld by manual metal arc technique.

Electrode type :-	Filler wire, mild steel, copper coated		
Electrode angle :-	Slope : 60-70 Tilt : 90		
Electrode size :-	0.8 mm		root run
	1.2 mm		capping run
Wire feed :-	220-240	in/min.	root run
	300	in/min.	capping run
Power :-	Direct current		
Electrode current :-	140-150	Amps	root run
	230-240	Amps	capping run
Voltage:-	24-25	Volts	root run
	26-27	Volts	capping run
Gas flow :-	13-15	litre/min.	root run
	26-27	litre/min.	capping run
Shielding gas:-	CO ₂		root run
	Argon		capping run
Operation :-	First run carried out by dip transfer metal inert gas (MIG). Second run was done by spray transfer metal active gas (MAG).		

Table 7 Formation of a sound weld by metal inert gas technique

3.7.2 DEFECTIVE WELDS CONTAINING GROSS DEFECTS

The experimental design provides for 30 specimens that have to be fabricated by welding in a controlled manner so that there is a distinct difference between sound and 'defective' welds. The 'defective' weld must appear to be superficially sound as otherwise it would be rejected in any basic screening process (we shall call this a category 3 weld). Many experiments were conducted to produce welds of this nature.

For example as seen in figure 32 to 36 category 2 welds that contain defects due to lack of side wall fusion, of incomplete root fusion, gross macro-porosity, or lack of root penetration were not suitable for this process. To produce a satisfactory category 3 weld fine control over the welding variables such as welding process, electrode voltage and current, and manipulation pattern is needed. In addition it was necessary to introduce FeS directly into the weld pool in order to allow a slight increase in the sulphur content of the fusion and heat affected zones.

The first decision was what type of welding process to use. Tests were done using manual metal arc, MIG, and MAG welding methods. Manual metal arc methods (see table 6 for conditions) were rejected because of lack of reproducibility. Further tests showed that a combination of MIG and MAG methods were more likely to produce this desired level of reproducibility.

The MIG technique was used for first pass and the MAG technique for a second pass, all welds were two pass welds. This technique was necessary to take advantage of the higher rate of metal deposition from the MAG technique, otherwise more passes would have been needed thus giving more opportunity for variations in weld quality.

Table 7 gives the electrode voltages and currents used for the root and capping runs. Initially the voltage and currents were set as low as possible in the belief that it would produce a defective weld through lack of fusion. The effects of this measure were so gross that it resulted in defects that were easily visible to the naked eye and thus did not fit the experimental design. Further experiments were done in raising the voltage and current above the norms but considerable burning of the weld took place and again the defects produced were too severe.

Once the weld voltage and current conditions are fixed then there is little choice over the wire feed and gas flow speeds, but there are many possible manipulation patterns i.e linear, zig-zag and spiral. Experiments showed that the spiral patterns gave better penetration and more reproducible welding conditions and these were ultimately chosen.

All the variations in welding conditions that relate to table 7 were not sufficient to produce reliable category 3 defective welds, because each time a departure from standard welding procedure took place the end result was a gross category 2 defect.

Consequently the standard welding practice described in table 7 had to be adhered to, but to produce the category 3 defective weld it was found by trial and error that the addition of a small amount of FeS to the weld -pool produced the desired effect of a weld that apparently appeared sound but whose mechanical properties would be inferior to those of sound welds. An example of such a category 3 defective weld is given in figures 35 and 36 where the defects are either small sulphide particles 0.4 μm in diameter (see scanning electron microscope photographs figure 55) or pores no greater than 0.06 mm in diameter.

Tables 8-20 are typical gross defects that can be produced due to any variations in the standard welding conditions. In order to produce the desired defective welds each of these conditions had to be checked, to make sure that the "defective welds" did not contain readily observable faults.

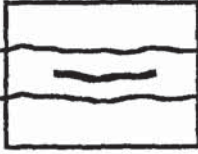
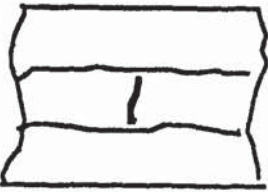
Weld Defect Class Cracks	Probable cause	Corrective action
 <p data-bbox="405 779 576 846">Longitudinal crack</p>	<p data-bbox="756 517 863 546"><u>General</u></p> <ol data-bbox="655 566 979 913" style="list-style-type: none"> 1. Incorrect electrode 2. High resistant of joint 3. Rapid cooling of weld 4. Improper joint preparation 	<ol data-bbox="1034 566 1369 913" style="list-style-type: none"> 1. Use proper electrode 2. Reduce rigidity of weldment ,use higher ductility welding filler metal. 3. Use pre-heat and/or inter pass heat to reduce cooling rate. 4. Use proper joint for welding process.
 <p data-bbox="376 1070 549 1099">Crater crack</p>	<p data-bbox="743 938 916 967"><u>Crater crack</u></p> <ol data-bbox="663 1003 911 1032" style="list-style-type: none"> 1. Unfilled crater 	<ol data-bbox="1034 1003 1385 1070" style="list-style-type: none"> 1. Fill crater with proper techniques
 <p data-bbox="344 1384 580 1413">Transverse crack</p>	<p data-bbox="708 1140 948 1169"><u>Transverse crack</u></p> <ol data-bbox="663 1193 995 1406" style="list-style-type: none"> 1. Incorrect electrode 2. Rapid colling 3. Welds too small for size of parts joined 	<ol data-bbox="1034 1193 1401 1406" style="list-style-type: none"> 1. Use proper electrode 2. Use larger electrode, higher welding currents or pre heat 3. Use larger weld possibly larger electrode

Table 8 Weld defects , cracks

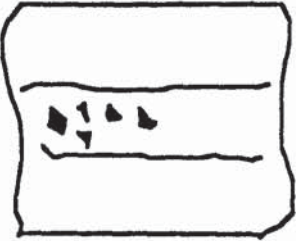
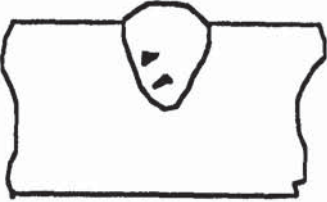
Weld Defects Class Cavities	Probable cause	Corrective action
	<p><u>General</u></p> <ol style="list-style-type: none"> 1. Welding over foreign material on surface such as, oil, moisture paint, etc. 2. Damp electrode 3. High sulphur level 4. Welding current too low 	<ol style="list-style-type: none"> 1. Clean bevels and area adjacent to the weld and keep clean 2. Use fresh dry electrodes that have not been exposed to dampness. 3. Use low hydrogen electrode type. 4. Increase welding current.
	<p><u>Gas shielded process</u></p> <ol style="list-style-type: none"> 1. Incorrect gas type 2. Incomplete gas coverage due to breeze, defective gas system, clogged nozzle etc. 3. Moisture in the shielding system. 4. poor gas coverage. 	<ol style="list-style-type: none"> 1. Use specified gas 2. Provide wind shield gas. Check efficiency of gas system such as broken pipes, gas valves, clean nozzle. 3. Check and make sure gas is dry. 4. Use proper nozzle, gas flow rate.

Table 9 Weld defects : Cavities

Weld defect class: Solid inclusions.	Probable cause	Corrective action
 	<ol style="list-style-type: none"> 1. Slag inclusion between passes. 2. Irregular surface of bevels. 3. Incorrect welding techniques, wrong current, voltage. 	<ol style="list-style-type: none"> 1. Remove solidified slag after each pass. 2. Provide smooth bevels. 3. Utilize correct welding techniques , current, voltage, design, electrode.

Table 10 Weld defects : Solid inclusions.

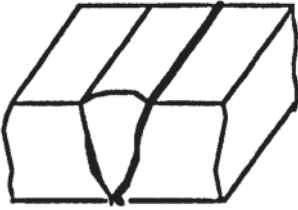
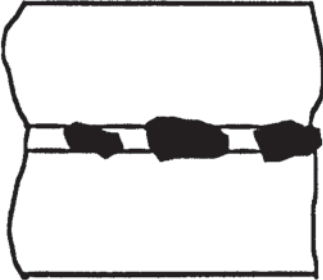
Weld defect class: Incomplete fusion	Probable cause	Corrective action
   	<p style="text-align: center;"><u>General</u></p> <ol style="list-style-type: none"> 1. Welding speed too fast 2. Electrode too large for joint detail. 3. Welding current too low. 4. Improper joint design such as excessive root face or minimum root opening. 5. Improper joint fit up such as root opening too small. 6. Irregular travel speed 7. Irregular arc length 	<ol style="list-style-type: none"> 1. Reduce welding speed 2. Utilize correct electrode size. 3. Increase welding current for more penetration. 4. Utilize correct joint detail. 5. Make correct set up. 6. High speed will reduce complete fusion, lower speed will cause complete fusion 7. Maintain proper arc length..

Table 11 Weld defects : Incomplete fusion.

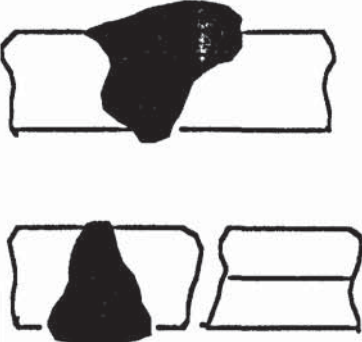
Weld defect class: Imperfect shape	Probable cause	Corrective action
	<p><u>Undercutting</u></p> <ol style="list-style-type: none"> 1. Faulty electrode manipulation. 2. Welding current too high. 3. Incorrect electrode size (usually too large). 4. Incorrect electrode for welding position. 5. Incorrect electrode angle. 	<ol style="list-style-type: none"> 1. Use uniform weave in groove welding pause at edge. 2. Use proper current for electrode size. 3. Use correct electrode size for size weld being made. 4. Use correct electrode with position capabilities . 5. Adjust electrode angle to fill undercut area.
	<p><u>Incorrect profile</u></p> <ol style="list-style-type: none"> 1. Excessive root penetration. 2. Travel speed too slow. 3. Incorrect electrode type 	<ol style="list-style-type: none"> 1. Root opening too wide 2. Welding current too high. 3. Use proper electrode type.

Table 12 Weld defects : Incorrect shape

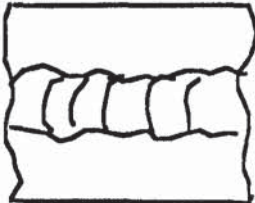
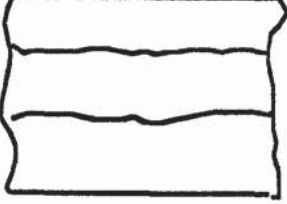
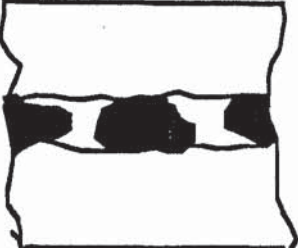
Weld defect class : Miscellaneous defects	Probable cause	Corrective action
	<p><u>Poor appearance</u></p> <ol style="list-style-type: none"> 1. Current too high or low. 2. Improper technique 3. Faulty electrode 4. Irregular travel speed 	<ol style="list-style-type: none"> 1. Use prescribed procedure. 2. Better skill required. 3. Fresh and correct type of electrode to be used. 4. Additional skill and practice is needed.
	<p><u>Excessive weld spatter</u></p> <ol style="list-style-type: none"> 1. Arc bloe. 2. Excessive welding current type and size of electrode. 3. Excessive long arc length high voltage. 4. Improper electrode type. 	<ol style="list-style-type: none"> 1. Use AC. 2. Adjust current. 3. Hold proper arc length and use correct arc voltage. 4. Utilize proper electrode type.
	<p><u>Poor tie-in</u></p> <ol style="list-style-type: none"> 1. Incorrect electrode angle. 2. Improper technique for restriking arc. 	<ol style="list-style-type: none"> 1. Use correct electrode angle. 2. Better skill.

Table 13 Weld defects: Miscellaneous.

Electrode type	
<u>Manual metal arc</u>	
1. Cellulosic	Good penetration characteristics but due to its weakness in resistance to cracking undercutting occurred, also crack along side of welds.
2. Rutile	Good ease of operation and arc striking ,but lack of penetration and loss of ductility in the joint was observed.
3. Iron oxide	High deposition rates are possible but joint was prone to cracking and loss of ductility.
4. Heavy coating	This is used for one pass operations, but excessive undercut and slag inclusions at the base of joints were observed
5. Basic coated low hydrogen	Good general welding characteristics were observed.
<u>Metal Inert Gas</u>	
1. Filler wire , mild steel copper coated.	Low hydrogen

Table 14 Electrode type

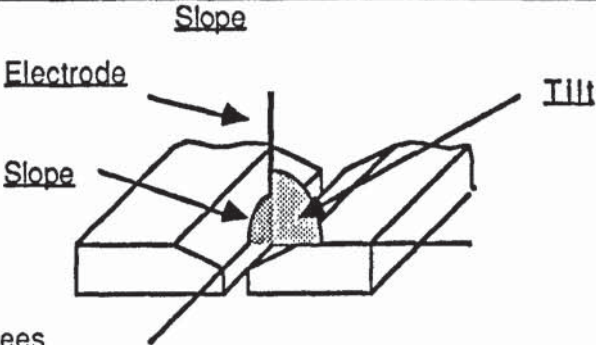
Electrode angle	Observation	
		
<u>Angle in degrees</u>		
40	Defects such as porosity	
50	" " "	
60	Good weld	
70		" "
80	Excessive penetration along sides and root collapse.	
90		
<u>Tilt</u>		
90	Sound weld obtained	
80	Unequal side fusion and irregular penetration.	
70		
60		" " " " "

Table 15 Electrode angle.

Plate geometry	Observation
<u>Angle in degrees</u>	
90	Excessive transitional
80	and longitudinal distortion
70	" " " "
60	Optimum angle for a sound weld
50	Lack of root penetration
40	and side wall fusion, micro cracking
<u>Root gap</u>	
<u>Distance in mm</u>	
0	Incorrect penetration
1	" " "
2	Optimum distance for a sound weld
3	Excessive penetration
4	" " "
5	" " "
<u>Root face</u>	
0	Excessive penetration
1	" " " "
2	Optimum distance for a sound weld
3	Lack of fusion
4	" "

Table 16 Plate geometry

Electrode current		Observation
<u>Using a 2.5 mm electrode</u>		
<u>Amps.</u>		
40		Lack of penetration and fusion
50		" " "
60		" " "
70	↕	Optimum for a sound weld
80		Excessive penetration and spatter
90		" " "
100		
<u>Using a 4.0 mm electrode</u>		
<u>Amps</u>		
120		Difficulty in striking an arc, lack of fusion to parent plate.
130		
140	↕	Optimum for a sound weld
150	Uncontrollable arc	Excessive penetration collapse of the under side of the joint.
160		

Table 17 Variation in current and electrode size

Power supply	Observation
AC	Heat input not controllable, Irregular welding
DC	Controllable heat input

Table 18 Variation in power supply for manual metal arc welding

Gas flow	Observation
<u>Liter/min.</u>	
10	Inadequate gas shield, scattered porosity
11	" " "
12	" " "
13	 Optimum for a good weld
14	
15	
16	Defects such as porosity
17	" "
18	

Table 19 Effects of variation of gas flow in MIG welding

Miscellenaeous variables	Observation
<u>Electrode extension on dip transfer</u>	
Long	Over heating of wire excessive spatter.
Short	Incorrect pre heating of filler wire, cold lapping,poor side wall penetration
<u>Wire size in dip transfer</u>	
0.8 mm	Good welding
1.2 mm	Excessive penetration and uncontrollable weld pool
<u>Voltage</u>	
High	Irratic arc with excessive penetration and uncontrollable weld pool
Low	Freezing of filler wire

Table 20 Miscellaneous variables

3.7.3 DEFECTIVE WELDS AVOIDING GROSS DEFECTS

A welding defect that would escape detection under commercial conditions is one in which the imperfection could only be resolved by microscopical examination. In large scale welding operations it is possible that contaminations by oil, grease or dirt prior to the welding operation might result in increasing the impurity level of the fusion zone and thereby have an effect on the adjacent zones through processes such as diffusion.

This type of possible defect has been simulated by artificially increasing the level of sulphide inclusions in the welded region. Due to the geometry of the plate, so that the category (2) defects be prevented from occurring, welding had to be done in two runs. Approximately two grams of FeS was smeared over the first run causing an increased volume fraction of sulphide inclusions in the steel, as shown in figure 38 and 39 due the slight increase in the volatility of the reactions occurring, during sulphidisation, other defects such as cavities and pores were also created (figure 38).

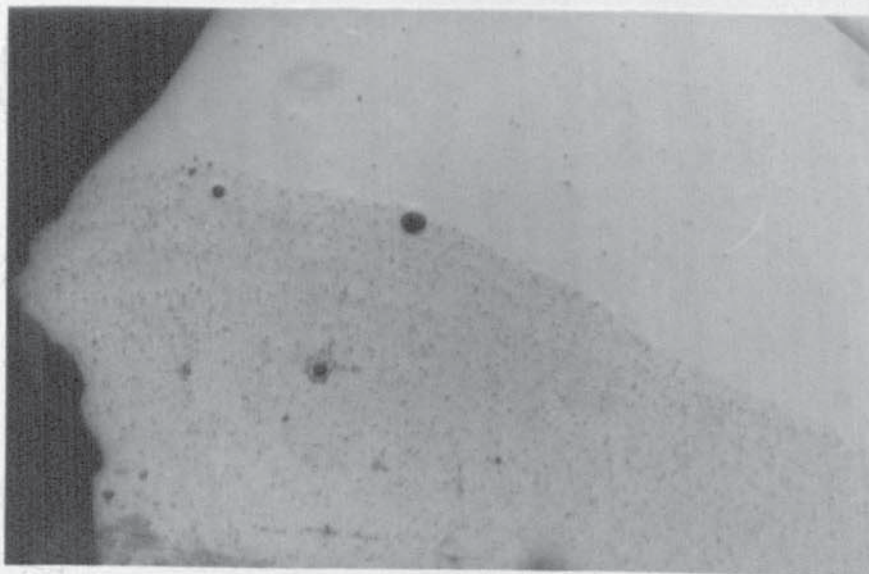


Figure 38 Increase in volume fraction of the sulphide particles magnification X40.

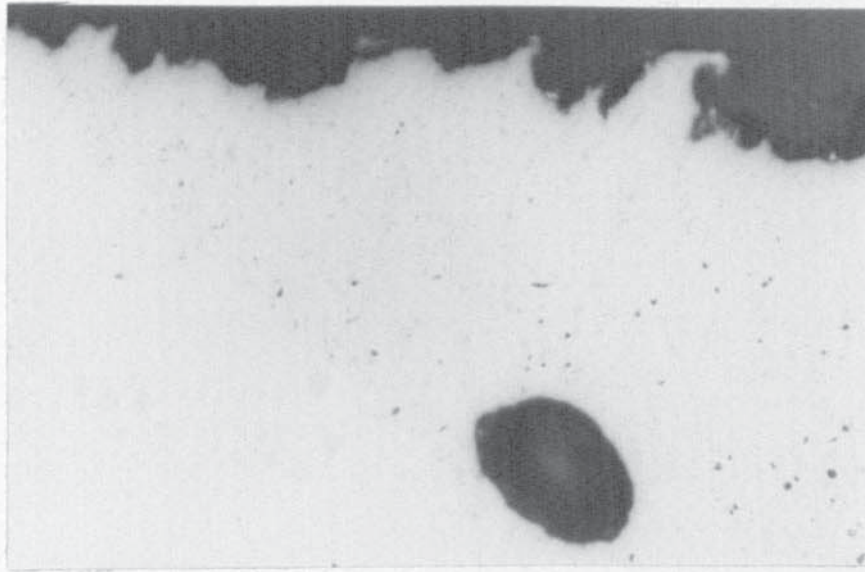


Figure 39 Increase in the volume fraction of the sulphide particles magnification X 160.

3.8 SPECIMENS

3.8.1 WELDED SPECIMENS

Approximately 20 mm from the both ends of the welded plates were discarded, this was mainly because of the inconsistency arising in the weld quality during start and stop of the weld runs. The remaining plate was cut into strips of ~36 mm width with the welds positioned in the centre of the plates (figure 30).

3.8.2 AS-RECEIVED SPECIMENS

The as-received specimens were cut with the rolling direction parallel and perpendicular to the parallel length of the specimens. The design calculations for the size of the specimen were based on the loading capacity of the already mentioned testing machines. They were then machined to BS18 : part 2 1971 shown in figures 40 and 41.

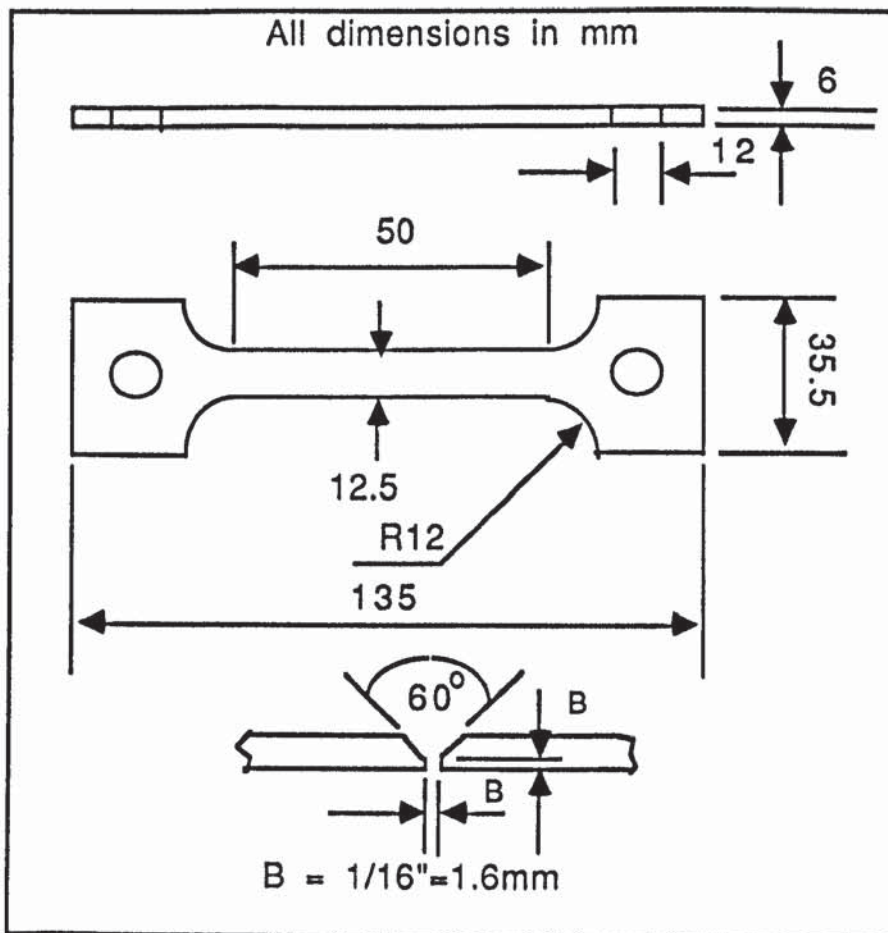


Figure 40 Diagrammatic representation of the specimen

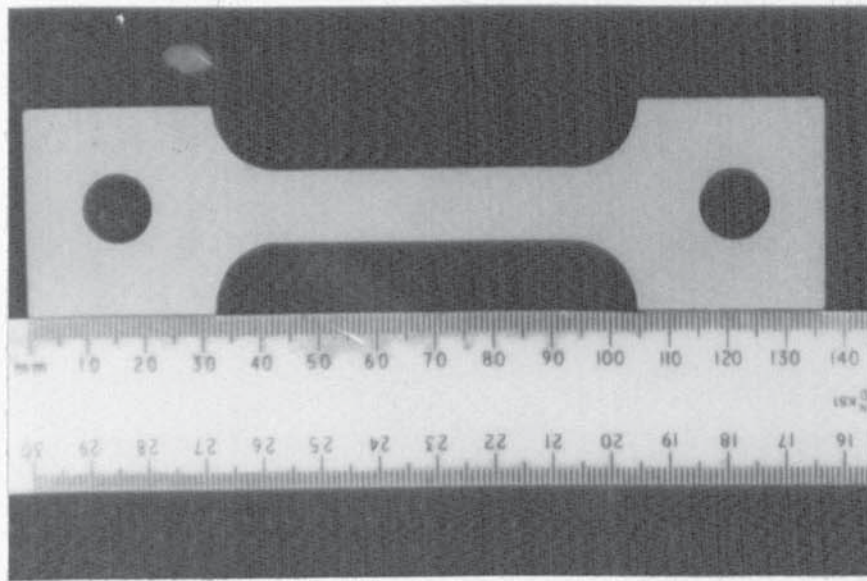


Figure 41 Specimen

The surface of the welded specimens were machined flat, polished, and etched with 2% and 4% solution of nital. This exposed the characteristic of each region of the weld and made various zones to be clearly visible with the naked eye. This simplified the problem of measuring the boundaries of each area of the weld. A mesh with overall dimensions of 50 X 12 mm with internal spacing of 1 X 1 mm was then printed on this surface, using the photographic technique explained in appendix 5 (figure 42). All the surfaces were lacquered except for one face which was exposed to sea water in the environmental testing.

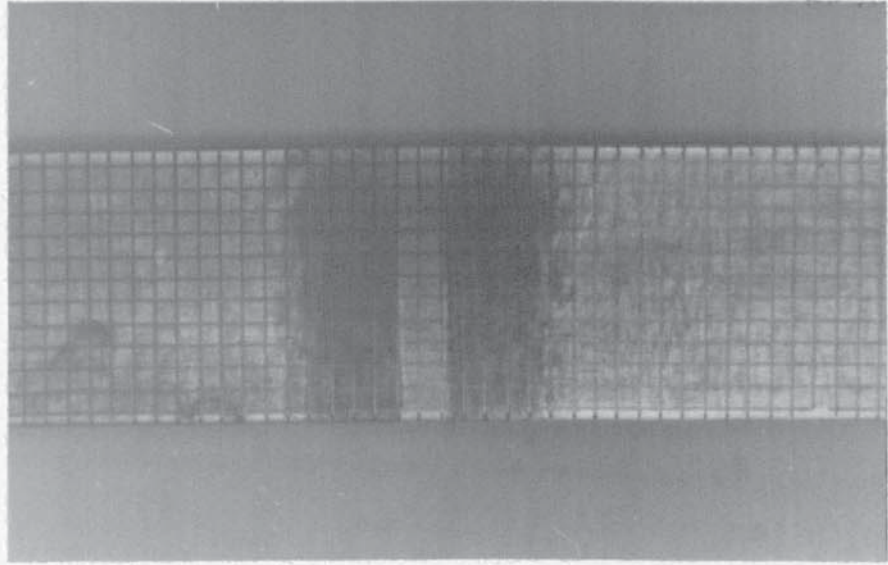


Figure 42 Printed grid on parallel length of the specimen showing the three distinct regions of the weld.

After a series of tests which were carried out on the welded specimens it was revealed that due to the higher strength of the welds compared with the parent plate deformation and eventual fracture had fallen outside the welded region. Hence in order to find the actual properties of the welds, a notch was introduced to force the deformation into the weld zone. The dimensions of a notch is shown in appendix 6. The presence or absence of a notch then became another variable in the experimental matrix.

3.9 ENVIRONMENTAL TESTING

All the prepared specimens were tested under three distinct environmental conditions;

- 1) Air
- 2) Sea water, stress corrosion condition
- 3) Sea water, hydrogen evolution.

Table 21 shows the number of different specimens tested in each of the above environments. All tests were carried out with the same slow strain rate . For corrosion and hydrogen tests, a special perspex tank and a stainless steel adapter was designed (figures 43, 44). The adapter, connecting pin and the end of the specimen which were submerged in the sea water were all protected against corrosion and the effect of creating a galvanic couple using lacquer filler materials and a polystyrene spray.

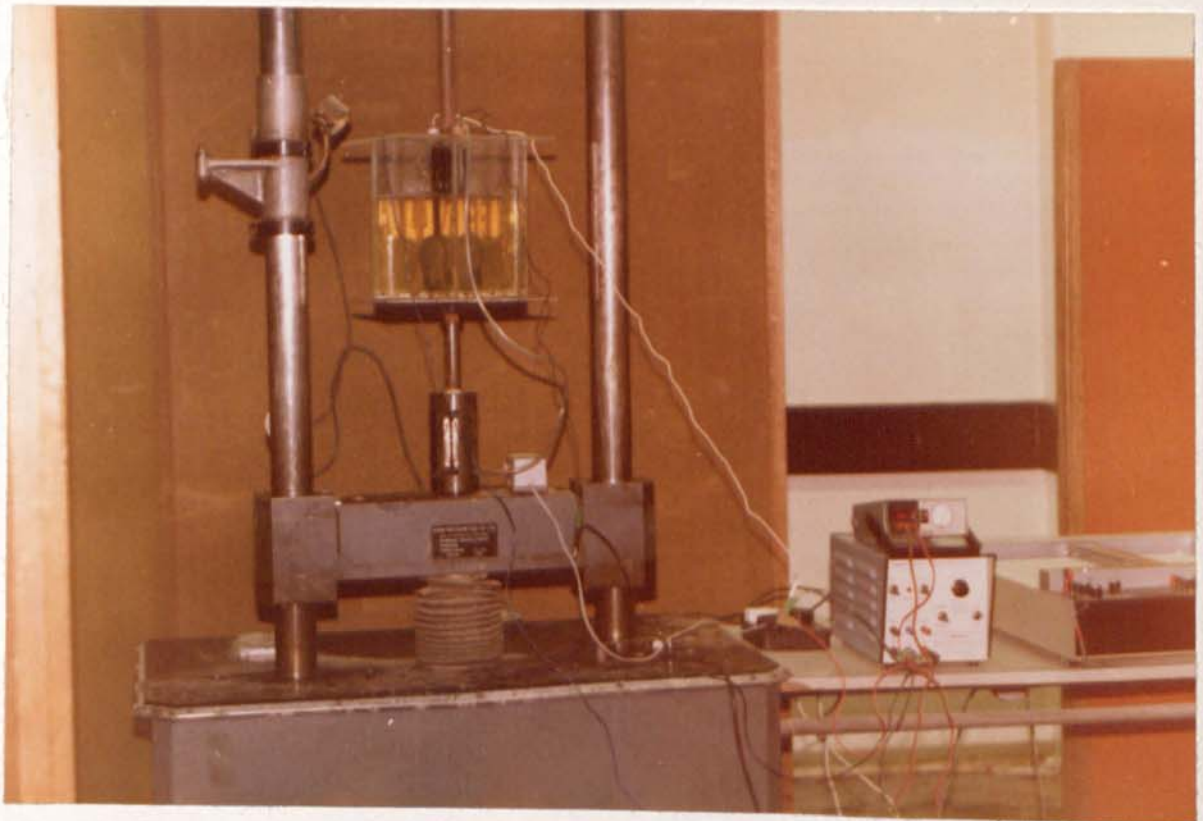


Figure 43 The experimental rig.

NO	Specimen	Heat treatment	Weld quality	No. of specimens to be tested in different Testing conditions		
				Air	SCC sea water	Hyd. evolution sea water
1	As received Parallel to RD	None	Without a weld	1	1	1
2	As received perpendicular to RD	None	Without a weld	1	1	1
3	Normalised	920 air cool	Without a weld	1	1	1
4	Normalised	920 air cool	Good	1	1	1
5	Normalised	920 air cool	Defective	1	1	1
6	Normalised	920 air cool	Good with a notch	1	1	1
7	Normalised	920 air cool	Defective with a notch	1	1	1
8	Quenched and tempered	920 OQ 600 air	Without a weld	1	1	1
9	Quenched and tempered	920 OQ 600 air	Good	1	1	1
10	Quenched and tempered	920 OQ 600 air	Defective	1	1	1
11	Quenched and tempered	920 OQ 600 air	Good with a notch	1	1	1
12	Quenched and tempered	920 OQ 600 air	Defective with a notch	1	1	1
13	Quenched and tempered	920 WQ 600 air	Without a weld	1	1	1
14	Quenched and tempered	920 WQ 600 air	Good	1	1	1
15	Quenched and tempered	920 WQ 600 air	Defective	1	1	1
16	Quenched and tempered	920 WQ 600 air	Good with a notch	1	1	1
17	Quenched and tempered	920 WQ 600 air	Defective with a notch	1	1	1

Table 21 Number of specimens tested in different environments

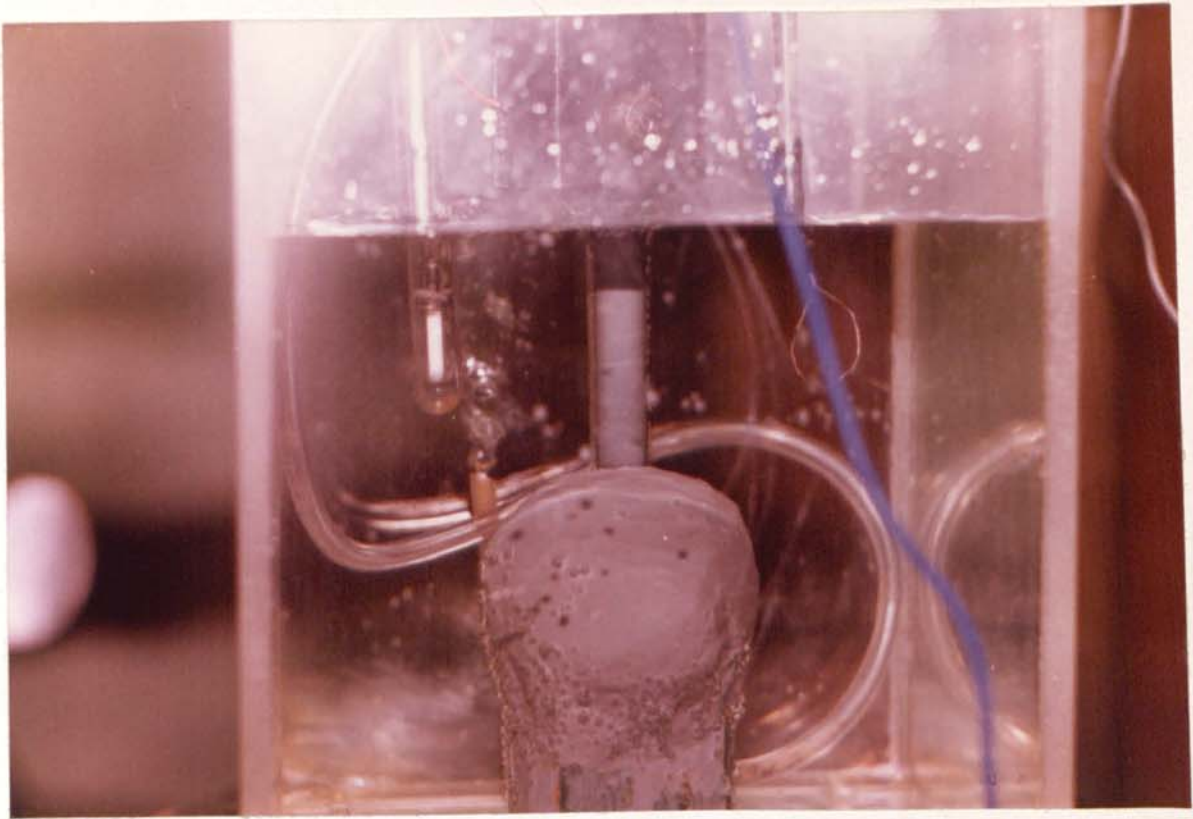


Figure 44 Close up view of the environmental test rig.

3.9.1 AIR TESTS

These tests were carried out for control purposes only, and gave the basic mechanical property data of the specimens used in the research.

3.9.2 ACCELERATED STRESS CORROSION TESTING IN SEA WATER

The most appropriate method of stress corrosion testing in a relatively short period of time seems to be the constant deflection rate test method. (71) . This involves the application of a relatively slow strain (10^{-5} _ 10^{-6} S^{-1}) to a specimen subjected to the appropriate electrochemical conditions.

Acceleration of the stress corrosion tests is usually done by increasing the aggressiveness of the environment i.e changing the composition, or by stimulating the corrosion reactions through potentiostatic polarisation. The electrolyte used for this purpose was the natural North sea water obtained from the east coast, outside Newcastle, two miles south of Blyth, where the water pollution was less. This was taken during the summer period. The composition of the sea water was kept constant for all tests, and the measure of consistency that was chosen was the chloride concentration which was measured by using titration technique and was found to be 19.82 parts per thousand .

Therefore the acceleration of the stress corrosion tests was done through the potentiostatic polarisation. For this purpose initially a sample of the steel was tested in a sea water using the Auto-stat (automatic potentiostat) over a range of varying potentials and currents to obtain the general polarisation curves (figure 45). Using the Auto-stat, the potential of ± 1000 mV was scanned through at a rate of 10 mV/sec., the polarisation data gave the corrosion rate of 16 mA / Cm² with E_{rest} of -540 mV.

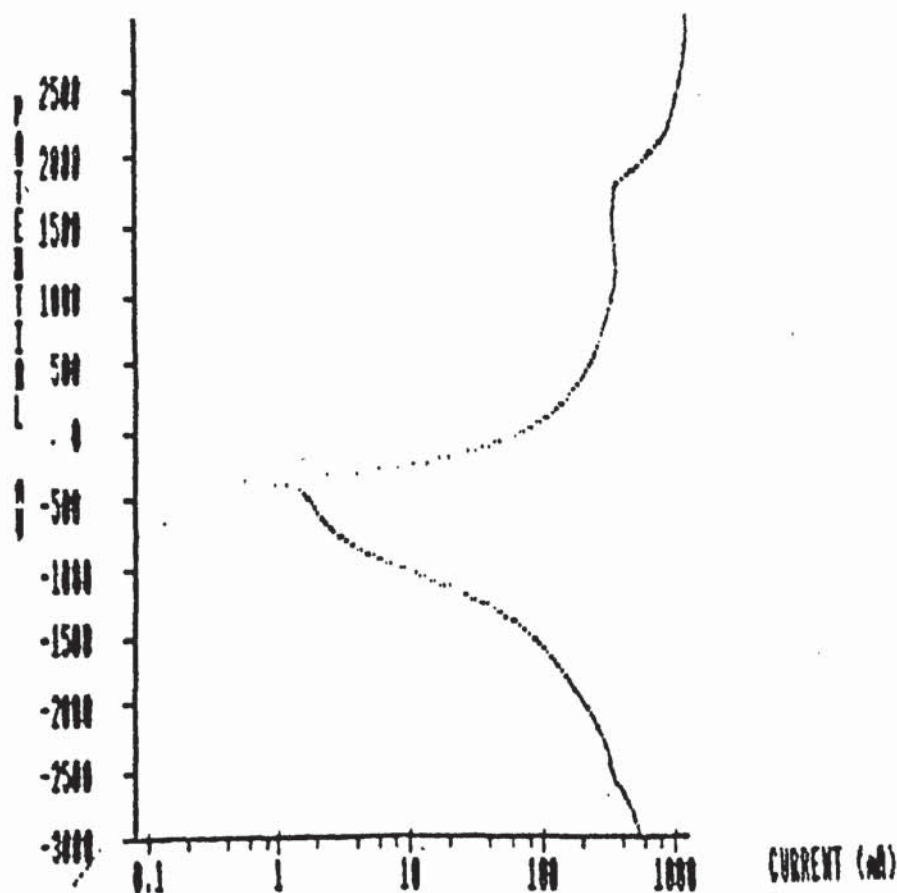


Figure 45 Polarisation curve obtained by using the Auto-stat.

In order to speed the corrosion process a potential of -350 mV was chosen for all the SCC tests. This potential conveniently falls in the corrosion range of the standardised Pourbaix diagram (figure 13). A diagram showing the arrangements of the corrosion cell is shown in figure 46.

3.9.3 TESTING IN SEA WATER WITH HYDROGEN EVOLUTION

These tests were conducted under potentiostatic conditions, in which the potential of $\sim -1.1\text{V}$ was used to keep a high enough potential difference between the anode and the cathode, this enabled the hydrogen to evolve as bubbles over the cathodic surface. The specimen acts as the cathode and becomes hydrogenated because of the adsorption of hydrogen ions into the metal, thereby facilitating the build up of dissolved hydrogen in the steel structure.

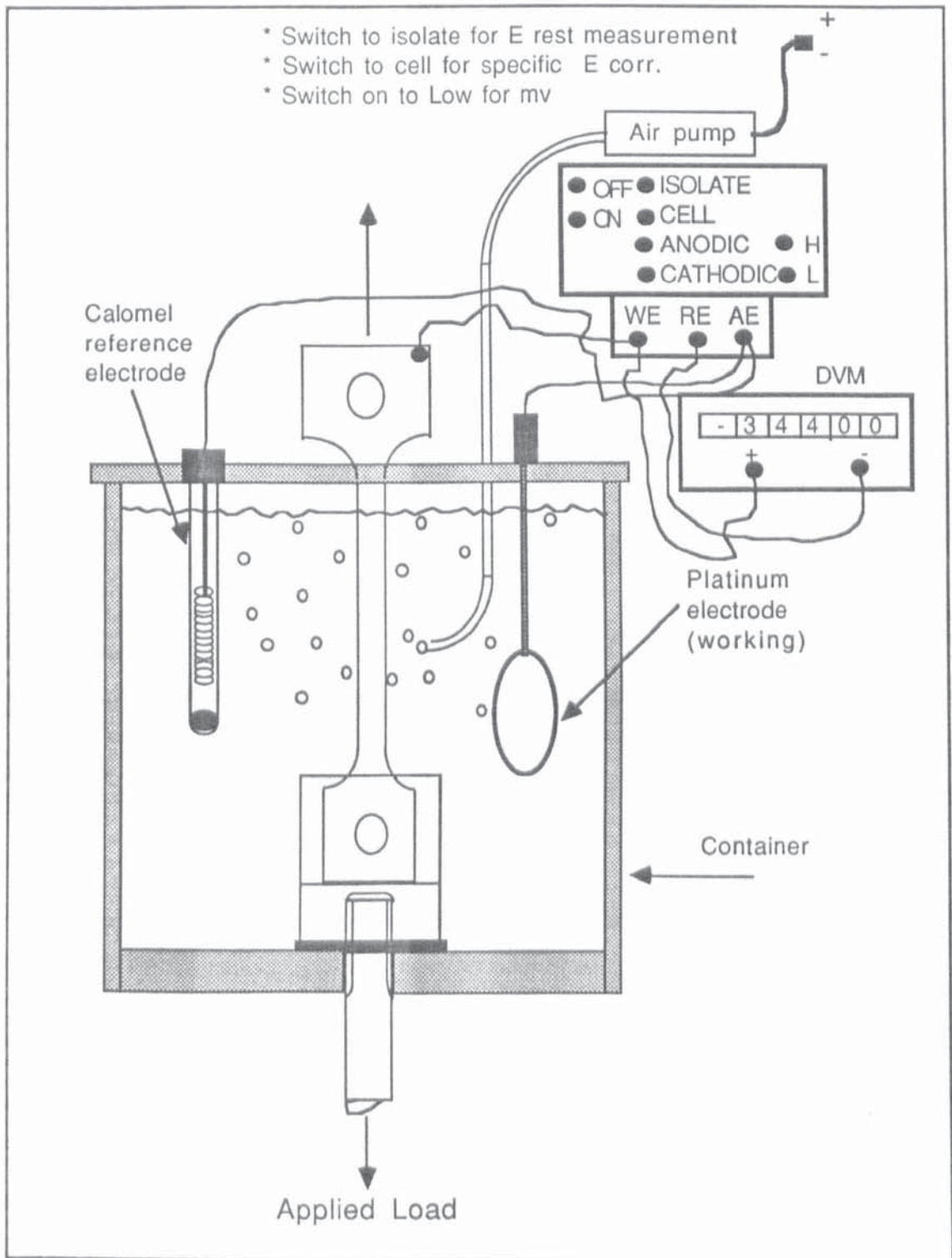


Figure 46 schematic diagram showing arrangements for the corrosion cell

CHAPTER 4

RESULTS AND ANALYSIS OF THE RESULTS

4. RESULTS AND ANALYSIS OF THE RESULTS

4.0 RESULTS

The results obtained from the research programme falls into three categories:

- I) Experimental (based on the laboratory testing of the specimens)
- II) Analytical, using the statistical methods of T-test of significance, analysis of variance and regression modelling.
- III) Analytical, using the finite element modelling technique.

The experimental results include mechanical and metallographical data. Mechanical properties reveal the elastic, plastic behaviour of the steel in the various environments.

The statistical work tests for the significance of the results bearing in mind the variations in recorded properties from test to test and seeks for those experimental variables that have the greatest influence on the five mechanical property parameters yield stress, U.T.S, fracture stress, percentage elongation and percentage reduction in area. Information about the fracture has also been included and this has been correlated with the variables.

The finite element results are considered for the possibility of analytical modelling of each test in various environments. The welded steel which is a material of non-uniform microstructure and has different mechanical properties in the region of parent metal, fusion zone and heat affected zone, has been modelled by linearisation of its mechanical properties. This is done by using plasticity module parameters that describe the yield stresses, the strains to failure and the slopes of the stress/strain plots. This modelled behaviour is compared with the actual behaviours of the material in the laboratory tests and the differences are discussed in detail.

4.1 EXPERIMENTAL RESULTS

Prior to each tensile test the dimensions of the specimens were accurately measured and recorded. These are tabulated separately for each batch and are shown in tables 22-25 in appendix 7. In tensile tests for normalised and oil quenched and tempered specimens it was found that the strength of the welds were actually higher than that of the parent plates, hence all deformations occurred outside the weld and within the parent plates. In order to obtain information about the mechanical properties of the welds themselves, deformation was forced through the welded zone of the specimens, through the selective reduction of the cross sectional area in the vicinity of the weld.

This was not necessary for the water quenched and tempered specimens, as the strength level of the welded zone was not higher than the parent metal. In the as received batch of the specimens, the air tests for the transverse and longitudinal rolling directions revealed that the mechanical properties did not vary significantly with respect to different directions, hence further tensile tests on specimens cut from different directions was unnecessary.

Figures 68-108 in appendix 6 show the stress/strain relationships obtained for each specimen during a tensile test. These diagrams represent testing of specimen in air, corrosion and hydrogen conditions respectively. Figures 50 and 51 show the main fracture characteristics of each test carried out in different environments. Figure 52 reveal the failure of the plates outside the welded zone, whilst figure 53 display the deformation which has occurred within the welded zone.

4.1.1 TENSILE TESTS

The results of tensile tests are given in table 26-28 and figures 47-49, and 68-108 appendix 6. The values reported are yield stress (YS), ultimate tensile stress (UTS), fracture stress (FS), % reduction in area and % elongation. Unless explained otherwise the original cross sectional areas and gauge lengths were used as the basis of the calculations.

When specimens were tested in the corrosion cell a considerable amount of metal was dissolved from the surface. For these specimens corrections were made to the effective cross sectional areas to take into account the extent of dissolution. For the welded specimens which fractured outside the weld, the elongation of the parent plate material was calculated using an effective gauge length which is the total gauge length minus the distance between the extremity of the affected zones.

The data in these tables show that the YS and UTS increased in the order of normalised, oil quenched and tempered, water quenched and tempered and in the case of welded specimens defective and sound welds. This reflects the effect of quench and tempering and weld quality upon the strength of the steels.

The YS of 623 N/mm² was maximum for WNW3 which is a water quenched and tempered steel without a weld and tested under hydrogen evolution conditions, whilst the maximum UTS of 685 N/mm² occurred when the same steel was tested in air. The minimum values of YS and UTS were found to be for HNW3 which is a normalised steel without a weld and tested in hydrogen environment.

From the results obtained it can be seen that there was no systematic change in the YS between the hydrogen charged and uncharged tensile specimens, although the UTS was consistently lower for the hydrogen charged specimens. The fracture strain has been greatly reduced in all the hydrogen charged specimens, and equally in specimens containing defective welds.

Typical stress Vs strain curves are reproduced in figures 47-49 which show the effect of weld defect and hydrogen charging upon the shape and extent of the flow curves compared to the uncharged and sound weld steels.

NO.	Specimen	Test in	Y.S	U.T.S	F.S	% Elong.	% R.A
			N/mm ²	N/mm ²	N/mm ²		
1	HNW1	Air	350	474	908	34.0	67.0
2	HNW2	Corrosion*	320	444	890	28.0	62.5
3	HNW3	Hydrogen	315	418	268	26.0	27.1
4	HGC7	Air	382	511	1167	+ 23.0	69.5
5	HGC6	Corrosion*	370	500	856	+ 20.8	60.3
6	HGC1	Hydrogen	337	502	176	+ 14.3	21.7
7	HB2	Air	379	514	1199	+ 24.1	71.9
8	HB3	Corrosion*	381	501	332	+ 18.4	68.5
9	HB5	Hydrogen	346	508	251	+ 20.0	36.1
10	HGC5	Air	443	621	1129	26.4	59.2
11	HGC8	Corrosion*	442	572	1030	22.6	58.1
12	HGC4	Hydrogen	446	580	408	12.5	24.1
13	HB8	Air	426	539	726	11.6	26.8
14	HB7	Corrosion*	400	537	271	12.4	32.3
15	HB6	Hydrogen	377	545	247	10.8	32.0

NOTE:

Specimens 1 - 3 HNW are without welds

Specimens 4 - 6 HGC are with sound welds

Specimens 7 - 9 HB are with defective welds

Specimens 10 - 12 HGC are sound welds and notched

Specimens 13 - 15 HB are defective welds and notched

* %RA and F.S are based on the reduced cross sectional areas brought about by corrosion.

+ In a composite specimen of weld and parent plate, the gauge length on which the elongation results are calculated is shorter by ~ 30%.

Table 26 General mechanical property results for normalised specimens.

NO.	Specimen	Test in	Y.S	U.T.S	F.S	% Elong.	% R.A
			N/mm ²	N/mm ²	N/mm ²		
1	HNW1	Air	350	474	908	34.0	67.0
2	HNW2	Corrosion*	320	444	890	28.0	62.5
3	HNW3	Hydrogen	315	418	268	26.0	27.1
4	HGC7	Air	382	511	1167	+ 23.0	69.5
5	HGC6	Corrosion*	370	500	856	+ 20.8	60.3
6	HGC1	Hydrogen	337	502	176	+ 14.3	21.7
7	HB2	Air	379	514	1199	+ 24.1	71.9
8	HB3	Corrosion*	381	501	332	+ 18.4	68.5
9	HB5	Hydrogen	346	508	251	+ 20.0	36.1
10	HGC5	Air	443	621	1129	26.4	59.2
11	HGC8	Corrosion*	442	572	1030	22.6	58.1
12	HGC4	Hydrogen	446	580	408	12.5	24.1
13	HB8	Air	426	539	726	11.6	26.8
14	HB7	Corrosion*	400	537	271	12.4	32.3
15	HB6	Hydrogen	377	545	247	10.8	32.0

NOTE:

Specimens 1 - 3 HNW are without welds

Specimens 4 - 6 HGC are with sound welds

Specimens 7 - 9 HB are with defective welds

Specimens 10 - 12 HGC are sound welds and notched

Specimens 13 - 15 HB are defective welds and notched

* %RA and F.S are based on the reduced cross sectional areas brought about by corrosion.

+ In a composite specimen of weld and parent plate, the gauge length on which the elongation results are calculated is shorter by ~ 30%.

Table 26 General mechanical property results for normalised specimens.

NO.	Specimen	Test in	Y.S	U.T.S	F.S	% Elong.	% R.A
			N/mm ²	N/mm ²	N/mm ²		
1	WNW1	Air	581	685	992	16.0	65.0
2	WNW2	Corrosion*	530	578	1151	16.0	65.0
3	WNW3	Hydrogen	623	637	1105	13.0	50.0
4	GW1	Air	570	628	1241	17.0	65.0
5	GW2	Corrosion*	433	594	1097	20.0	64.0
6	GW3	Hydrogen	488	602	878	14.0	54.0
7	BW1	Air	408	596	553	7.00	26.0
8	BW2	Corrosion*	439	536	372	7.00	32.0
9	BW3	Hydrogen	412	450	304	4.00	17.0

NOTE:

Specimens 1 - 3 WNW are without welds

Specimens 4 - 6 GW are with sound welds

Specimens 7 - 9 BW are with defective welds

* %RA and F.S are based on the reduced cross sectional areas brought about by corrosion.

Table 28 General mechanical property results for water quenched and tempered specimens.

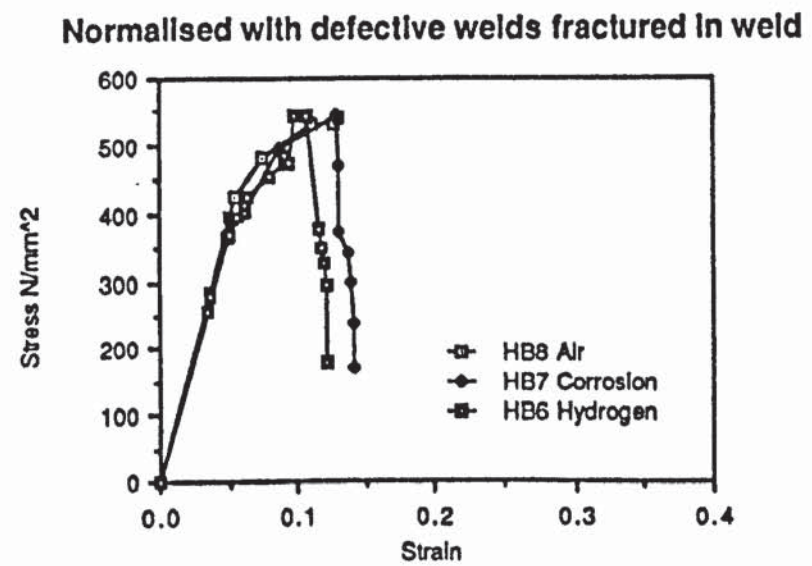
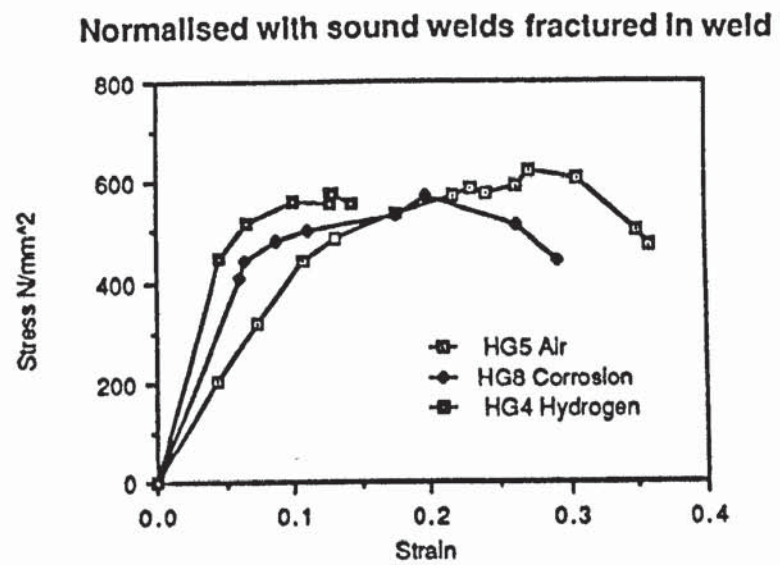
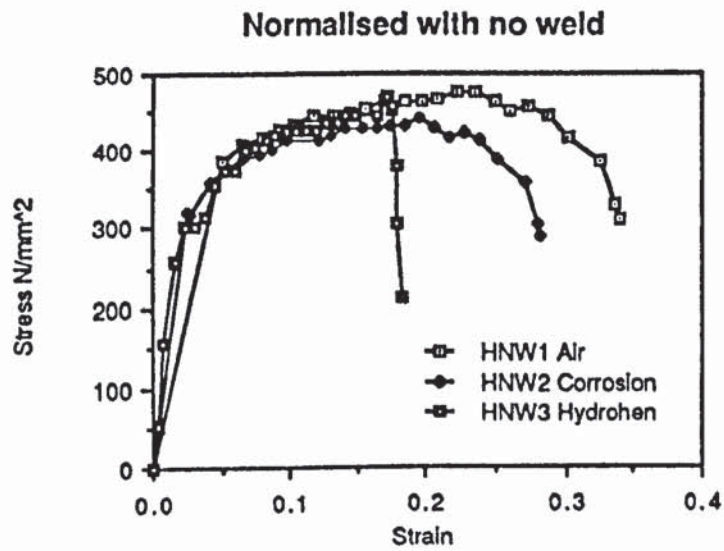


Figure 47

Stress strain curves for normalised steels containing no welds, sound welds and defective welds tested in air, corrosion and hydrogen environments.

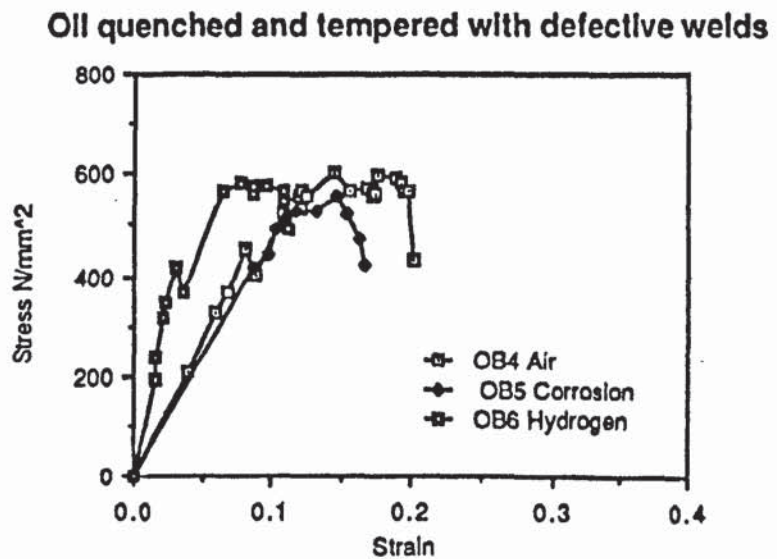
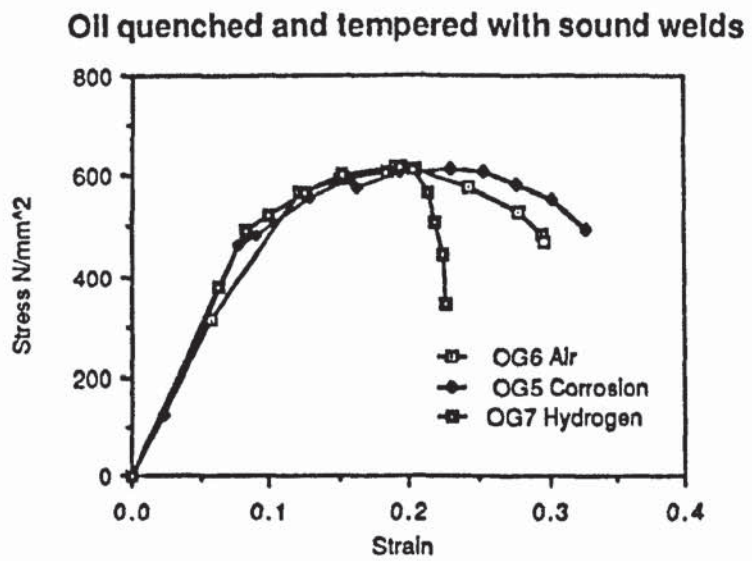
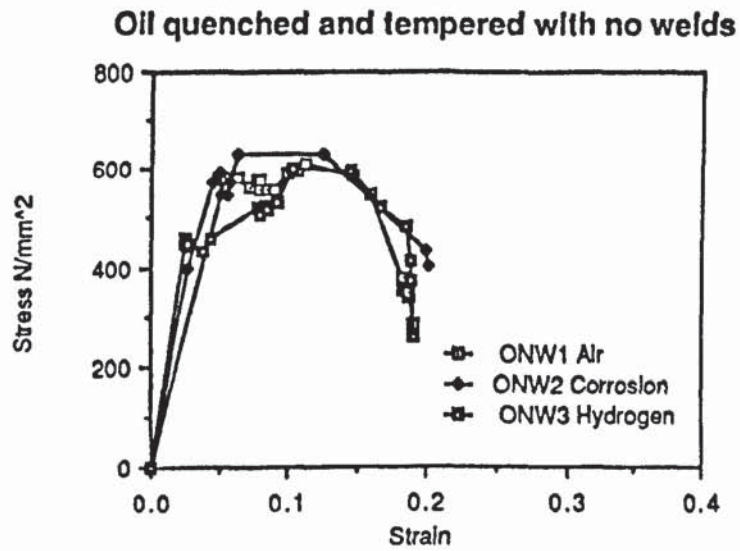
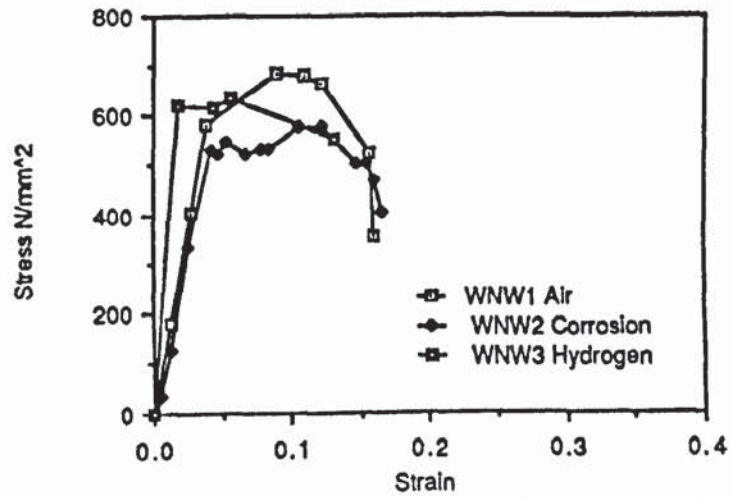


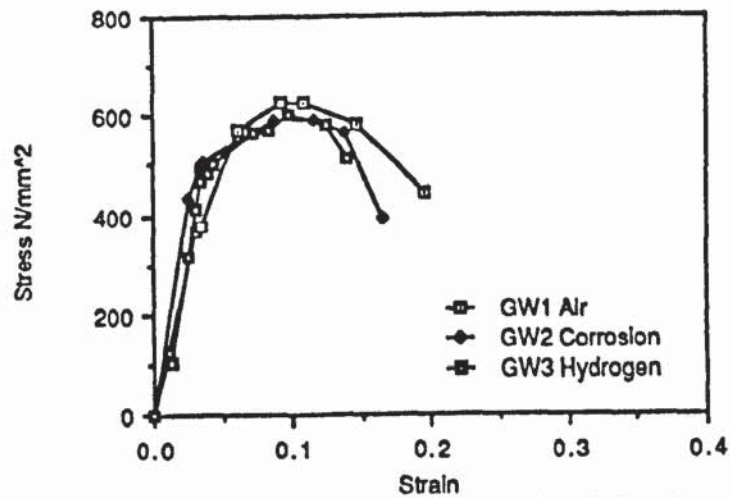
Figure 48

Stress strain curves for oil quenched and tempered steels containing no welds, sound welds and defective welds tested in air, corrosion and hydrogen environments.

Water quenched and tempered with no welds



Water quenched and tempered with sound welds



Water quenched and tempered with defective welds

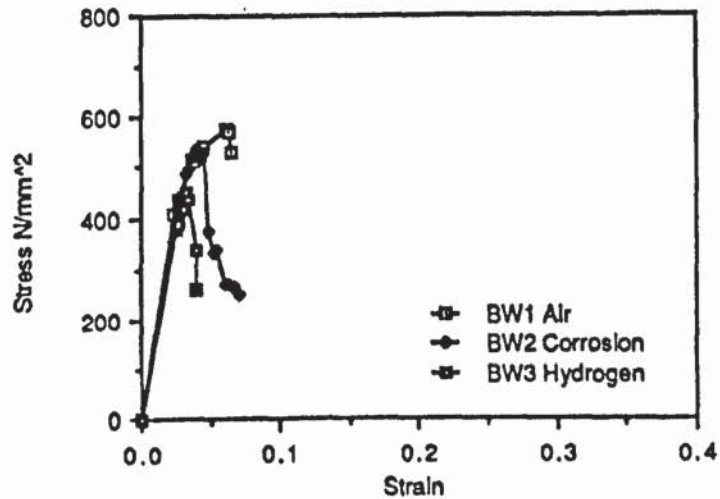


Figure 49

Stress strain curves for water quenched and tempered steels containing no welds, sound welds and defective welds tested in air, corrosion and hydrogen environments.

4.1.2 METALLOGRAPHICAL EXAMINATIONS

The most frequently observed inclusion phase was MnS the shape of which varied from spherical to ellipsoidal (Figure 55). Observations of SEM samples of defective welds revealed many of the inclusion clusters to be preferentially situated. Figures 55, 56 show a typical type of fracture surface observed for the tensile specimen. This example is a classical "cup and cone" type fracture which has been found for all the steels tested, figures 54, 55 show details of the fracture surface at higher magnifications.

The fracture surfaces which were observed for tensile specimens displayed many characteristics in common, therefore to prevent repetition in describing these and concentrate upon the principal aim of the fractographic study i.e compare the fracture appearance between the sound and defective welds further descriptions of the fracture surfaces for tensile tests will not be made.

For all the steels tested in absence of hydrogen fracture occurred by micro void coalescence (MVC). Comparing the two fracture surfaces it can be seen that the dimples occurring upon the defective specimen were markedly larger than those of sound welds. In both of these fracture surfaces the dimples seem to be equiaxed. Upon these sections dimples which contain unfractured inclusions can be seen, it can also be seen from figure 57 covered with, small, apparently undeformed cluster of inclusions which can be responsible collectively for the formation of a single dimple.

There was no anisotropy of fracture appearance found for either of the two specimens, although this seems to be commonly related to the orientation of inclusions and hence their shape in respect to the testing directions. The majority of inclusions in these steels which remained within the dimples after the fracture seemed to be globular in shape.

As a general observation the fracture Mode did not change from micro void coalescence (MVC) for any of the specimens as a result of addition of inclusions or hydrogen charging but for the hydrogenated specimens the resulting fracture appearance was more "feathery" i.e a qualitative appraisal of the dimple size would suggest they had become fine, and more numerous in comparison to the uncharged specimens.

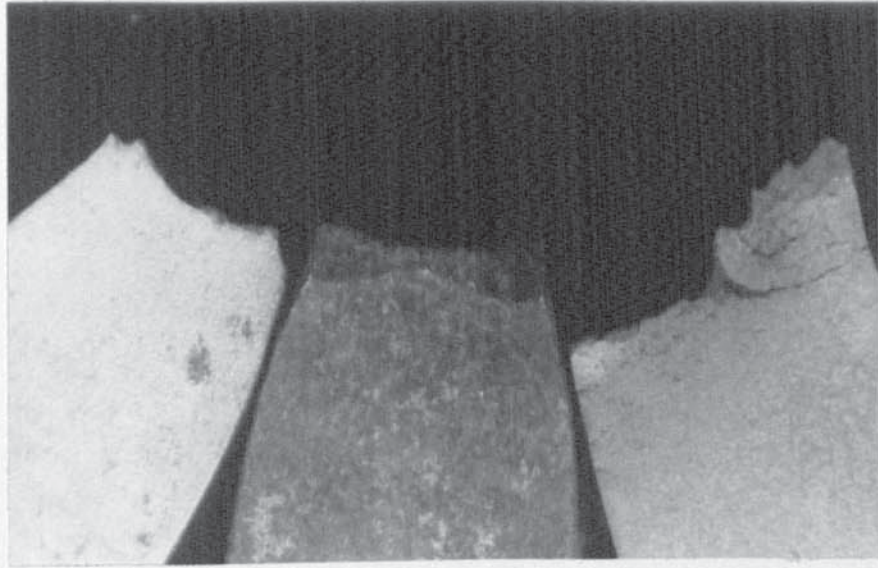


Figure 50 Fractured specimens in three different environments.

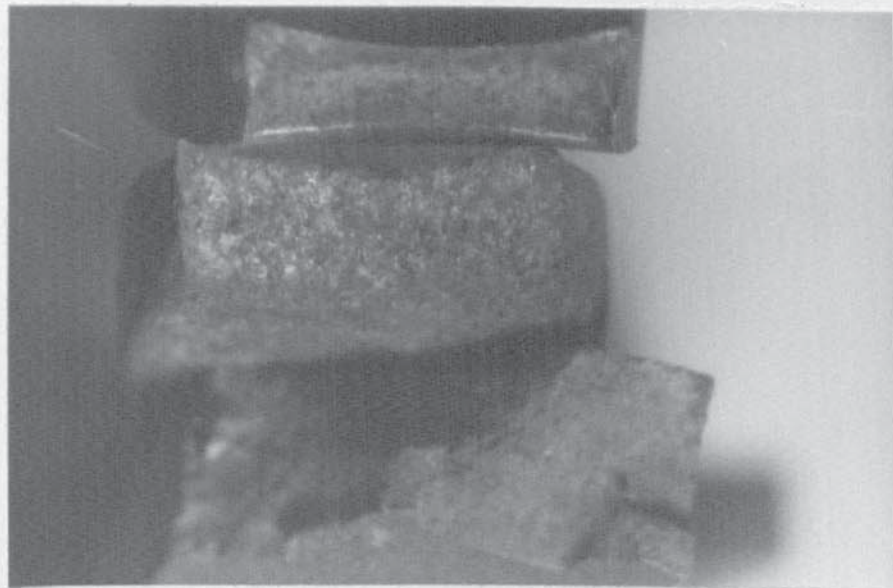


Figure 51 Fracture characteristics of different tests in air, corrosion and hydrogen environments.

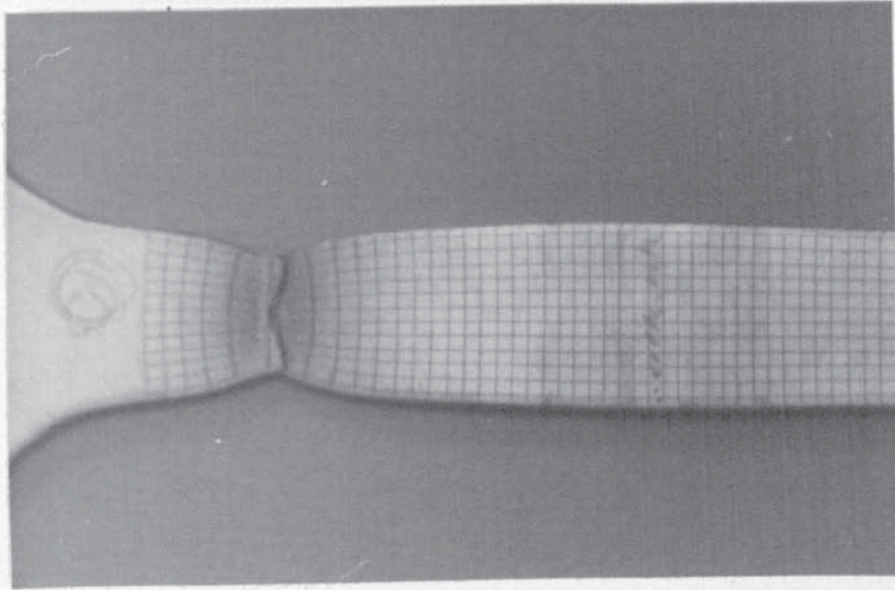


Figure 52 Failure of the specimen outside the weld.

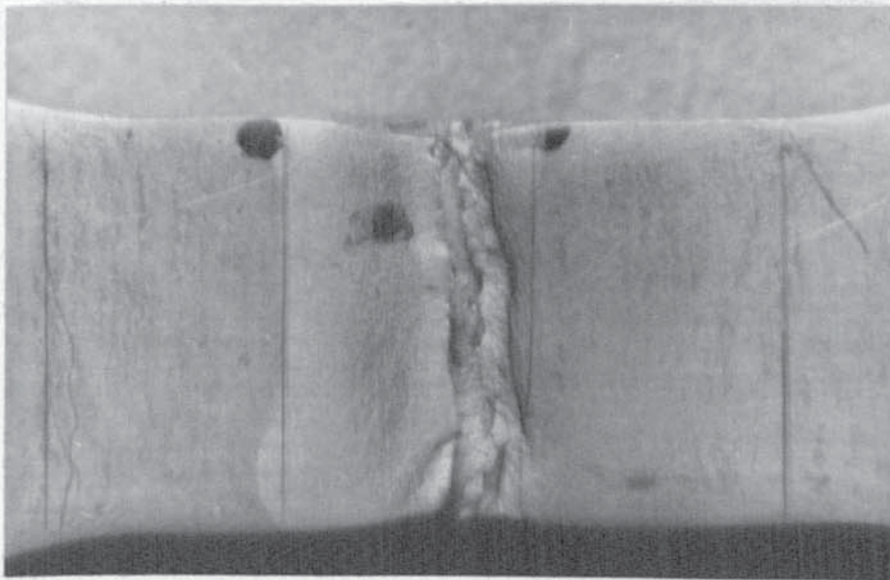


Figure 53 Deformation through the weld.

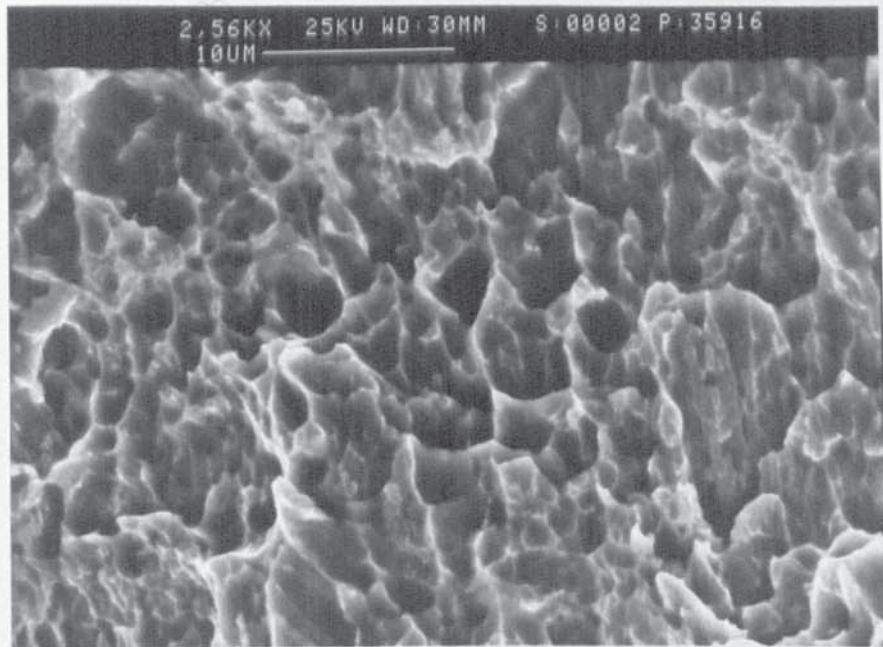


Figure 54 SEM details of fracture surface for tensile test specimen with a sound weld magnification X 2.6K

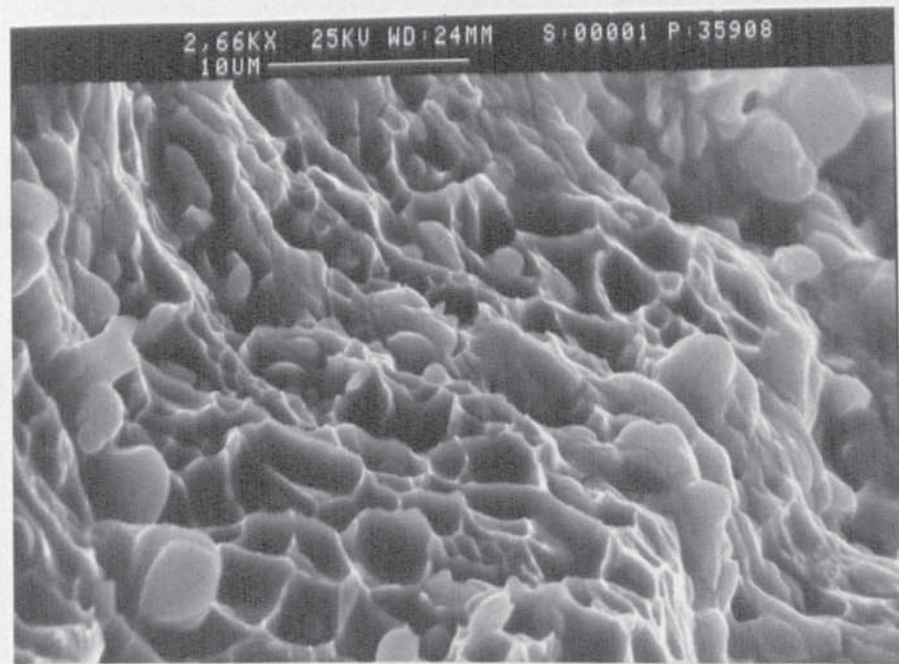


Figure 55 SEM details of fracture surface for tensile test specimen with a defective weld magnification X 2.6K

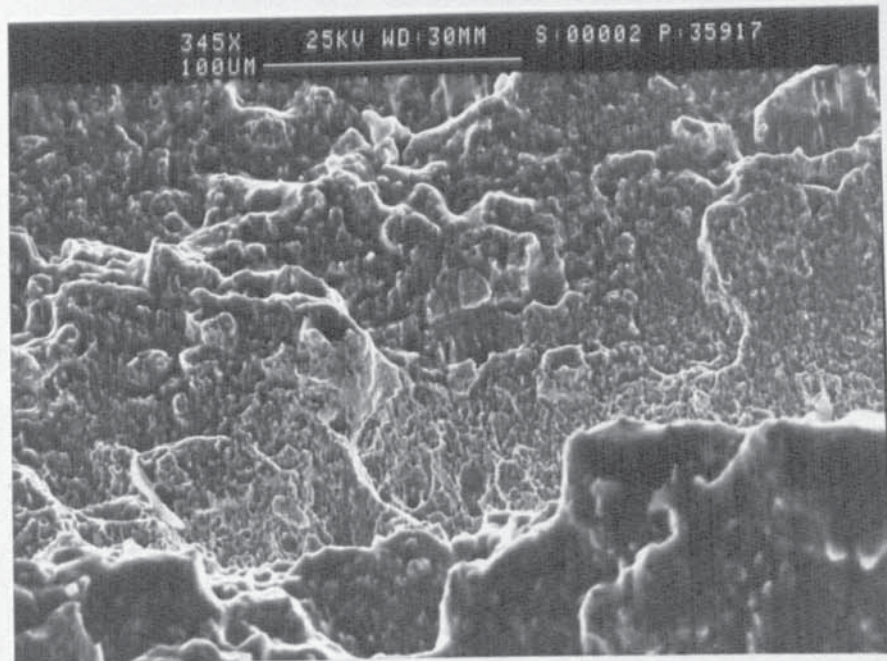


Figure 56 SEM details of fracture surface for tensile test specimen with a sound weld magnification X 350

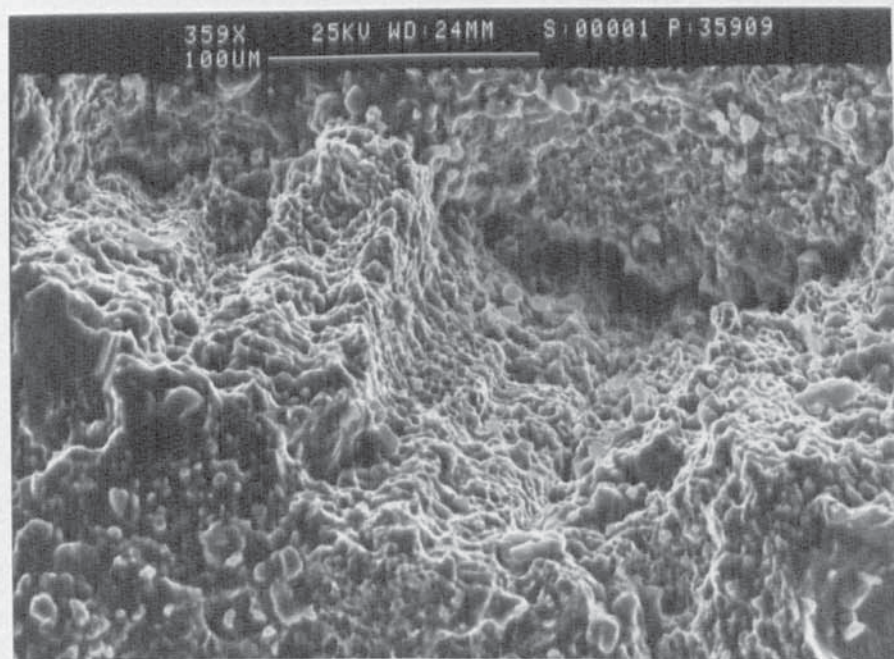


Figure 57 SEM details of fracture surface for tensile test specimen with a defective weld magnification X 360

4.2 THE STATISTICAL RESULTS

The statistical analyses were conducted using the SPSSX software package run on the Vax-cluster computer. The mechanical property results were entered in the data file in their cardinal form. The conditions that the material was subjected to were entered as cardinal quantities and a coding scheme had to be devised. This was as follows:

<u>Parameter</u>	<u>Variable name</u>	<u>code</u>	<u>Condition</u>
Heat treatment	HEAT	1	Normalised
		2	Quenched in oil and tempered.
		3	Quenched in water and tempered.
Welding	WELD	1	No weld (plain specimen).
		2	Sound Weld.
		3	Defective (category 3 weld).
Notch	NOTCH	1	No notch (plain specimen).
		2	Notched at weld.
Environment	ENVIRON	1	Air test.
		2	Corrosion test.
		3	Hydrogen evolution test.
Fracture path	FRACT	1	Fracture through parent plate.
		2	Fracture through the weld.

A copy of the data file is shown in table 29

For the regression modelling involving variables that represent two-way and three-way interactions the coding scheme had to be modified in the following way to ensure the integrity of the newly created variables.

<u>Variables</u>	<u>Recode</u>
HEAT	1 becomes 0 2,3 become 1
WELD	1,2 become 0 3 becomes 1
NOTCH	1 becomes 0 2 becomes 1
ENVIRON	1,2 become 0 3 becomes 1
FRACT	1 becomes 0 2 becomes 1

The data file (Table 29) matches the re-coded variables for the regression modelling.

ID	TABLES	NUMBER	HEAT	WELD	FRACT	ENVIRON	YS	UTS	FS	ELONG	RA	NOTCH
1	26	1	0	0	0	0	342	474	908	34.0	67.0	0
2	26	2	0	0	0	0	320	444	890	28.0	62.5	0
3	26	3	0	0	0	1	315	418	268	26.0	27.1	0
4	26	4	0	0	0	0	382	511	1167	23.0	69.5	0
5	26	5	0	0	0	0	295	472	856	20.8	60.3	0
6	26	6	0	0	0	1	337	502	176	14.3	21.7	0
7	26	7	0	1	0	0	379	514	1199	24.1	71.9	0
8	26	8	0	1	0	0	381	501	332	18.4	68.5	0
9	26	9	0	1	0	1	346	508	251	20.0	36.1	0
10	26	10	0	0	1	0	443	621	1129	26.4	59.2	1
11	26	11	0	0	1	0	442	572	1030	22.6	58.1	1
12	26	12	0	0	1	1	446	580	408	12.5	24.1	1
13	26	13	0	1	1	0	426	539	726	11.6	26.8	1
14	26	14	0	1	1	0	400	537	271	12.4	32.3	1
15	26	15	0	1	1	1	377	545	247	10.8	32.0	1
16	27	1	1	0	0	0	580	610	798	19.0	67.0	0
17	27	2	1	0	0	0	562	596	1350	20.0	70.0	0
18	27	3	1	0	0	1	454	600	510	19.0	49.0	0
19	27	4	1	0	0	0	413	504	1503	28.0	72.0	0
20	27	5	1	0	0	0	368	492	1061	31.0	67.0	0
21	27	6	1	0	0	1	379	532	263	22.0	28.0	0
22	27	7	1	1	0	0	409	543	1048	25.0	65.0	0
23	27	8	1	1	0	0	432	542	1083	25.0	68.0	0
24	27	9	1	1	0	1	366	518	217	17.0	26.0	0
25	27	10	1	0	1	0	462	612	1036	33.0	52.0	1
26	27	11	1	0	1	0	459	502	959	30.0	51.0	1
27	27	12	1	0	1	1	511	617	488	23.0	30.0	1
28	27	13	1	1	1	0	449	572	583	20.0	28.0	1
29	27	14	1	1	1	0	405	607	627	19.0	33.0	1
30	27	15	1	1	1	1	433	550	497	11.0	16.0	1
31	28	1	1	0	0	0	581	685	992	16.0	65.0	0
32	28	2	1	0	0	0	530	578	1151	16.0	65.0	0
33	28	3	1	0	0	1	623	637	1105	13.0	50.0	0
34	28	4	1	0	0	0	570	628	1241	17.0	65.0	0
35	28	5	1	0	0	0	433	594	1097	20.0	64.0	0
36	28	6	1	0	0	1	488	602	878	14.0	54.0	0
37	28	7	1	1	1	0	408	596	553	7.0	26.0	0
38	28	8	1	1	1	0	439	536	372	7.0	32.0	0
39	28	9	1	1	1	1	412	450	304	4.0	17.0	0

0
Number of cases read: 39 Number of cases listed: 39
116-Jan-90 modelling the results

Fract 0 In parent plate

Fract 1 In weld

Table 29 Data file for statistical analysis.

4.2.1 T-TEST OF SIGNIFICANCE

These were conducted for each mechanical property parameter in turn and the results are summarised in the following table.

	Norm v WQ	OQ v WQ	Plain v Sound	Sound v Defective	Plain v Notch	Air v Corrosion	Air v Hydrogen
Yield stress	Yes	-	-	-	-	-	-
U.T.S	Yes	-	-	-	-	-	-
Fracture stress	-	-	-	Yes	-	-	Yes
% Elongation	Yes	Yes	-	Yes	-	-	Yes
% RA	-	-	-	-	Yes	-	Yes

Yes Significance of separate variance estimate < 0.05
 - > 0.05 (i.e lost in the scatter of the results)

The raw data is given in appendix 8 section 8.1-8.8

Table 30 T- test results

The column headings in the table give the variables involved in the two-sample T test. For example, Norm v WQ indicates that a comparison was made of all normalised heat treatment tests against the water quenched and tempered heat treatment tests, the oil quenched and tempered tests being excluded. A 'Yes' in the table indicates a greater than 95% probability that the difference in the means of the test results is not due to chance. For example the yield stress of normalised steel is significantly different from those that have been water quenched and tempered.

Examining the table as a whole the following inferences can be made.

- i) The difference between normalising and water quenching is the only factor that significantly effects the yield stress and U.T.S results.
- ii) The fracture stress and % reduction in area are significantly difference in tests where the environment includes hydrogen evolution as opposed to those conducted in the neutral air test.
- iii) Additionally the fracture stress is affected by higher sulphur contents in the weld, and the % reduction in area is affected by the presence of notches in the centre of the welded test pieces.
- iv) The elongation results were the most complex. It appears that elongation is a function of heat treatment, sulphur content of the weld and the presence or not of hydrogen evolution conditions in the environment. It is thought that the difference revealed between the oil quenched and water quenched tests to be a statistical accident.

4.2.2 ANALYSIS OF VARIANCE

An analysis of variance examines not only the main effects of the variables, but also provides information on the effects of possible two-way or three-way interactions. For this test a full experimental matrix is required and so it had to be limited to the variables HEAT, WELD, and ENVIRON. (appendix 8.9-8.10 page 246-249)

The following table gives the results of the F- statistics and ticks in the table 31 indicate to those variables or combinations of variables in which there is a greater than 95 % probability, and there is a significant difference between the population means. The results of the main effects are similar to those of the T- tests . Of the two - way effects only the combination of HEATxWELD gives a significant result for the yield stress, U.T.S. and % elongation.

A possible interpretation of this result is that the presence of extra sulphide particles in the weld has a greater effect on these mechanical properties when the steel has been subjected to a previous thermal history of water quenching and tempering compared with normalising. It is also true to say that there is a greater degree of uncertainty with this second order effect than with the main effects. There is no evidence for existence of three-way interactions.

	Main effects			Two - way interactions			Three - way interactions
	Heat	Weld	Env	HxW	HxE	WxE	HxWxE
YS	/	-	-	/	-	-	-
U.T.S	/	-	-	/	-	-	-
F.S	-	/	/	-	-	-	-
Elon.	/	/	/	/	-	-	-
RA	-	/	/	-	-	-	-

Table 31 Analysis of variance

There is no evidence that the magnitude of the effect of the environment is linked to the previous history of the specimens.

4.2.3 REGRESSION MODELLING

The results were first divided into two sections - one in which the specimens all fractured through the parent plate and the other in the specimens all failed through the welded zone. The mechanical property parameters was chosen as the dependent variable and multiple linear regression models were derived for yield stress, U.T.S, fracture stress, % elongation and % reduction in area in turn. The independent variables that were included were the main effect HEAT, WELD, and ENVIRON, the two way effects HEATxWELD, HEATxENVIRON, and WELDxENVIRON, and the three way effect HEATxWELDxENVIRON. (Appendix 8.11-8.12 page 250-253)

The forward method of regression analysis was used in which the most significant variable was searched for and then other variables were added one at a time to improve the goodness of fit. This continued until a cut - off situation was reached in which the F-statistics probability of the next likely variable was less than or equal to 0.05.

The following gives the results of the regression models for the parent plate and welds for each mechanical property parameter. The associated % goodness of fits (% r^2 statistics) are also included.

<u>Yield stress</u>		<u>Goodness of fit</u>
Parent plate	YS = 344.11 + 154.31xHEAT - 96.08xHEATxWELD	57%
Weld	YS = 446.62 - 48.57xWELD +27.76xHEAT	67%
<u>U.T.S</u>		
Parent plate	U.T.S = 482.67 + 94.73xHEAT	50%
Weld	U.T.S = 572.00 - 72.00xHExWELDxENVIRON	29%
<u>ES</u>		
Parent plate	F.S = 866.47 - 583.75xENVIRON + 281.24xHEAT	61%
Weld	F.S = 1038.50 - 516.5xWELD - 590.5xENVIRON +417.83xWELDxENVIRON	84%
<u>ELONG</u>		
Parent plate	ELONG = 22.83 - 4.67xENVIRON	17%
Weld	ELONG =13.25 - 12.46xWELD - 10.25xENVIRON +11.44xNOTCH + 6.62xHEAT + 6.02xWELDxENVIRON	96%
<u>RA</u>		
Parent plate	R.A = 66.73 - 38.43xENVIRON + 16.95xHEATxENVIRON -19.25xHEATxWELDxENVIRON	89%
Weld	R.A = 55.08 - 25.39xWELD - 28.03xENVIRON + 30.34xWELDxENVIRON - 15.50xHETAxWELDxENVIRON	96%

Table 32 Comparison of regression results

In all these models the constant represents the average result for the control condition i.e normalised steel, no sulphur addition, no H₂ in the environment and no machined notches. When the regression model was relatively simple the goodness of fits were poor indicating that multiple linear relationships were not appropriate. In these cases where the goodness of fit is high (i.e ~ 90% or more) then the model was complex and difficult to interpret in a logical fashion.

In general terms it can be seen from the pattern of results that quenching and tempering tends to raise the mechanical property stress parameters as opposed to normalising; and that introducing either sulphur into the welds or hydrogen in to the environment tends to reduce either the engineering stresses or the ductilities.

4.3 FINITE ELEMENT RESULTS

In order to model the behaviour of the specimens the PAFEC finite element package was used. Figure 59 is an example of the input data representing the geometry, loads and restraints bearing on the tensile test piece. Also included is a description of the plasticity parameter.

The output from PAFEC comes in the form of output files which contain the displacement and stresses for each node. The output files are very large, and difficult to interpret hence the output is best represented graphically. In this form of output the specimen shape is drawn and the displacements occurring during deformation are superimposed. Stress contours can also be obtained. Figures 58,60 and 61 represent examples of graphical outputs for various specimens.

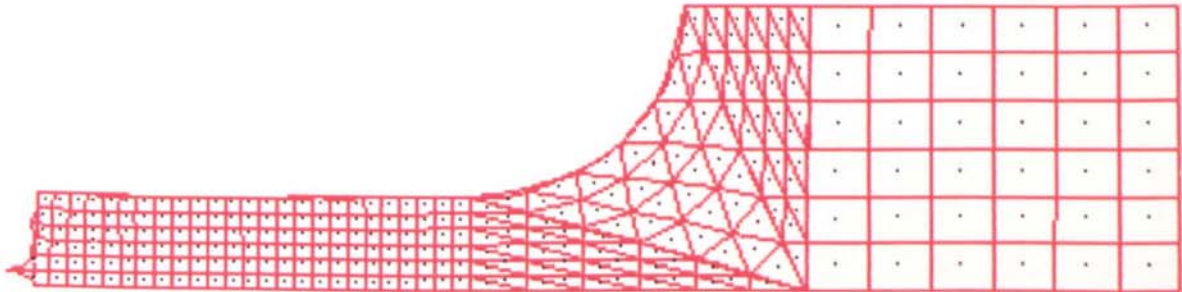


Figure 58 A typical graphical output from a PAFEC data file representing a deformed specimen.

```

$ TY WNW1.DAT
TITLE WNW1 WATER QUENCHED SPECIMEN WITH NO WELD (AIR TEST)
C
CONTROL
CONCATENATE,OUTPUT
PLASTIC
PHASE=10
CONTROL.END
MODES
MODE NUMBER      X      Y
  1              0      0
  2              7      0
  3              0      6
  4              7      6
  5             25      0
  6             25      6
  7             45      0
  8             37      18
  9            33.565  9.435
 10             45      18
 11             68      0
 12             68      18

ELEMENTS
PROPERTIES-1
NUMBER  ELEMENT TYPE      TOPOLOGY
  1     36210             1 2 3 4
  2     36210             2 5 4 6
  3     36110             5 7 6
  4     36110             6 7 8 0 0 9
  5     36110             7 8 10
  6     36210             7 11 10 12

PAFBLOCK
BLOCK NUMBER  TYPE  ELEMENT TYPE  N1  N2  N3      TOPOLOGY
  1           1     36210         1   2   0      1 2 3 4
  2           1     36210         3   2   0      2 5 4 6
  3           2     36110         2   2   2      5 7 6
  4           2     36110         2   2   2      6 7 8 0 0 9
  5           2     36110         2   2   2      7 8 10
  6           1     36210         2   2   0      7 11 10 12

MESH
REFERENCE      SPACING LIST
  1             7
  2             6
  3            18

PLATES AND SHELLS
PLATE NUMBER  MATERIAL NUMBER  THICKNESS
  1             11             6

MATERIAL
MATERIAL NUMBER      E      NU      RO
 11                 20923      0.3    7800E-9

LOADS
CASE OF LOAD  NODE NUMBER  DIRECTION OF LOAD  VALUE OF LOAD
  1            1            1            - 516
  1            48           1            - 2064
  1            71           1            - 1032
  1            16           1            - 2064
  1            115          1            - 1032
  1            136          1            - 2064
  1            3            1            - 516

RESTRAINTS
NODE NUMBER  PLANE  DIRECTION
 11           1      1
 11           2      2
 12           1      1
 12           2      2

INCREMENTAL

 11           1      1
 11           2      2
 12           1      1
 12           2      2

INCREMENTAL
GAUSS.PRT  DISP.PR  NODAL STRESS.PRT  STEP LIST
 1          1          1          85 15

YIELD
PLASTIC GROUP
 1          1

PLASTIC
PLASTIC TYPE  PROP
 1           1  SBI 2080

STRESS ELEMENT
START FINISH  STEP
 1    1000    1

IN.DRAW
DRAWING NUMBER  TYPE NUMBER
 1              3

OUT.DRAW
DRAWING NUMBER  PLOT TYPE
 2              20

END OF DATA
$

```

Figure 59 A typical PAFEC input data file.

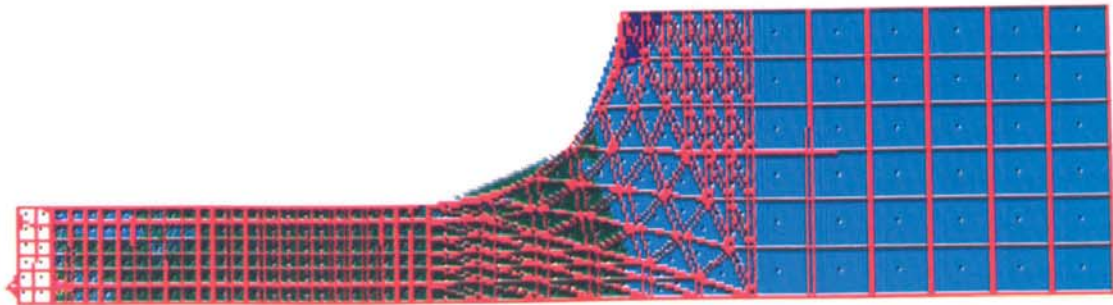


Figure 60 A typical graphical output from a PAFEC data file representing the superimposed deformed specimen.

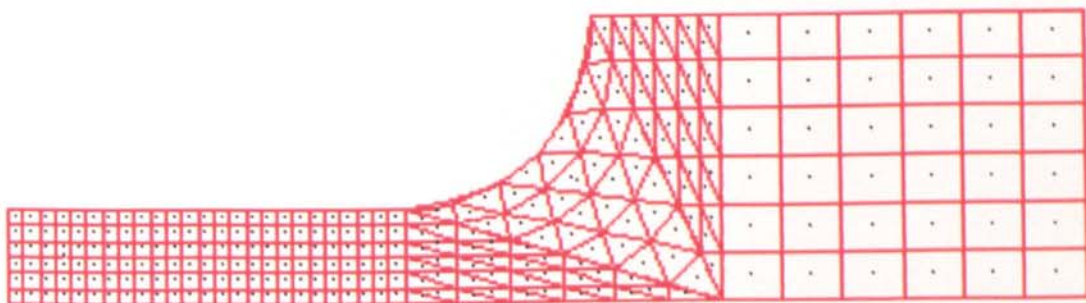


Figure 61 A typical graphical output from a PAFEC data file representing an undeformed specimen.

4.4 ANALYSIS OF THE FINITE ELEMENT RESULTS

From the graphical output of the PAFEC, the way in which elongation was divided between the parent plate and the weld was recorded. For the comparison of this data and the actual test results tables 33-35 were compiled. In these tables the elongations of plane and welded specimens in three environments for both the experimental and the finite modelling results are given. The elongations are expressed in terms of ratios of total gauge length for example;

Experimental extension:

$$\begin{array}{rcl}
 \text{Parent plate exp.} & = & 10.5 \\
 & & \frac{10.5}{14.8} = 0.71 \\
 \text{Weld exp.} & = & 4.30 \\
 & & \frac{4.30}{14.8} = 0.29 \\
 \text{Total exp.} & = & 14.8 \\
 & & \frac{14.8}{14.8} = 1.00
 \end{array}$$

Specimen	Air(Exp.)	Air(Mod.)	Corr(Exp.)	Corr(Mod.)	Hyd.(Exp.)	Hyd.(Mod.)
HNW						
PP	1.00	1.00	1.00	1.00	1.00	1.00
Weld	0.00	0.00	0.00	0.00	0.00	0.00
Tot. Elon	1.00	1.00	1.00	1.00	1.00	1.00
HG						
PP	0.71	0.77	0.74	0.83	0.82	0.86
Weld	0.29	0.23	0.26	0.17	0.18	0.14
Tot. Elon	1.00	1.00	1.00	1.00	1.00	1.00
HB						
PP	0.86	0.92	0.84	0.82	0.86	0.88
Weld	0.14	0.08	0.16	0.18	0.14	0.12
Tot. Elon	1.00	1.00	1.00	1.00	1.00	1.00

Table 33 Comparison of the experimental and finite element modelled results for the normalised specimens in terms of ratios.

- * HNW1 Normalised without weld
- * HB Normalised with defective weld
- * Tot.Elon. Total elongation
- * HG Normalised with sound weld
- * PP Parent plate

Specimen	Air(Exp.)	Air(Mod.)	Corr(Exp.)	Corr(Mod.)	Hyd.(Exp.)	Hyd.(Mod.)
ONW						
PP	1.00	1.00	1.00	1.00	1.00	1.00
Weld	0.00	0.00	0.00	0.00	0.00	0.00
Tot. Elon.	1.00	1.00	1.00	1.00	1.00	1.00
OG						
PP						
Weld	0.70	0.85	0.72	0.82	0.73	0.82
Tot. Elon.	0.30	0.15	0.28	0.18	0.27	0.18
OB	1.00	1.00	1.00	1.00	1.00	1.00
PP						
Weld	0.80	0.83	0.81	0.88	0.78	0.81
Tot. Elon.	0.20	0.17	0.19	0.12	0.22	0.19
	1.00	1.00	1.00	1.00	1.00	1.00

Table 34 Comparison of the experimental and finite element modelled results for the oil quenched and tempered specimens in terms of ratios.

- *ONW Oil quenched and tempered, without the weld.
- *OG Oil quenched and tempered, with sound weld.
- *OG Oil quenched and tempered, with defective weld.

- * PP Parent plate.
- * Tot. Elon. Total elongation.

Specimen	Alr(Exp)	Alr(Mod)	Corr(Exp)	Corr(Mod)	Hyd(Exp)	Hyd(Mod)
WNW						
PP	1.00	1.00	1.00	1.00	1.00	1.00
Weld	0.00	0.00	0.00	0.00	0.00	0.00
Tot. Elon.	1.00	1.00	1.00	1.00	1.00	1.00
GW						
PP		0.69		0.69		0.71
Weld		0.31		0.31		0.29
Tot. Elon.	1.00	1.00	1.00	1.00	1.00	1.00
BW						
PP		0.73		0.76		0.53
Weld		0.27		0.24		0.47
Tot. Elon.	1.00	1.00	1.00	1.00	1.00	1.00

Table 35 Comparison of the experimental and finite element modelled results for the water quenched and tempered specimens in terms of ratios.

- * WNW Water quenched and tempered, without the weld.
- * GW Water quenched and tempered, with sound weld.
- * BW Water quenched and tempered, with defective weld.

- *PP Parent plate
- * Tot. Elong. Total elongation

In subsequent tables 36-38 the elongations predicted by the model and that obtained in the experiment are expressed in terms of the % elongation calculated individually for the parent plate the weld and the combination of both. For example for the specimen without a weld the 50 mm parent plate was extended to 67 mm hence a % elongation of 34%. For a specimen containing a weld the % elongation for weld and parent plate was calculated separately. So for a 14 mm weld which was extended to 17.92 mm % elongation of 28% is obtained and the parent plate for the same steel has extended from 36 mm to 40.8 mm, % elongation of 30%. The overall extension calculated would not be the sum of these elongations but calculated separately i.e a 50 mm composite parallel length which has extended to 58.72 has a % elongation of 30 % etc.

Specimen	Air(Exp.)	Air(Mod.)	Corr(Exp.)	Corr(Mod.)	Hyd.(Exp.)	Hyd.(Mod.)
HNW						
PP	34	22	28	18	26	18
Weld	00	00	00	00	00	00
Tot. Elon.	34	22	28	18	26	18
HG						
PP	30	14	29	17	23	09
Weld	28	10	23	07	11	03
Tot. Elon.	30	13	27	12	19	07
HB						
PP	33	17	26	09	26	10
Weld	12	03	13	05	10	03
Tot. Elon.	27	13	21	08	21	08

Table 36 Comparison of the experimental and finite element modelled results for the normalised specimens in terms % elongations.

Specimen	Air(Exp.)	Air(Mod.)	Corr(Exp.)	Corr(Mod.)	Hyd.(Exp.)	Hyd.(Mod.)
CNW						
PP	19	15	20	12	19	12
Weld	00	00	00	00	00	00
Tot. Elon.	19	15	20	12	19	12
HG						
PP	29	13	30	13	23	11
Weld	28	05	27	07	20	05
Tot. Elon.	28	11	29	11	22	09
HB						
PP	29	11	27	13	19	08
Weld	17	05	15	04	10	05
Tot. Elon.	25	10	24	10	16	07

Table 37 Comparison of the experimental and finite element modelled results for the oil quenched and tempered specimens in terms of % elongation.

Specimen	Air(Exp.)	Air(Mod.)	Corr(Exp.)	Corr(Mod.)	Hyd.(Exp.)	Hyd.(Mod.)
WNW						
PP	16	10	16	10	13	09
Weld	00	00	00	00	00	00
Tot. Elon.	16	10	16	10	13	09
GW						
PP		11		09		07
Weld		11		10		07
Tot. Elon.	16	10	20	10	14	07
BW						
PP		06		06		04
Weld		05		05		03
Tot. Elon.	07	06	07	06	04	04

Table 38 Comparison of the experimental and finite element modelled results for the water quenched and tempered specimens in terms of % elongations.

In tables 39 and 40, the % elongation for the modelled results are shown as a proportion of the actual experimental results. The mean value from table 36 for the modelled values are 66% of the actual experimental results, the remaining 34 % which is not shown in the finite element analysis could be due to the metallurgical factors. Figures 62 - 64 are used to represent the comparative data obtained for the experimental and finite element results.

Table 40 simply converts the difference between the modelled and the experimental results into percentage for example;

$$\text{HNW Air test} \quad \frac{\text{Mod.}}{\text{Exp.}} = \frac{22}{34} = 65\%$$

Specimen	Air	Corrosion	Hydrogen
HNW			
(Exp.)	34	28	26
(Mod.)	22	18	18
ONW			
(Exp.)	19	20	19
(Mod.)	15	12	12
WNW			
(Exp.)	16	16	13
(Mod.)	10	10	09

Table 39 % elongations for the experimental and finite element modelled results.

Specimen	Air	Corrosion	Hydrogen
HNW (Mod.)	65	64	69
ONW (Mod.)	79	60	63
WNW (Mod.)	63	63	69

Table 40 Elongation of the modelled results as a % of the actual experimental results.

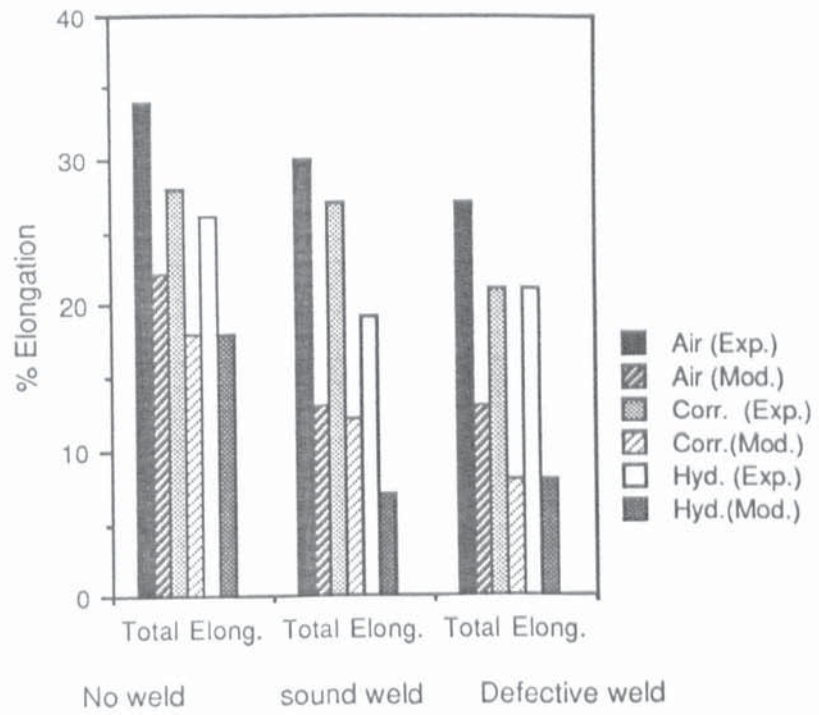


Figure 62 % Elongation for Normalised specimens.(Graphical presentation of table 36)

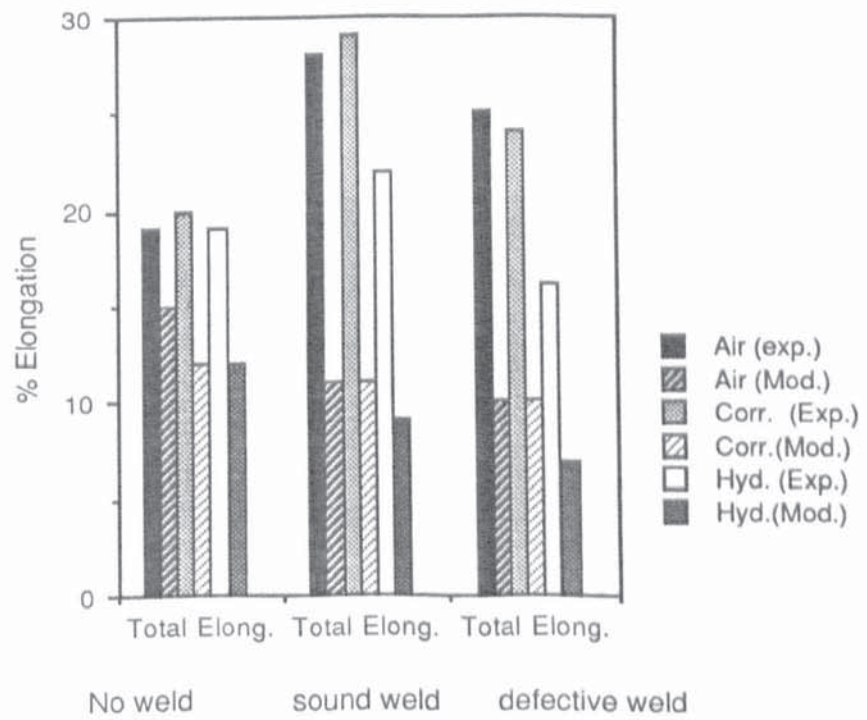


Figure 63 % elongation for OQ and tempered specimens

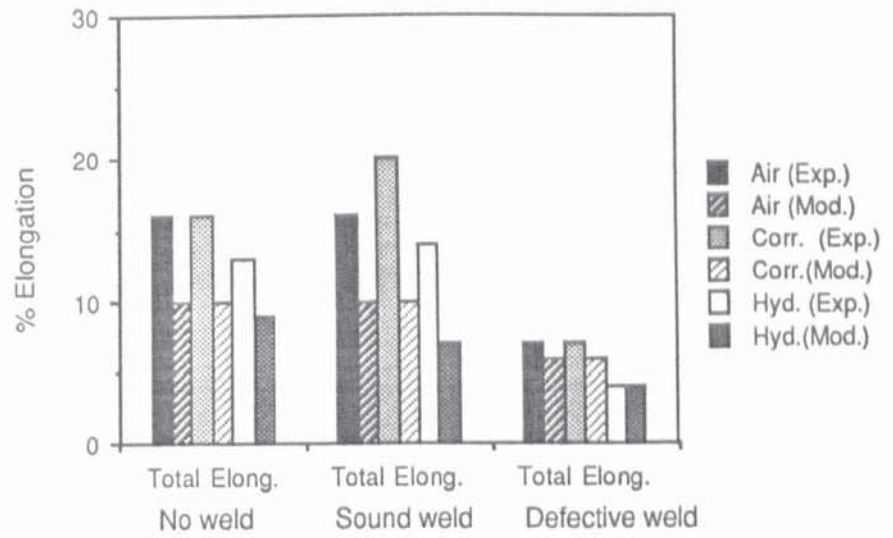


Figure 64 % Elongation for water quenched and tempered specimens

CHAPTER 5

DISCUSSION OF THE RESULTS

5.0 DISCUSSION OF THE RESULTS

5.1 OVERVIEW

Throughout the whole of this project only one type of steel has been examined. The reason for this is that it was considered important for the research to concentrate on the behaviour of a steel normally specified by the offshore industry for the key nodal components of the supporting jackets. Normally these steels are manufactured by hot rolling from the ingot stage and will thus exhibit directionality of mechanical properties. Moreover it is possible to give various heat treatments to the rolled steels and this research has considered these combinations of variables.

The nodal joints are effectively welded tubes and therefore the performance of these welds needed to be investigated closely under conditions that represented various types of environment found in the North sea. Specimens without welds were included in the experimental design for control purposes so as to give a yard stick of comparison. During welding, under conditions found in the offshore construction yards, it is possible for some contamination to take place in the weld pool and the research simulated this possibility by a small addition of FeS or not to the weld pool so that the local sulphur content of some welds was raised. This then enables the sensitivity of the steel to such contaminations to be studied.

The performance of the steels in the different environments was measured through mechanical property tests and fractographic and metallographic examinations. Finally finite element simulations of the mechanical property tests were conducted to produce some evidence of the relative importance of mechanical and metallurgical factors in determining the overall behaviour of the material.

5.2 DIRECTIONALITY OF THE SPECIMEN

To test whether any directionality in the specimens brought about by the processing conditions had any influence on the mechanical property results, plain tensile test specimens were cut from the longitudinal and transverse directions of the hot rolled sheet. As shown in figures 107-108 appendix 6, there was no significant difference

found in our tests between the yield stresses, ultimate tensile strengths or elongation to failure of the steels cut from the two different directions. Metallographic examination showed some elongation of the ferrite grains in the rolling direction but this elongation was small compared to the considerable distortion of the grain adjacent to any fracture surface. The steel used in this research has relatively low S and P contents and is a fairly pure material. Consequently it is very ductile and the considerable ductility masks any differences due to directional effects. For this reason this factor was not explored further.

5.3 HEAT TREATMENT

The heat treatments were chosen to develop different metallographic structures and hence varying strengths and ductilities. This was done because all the tests in this research were based on one batch of steel. In the commercial world steels from different batches will have a range of chemical compositions and hence strength and ductilities, even though they are manufactured to the same nominal specification. Different heat treatments were therefore used to create steels possessing a range of properties in order to investigate the relationship between the mechanical properties of the steel and its durability under conditions normally experienced by offshore installations.

Metallographic examination showed the significant difference between the various heat treated structures to be one of scale. The statistical analysis of the results showed that heat treatment was a significant variable affecting both the yield stress and the U.T.S of the steel. The regression models page 148-table 32 demonstrated that for the parent plate there was a positive coefficient associated with the variable HEAT in relation to the dependent variables yield stress and U.T.S. This shows that heat treatments that involve quenching and tempering of the steel give consistently higher strength than normalising. This can either be attributed to the finer scale of the structures (i.e. Petch strengthening) or due to the different shape and distribution of the carbides which vary from a lamellar form for normalised steel to a finer more uniformly dispersed form for the quenched steels. It is probable that both of these factors play a role in increasing the strength of the steels.

The ductility of the steels as measured by percent elongation and percent reduction in area is more affected by the conditions of welding and the type of environment than the heat treatment. The regression models are quite complicated and are difficult to interpret although the T-tests values are respectively +3.01 (appendix 8.1 page 231) for the comparison of normalised and water quenched specimens and +4.27 (appendix 8.2 page 233) for the comparison of oil quenched and water quenched specimens) . This shows that in each case the elongations of the water quenched and tempered are significantly lower than those of other heat treatments.

This is compatible with the classical concept of strength and ductility being inverse properties and is related to the degree of ease or difficulty that dislocations are able to move through the structure during plastic deformation. The finer particles produced by water quenching and tempering are more probably effective as barriers to moving dislocations than coarser ones.

When a fusion weld is introduced into a specimen the yield strength and ductility is usually different from that of the parent plate owing to the high rates of cooling from the austenite region when the weld is formed. Examination of the mechanical properties of the normalised and oil quenched and tempered specimens compared with the welded specimens (figures 47-48 page 135-136) showed that the cooling rates of the welds were in excess of those normally experienced during air cooling and oil quenching. However the properties of the water quenched and tempered steels were similar to those of welded structures (figure 49 page 137) and this indicates that the rate of cooling during welding is of the same magnitude to water quenching. This result has been brought about by the relatively thin section of the composite tensile test piece.

When the welded specimens are considered the coefficient relating to variable HEAT is much lower (27.76 compared to 154.31, table 32 page 148) indicating a weaker influence. This is because welding the specimen imposes a new quenching and tempering heat treatment making the previous treatment less relevant in influencing the ultimate strength of the material

Overall the influence of heat treatment is predictable in terms of the different types of structure produced and the greater variations possible in the manufacture of the welds is always likely to override the influence of variations in heat treatment.

5.4 THE WELDED JOINTS

In some of the mechanical property tests material was machined from the edge of the specimen to reduce the cross-sectional area locally in the vicinity of the weld in order to force deformation in the welded region of the composite test pieces. This was necessary in order to be able to measure the mechanical properties of the welded region. As the T-test results show (Table 30 page 145) only the reduction in area results are significantly different for those specimen in which the deformation has been forced through the weld by the introduction of a notch, the T-value being +2.97 (appendix 8.5 page 239) This indicates that the ductility of the weld is significantly lower than that of the plain specimen even though both have received the same treatments.

The reduction in area is a measure of ease of cavity or void formation and elongation during the final stages of deformation prior to failure; the lower the reduction in area the more readily these defects form during the local contraction of the specimens. When welds are created gas from the atmosphere can be absorbed into the weld pool and this can result in oxide formation or even porosity if the oxides are instable (see figure 38 page 117). Any particle can act as a nucleus for a cavity, or a pore can become one itself, and thus contribute to a lower reduction in area during localised deformation.

The macroscopic structure of the weld also has to be taken into account for the failure characteristics of the welded region is partly affected by the considerable structural difference between the weld and the parent plate. The boundary between the two zones is a region of plastic constraint.

This view is reinforced by the revelation that the fracture path follows the boundary between the two structures. Also due to the geometry of the weld in relation to the tensile axis of the specimen, the boundary line approximates to the direction of the maximum shear stress in the mechanical test causing the ultimate weld failure to be a shear fracture (figure 66). This is in contrast to the conventional ductile fracture mechanism of the parent plate where no boundaries of strain concentration occur.

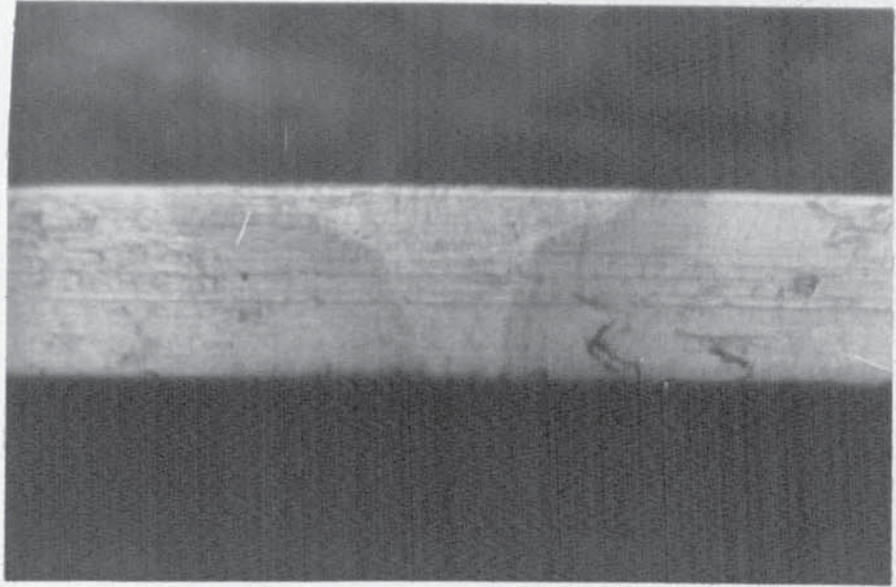


Figure 65 The boundary between different welded zones

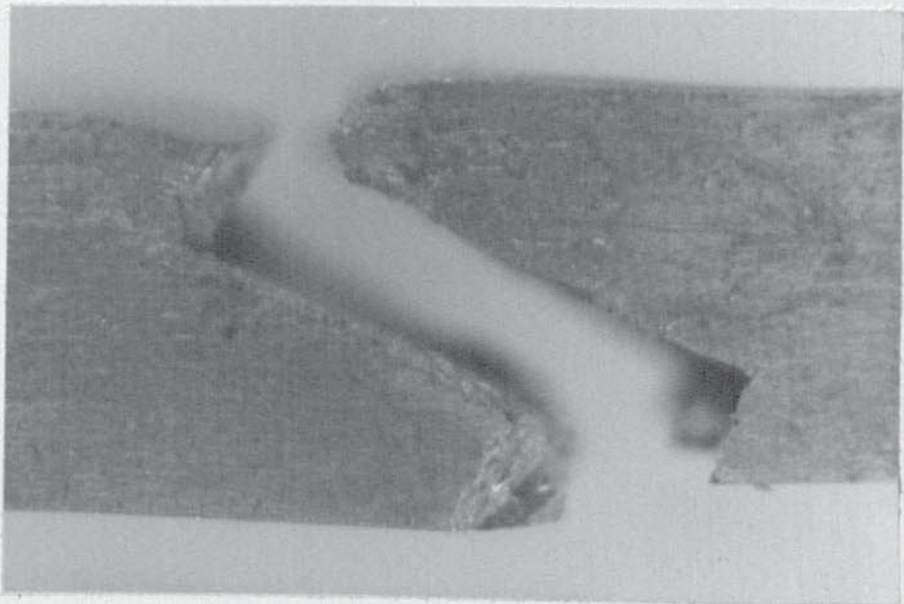


Figure 66 The ultimate weld failure shown as a shear fracture.

Iron sulphide was introduced into the weld pool of some of the welds to simulate the production of an inferior weld which generally would not be detected by conventional NDT techniques or show any indication on its surface that there was a reduction in quality. Not all of the iron sulphide would actually dissolve into the weld-pool for most would remain on the surface and eventually be removed when the welds were dressed. The small amount of iron sulphide which did dissolve would then diffuse through the fusion zone in the form of S^{2-} ions and recombine with Fe^{++} atoms during the transformation of the steel through the austenitic region.

As indicated above the critical region is the boundary between the fusion zone and the heat affected zone. The metallographic evidence points to a higher concentration of sulphide particles in this region than elsewhere and using quantitative metallographic techniques the local S concentration is estimated to be 0.037% S compared to the 0.005% S in the clean steel. Conventional chemical analysis is not appropriate in this context because of the difficulty of sampling from this critical boundary zone. However it is appropriate to examine the details of the fracture surfaces using the great depth of field of the scanning electron microscope.

These fractographs (Figure 54-57 page 141-142) reveal the dimples associated with conventional ductile failure and in the case of the specimens containing the higher localised sulphur contents, they show individual sulphide particles associated with some of the dimples. The particles can be seen in figure 55 page 141 to be approximately spherical in shape and $0.4\mu m$ in diameter. In these fractographs there is a range of dimple sizes but those specimens that have higher sulphur contents generally exhibit average dimple sizes about twice those of the very low sulphur content steels. Thus there is some evidence of a direct relation between the sulphur content and the ease with which cavities are nucleated. The T-test which analysed the results of the sound and defective welds gave a T-value of 1.96 (appendix 8.4 page 237) which was significant at 94% level, although missing the previous cut-off point of 95%.

The main effect of the sulphide particles is to form incoherent boundaries with the matrix which can act as nuclei for crack growth along the lines of maximum shear stress. The fractography supports this view because the only difference in morphology of the fracture paths were due to the difference in ductility between the good and the deliberately contaminated welds.

The Department of Energy Guidance on the design and construction of offshore installations, third edition 1984, states that welded steel structures shall be examined by an appropriate NDT technique after the final heat treatment. But no particular guidance has been given on defect acceptance levels except that they should be agreed between the owner and the certifying authority. It is most unlikely that sulphide particle $0.4\mu\text{m}$ in diameter would be detected by any NDT method of examination. Thus it can be concluded that the 25% decrease in % reduction in area due to defective welds in these experiments would not be avoided by the rejection of the constructions after the NDT examinations.

5.5 THE EFFECT OF THE ENVIRONMENT

5.5.1 THE AIR TESTS

The mechanical properties of all of the specimens within the environmental matrix were tested in air primarily for purposes of control. It is assumed that air is an inert medium for room temperature tests and that in the results of these tests the environment plays no part.

5.5.2 THE CORROSION ENVIRONMENT

In this series of tests the specimens are being deformed plastically at the same time as the steels are corroding within an electrolytic cell. The potentiostatic conditions within the cell ensures that when either the specimen dimensions change due to deformation or that films due to the formation corrosion products build up on the surface of the specimens, then the cell voltages do not change and the rate of corrosion is kept constant. The combination of cell potential and current density has also been controlled within fine limits to prevent either passivity, cathodic protection or pitting of the specimen taking place during the test.

These conditions then create an environment which would theoretically be suitable for developing stress corrosion cracking conditions within the specimen providing the mechanical conditions are suitable. To ensure this latter point the strain rate of all the tests was confined to 10^{-4} S^{-1} which corresponds to a rate of deformation at which the phenomenon of stress corrosion cracking has been observed in other constructional steels.

The results of all the corrosion tests had two things in common. One was that the phenomenon of stress corrosion was never observed, and the other was that once allowance had been made for loss of metal by dissolution during the corrosion tests then there was no significant difference in the mechanical properties compared with the air tests.

This is underlined by the T-tests conducted on two groups of specimen, one being those that had been subjected to the potentiostatic conditions and the other being the control air tests. In every case any differences that were observed between the means of the test results for the two groups were a function of the size of the sample. These same differences could have been observed simply by random selection from the population as a whole.

There are two possible explanations of these results. One is that the steels used in this investigation are simply not susceptible to stress corrosion cracking. This is not an unreasonable conclusion because this particular grade of steel has been chosen for use in the North sea because of its reported (1, 5, 6) stability in this respect. An alternative explanation concerns the actual rate of corrosion. During a test lasting up to 12 hours in duration, the amount of metal loss by dissolution could be the equivalent of losing 17% of the original cross-section area of the specimen.

This represents a tremendously accelerated rate of corrosion and it has been brought about by the desire to keep the corrosion conditions within the region of the Pourblax diagram where the phenomenon of stress corrosion could possibly take place without the risk of hydrogen evolution at the surface of the specimen.

The dynamic characteristics of the tests, always ensuring that the threshold stress is exceeded, causes more rapid rates of deformation compared with what would occur in a commercial environment, and it is possible that a true balance may not have been achieved between the rates of dissolution and the rates of cracking that would be

possible at the imposed deformation rates. As indicated in the review a potent electrolyte would need to promote this critical balance between stress corrosion susceptibility and the alternative of passivity. If this critical balance was not present in the tests conducted in this work, then the phenomenon of stress corrosion could be inhibited. If this critical balance does exist for this type of steel, then the range of conditions in which it occurs is very limited indeed.

5.5.3 HYDROGEN EVOLUTION

In these tests, the potential across the electrolytic cell was reduced so that the combination of potential and current density conditions brought the specimens into the cathodic protection region of the Pourbaix diagram so that hydrogen evolution would take place at the surface of the specimen which is the cathode in the cell.

The results of all these tests had a dramatic effect on the ductility of the steel. Compared with the air tests, the biggest decrease in ductility was represented by the reduction in area results for the plain specimens. This result is confirmed by the high T-test value of 4.16 for the comparison of air and hydrogen evolution tests (appendix 8.7 page 243). The welded specimens exhibited smaller elongations, and when fracture took place it tended to occur at the boundary between the fusion and heat affected zones. This boundary was more closely followed by the fracture path in the case of the welded specimens deliberately contaminated with iron sulphide. The scanning electron fractograph (figure 55 page 141) shows clearly the presence of small FeS particles at the fracture surface.

Hydrogen can exist in two forms in these steels i.e the molecular or atomic form. To cause embrittlement hydrogen atoms need to enter the lattice to bring about the reduction in internal strain energy necessary to enable a crack to propagate more easily through the structure. The plain specimen in having few interfaces, have fewer sites where atomic hydrogen can recombine into molecular hydrogen and are therefore more prone to failure by the strain energy reduction mechanism. The welded specimens do possess these interfaces, for example between the different welding zones, and it is in these additional places where molecular hydrogen can form localised regions of high pressure.

Fracture of a steel in hydrogen can be separated into three distinct stages;

- i) Crack Initiation
- ii) Slow crack growth and
- iii) Rapid unstable fracture.

These stages can be represented by the crack growth rate/stress intensity plot (figure 19). It is the second of these stages that is the most relevant to this research and can be thought of being a direct result of the hydrogen transport process. The rate of crack growth is believed to be controlled by the rate of diffusion of the hydrogen to an area near the crack tip. Referring to corrosion fatigue crack growth data, the effect of hydrogen is demonstrated in (figure 67). Here hydrogen was generated on the specimen surface by the applied potential of -1200 mv and caused appreciable local embrittlement resulting in a marked increase in surface crack growth rate.

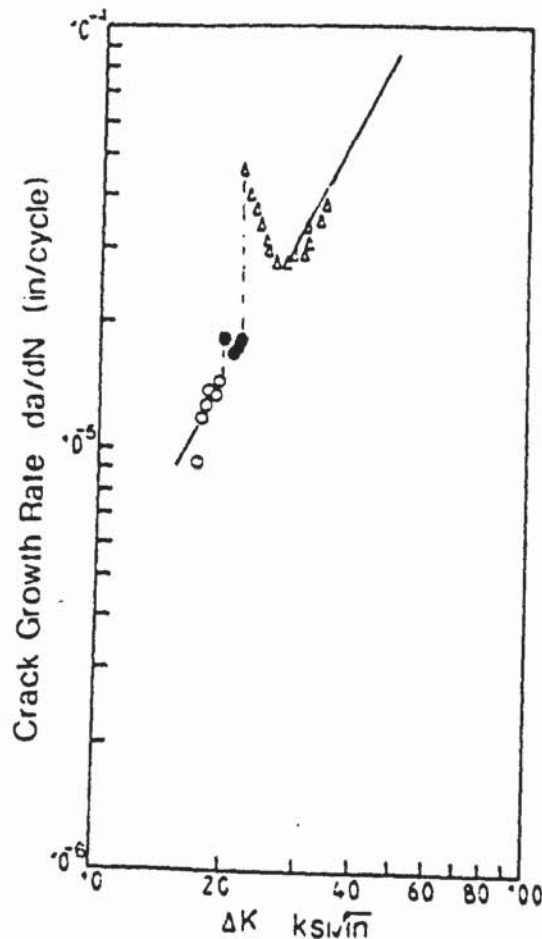


Figure 67 Corrosion fatigue crack growth data, indicating limited diffusion of hydrogen in thick specimens, 0.6 cpm open circuit; 0.6 cpm 800 mV sce.; Δ , 0.6 cpm 1200 mV sce.

The degradation of the steel under conditions of hydrogen evolution depends on the relation between the position of the crack tip and the structural feature of the steel. In plain specimens the hydrogen transport process to the crack tip depends more on lattice diffusion of atomic hydrogen, but in welded specimens there is considerably more room along the internal boundaries between the fusion weld and the heat affected zone and this gives more of an opportunity for molecular hydrogen to play a role in the embrittlement process. When welded specimens are contaminated with sulphur then in addition there are channels for diffusion at the particle-matrix interface.

The regression modelling results show that ductility as described by % elongation and % reduction in area, involves for the welded samples both the parameters WELD and ENVIRON as main effect in reducing the ductility of steel (table 32 page 148). This confirms that the sensitivity of the ductility of the steel is related to both the hydrogen evolution conditions and the sulphur contamination, and can be explained by an argument based on the easier transport of hydrogen to the crack tip along structural features which have greater atomic discontinuities than are associated with the lattice and grain boundaries in plain specimens.

5.6 THE FINITE ELEMENT ANALYSIS

When the choice of specimen dimensions was made a number of considerations were involved. One was that the specimen thickness of 6 mm was selected in order that when the testing was performed the result would be representative of the bulk material. It was important to ensure that plane stress conditions did not exist otherwise the tests could not fail by a fracture mechanism typical of the bulk material which is brought about by the presence of triaxial stresses. Once the thickness was chosen the width/thickness ratio had to be controlled within relatively fine limits. A second consideration was that the loads at which the specimens would deform plastically had to be comfortably within the 10 tonne capacity of the Mand testing machine.

A consequence of these constraints on specimen dimensions was that during deformation not all the plastic flow was confined to the gauge length, but significant distortions in the regions of the fillets took place due to some stress concentration in that area. Although this did not directly affect the quoted mechanical property results because the strength and ductilities were calculated from gauge length dimensions, and fillet areas were protected in the environmental tests; the patterns of flow should be considered in the specimen as a whole rather than just confining ones attention to the gauge length.

To provide more information on this, each type of test within the experimental matrix was subjected to a finite element simulation which would predict flow in the specimen as a whole and provide a basis for comparison with the actual mechanical property tests. These simulations do not represent true plastic deformation, but an approximation of it. The strain to fracture of a given specimen was divided into a number of regions and a linear elastic simulation using different values of apparent modulus (to simulate work hardening) was concluded for each strain increment in succession until the simulated specimen had exhibited the same strain to failure as the actual test.

From the finite element analysis plots, the way in which the strain to failure was divided between the gauge length and the fillets was recorded. When this data was compared with the actual tests, it was possible to compile tables 33-35 page 153-155 which give the elongations of tests on plain and welded specimen in the three environments both for the actual experimental tests and the finite element modelling. In subsequent tables 36-38 page 156-158 the actual elongations occurring in the parent plate and the welded zones are given as well as the total elongation for the test piece as a whole. The values obtained for the finite element model are compared with

the values obtained from experiment.

In each case the elongation in the gauge length predicted by the model is less than that occurring in the tests, and the results were independent of the nature of the environment. The difference is due to the fact that experimental tests revealed localised as well as general deformation as the failure point was approached. The finite element analysis could only simulate general elongation. The localised deformation is brought about by the gradual development of voids or cavities with strain which ultimately link up to cause internal tears which then gradually grow to give rise to ruptures leading to ductile failure.

Table 39 page 159 gives the elongation of the modelled results as a % of the actual experimental results. The modelled results are consistently lower than the experimental results and the amount is fairly consistent (with one exception) for the air, corrosion, and hydrogen evolution tests in normalised, unnotched samples. This consistent difference is interpreted to imply a consistent amount of localised deformation occurring in tensile test specimens just prior to fracture.

Because these were unnotched specimens and the weld was stronger than the parent plate for the normalised structures, the failure always took place with the parent plate zone of the composite specimens. The amount of localised deformation then appears to be independent of the environment to which the specimens are subjected. This is the main conclusion that stems from the dual metallurgy / continuum approach used in this research. This is a result that was expected for the comparison of the air and corrosion tests for there was plenty of evidence to show that corrosion did not modify the mechanical properties of the steels, but merely weakened them through the reductions in cross sectional area. But in the case of hydrogen evolution conditions genuine embrittlement took place.

However as can be seen in figure 70 appendix 6 the fall in stresses prior to failure was more abrupt. This is due to rapid crack propagation as opposed to more gradual development of cavities in the other tests, although in the case of the hydrogen evolution the rate of fall of the stress is many times higher in air tests, the magnitude of the fall before failure is little different from the air tests. This observation gives some supports to the dual metallurgy / continuum approach as it appears in the case of the hydrogen tests that the amount of localised deformation and / or fracture is similar to the air tests but is confined in a much smaller volume of the specimen due to the difference in mechanism when localised failure takes place.

Even in the case of the plain specimens embrittled by hydrogen, there was still the same proportional amount of localised deformation prior to the failure and no truly brittle fracture caused by a cleavage mechanism occurred. These results give more evidence to the pressure theory of hydrogen embrittlement than to the strain energy reduction mechanism. Similar comparisons for the welded specimens (table 39-40 and figures 62-64 page 159-161) show a significant reduction in the amount of elongation predicted by the finite element simulation compared with the plain specimens. The explanation lies in the nature of the welded zone which, in consisting of regions where the mechanical properties vary quite considerably, cause strain concentrations and produce areas of constraint.

Although the finite element modelling takes into account the varying mechanical properties, it did not take into account the detailed structure of the weld when considered in three dimensions. The net effect of this discrepancy causes the model to predict lower gauge length elongations than those obtained by experiment.

As with the plain specimens the different environments do not give rise to further discrepancies in the model predictions and the same applies to the deliberately contaminated welds. This indicates that the balance between localised and general deformation in the welded specimen is not a function of the environment or purity. This supports the conclusion that corrosion, hydrogen embrittlement or sulphide particles may modify the stresses and strains at which fracture may take place, but do not fundamentally alter the manner in which the deformation takes place. Corrosion and sulphide particles tend to reduce effective cross sectional areas and provide some interfaces, and hydrogen produces internal pressures that affect the need for such high applied stresses for deformation, but none of these mechanisms converts a ductile steel into a truly brittle one.

5.7 COMMERCIAL IMPLICATIONS

The offshore industry is concerned about the durability of the steels specified for use in North sea environments. This involves both a combination of steady stresses and fatigue. This research confines its attention to steady stresses of plain components and welds in corroding conditions.

Because of time limitations imposed on this work, the environmental tests had to be considerably accelerated and it is possible that the acceleration has been so great as to limit the commercial interest in the results. Nevertheless there are some general conclusions that are worth pointing out to the industry.

- I) The choice of BS4360 for the steel specification is a good one as there is no evidence that this material is particularly sensitive to embrittlement compared with other possible materials.
- II) Whereas some marginal improvement in mechanical properties can be achieved by selecting water or oil quenching and tempering instead of normalising, the magnitude of the benefit would not justify the cost.
- III) The conditions under which the welding is done is important particularly in avoiding absorption of hydrogen through damp conditions and in appropriate pre and post weld heat treatments, and in avoiding other contamination of the weld pool. This imposes a considerable challenge in quality control in large constructional yards. Even though a weld may be satisfactory from both visual and NDT inspection, it is still possible for the weld quality to be insufficient for the North sea environment. The reductions in durability due to incomplete control of welding conditions can be greater than those brought about by the subsequent exposure of the steels to the hostile North sea elements.
- IV) Good welding practice leads to material that is stronger than the parent plate, but is still more susceptible to the rigours of the environment.

- v) General corrosion of the steels without hydrogen evolution at their surface does not reduce the durability but only reduces the load bearing capacity due to loss of metal caused by dissolution.

- vi) Corrosion conditions that involve hydrogen evolution cause significant reductions in durability. This emphasises the important of full potentiostatic control of the corrosion processes that are taking place in the immersed offshore structures to ensure that the electrochemical conditions correspond to the rest potential of the steel when related to the Pourblax diagram.

- vii) Finite element modelling is useful in predicting the outcome of uniform deformation conditions, but not involving local deformations prior to fracture processes. Its applicability in durability analysis is thus limited.

CHAPTER 6

CONCLUSIONS

6.0 CONCLUSIONS

- 1) Differences in the variation of mechanical properties with specimen direction are completely masked by the high ductility of what is considered to be a clean steel.
- 2) The heat treatments that produced finer structures caused enhance yield stresses and lower ductilities through making the passage of dislocations from one grain to another more difficult during the plastic deformation.
- 3) The rate of cooling during the welding of the composite test pieces produces structures whose mechanical properties are similar to those of water quenched and tempered specimens.
- 4) The boundary between the fusion zone and the heat affected zone of the welds acts as a surface of plastic constraint which accounts for the reduced elongation to fracture and the shear failure morphology of the fracture process. This is in contrast to the plain specimens where no such zones of strain concentration occur.
- 5) The welds which were deliberately contaminated with FeS, have slightly reduced strengths and greatly reduced ductilities. This effect has been explained by considering the sulphide particles acting as crack initiators and thereby increases the localised stresses the matrix has to bear.
- 6) It is assumed that air is an inert medium for room temperature tests and in the results of these tests, the environment plays no part.
- 7) The results of all the stress corrosion tests had two things in common, one was that the phenomenon of stress corrosion was never observed and the other was that once the allowance had been made for loss of metal by dissolution during the corrosion tests, then there was no significant difference in the mechanical properties, compared with the air tests.

- 8) The results of all hydrogen evolution tests had a dramatic effect on the ductility of the steel. Compared with the air tests the biggest decrease in ductility was represented by the reduction in area results for the plain specimens.
- 9) The welded specimens exhibited smaller elongations, and when fracture took place it tended to occur at the boundary between the fusion and heat affected zones. This boundary was more closely followed by the fracture path in the case of the welded specimens deliberately contaminated with iron sulphide.
- 10) Overall it may be inferred that in the complete set of tests there are two mechanisms operating by which hydrogen impairs the ductility of the tests. One is the strain energy reduction mechanism caused by atomic hydrogen in solution and the other is the pressure mechanism caused by molecular hydrogen at interface. The former is more appropriate for plain specimens and the latter is more relevant for the welded and deliberately contaminated specimens.
- 11) The SEM fractographs reveal the dimples associated with conventional ductile failure. The particles are approximately spherical in shape, and although the fractographs show a range of dimple sizes, but those specimens that have higher sulphur contents generally exhibit dimple sizes about twice those of the very low sulphur content steels.
- 12) T-tests analysis show that the difference between the normalising and water quenching is the only factor that significantly effects the yield stress and U.T.S results. The fracture stress and % reduction in area are significantly different in tests where the environment includes hydrogen evolution as opposed to those conducted in the neutral air test. Additionally the fracture stress is affected by higher sulphur contents in the weld, and the % reduction in area is affected by the presence of notches in the centre of the welded test pieces. The elongation results seems to be a function of heat treatment, sulphur content of the weld and presence or not of hydrogen evolution.

- 13) The results of analysis of variance indicate that the presence of extra sulphide particles in the weld has a greater effect on those mechanical properties when the steel has been subjected to a previous thermal history of water quenching and tempering compared with normalising. There is also a greater degree of uncertainty with the second order effect than with the main effects, whilst there is no evidence for existence of a three-way interactions.
- 14) When the regression model was relatively simple the goodness of fits were poor indicating that multiple linear relationships were not appropriate. In these cases where the goodness of fit is high (i.e. ~ 90% or more) then the model was complex and difficult to interpret in a logical fashion.
- 15) The results of the finite element simulations show that the elongation predicted by the model is less than that occurring in the tests. This indicates that experimental tests revealed localised as well as general deformation as the failure point was approached, whilst the finite element analysis could only simulate general elongations.
- 16) Different environments and weld contaminations do not give rise to further discrepancies in the model predictions, hence the balance between localised and general deformation in the welded specimen is not a function of the environment or purity.

CHAPTER 7

FUTURE WORK

Z. FUTURE WORK

In conducting this research a number of decisions were made to limit the scale of the problems to fit with the time and equipments limitations.

The first decision was to confine the work to one grade of steel, BS 4360 50E, which is commonly used for North Sea structures. In determining the durability the salinity and pH of the North Sea was replicated in the environmental tests and the choice of strain rate, mode of stressing, and electrochemical conditions was made to promote the phenomenon of stress corrosion cracking should the steel be sensitive to it.

The chosen steel was a medium strength version of HSLA steels and it was more likely to exhibit stress corrosion phenomenon in its water quenched and tempered condition. In the event this did not occur and there is a strong argument for basing future work on higher tenacity steels. Changing the chemical composition of the steel would necessitate re-examining the pourbaix diagram and adjusting the combination of cell voltage and current to develop optimum condition for corrosion and hydrogen evolution.

The difficulty with relying on measurements of mechanical properties based on steady stresses is the lack of information gained on crack propagation rates. Cracks can be made to propagate at modest stress levels under fatigue conditions and thereby enable the researcher to determine the relationship between the crack propagation rates and the change in stress intensity. From such data the characteristics of the embrittlement can be better understood. Thus future work should involve fatigue studies.

Because of the need for the oil rig to withstand shocks caused either by minor collisions or the pounding of waves and wind, it is important to conduct studies of the energies absorbed during fracture and the morphology of the fracture process of the welds under high strain rate conditions. This could best be done by conducting fast

bend tests on bars containing welds that were notched with root radii in either the fusion or heat affected zones.

The finite element calculations in this research considered the specimen as a thin two dimensional plate. In reality the specimen was 6 mm thick and the calculations could be refined by taking into account the through thickness dimension.

The finite element calculations were based on incremental amounts of linear elasticity with varying apparent elastic modulus at each stage to represent the work hardening process. This is a crude model and again if time permitted, it could be refined to incorporate true plastic flow by reducing the incremental width and applying power law criteria to the stress- strain relationship.

The finite element calculations for the parent plate and the weld were done separately and then added together to model the whole welded specimen. The specimen could be regarded as a single composite with varying mechanical properties to represent the parent plate, the heat affected zone and the fusion zone. The three dimensional geometry of the fusion zone would also be taken into account.

CHAPTER 8

REFERENCES

REFERENCES

1. GRAFF, W.J.
Introduction to Offshore Structures, Gulf Publishing, 1981.
2. Institute of Oceanographic Science, Data from Marine Information Advisory Service.
3. MYERS, J.J.
"Hand Book of Ocean and Underwater Engineering", Mc Graw Hill Book Co., New York, 1969.
4. HOWARD ROGERS, T.
"Marine Corrosion", George Newness LTD, London 1968.
5. COTTON, H.C.
"Materials requirements for Offshore Structures", Phil. Trans. R. Soc. London, sep. 1982.
6. COTTON, H.C.
"Welded Steels for Offshore Constructions", Proc. Inst. Mech. Eng., 1979; Vol.193, P.193.
7. WILSON, A.D.
"Characterizing Inclusion Shape Control in Low Sulphur C-Mn-Nb Steels, presented International conference on technology and application of High Strength Low Alloy Steels, Philadelphia, October 3-6, 1983, reprints 8306-012.
8. Offshore Installation: Guidance on Design and Construction ISBN 0-11-7011185, Department of Energy HMSO, London, 1984.
9. Code of Practice for Fixed Offshore Structures-BS56235, 1982, Publisher British Standard Institution.

10. Recommended Practice for Planning Design and Constructing Fixed Offshore Platforms, API-RP2A Jan. 1981.
11. "Towards Improved Toughness and Ductility", Climax Molybdenum Co. LTD.,Tokyo, 1972.
12. Microstructure and Design of Alloys Publ.No.36, The Institute of Metals/Iron and Steel Institute, London, 1973.
13. GRAY, J.M.
"Processing and Properties of Low Carbon Steel", Metallurgical Science of AIME, New York. 1973.
14. "Mechanical Working and Steel Processing", Proceedings of 14th-19th Conferences, AIME, New York, 1972-1977.
15. "Controlled Processing of HSLA Steels", Proceedings of York Conference, British Steel Corporation, 1976.
16. KORCHYNSKY, M.
"Microalloying 75", Union Carbide Corporation, New York, 1977.
17. BALLANCE, J.B.
"Hot Deformation of Austenite", AIME, New York, 1977.
18. "Structural Steels for Eighties", AIME, Warrendale, 1977.
19. " Low Carbon Steels for the Eighties", The Institution of Metallurgists, London, 1977.
20. HAESSNER, F.
"Recrystallisation of Metallic Materials", Paper presented at a seminar, Stuttgart, Rieder-Verlag GMBH, 1971.
21. "Dual Phase and Colled Processing of Vanadium Steels", Proceedings of Berlin Conference, Vanitec, 1978.

22. ROTHWELL, A.B. and GRAY, J.M.
"Welding of HSLA (Microalloyed) Structural Steels", ASM, Cleveland, 1978.
23. DOANNE, D.V. and KIRKALDY, J.S.
"Hardenability Concepts With Applications to Steels", AIME, Warrendale, 1978.
24. "Pipe welding", Proceeding of International Conference, The Metals Society, London, 1979.
25. KOT, R.A and MORRIS, J.W.
"Structure and Properties of Dual Phase Steels, AIME, Warrendale, 1979.
26. "Vanadium in High Strength Steels" , Publication No. 140, Vanitic, London, 1979.
27. "Vanadium in Rail Steels", Proceedings of Vanitec Chicago Conference, Vanitec, London, 1979.
28. "Arctic Pipe Line", Proceedings of Golden Gate Conference, San Francisco, ASM, Cleveland, 1979.
29. ABRAMS, H. , MC NAIR, G.N., NAIL, D.A, SOLOMON, H.D.
"Micon 78" Optimisation of Processing Properties and Service Performance Through Microstructural Control, STP 672, ASTM, Philadelphia, 1979.
30. SELLARS, C.M. and DAVIES, G.J.
"Hot working and Forming Processes", Proceedings of an International Conference, The Metals Society, London, 1980.
31. "Technology and Applications of Vanadium Steels", Proceedings of Vanitec Conference Karkow, Poland, Published by Vanitec, 1980.
32. DE ARDO, A.J, RATZ, G.A, and WRAY, P.J.
"Thermomechanical Processing of Microalloyed Austenite", Proceedings of Conference, Pittsburg, Pennsylvania, 1981.

33. "Steels for line pipe and pipeline fittings", (Proc. Conf.), Metals Society and Welding Institute, London, 1981.

34. KORCHYNSKY, M.
"HSLA Steels Technology and Applications", (Proc. Conf.), Philadelphia, USA, 1983.

35. HONEYCOMBE, R.W.K.
Trans. Jap. Inst. of Metal, 1983, No. 4, P. 24.

36. PAXTON, H.W.
"Alloys for Eighties", Climax. Moly. Co. LTD., London, 1981.

37. USUI, T., YAMAD, K., MIYASHITA, Y., TANABE, H., HANMYO, M., and TAGUCHI, K.
(Proc. Conf.), Scan Inject 2, 2nd International Conference on Injection Metallurgy, Papers-MEFOS-Jernkontoret, Part 2, June 1980, Lulea, Sweden.

38. SMITH, S., and HARDY, C.W.
"Refractory Selection and Engineering for Redcar 14 m Blast Furnace", Iron Making & Steel Making, 1981, Vol. 8, No. 4, P. 153.

39. PICKERING, F.B.
"Physical Metallurgy and Design of Steels", Applied Science Publication, London, 1978.

40. JONES, C.L, RODGERSON, P. and BROWN, A.
Ref. 34, P. 809.

41. INAGAKI, H., TANIMURA, M., MATSUSHIMA, I. and NISHIMURA, T.
"Effect of Cu on The Hydrogen Induced Cracking of The Pipe Line Steel", Trans. I.S.I.J, Vol.18, 1978, P. 149.

42. PICKERING, F.B
Ref. 16, P.3.

43. BELLLOT, J. and GANTOIS, M.
"Influence of Sulphur and Tellurium Compounds on The Hot Deformability and Mechanical Properties of Steels", Trans. I.S.I.J., Vol.8, 1978, P. 546.

44. SPITZIG, W.A.
"Effect and Shape of Sulphide Inclusions on Anisotropy of Inclusion Spacings and on Directionality of Ductility In Hot-Rolled C-Mn Steels",Met. Trans., Vol.15A, 1984, P.1259.
45. JONES, C.L., RODGERSON, P. and BROWN, A.
Ref. 34, P. 809.
46. LE BON, A.B. and DE SAINT-MARTIN, L.N.
Ref. 16, P. 72.
47. KOSASAN, I., OUCHI, C., SAMPEI-TAND OKITA, T.
Ref. 16, P. 100.
48. IRVINE, K.J., PICKERING, F.B., and GLADMAN,T.
Journal of Iron & Steel Institute, Vol. 205,1967, P. 161.
49. IRVINE, K.J., GLADMAN, T., ORR, J. and PICKERING, F.B.
"Controlled Rolling of Structural Steels", Journal of Iron & Steel Institute, Vol. 208,1970, P. 717.
50. COLDERN, A.P., BLISS,V. and OAKWOOD,T.G.
Ref. 32, P. 591.
51. ROBERTS, W.
"The evolution of Microstructure During Controlled Rolling",Scandinavian Journal of Metallurgy, Vol. 9, 1980, P.13.
52. HEEDMAN,P.J. and SJOSTROM,A.
"Controlled Rolling Schedules for Increased Plate Production",Ibid, Vol.9, 1980, P.21.
53. NILSSON, T.
"Controlled Rolling of Mn-Mo HSLA-Steel Plate", ibid, Vol. 9, 1980, P.69.
54. ROBERTS, W.
Ref. 34, P.33.

55. ZHENG, Y. AND DE ARDO, A. J.
Ref. 34, P.85.

56. ROBERTS,W., SANBERG, A.,SIWECKI,T. AND WARLEFORS,T.
Ref.34, P. 67.

57. COLDREN, A.P., OAKWOOD, T.G. AND TITHER,G.
Ref. 34, P. 755.

58. ALMOND, E.A., MITCHELL,P.S. AND IRANI, R.S.
Metals technology, 1979, P.205.

59. SHARP, J.V.
"The Use of Steel and Concrete in the Construction of North Sea Oil and Gas
Production Platforms", J. Material Sci., Vol. 14,1979, P.1773.

60. COTTON, H.C.
Conference Manufacturer, Fabrication and Operation of Pipe Lines,
Strachlyde, Sep. 1982 : Metals Society.

61. GRAFF, W.J.
"Introduction to offshore structures", Design fabrication and installation,
Gulf publishing co., Houston, Texas, 1981.

62. PETERSON, M.L.
"Evaluation and selection of steel for welded offshore drilling and production
stuctures", 1969, offshore technology conference preprints, paper 1075.

63. "Commentary on high restrained welded connections"
Engineering Journal, American Institute of Steel Construction, Vol. 10, No.
3, 1973, P. 61-73

64. CHANDLER, K.A.
"Marine and offshore corrosion", Butterworths book co., London, 1976.

65. SHRIER, L.L.
"Corrosion", 2nd. ed., vol. 1, Butterworths book co., London, 1976.

66. FONTANA, M.G. AND GREENE, N.D.
"Corrosion Engineering", 2nd ed., Mc Grawhill International Book co., 1983.
67. HOWARD ROGERS, T.
"Marine Corrosion", George Newness LTD, London, 1968.
68. WYATT, B.S.
Anti Corrosion, Vol. 24, 1977, P. 5.
69. SCULLY, J.C.
"The Fundamentals of Corrosion", Chapter 4, 2nd ed., Oxford : Pergamon, 1975.
70. CHILTON, J.P.
"Principles of Metallic Corrosion", Chapter 4, 2nd ed., London : The Chemical Society, 1968.
71. PARKINS, R.N.
"Corrosion", Vol.1, Section 8.19, edited by Shreir, L.L., 2nd ed. London, Newnes-Butterworths, 1976..
72. SCULLY, J.C.
"Environmental Variables and SCC Propagation Rates".
73. PHELP, E.H.
"The Interaction of Strain Rate and Repassivation Rate in Stress Corrosion Crack Propagation", Corr. Sci., Vol. 20, P. 997-1016.
74. PUGH, E.N.
"Progress Towards Understanding The Stress Corrosion Problem", Vol. 41, No. 9, Sep. 1985, Corrosion-NACE.
75. ZAPFFE, C.A., and SIMS, C.E.
1941, J. Met. Trans., AIME, Vol. 145, P. 225-259.
76. DEKAZINCZY, F.A.
1954, J. Iron Steel Inst., Vol.177, P. 85-92.

77. BILBY, B.A., and HEWITT, J.
1962. *Acta Metall.*, Vol. 10, P. 587-600.

78. TETELMAN, A.S and ROBERTSON, W.D.
Trans. TMS-AIME ,Vol.224, 1962, P. 775-783.

79. PETCH, N.O., and STABLES, P.
Nature, London, Vol. 169, 1952,P. 842-843.

80. BARNETT, W.J and TROIANI, A.R.
J. Met. Trans. AIME, Vol. 209, 1957, P. 486-494.

81. BASTEIN, P., and AZOU, P.
Proc. World Metall. Cong.; First American Society of Metals, 1951,
P.535-552.

82. LYNCH, S.P.
Met. Forum 2, 1979, P. 182-200.

83. ZIENKIEWIZ, O.C.
"The finite element method In engineering science", McGrawhill Book
company, New York, 1971.

84. RICHARDS, T.H.
"Engineering methods in stress analysis", Ellis-Horwood series in
engineering science, London, 1977.

85. MENDELSON, A.
"Plasticity : Theory and application, MacMillan, New York, 1968.

86. CRANDALL, S.H., DAHL, N.C.
"An introduction to the mechanics of solids", 2nd. ed., McGraw-Hill, New
York, 1972.

87. HOFFMAN,O., SACHS, G.
"Theory of plasticity", McGraw-Hill, New York, 1953.

88. JOHNSON, W. AND MELLOR, B.P.
"Engineering plasticity", Van Nostrand, London, 1976.
89. ZIENKIEWIZ, O.C.
"The finite element method In engineering science", McGraw-Hill, 1971.
90. ZIENKIEWIZ, O.C., PAREKH, C.J.
"Transient field problems", two dimensional and three dimensional analysis by isoparametric finite elements. IJNME 2, 61-71 , 1970.
91. HILL, R.
"Mathematical theory of plasticity," Clarendon press, Oxford, 1950.
92. PROVAN, J.W.
"Fatigue failure of polycrystalline metals, cavities and cracks in creep and fatigue." Ed. by J. Gittus Applied Science Publishers, 1981, P.208.
93. ASHBY,M.F. AND JONES, D.R.H.
Engineering materials, Pergamon, 1985.
94. WEBSTER, S.E., AUSTER, I.M. AND RODD, W.J.
"Fatigue, corrosion fatigue and stress corrosion of steels for offshore structures." CEC Technical Steel Research. 1985.
95. MADDOX, S.J.
"Designing against fatigue fracture.", Metals and Materials, 1989, P. 727.
96. NORRING, K. AND NILSSON, K.
"Development of a steel resistant to lamellar tearing - Z - Steel, Paper presented at the Sixth Annual Offshore Technology Conference, Texas, May 6-8, 1974.

CHAPTER 9

APPENDICES

APPENDIX 1

NERNST EQUATION

Generally, an electrode reaction can be written



Where;

Ox - Oxidised species

Red - Reduced species

Z - Change in ionic charge in an electrode

According to thermodynamics of chemical equilibria, the free energy change in general case (ΔG) and standard (ΔG°) are connected by the relationship;

$$\Delta G = \Delta G^\circ + RT \ln \frac{[\text{Red}]}{[\text{Ox}]}$$

Where;

R - Gas constant

For corresponding electrode potentials, division by $-ZF$ gives the equations

$$E_{\text{eq.}} = E^\circ - \frac{RT}{ZF} \ln \frac{[\text{Red}]}{[\text{Ox}]}$$

or,

$$E_{\text{eq.}} = E^\circ + \frac{RT}{ZF} \ln \frac{[\text{Ox}]}{[\text{Red}]}$$

Where;

E° is the standard electrode potential for the reaction $= -G^\circ / ZF$ and

E_{eq} is the reversible electrode potential for the system.

This is the general form of the so called NERNST equation, which shows the variation of electrode potentials of participating substances. The dependence of electrode potentials on hydrogen ion concentration or pH is of particular importance.

APPENDIX 2

FORMULATING THE DISCRETE STIFFNESS EQUATIONS

The strains at any point within the element may be expressed in terms of the element nodal displacements. This can be done by a suitable differentiation of the displacements defined by equation;

$$\{q\}^e = [N] \{q\}^e \dots\dots\dots (1)$$

Where;

- $\{q\}$ - is the displacement field within the elements
- $\{q\}^e$ - is a vector of element nodal displacements and
- $[N]$ - is the shape function.

so that;

$$\{\epsilon\}^e = [\delta][N]\{q\}^e$$

or;

$$\{\epsilon\}^e = [B] \{q\}^e \dots\dots\dots(2)$$

Where;

- $\{\epsilon\}^e$ is the element strain vector;
- $[\delta]$ is a matrix of differential operators; and
- $[B]$ contains the appropriate derivatives of $[N]$

The strain energy stored in a typical element is (83);

$$U^e = 1/2 \int_{vol.} \{\epsilon\}^{et} [D] \{\epsilon\}^e dvol \dots\dots\dots(3)$$

substituting from equation (1)

$$U^e = 1/2 \{q\}^{et} \int_e [B]^t [D] [B] dvol \{q\}^e$$

or;

$$U^e = 1/2 \{q\}^{et} [k]^e \{q\}^e \dots\dots\dots(4)$$

The matrix

$$[k]^e = \int_{\theta} [B]^t [D] [B] dvol \dots\dots\dots(5)$$

is the element stiffness matrix.

Now, the total strain energy stored in the system is:

$$U = \sum_{e=1}^n U^e \dots\dots\dots(6)$$

Where n is the total number of elements in the assemblage. If all the element nodal displacements are denoted by :

$$\{q\} = \{q\}^e = \begin{matrix} \{q\}^1 \\ \{q\}^2 \\ \{q\}^3 \end{matrix} \dots\dots\dots(7)$$

and the element stiffness matrices are displayed as :

$$[K] = \begin{matrix} [K]^1 & & \\ & [K]^2 & \\ & & [K]^3 \end{matrix} \dots\dots\dots(8)$$

The equation (5) can be written as :

$$U = 1/2 \{q\}^t [K] \{q\} \dots\dots\dots(9)$$

Because the displacements are matched at the nodes; a compatible or connection matrix [C] is formed which expresses the necessary compatibility between the locally and globally measured displacements, therefore:

$$\{q\} = [C] \{q\} \dots\dots\dots(10)$$

Where $\{q\}$ is the vector of system generalised co-ordinates. Equation (9) can be expressed in terms of $\{q\}$. That is;

$$U = 1/2 \{q\}^t [C]^t [K] [C] \{q\}$$

or

$$U = 1/2 \{q\}^t [K] \{q\} \dots\dots\dots(11)$$

Where $[K]$ is the assemblage or system stiffness matrix. In order to establish the stiffness equilibrium equations, the total potential of the applied loads must be determined. If the external applied loads are denoted by $(Q^1, Q^2, \dots\dots\dots Q^N)$ corresponding to $(q^1, q^2, \dots\dots\dots q^N)$, then

$$\Omega = -\{q\}^t \{Q\} \dots\dots\dots(12)$$

Where N is the total number of nodal degrees of freedom that is, the total number of equations to be solved for the assemblage. The total potential energy in the discrete system is then,

$$V = 1/2 \{q\}^t [K] \{q\} - \{q\}^t \{Q\} \dots\dots\dots(13)$$

Now, the principle of minimum potential energy to the assemblage is applied, i.e for equilibrium $\delta V = 0$, so that:

$$\{\delta q\}^t ([K] \{q\} - \{Q\}) = 0$$

But δq are arbitrary so that:

$$[K] \{q\} = \{Q\}$$

These are the required equilibrium equations for the 'assembled' approximate system.

ELASTIC-PLASTIC BEHAVIOUR

To relate two and three dimensional problems to the one dimensional uniaxial case it is convenient to work with the equivalent stress and the equivalent strain.

The equivalent stress is given by (85, 86, 87, 88) ;

$$\sigma_{eq} = 2^{-1/2} ((\sigma_{xx} - \sigma_{yy})^2 + (\sigma_{yy} - \sigma_{zz})^2 + (\sigma_{zz} - \sigma_{xx})^2 + ((\sigma_{xy}^2 + \sigma_{yz}^2 + \sigma_{zx}^2)))^{1/2} \dots\dots\dots(1)$$

For the equivalent strain it is convenient, after yielding has taken place, to divide the components of strain into elastic and plastic parts

$$\begin{aligned} \epsilon_{xx} &= \epsilon_{xxel} + \epsilon_{xxpl} & \epsilon_{yy} &= \epsilon_{yyel} + \epsilon_{yypl} & \epsilon_{zz} &= \epsilon_{zzel} + \epsilon_{zzpl} \\ \epsilon_{xy} &= \epsilon_{xyel} + \epsilon_{xypl} & \epsilon_{yz} &= \epsilon_{yzel} + \epsilon_{yzpl} & \epsilon_{zx} &= \epsilon_{zxel} + \epsilon_{zxpl} \dots\dots\dots(2) \end{aligned}$$

The elastic parts of the strain components are related to the stresses by the usual Hooke's law. The plastic parts of the strain components contribute nothing towards the stresses and form the residual strains after unloading. Before yielding the plastic parts of strain are zero.

The equivalent strain is given by;

$$\epsilon_{eq} = \epsilon_{eqel} + \epsilon_{eqpl} \dots\dots\dots(3)$$

Where the elastic part is given by;

$$\epsilon_{eqel} = \sigma_{eq} / E = 1/(2(1+\nu))^{1/2} ((\epsilon_{xxel} - \epsilon_{xxpl})^2 + (\epsilon_{yyel} - \epsilon_{yypl})^2 + (\epsilon_{zzel} - \epsilon_{zzpl})^2 + 1.5 (\epsilon_{xyel}^2 + \epsilon_{yzel}^2 + \epsilon_{zxel}^2))^{1/2} \dots\dots\dots(4)$$

and the plastic part is given by the sum of the increments of the equivalent plastic strain (85, 86, 88), which are given by ;

$$\delta \epsilon_{eqpl} = 1/(1.5 \times 2)^{1/2} \left((\delta \epsilon_{xxpl} - \delta \epsilon_{yypl})^2 + (\delta \epsilon_{yypl} - \delta \epsilon_{zzpl})^2 + (\delta \epsilon_{zzpl} - \delta \epsilon_{xxpl})^2 + 1.5 (\delta \epsilon_{xypl}^2 + \delta \epsilon_{yzpl}^2 + \delta \epsilon_{zpxpl}^2)^{1/2} \right) \dots \dots \dots (5)$$

Here the 1.5 replaces the (1+ν) as the plastic strains involve no volume change.

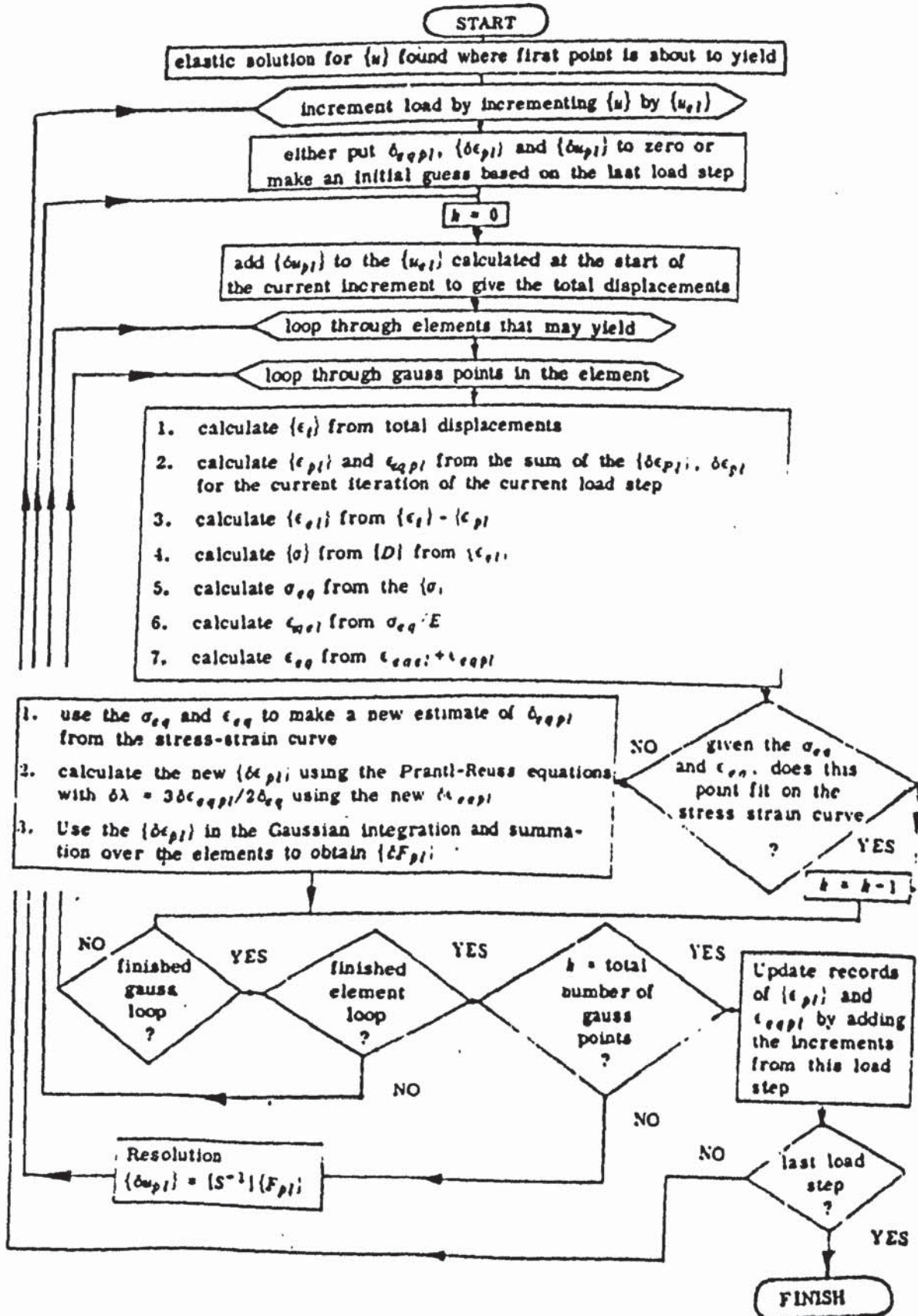
$$\delta \epsilon_{xypl} + \delta \epsilon_{yzpl} + \delta \epsilon_{zpxpl} = 0 \dots \dots \dots (6)$$

The constant $2^{-1/2}$ in the expression for equivalent stress and $1/(2(1+\nu))^{1/2}$, $1/(1.5 \times 2)^{1/2}$ in the expression for equivalent strain are chosen so that the equivalent stress and equivalent strain for the uniaxial case are that the $\delta \sigma_{xx}$ and ϵ_{xx} . When the equivalent stress becomes greater than the uniaxial yield stress, then yielding takes place. the yield condition

$$\sigma_{eq} > \sigma_{yield} \dots \dots \dots (7)$$

is the well established von Mises yield criterion (85, 86, 87, 88, 89, 89, 90, 91). The expression for the equivalent plastic strain is used because in addition to being in a similar form to that for the equivalent stress the plastic stress-strain relations and the 'equivalent of plastic work (85, 89, 87). This is an assumption that the strain hardening (or strain softening) is a function only of the plastic work, which must be positive or zero for any deformation. The plasticity solution for PAFEC methods are given in appendix 4 .

PLASTICITY SOLUTION FLOW DIAGRAM



THE GRIDS PRINTING TECHNIQUE

1. Polish the specimens and for the welded ones etch them with 2% solution of nital.

2. Clean the surface of the specimen on which the grid is to be printed with a solvent for eg. thinner.

3. Coat the surface of the specimen evenly with the solution of Kodak photo-resist, this must be allowed to dry over a long period of time (overnight) or kept in an oven for approximately one hour. The thinner the coating, the better the resolution of the grids.

4. A prepared grid of the required size is put on the surface area of the specimen, and then this is exposed to ultra violet light for approximately one minute.

5. The specimen is inserted in the developer and agitated for approximately two minutes.

6. Following this it is inserted in the dye for about five seconds, if the image is too light the time should be slightly extended but not too much otherwise the photo-resist will be washed off.

7. The specimen is then washed in a solution of water and detergent, and then rinsed off with a water spray.

8. Finally it is dried with a blowdrier and care must be taken so that all the water droplets are removed, otherwise the exposed surface of the specimen will rapidly corrode.

HNW1:

Normalised specimen with no weld tested in air. The stress strain curve is a typical one for a ductile steel with yield value of 350 N/mm^2 UTS of 474 N/mm^2 , 34% elongation and reduction in area of 67%. Fracture appearance is a classic "cup and cone" with evidence of shear along the edges.

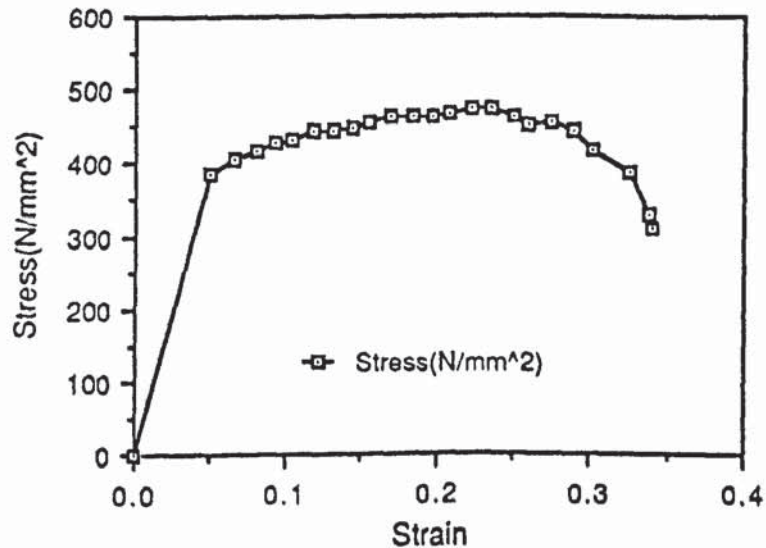


Figure 68 stress-strain relationship for HNW1

HNW2:

Normalised specimen with no weld tested under corrosion conditions. The stress strain curve generally resembles that of the HNW1 with slightly lower values of yield strength 320 N/mm^2 UTS of 444 N/mm^2 , 28% elongation and reduction area of 62.5%, this is mainly due to general loss of metal caused by the corrosion which reduced the cross sectional area of the material by approximately 7.5%. Fracture appearance is of a classic cup and cone with slightly finer dimples and general formation of corrosion products on the surface.

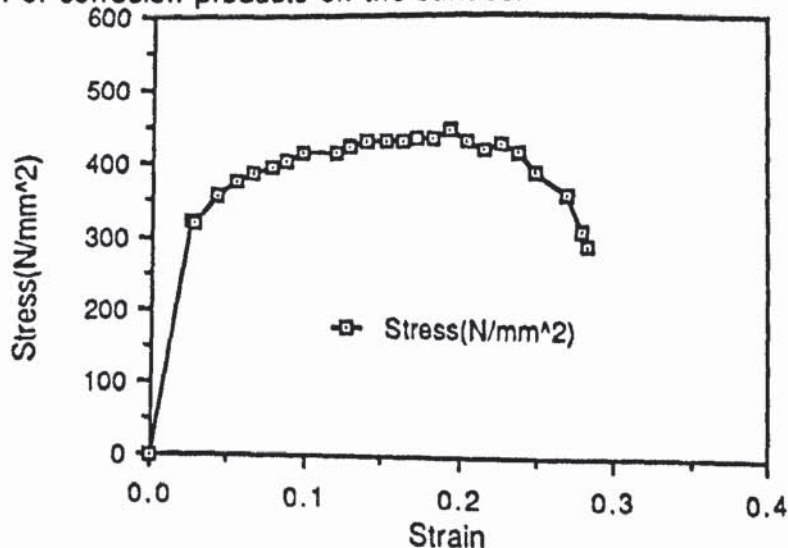


Figure 69 Stress-strain relationship for HNW2

HNW3:

Normalised specimen, no weld tested under hydrogen evolution conditions. The stress strain curve and general mechanical properties are significantly different from HNW1 and HNW2 with yield stress of 315 N/mm^2 UTS value of 418 N/mm^2 , 26% elongation and greatly reduced reduction of area value of 27.1%. Although the fracture appearance resembles the ductile cup and cone but it seems to be much more smoother than the specimens tested in air and under general corrosion conditions, there is also some evidence of change of direction in the direction of fracture from xx plane to the yy plane as well as few stepwise cracks within the vicinity of the fracture surface.

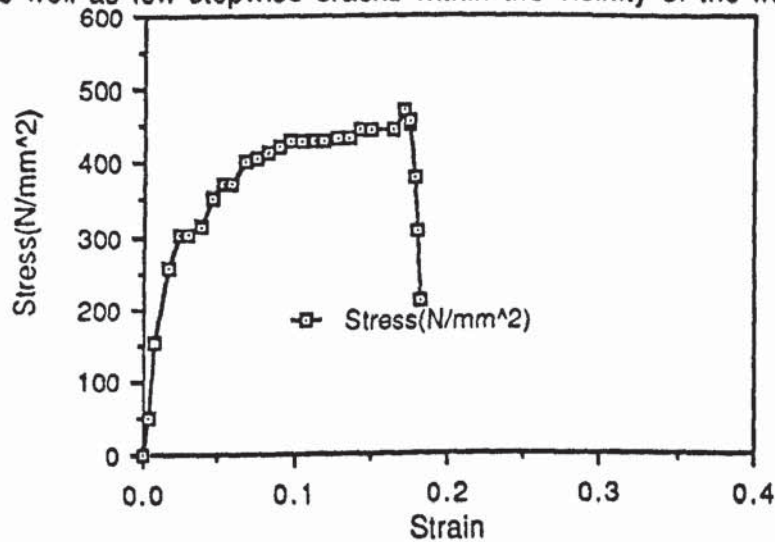


Figure 70 Stress-strain relationship for HNW3

HGC7:

Normalised specimen with sound weld tested in air. Due to higher strength of the weld the failure has occurred outside the weld in the parent plate portion of the parallel length. Yield stress value of 382 N/mm^2 , UTS of 511 N/mm^2 , 23% elongation and 69.5% reduction of area. The higher strength is mainly associated with the quenching effect caused by the parent plate and slight change in the microstructure.

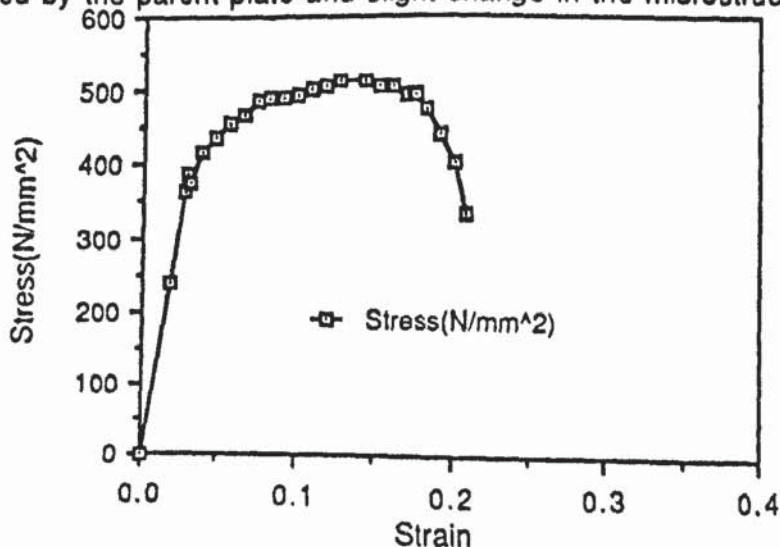


Figure 71 Stress-strain relationship for HGC7

HGC6:

Normalised specimen with sound weld tested under corrosion conditions. Apart from slight reduction in the mechanical properties which is mainly due to general loss of metal compared with HGC7 there is no evidence of any major change yield stress of 370N/mm^2 , UTS value of 500N/mm^2 20.8% elongation and 60.3% reduction in area. The failure is outside the weld within the parent plate. There is no significant change in the fracture appearance.

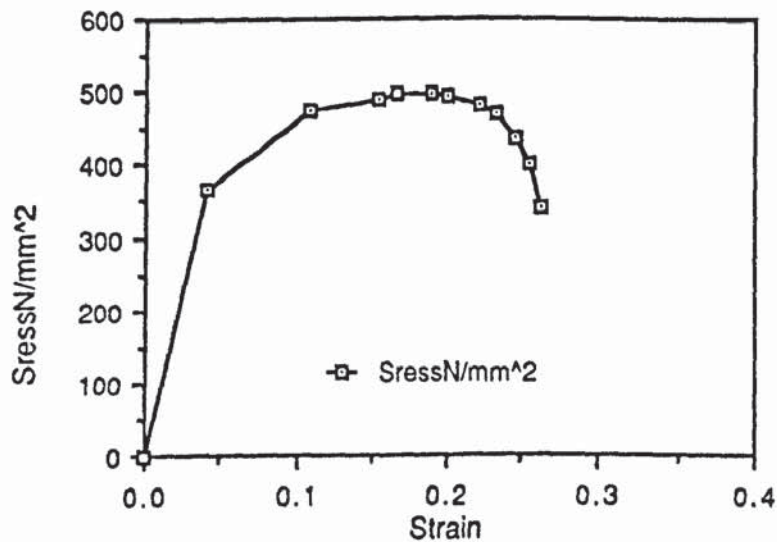


Figure 72 Stress-strain relationship for HGC6

HGC1:

Normalised with sound weld tested under hydrogen evolution conditions. Yield stress of 377N/mm^2 , UTS of 500N/mm^2 14.4 % elongation and 21.7% reduction in area, as expected these indicate to a general reduction in the mechanical properties. The fracture appearance is very similar to the normalised specimen without the weld (HNW3) with no clear evidence of a 45° shear failure, there are also some stepwise cracks within the vicinity of the fracture area.

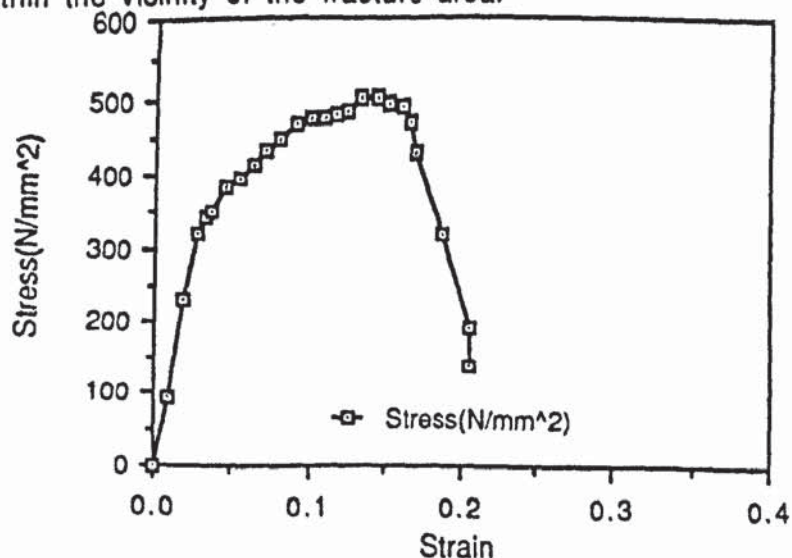


Figure 73 Stress-strain relationship for HGC1

HB2:

Normalised, defective weld tested in air. Although there is a defective weld within the matrix of the steel nevertheless it has higher strength than the actual parent plate, hence the failure has occurred in the parent plate outside the welded region. Because of this effect the general behaviour of this category of test specimens very closely resemble those containing sound welds. Yield stress 379 N/mm², UTS 514 N/mm², 24.1% elongation and 71.9% reduction in area values.

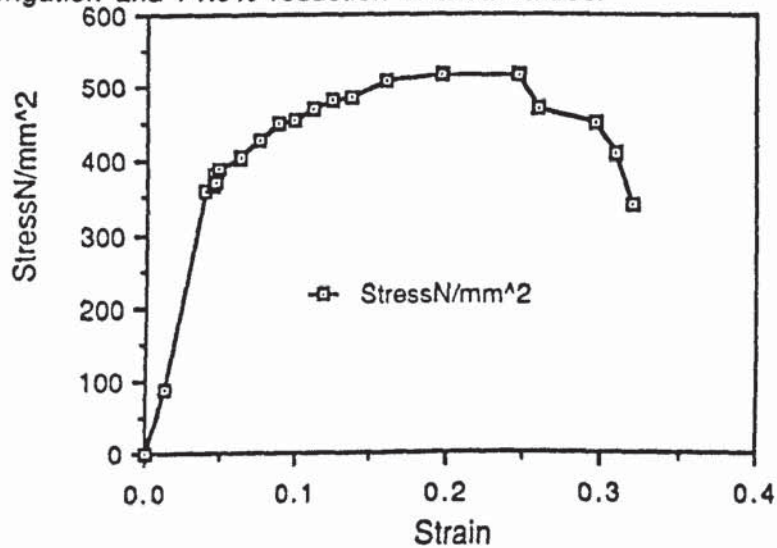


Figure 74 Stress-strain relationship for HB2

HB3:

Normalised, with defective weld tested under corrosion conditions. Same comments given for HB2 can be give for this specimen. The stress strain curve is not very smoothly drawn mainly because of number of data points available. Yield stress of 381 N/mm², UTS 501 N/mm², 18.4% elongation and 68.5% reduction in area.

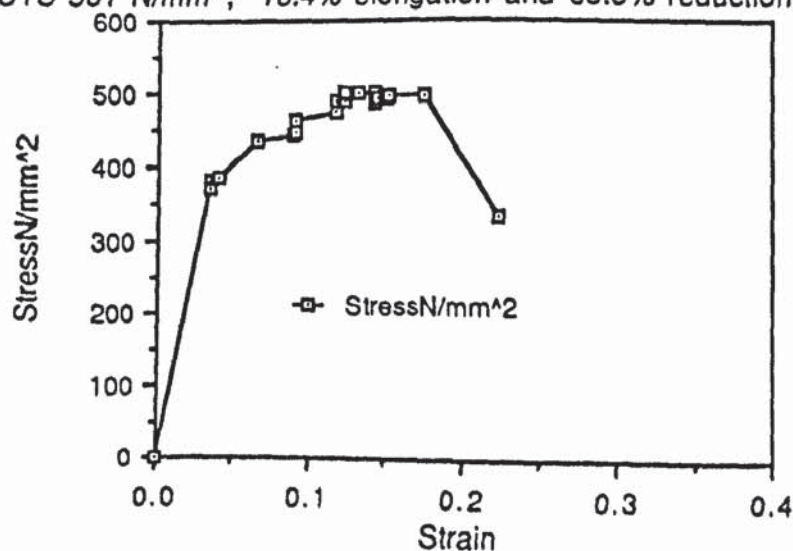


Figure 75 Stress-strain relationship for HB3

HB5:

Normalised, defective weld tested under hydrogen evolution conditions. Yield stress of 346 N/mm^2 and the YTS value of 508 N/mm^2 are similar to the same specimen containing sound weld and tested under same conditions, but 20% elongation and 36.1% reduction in area values are significantly different.

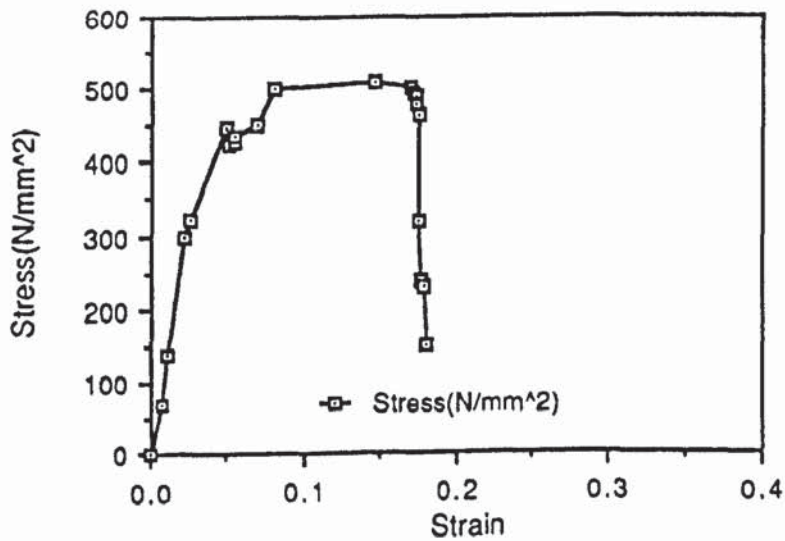


Figure 76 Stress-strain relationship for HB5

HGC5:

Normalised with sound weld and notched, tested in air. In order to obtain more information about the mechanical properties of the welds, a smooth notch has been introduced within the welded zone. The yield stress of 443 N/mm^2 and UTS of 621 N/mm^2 refer to approximately 30% increase in strength for the weld 26.4% elongation and 59.2% reduction in area indicate to the ductility of the weld which has not been greatly changed and fractography results confirm this. Apparent modulus of elasticity is significantly different to the previous tests mainly due to the lower stress strain ratio.

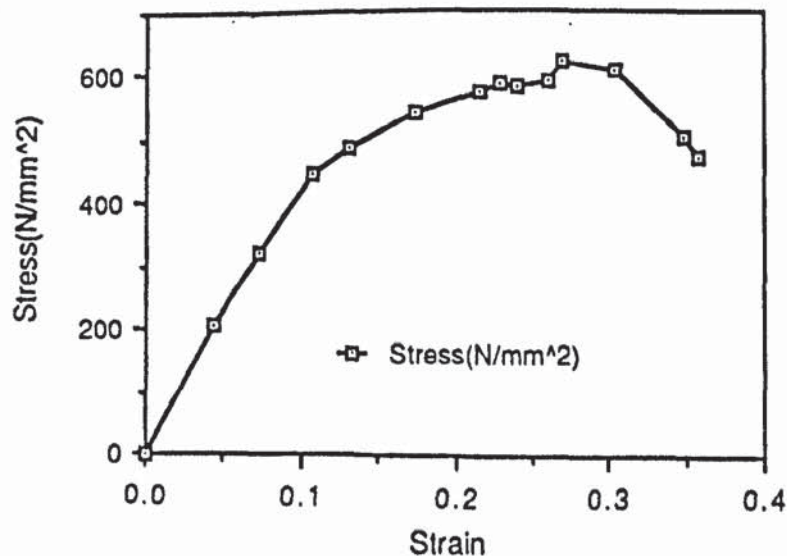


Figure 77 Stress-strain relationship for HGC5

HGC8: Normalised with sound weld and notched, tested under general corrosion conditions. Mechanical property results are not significantly different to the air test specimen, i.e. yield stress of 442 N/mm² UTS 572 N/mm² 22.6% elongation and 58.1% reduction in area. The apparent modulus of elasticity is also different. Because of the shorter duration of these tests compared with the unnotched specimens the corrosion environment has not greatly altered the mechanical properties since there has been significantly less loss of metal due to this effect.

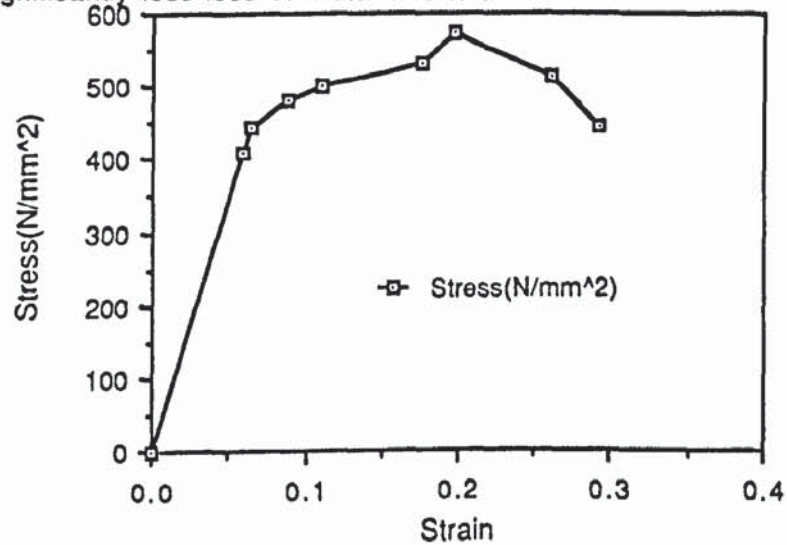


Figure 78 Stress-strain relationship for HGC8

HGC4: Normalised with sound weld and notched, tested under hydrogen evolution condition. The yield stress of 446 N/mm² is not greatly different from air and corrosion tests, but there is a slight reduction in UTS to 580 N/mm² 12.5% elongation and 24.1% reduction of area value are much smaller an order of 2.1 and 2.5 times. The brittleness of the steel due to the effect of the hydrogen can be seen from the stress strain curve, although the fracture appearance does not indicate to any change in the fracture mode, it only refers to smoother facets on the fracture surface and few cracks around the fractured area.

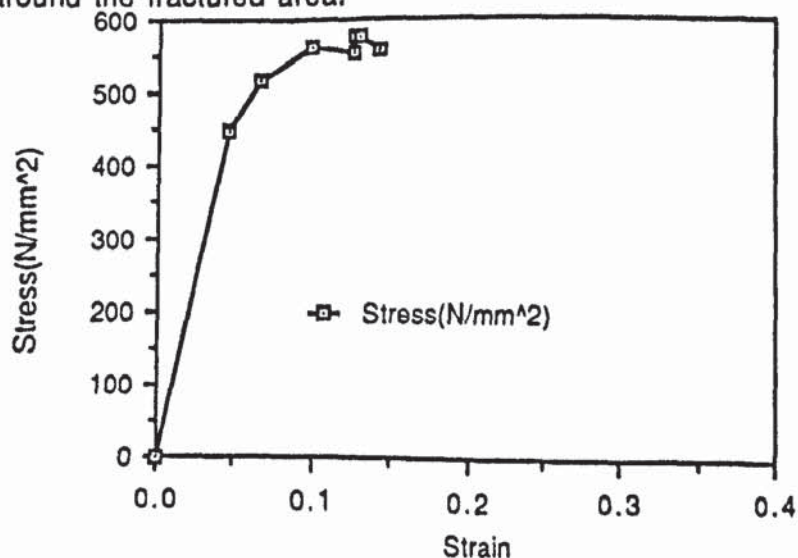


Figure 79 Stress-strain relationship for HGC4

HB8:

Normalised with defective weld and notched tested in air. As expected compared with the air test specimen all the mechanical properties have been deteriorated due to the effect of the added inclusions. Yield stress of 426 N/mm^2 , UTS of 539 N/mm^2 , 11.6% elongation and 26.8% reduction in area. The stress strain curve is very similar to that of the hydrogen test, i.e. it seems that the detrimental effects of the additions of defects and hydrogen embrittlement are also similar. Fracture surface clearly shows two distinct zones, a coarse surface which appears dark with nodular type of dimples and a much smoother surface with less evidence of the cup and cone.

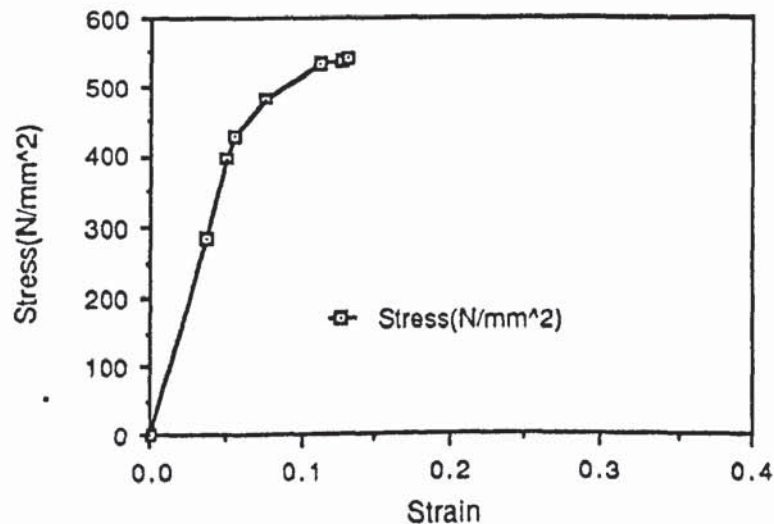


Figure 80 Stress-strain relationship for HB8

HB7:

Normalised defective notched specimen, tested under the corrosion conditions. Although the yield stress has been reduced to 400 N/mm^2 compared to the notched specimen containing a weld defect the UTS value of 537 N/mm^2 and 12.4% elongation are almost the same, but there is a significant increase in the reduction of area value to 32.3%. Again the stress strain curve very closely resembles that of a hydrogen specimen with the tearing effects of metal ligaments in a stepwise fashion, with the built up of triaxial stresses within the voids. Fractography indicates to a fracture surface of a ductile mode with some areas free from the added inclusions resulting in a classical cup and cone and parts which contain more defects showing a tearing effect.

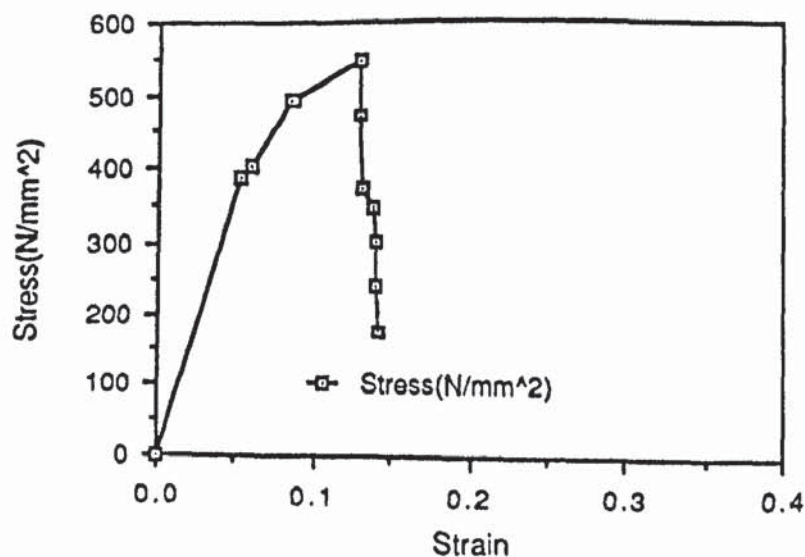


Figure 81 Stress-strain relationship for HB7

HB6:

Normalised defective weld notched, tested under hydrogen evolution conditions. yield stress of 377 N/mm^2 , and UTS 545 N/mm^2 are smaller than the sound welds, i.e a reduction in strength of 11.5% and 6% approximately. 10.8% elongation and 32% reduction in area values. Fractography shows some evidence of a 45° shear along the yy plane and some evidence of two different fracture surfaces similar to the HB7 specimen with a band of colonies of inclusions separating the two regions.

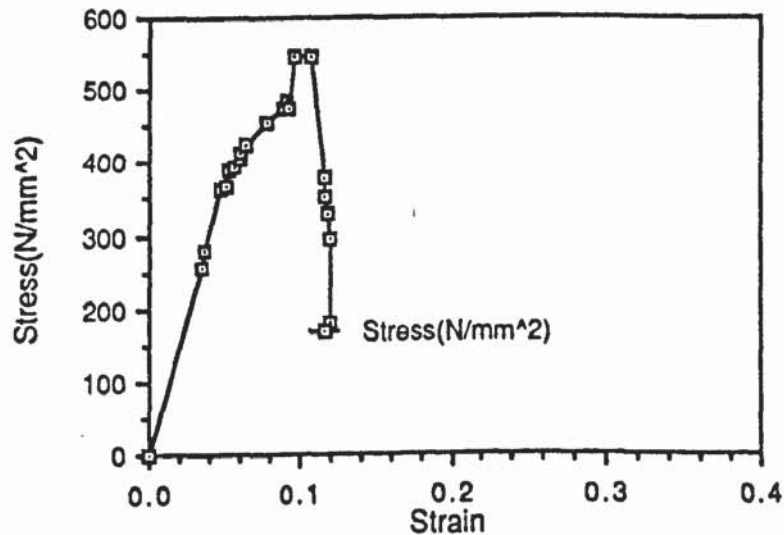


Figure 82 Stress-strain relationship for HB6

ONW1:

Oil quenched and tempered with no weld, tested in air. Yield stress of 580 N/mm^2 and UTS of 610 N/mm^2 19 % elongation and 67 % reduction in area. As expected due to the quench and tempering effect there is an increase in strength level compared with the normalised condition but there is a reduction of factor of x2 in % elongation. Fracture appearance is same as the HNW1.

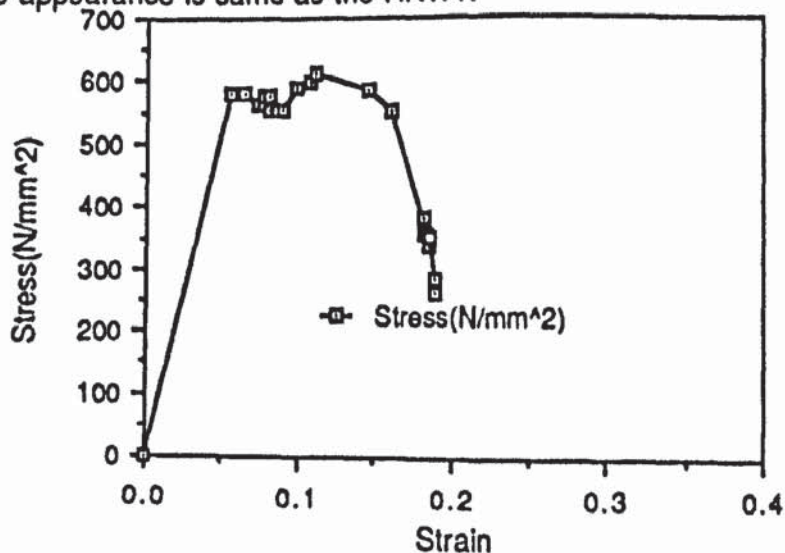


Figure 83 Stress-strain relationship for ONW1

ONW2:

Oil quenched and tempered with no weld, tested in corrosion. YS of 562 N/mm², UTS of 595 N/mm² are slightly lower than the air test with 20% elongation and 70% reduction in area. Generally the characteristic of this specimen is very similar to the air test specimen.

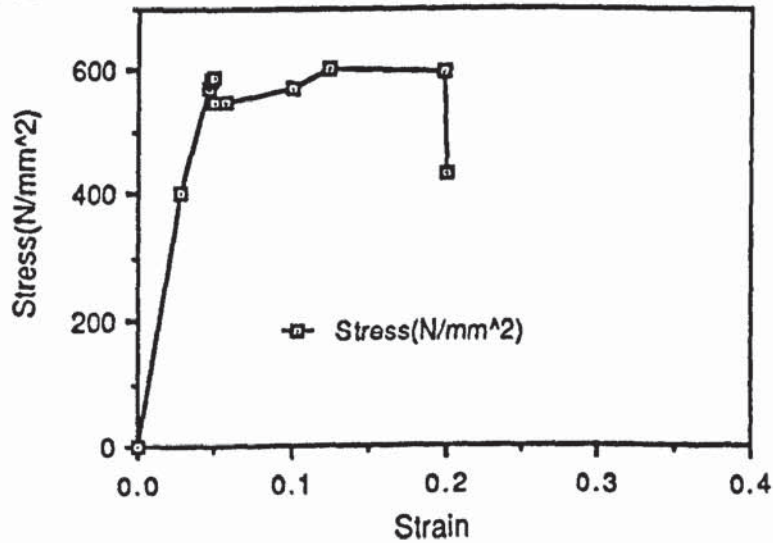


Figure 84 Stress-strain relationship for ONW2

ONW3:

Oil quenched and tempered with no weld, tested in hydrogen environment. YS is reduced by 20% to 454 N/mm² and reduction of area by 26% to 49% compared with the air test, but the UTS and % elongation is approximately the same. There is evidence of shear along the edges and smoother facets with few small cracks around the fracture surface, but no change in the fracture mode or the direction.

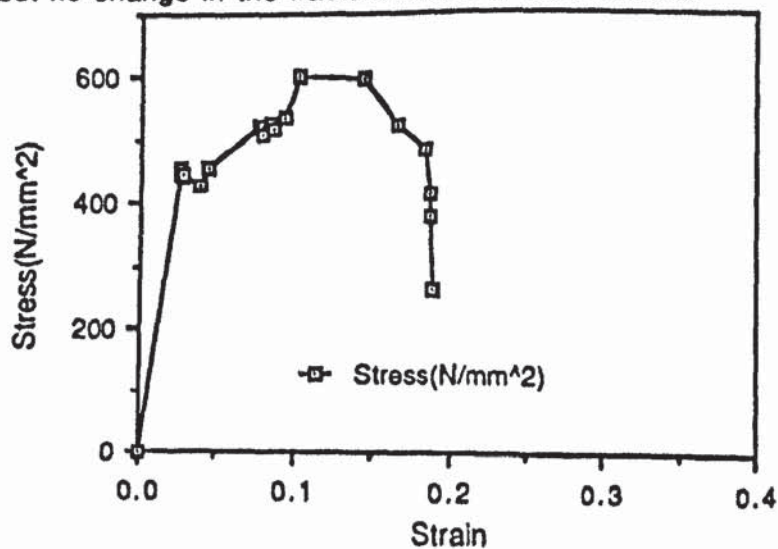


Figure 85 Stress-strain relationship for ONW3

OG1:

Oil quenched and tempered with sound weld , tested in air. Although the oil quenching has increased the strength of the steel but not to the same level as the welds hence the fracture of specimens has occurred out side the weld and within the parent plate. Generally the same mechanical characteristics of normalised steel is possessed by this specimn.

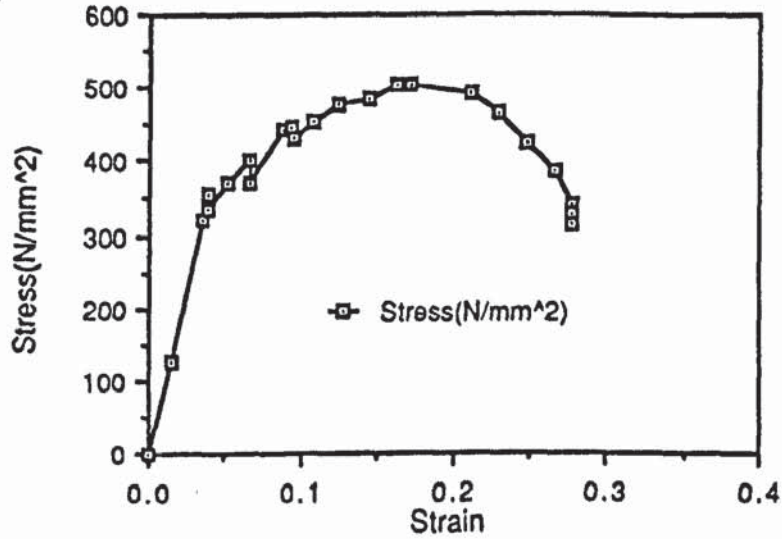


Figure 86 Stress-strain relationship for OG1

OG4:

Oil quenched and tempered with sound weld tested in corrosion conditions. Fracture is outside the weld and within the parent plate , same explanation as above can be given for this steel.

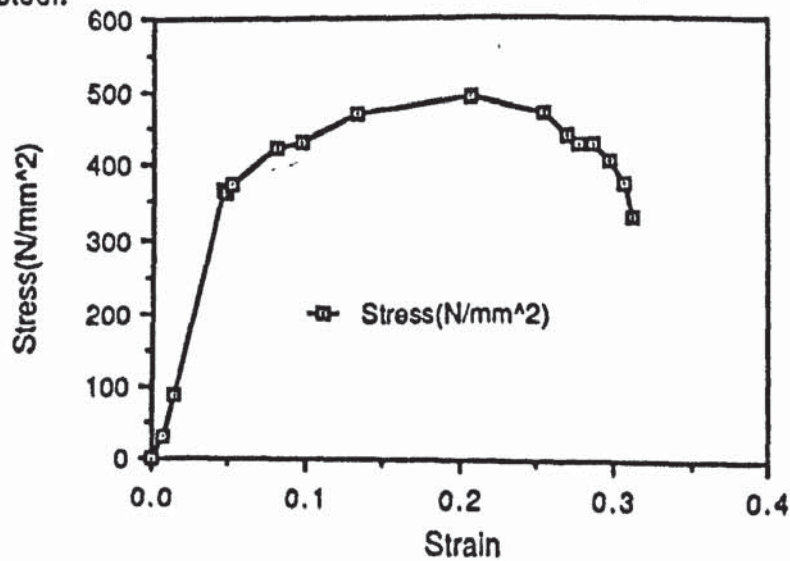


Figure 87 Stress-strain relationship for OG4

OG3:

Oil quenched and tempered with sound weld tested in hydrogen. The only major difference with the previous two steels is the reduction in area value of 28% which is reduced by a factor of x 2.7.

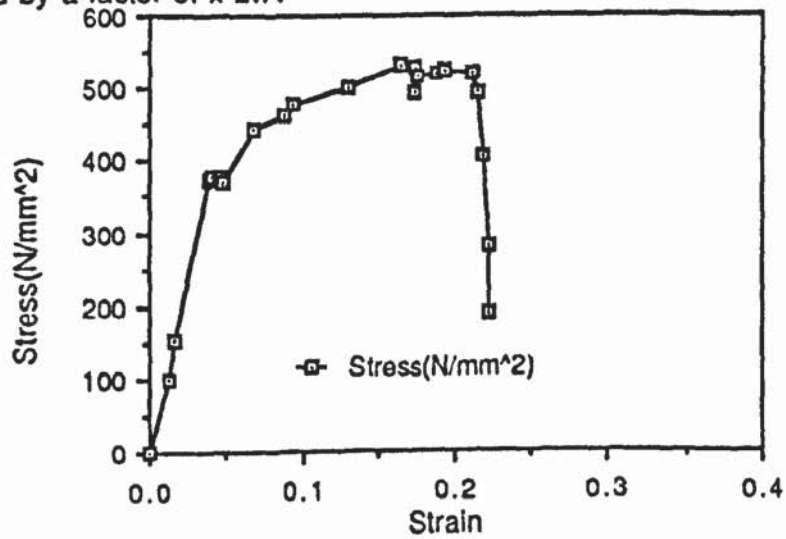


Figure 88 Stress-strain relationship for OG3

OB1:

Oil quenched and tempered with defective weld tested in air. Although the steel contains a defective weld, but the strength of it has not been greatly affected, hence the failure is still within the parent plate, therefore the properties of these steels are very much the same as the OG group without the notch.

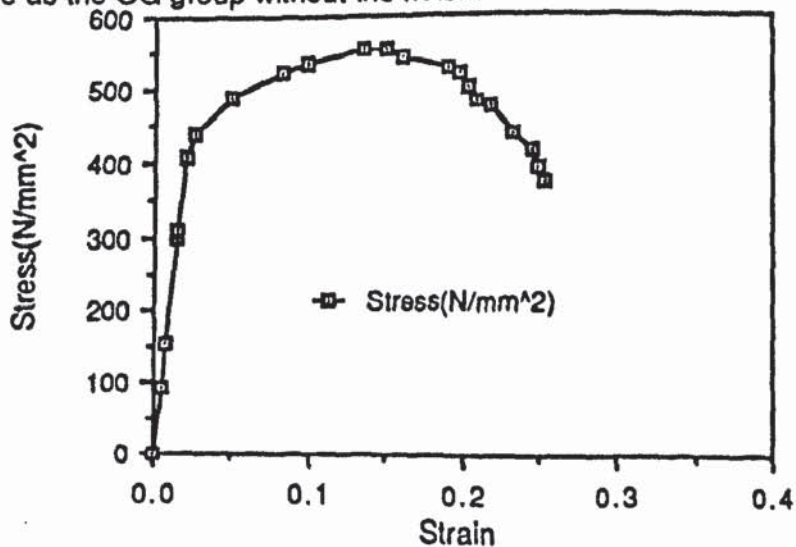


Figure 89 Stress-strain relationship for OB1

OB2:

Oil quenched and tempered with defective weld, tested in corrosion.
Same comments as OB1.

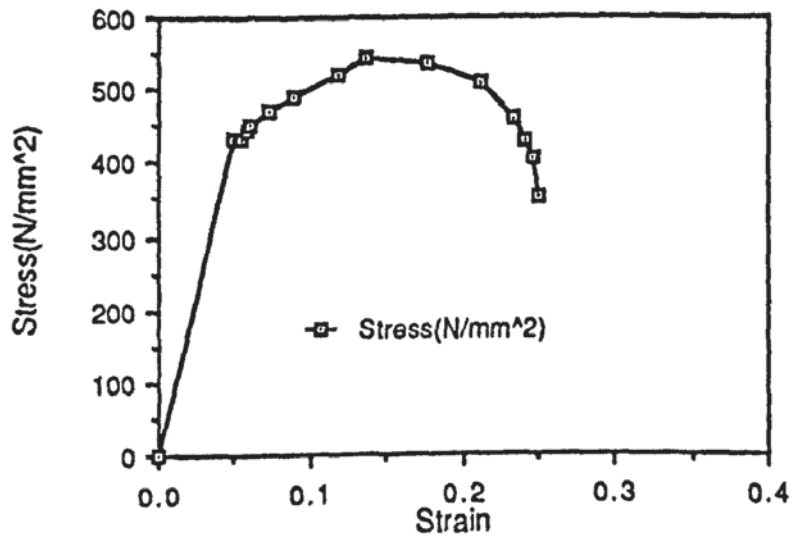


Figure 90 Stress-strain relationship for OB2

OB3:

Oil quenched and tempered with defective weld tested in hydrogen.
Same comments as the OB1.

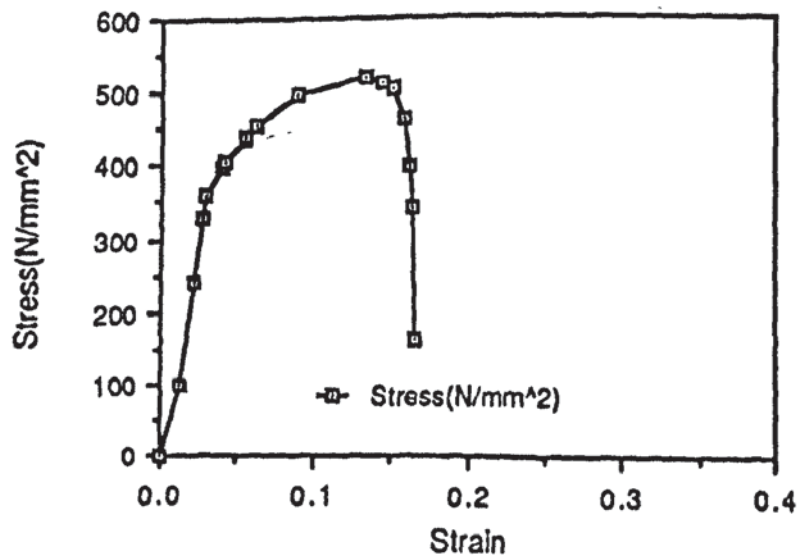


Figure 91 Stress-strain relationship for OB3

OG5:

Oil quenched and tempered with a sound weld and notched tested in air. YS of 462 N/mm² and UTS of 612 N/mm² indicates to the higher strength of the weld. The reduction in area value has reduced to 52% but the % elongation is slightly higher and this can readily be seen from the stress- strain curve. The apparent modulus of elasticity is not as steep as the previous ones due to the stress-strain ratio of the welds.

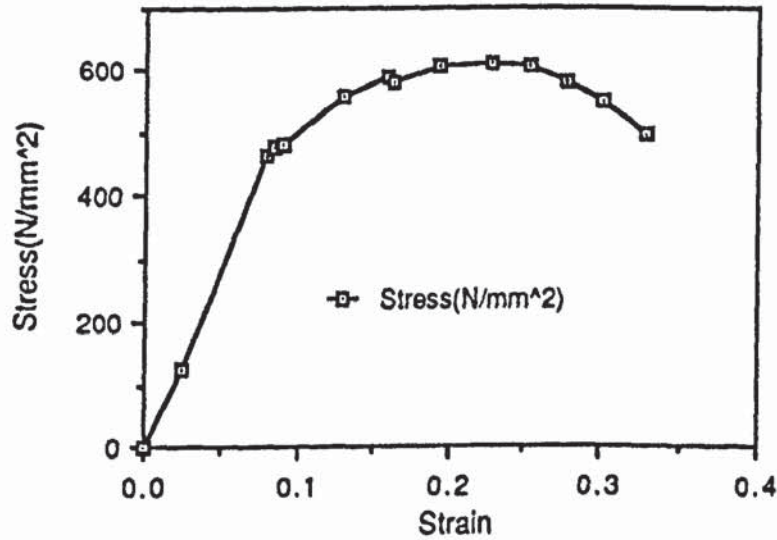


Figure 92 Stress-strain relationship for OG5

OG6:

Oil quenched and tempered with sound weld and notched, tested in corrosion. The mechanical properties and the fracture appearance very much is similar top the air test specimen, this could be mainly due to the lower time period which specimen has spent in the corrosion environment. Nevertheless the fracture strength has slightly been reduced.

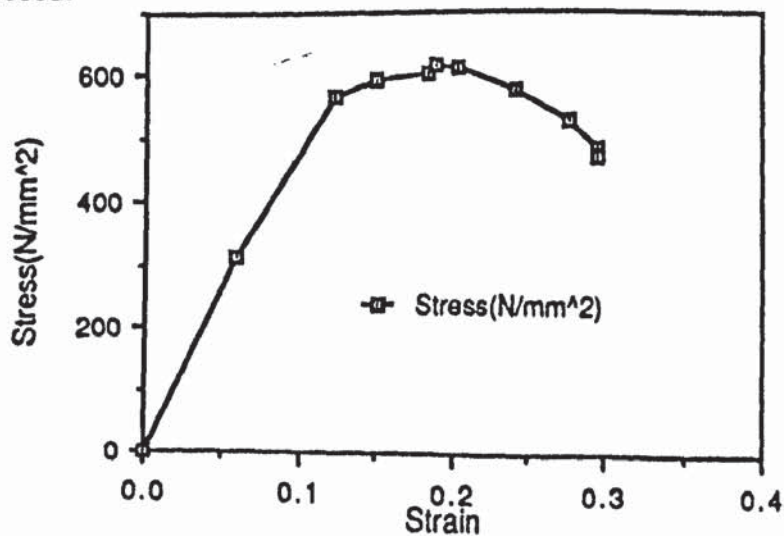


Figure 93 Stress-strain relationship for OG6

OG7:

Oil quenched and tempered with sound weld and notched, tested in hydrogen. The main effect of hydrogenation seems to be on the lowering of the fracture strength and reduction of plastic strain.

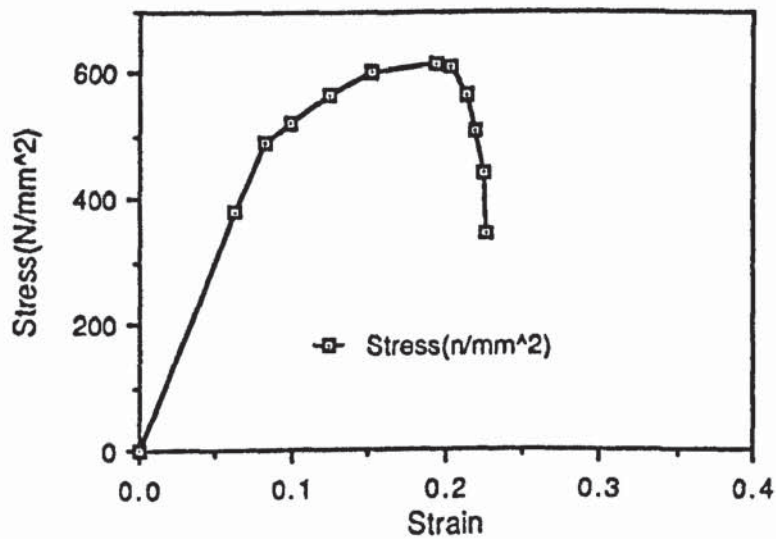


Figure 94 Stress-strain relationship for OG7

OB4:

Oil quenched and tempered with defective weld and notched, tested in air. The YS and UTS have been reduced by approximately 3 and 7 % to 449 and 572 N/mm², but the % elongation and % reduction in area have been reduced by approximately X1.7 and X2.0 compared with the air test specimen. The effect of deterioration of the weld quality upon the mechanical properties of the steel seems to be same as the hydrogen effect. The plastic deformation of the steel somehow is irregular.

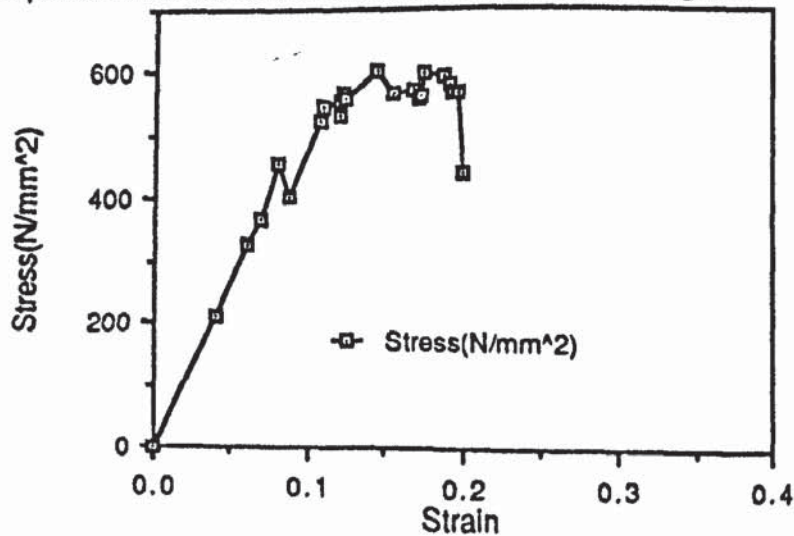


Figure 95 Stress-strain relationship for OB4

OB5:

Oil quenched and tempered with defective weld and notched, tested in corrosion. The main significant difference between this and the air test specimen is the reduction in plastic strain.

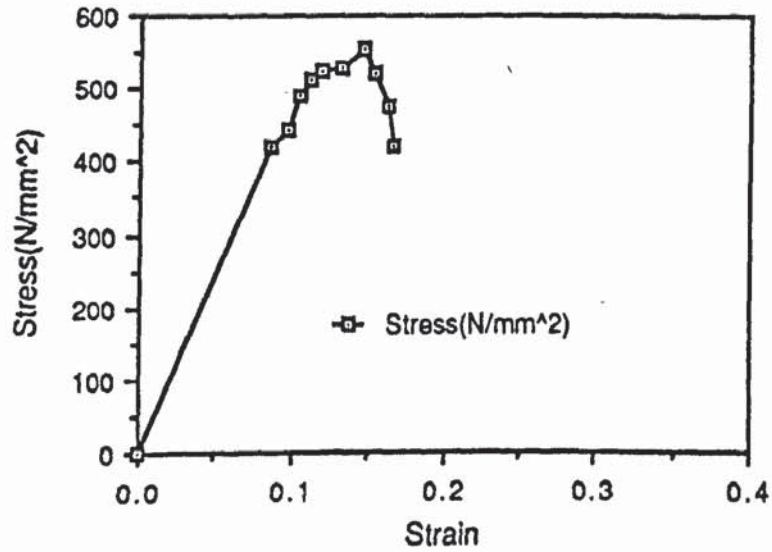


Figure 96 Stress-strain relationship for OB5

OB6:

Oil quenched and tempered with defective weld and notched, tested in hydrogen. There is a slight reduction in strength both YS and UTS, but the reduction in plastic strain is very significant, this is due to combination of deleterious effects of weld quality and the hydrogen environment. The fluctuation of points on the stress strain curve could partly be due to this effect and partly due to the testing error caused by the vibration in the machine.

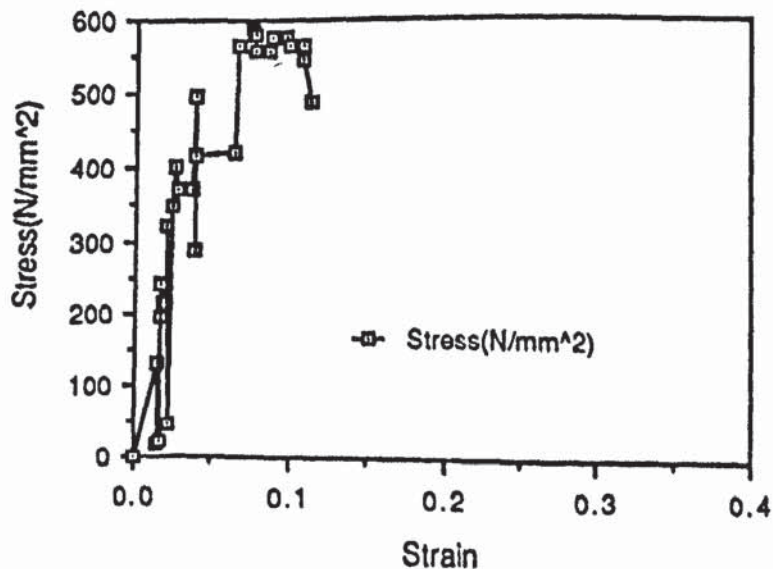


Figure 97 Stress-strain relationship for OB6

WNW1:

Water quenched and tempered with no weld, tested in air. The maximum UTS value of 685 N/mm^2 is achieved due to water quenching, in return the ductility has been reduced to 16 % elongation value.

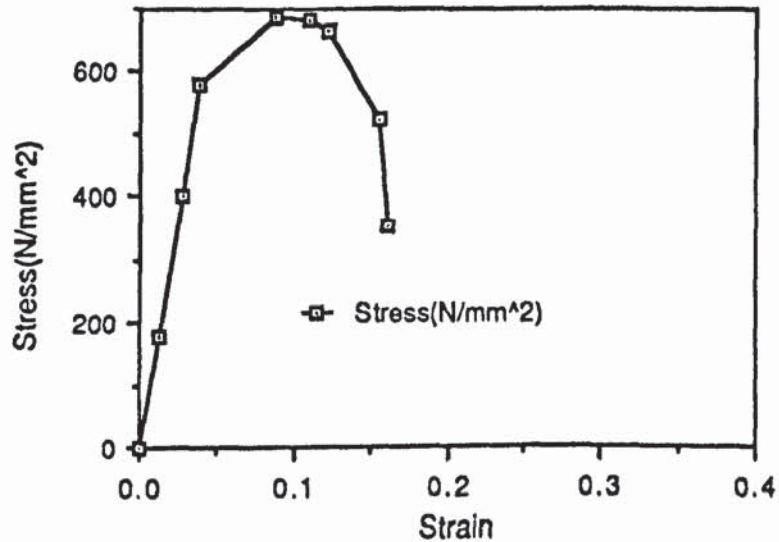


Figure 98 Stress-strain relationship for WNW1

WNW2:

Water quenched and tempered with no weld, tested in corrosion. The strength level compared with the air test specimen has slightly reduced but % elongation and % reduction in area value remain the same. There is no significant difference in fracture appearance.

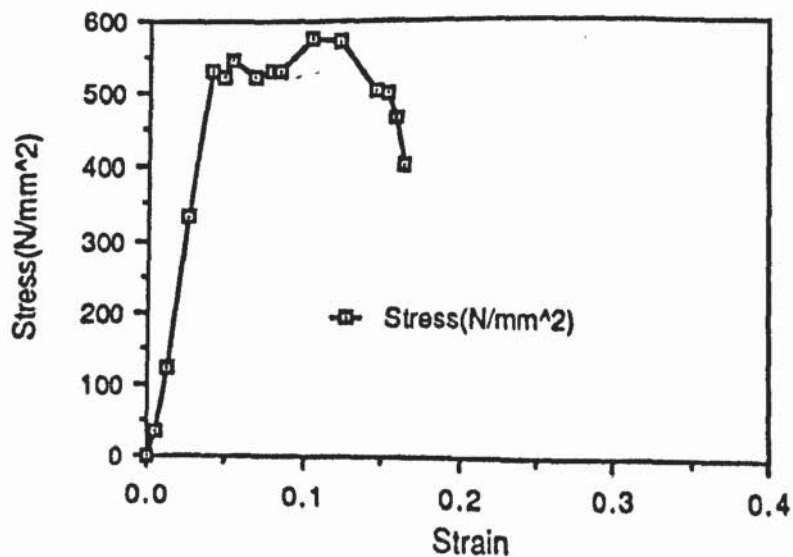


Figure 99 Stress-strain relationship for WNW2

WNW3:

Water quenched with no weld tested in hydrogen. The fracture strength compared to the normalised and oil quenched and tempered specimen has not been reduced, nor the strength level, but there is a slight drop in the reduction in area values and % elongation. The stress strain curve is not a smooth one due to the lack of data points.

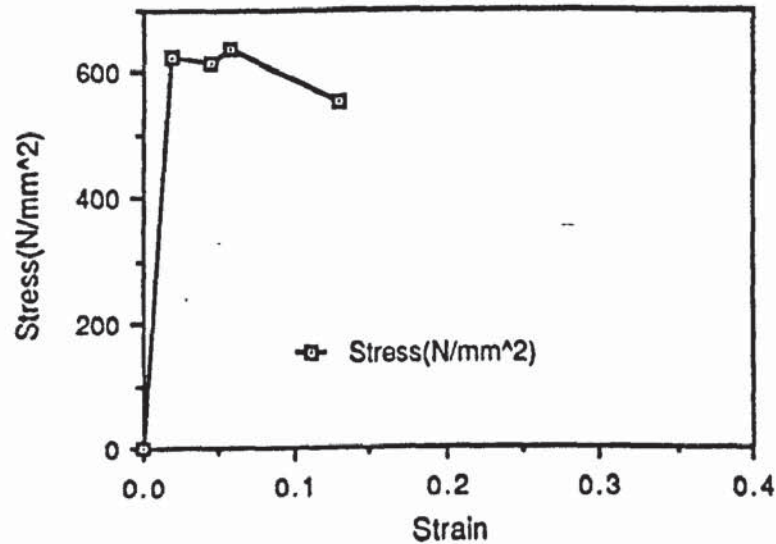


Figure 100 Stress-strain relationship for WNW3

GW1:

Water quenched and tempered with good weld, tested in air. The only main effect of welding has been slight drop in strength. Because the strength of the weld and the water quenched steel are approximately the same level, the fracture has been within the weld.

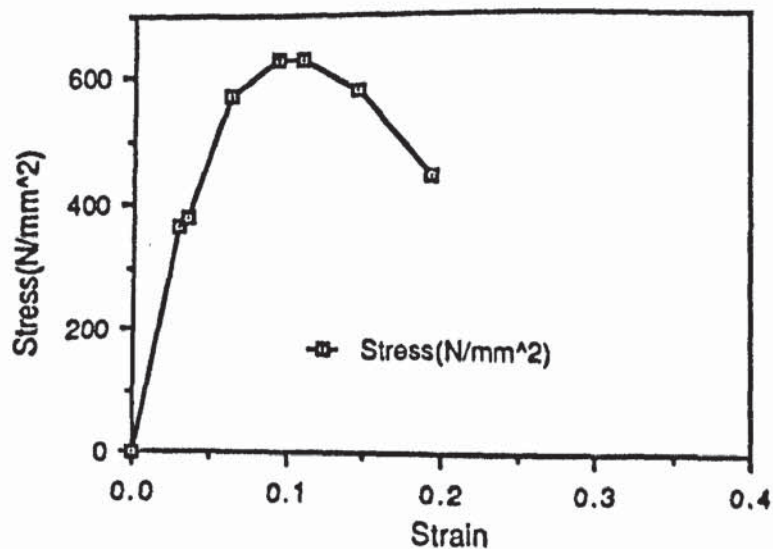


Figure 101 Stress-strain relationship for GW1

GW2:

Water quenched and tempered with sound weld, tested in corrosion. There has been a slight drop in strength and plastic strain. No significant change of fracture appearance or morphology has been observed. Fracture of the specimen has occurred within the welded zone.

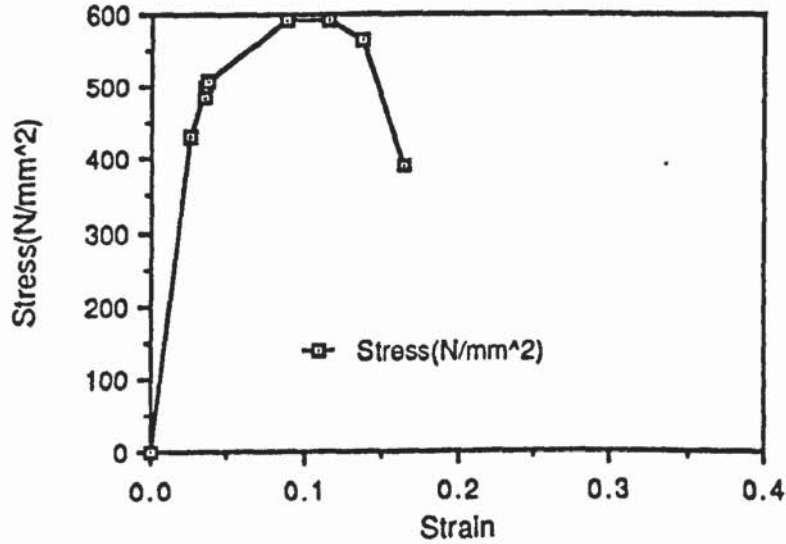


Figure 102 Stress-strain relationship for GW2

GW3:

Water quenched and tempered with sound weld tested in hydrogen. Apart from the 14% elongation compared with 17% for air test, there is no significant change in mechanical properties nor the fracture appearance between this specimen and those tested in air and corrosion.

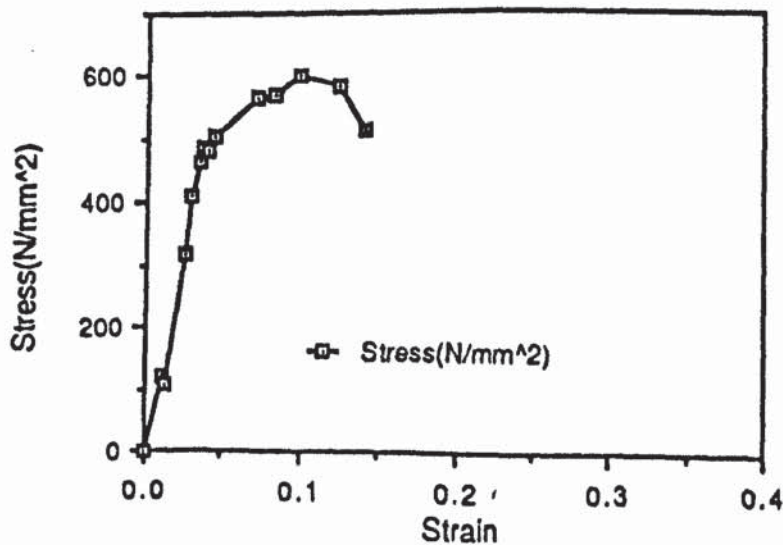


Figure 103 Stress-strain relationship for GW3

BW1:

Water quenched and tempered with defective weld, tested in air. The YS has reduced by about 30% to 408 N/mm² and the UTS by 13% to 596 N/mm² compared with the plane specimen. There has been a very significant drop in the ductility with 7% elongation and 26% reduction in area value, with a sudden failure after yielding.

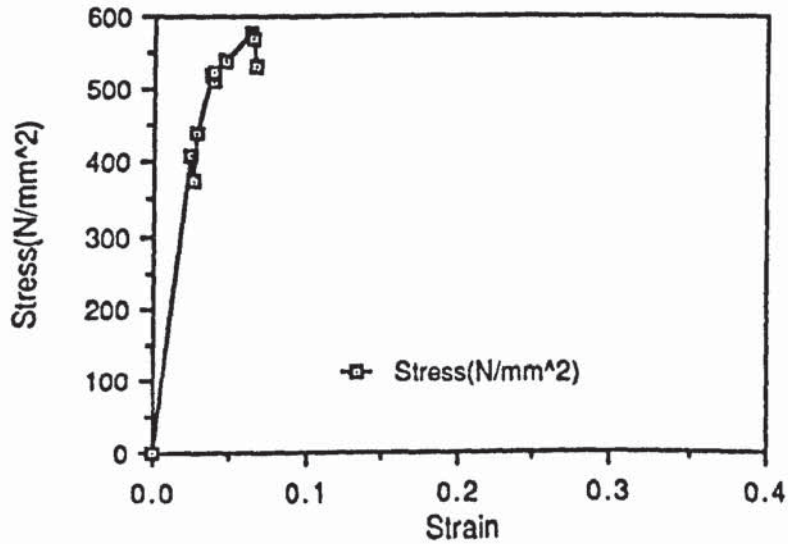


Figure 104 Stress-strain relationship for BW1

BW2:

Water quenched and tempered with defective weld, tested in corrosion. There is a further drop in YS, UTS and FS with more or less same ductility.

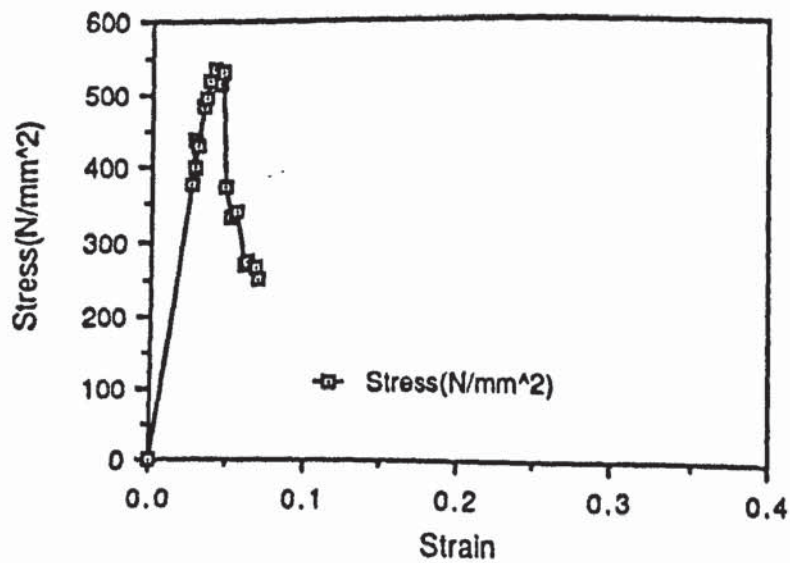


Figure 105 Stress-strain relationship for BW2

BW3:

Water quenched and tempered with defective weld, tested in hydrogen. This a worst case condition with X3 reduction in the elongation to 4% and approximately X4 in the reduction in area value to 17% compared with the air test specimen. There is also a significant drop in YS and UTS values to 412 and 450 N/mm², with almost an immediate failure after the UTS value has been reached.

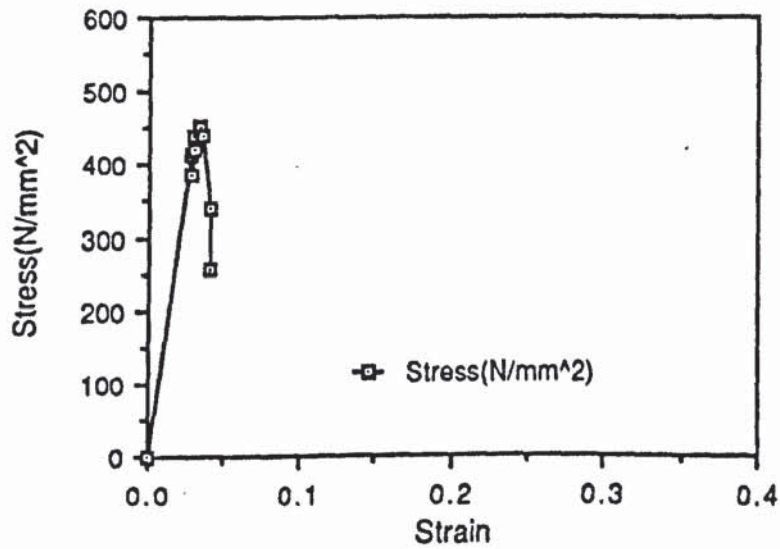


Figure 106 Stress-strain relationship for BW3

AS RECEIVED TRANSVERSE:

As recieved plate with specimen cut from the transverse to the rolling direction, tested in air. The mechanical properties truly represent that of a ductile steel with a cup and cone fracture surface.

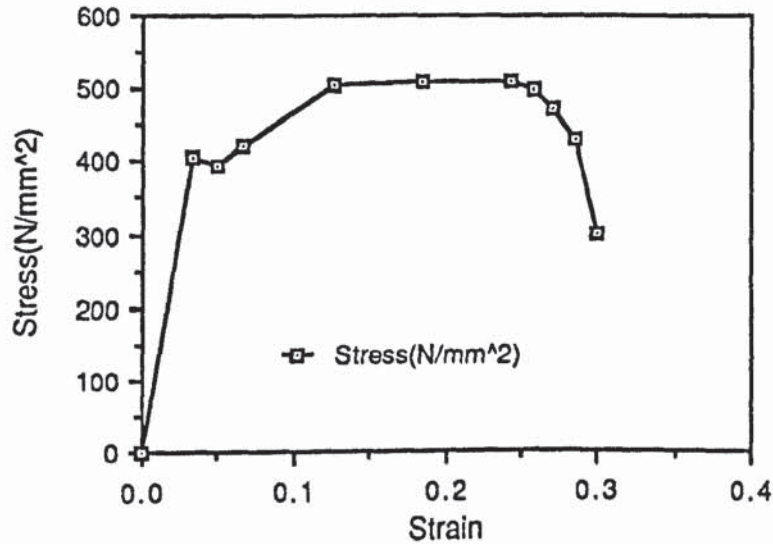


Figure 107 Stress-strain relationship for Transverse

AS RECEIVED LONGITUDINAL:

As recieved plate with specimen cut from the longitudinal to the rolling direction, tested in air. The mechanical properties truly represent that of a ductile steel with a cup and cone fracture surface.

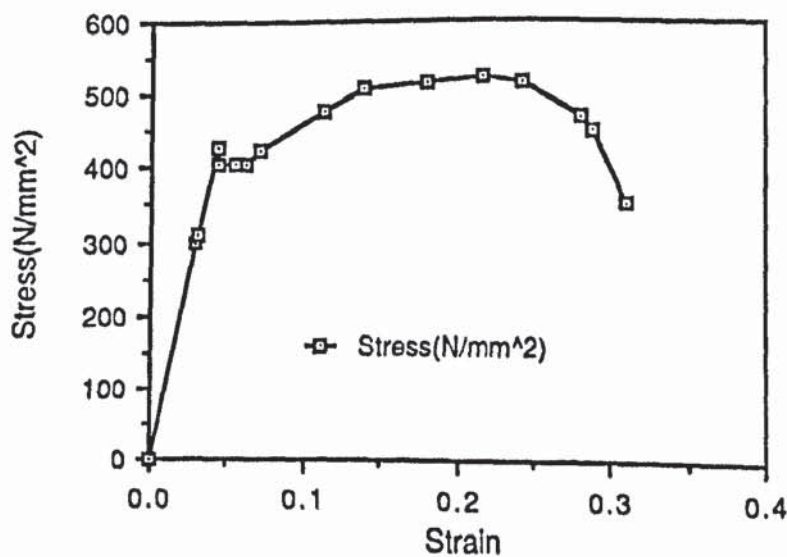


Figure 108 Stress-strain relationship for longitudinal

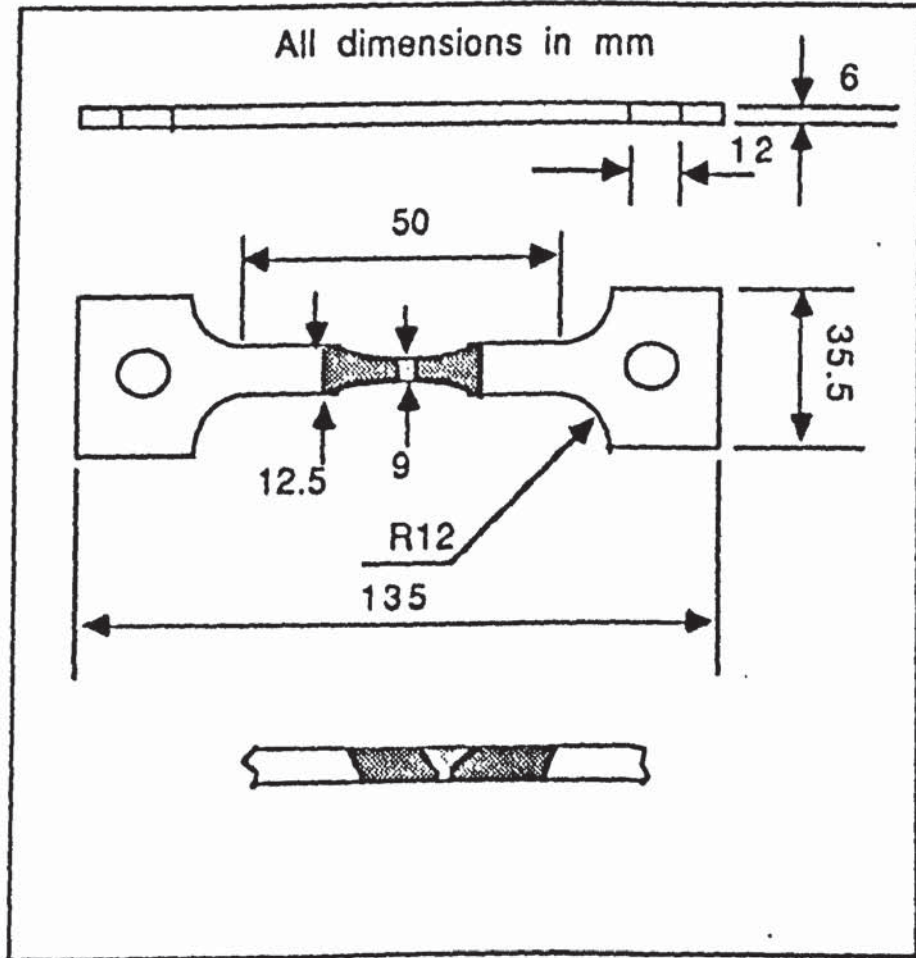


Figure 109 Diagrammatic representation of a notched specimen

APPENDIX 7

TABLES

No.	Specimen	Test in	Thickness (mm)		Width (mm)		Parallel Length (mm)		Ao mm ²	Af mm ²
			Before	After	Before	After	Before	After		
1	HNW1	Air	5.64	3.05	12.5	7.62	51.0	68.0	70.6	23.3
2	HNW2	Corr.	5.22	3.22	11.4	7.67	50.0	64.0	60.5	22.7
3	HNW3	Hydr.	5.60	4.87	12.6	10.8	50.0	63.0	70.7	51.5
4	HGC7	Air	4.87	2.32	12.5	8.00	35.0	45.5	60.8	18.6
5	HGC6	Corr.	4.68	3.04	12.4	7.60	38.0	48.0	58.1	23.1
6	HGC1	Hydr.	4.84	4.27	12.5	11.1	36.0	42.0	60.5	47.4
7	HB2	Air	5.08	2.32	12.3	7.55	36.0	47.5	62.4	17.5
8	HB3	Corr.	4.91	2.25	12.5	8.16	40.0	49.0	61.1	18.4
9	HB5	Hydr.	4.88	3.65	12.4	10.6	36.0	45.0	60.5	38.8
10	HGC5	Air	4.88	3.00	9.10	6.20	12.0	16.3	44.3	18.6
11	HGC8	Corr.	4.87	3.20	7.10	4.50	12.0	15.5	34.3	14.4
12	HGC4	Hydr.	4.85	4.55	6.80	5.50	11.9	13.6	33.0	25.5
13	HB8	Air	4.87	4.10	6.90	6.00	13.7	15.5	33.6	24.6
14	HB7	Corr.	4.88	4.06	7.00	5.70	12.0	13.7	34.4	23.1
15	HB6	Hydr.	4.87	3.90	7.00	5.90	12.4	13.9	33.9	23.0

- HNW Normalised specimens with no weld
HGC (7-6-1) Normalised specimens with sound welds
HB (2-3-5) Normalised specimens with defective welds.
HGC (4-5-8) Normalised specimens with sound welds and notched.
HB (6-7-8) Normalised specimens with defective welds and notched.

Table 22 Specimen dimensions for the normalised batch

No.	Specimen	Test in	Thickness (mm)		Width (mm)		Parallel Length (mm)		Ao mm ²	Af mm ²
			Before	After	Before	After	Before	After		
1	ONW1	Air	4.90	2.54	12.6	7.94	50.0	59.5	61.7	20.2
2	ONW2	Corr.	4.68	2.29	12.2	7.46	50.0	60.0	57.3	17.1
3	ONW3	Hydr.	4.90	3.10	12.3	9.90	50.0	59.5	60.5	30.5
4	OG1	Air	4.86	2.16	12.5	7.83	36.0	46.0	60.6	16.9
5	OG4	Corr.	4.58	2.40	12.4	7.82	33.5	44.0	56.8	18.8
6	OG3	Hydr.	4.82	3.79	12.5	11.4	36.0	44.0	60.3	43.2
7	OB1	Air	4.81	2.71	12.6	7.83	39.5	49.5	60.4	21.3
8	OB2	Corr.	4.59	2.41	12.4	7.63	38.0	47.5	56.9	18.4
9	OB3	Hydr.	4.49	3.79	12.5	10.9	39.0	45.5	56.0	41.3
10	OG5	Air	4.81	3.00	8.52	6.54	12.8	17.0	41.0	19.6
11	OG6	Corr.	4.72	3.23	8.34	6.02	13.5	17.5	39.4	19.4
12	OG7	Hydr.	4.82	4.03	8.45	7.14	13.2	16.2	40.9	28.8
13	OB4	Air	4.65	3.95	8.60	7.28	12.5	15.0	40.0	28.6
14	OB5	Corr.	4.61	3.75	8.52	7.05	12.0	14.3	39.3	26.4
15	OB6	Hydr.	4.65	4.46	8.52	7.48	13.3	14.8	39.6	33.4

- ONW Oil quenched and tempered specimens with no weld
OG (1-4-3) Oil quenched and tempered specimens with sound welds
OB (1-2-3) Oil quenched and tempered specimens with defective welds.
OG (5-6-7) Oil quenched and tempered specimens with sound welds and notched.
OB (4-5-6) Oil quenched and tempered specimens with defective welds and notched.

Table 23 Specimen dimensions for the oil quenched and tempered batch.

No.	Specimen	Test in	Thickness (mm)		Width (mm)		Parallel Length (mm)		Ao mm ²	Af mm ²
			Before	After	Before	After	Before	After		
1	WNW1	Air	4.30	2.25	12.6	8.53	50.0	58.0	54.2	19.2
2	WNW2	Corr.	4.10	2.08	12.3	8.44	50.0	58.0	50.7	17.5
3	WNW3	Hydr.	4.30	2.87	12.5	9.42	50.0	56.5	53.7	27.0
4	GW1	Air	4.40	2.40	12.5	8.15	50.0	58.2	55.0	19.4
5	GW2	Corr.	4.80	2.59	12.5	8.25	50.0	60.0	60.0	21.4
6	GW3	Hydr.	4.80	3.26	12.5	8.60	50.0	57.0	60.0	28.0
7	BW1	Air	4.80	3.82	11.5	10.7	50.0	53.5	55.2	40.8
8	BW2	Corr.	4.70	3.93	12.0	9.87	50.0	53.5	56.4	38.8
9	BW3	Hydr.	4.90	4.10	12.5	12.4	50.0	52.0	61.3	50.8

WNW Water quenched and tempered specimens with no weld
 G W Water quenched and tempered specimens with sound welds
 WB Water quenched and tempered specimens with defective welds.

Table 24 Specimen dimensions for the Water quenched and tempered batch.

No.	Specimen	Test in	Thickness (mm)		Width (mm)		Parallel Length (mm)		Ao mm ²	Af mm ²
			Before	After	Before	After	Before	After		
1	Transverse	Air	5.98	3.00	12.5	7.71	50.0	65.0	74.8	23.1
2	Longitudinal	Air	6.00	3.12	12.5	7.66	50.0	65.5	75.0	23.9

Table 25 Specimen dimensions for the as-received batch

APPENDIX 8

STATISTICAL ANALYSIS

APPENDIX 8.1 T-TEST FOR NORMALISED VS WATER QUENCHED

0- - - - - T - T E S T - - - - -

GROUP 1 - HEAT ED 1: normal-ised
 GROUP 2 - HEAT ED 3: water quenched

Variable	Number of Cases	Mean	Standard Deviation	Standard Error
YS yield stress				
GROUP 1	15	375.4000	49.195	12.702
GROUP 2	9	498.2222	80.641	26.880

F Value	2-tail Prob.	t Value	Degrees of Freedom	2-tail Prob.	t Value	Degrees of Freedom	2-tail Prob.
2.69	.101	-4.66	22	.000	-4.13	11.64	.001

Variable	Number of Cases	Mean	Standard Deviation	Standard Error
UTS ultimate tensile stress				
GROUP 1	15	515.8667	52.827	13.640
GROUP 2	9	589.5556	66.645	22.215

F Value	2-tail Prob.	t Value	Degrees of Freedom	2-tail Prob.	t Value	Degrees of Freedom	2-tail Prob.
1.59	.427	-3.00	22	.007	-2.83	14.03	.013

APPENDIX 8.1 CONT.

----- T - T E S T -----

GROUP 1 - HEAT EQ 1: normal-ised
 GROUP 2 - HEAT EQ 3: water quenched

Variable	Number of Cases	Mean	Standard Deviation	Standard Error
FS	fracture stress			
GROUP 1	15	657.2000	388.189	100.230
GROUP 2	9	854.7778	354.448	118.149

		Pooled Variance Estimate		Separate Variance Estimate	
F Value	2-tail Prob.	t Value	Degrees of Freedom	t Value	Degrees of 2-tail Prob.
1.20	.823	-1.25	22	.226	-1.28 18.26 .218

Variable	Number of Cases	Mean	Standard Deviation	Standard Error
ELONG	percentage elongation			
GROUP 1	15	20.3267	6.932	1.790
GROUP 2	9	12.6667	5.431	1.810

		Pooled Variance Estimate		Separate Variance Estimate	
F Value	2-tail Prob.	t Value	Degrees of Freedom	t Value	Degrees of 2-tail Prob.
1.63	.494	2.83	22	.010	3.01 ✓ 20.24 .007

----- T - T E S T -----

GROUP 1 - HEAT EQ 1: normal-ised
 GROUP 2 - HEAT EQ 3: water quenched

Variable	Number of Cases	Mean	Standard Deviation	Standard Error
RA	percentage reduction in area			
GROUP 1	15	47.8067	19.266	4.974
GROUP 2	9	48.6667	18.908	6.303

		Pooled Variance Estimate		Separate Variance Estimate	
F Value	2-tail Prob.	t Value	Degrees of Freedom	t Value	Degrees of 2-tail Prob.
1.04	.999	-.11	22	.916	-.11 17.25 .916

APPENDIX 8.2 T-TEST FOR OIL QUENCHED VS WATER QUENCHED

----- T - T E S T -----

GROUP 1 - HEAT EQ 2: oil quenched
 GROUP 2 - HEAT EQ 3: water quenched

Variable	Number of Cases	Mean	Standard Deviation	Standard Error
YS yield stress				
GROUP 1	15	445.4667	64.147	16.563
GROUP 2	9	498.2222	80.641	26.880

		* Pooled Variance Estimate *			* Separate Variance Estimate *		
F Value	2-tail Prob.	t Value	Degrees of Freedom	2-tail Prob.	t Value	Degrees of Freedom	2-tail Prob.
1.58	.434	* -1.77	22	.090	* -1.67	14.07	.117

Variable	Number of Cases	Mean	Standard Deviation	Standard Error
UTS ultimate tensile stress				
GROUP 1	15	559.8000	44.790	11.565
GROUP 2	9	589.5556	66.645	22.215

		* Pooled Variance Estimate *			* Separate Variance Estimate *		
F Value	2-tail Prob.	t Value	Degrees of Freedom	2-tail Prob.	t Value	Degrees of Freedom	2-tail Prob.
2.21	.185	* -1.31	22	.203	* -1.19	12.40	.257

APPENDIX 8.2 CONT.

----- T - T E S T -----

GROUP 1 - HEAT EQ 2: oil quenched
 GROUP 2 - HEAT EQ 3: water quenched

Variable	Number of Cases	Mean	Standard Deviation	Standard Error
FS fracture stress				
GROUP 1	15	801.5333	384.141	99.185
GROUP 2	9	854.7778	354.448	118.149

		Pooled Variance Estimate		Separate Variance Estimate	
F Value	2-tail Prob.	t Value	Degrees of Freedom	t Value	Degrees of Freedom
1.17	.848	-.34	22	.739	18.11
					2-tail Prob. .734

Variable	Number of Cases	Mean	Standard Deviation	Standard Error
ELONG percentage elongation				
GROUP 1	15	22.8000	5.931	1.531
GROUP 2	9	12.6667	5.431	1.810

		Pooled Variance Estimate		Separate Variance Estimate	
F Value	2-tail Prob.	t Value	Degrees of Freedom	t Value	Degrees of Freedom
1.19	.831	4.18	22	4.27	18.21
					2-tail Prob. .000

----- T - T E S T -----

GROUP 1 - HEAT EQ 2: oil quenched
 GROUP 2 - HEAT EQ 3: water quenched

Variable	Number of Cases	Mean	Standard Deviation	Standard Error
RA percentage reduction in area				
GROUP 1	15	48.1333	19.555	5.049
GROUP 2	9	48.6667	18.908	6.303

		Pooled Variance Estimate		Separate Variance Estimate	
F Value	2-tail Prob.	t Value	Degrees of Freedom	t Value	Degrees of Freedom
1.07	.963	-.07	22	.948	17.46
					2-tail Prob. .948

APPENDIX 8.3 T-TEST FOR PLAIN SPECIMEN VS WELD

0- - - - - T - T E S T - - - - -

GROUP 1 - WELD EQ 1: plain specimen
 GROUP 2 - WELD EQ 2: sound weld

Variable	Number of Cases	Mean	Standard Deviation	Standard Error
yield stress				
GROUP 1	9	478.5556	123.693	41.231
GROUP 2	15	428.5333	69.615	17.975

		Pooled Variance Estimate			Separate Variance Estimate		
F Value	2-tail Prob.	t Value	Degrees of Freedom	2-tail Prob.	t Value	Degrees of Freedom	2-tail Prob.
3.16	.058	1.28	22	.215	1.11	11.10	.290

0

Variable	Number of Cases	Mean	Standard Deviation	Standard Error
ultimate tensile stress				
GROUP 1	9	560.2222	92.392	30.797
GROUP 2	15	556.0667	55.386	14.301

		Pooled Variance Estimate			Separate Variance Estimate		
F Value	2-tail Prob.	t Value	Degrees of Freedom	2-tail Prob.	t Value	Degrees of Freedom	2-tail Prob.
2.78	.090	.14	22	.891	.12	11.52	.905

0

APPENDIX 8.3 CONT.

----- T - T E S T -----

GROUP 1 - WELD ED 1: plain specimen
 GROUP 2 - WELD ED 2: sound weld

Variable	Number of Cases	Mean	Standard Deviation	Standard Error
FS fracture stress				
GROUP 1	9	885.7778	330.957	110.319
GROUP 2	15	886.1333	382.521	98.767

		Pooled Variance Estimate		Separate Variance Estimate	
F Value	2-tail Prob.	t Value	Degrees of Freedom	t Value	Degrees of Freedom
1.34	.699	.00	22	.998	18.99

Variable	Number of Cases	Mean	Standard Deviation	Standard Error
ELONG percentage elongation				
GROUP 1	9	71.2222	6.760	2.253
GROUP 2	15	22.5067	6.346	1.639

		Pooled Variance Estimate		Separate Variance Estimate	
F Value	2-tail Prob.	t Value	Degrees of Freedom	t Value	Degrees of Freedom
1.13	.798	-.47	22	.644	16.12

----- T - T E S T -----

GROUP 1 - WELD ED 1: plain specimen
 GROUP 2 - WELD ED 2: sound weld

Variable	Number of Cases	Mean	Standard Deviation	Standard Error
RA percentage reduction in area				
GROUP 1	9	58.0667	13.802	4.601
GROUP 2	15	51.7267	17.243	4.452

		Pooled Variance Estimate		Separate Variance Estimate	
F Value	2-tail Prob.	t Value	Degrees of Freedom	t Value	Degrees of Freedom
1.56	.535	.94	22	.360	19.98

APPENDIX 8.4 T-TEST FOR SOUND WELD VS DEFECTIVE WELD

0- - - - - T - T E S T - - - - -

GROUP 1 - WELD EQ 2: sound weld
 GROUP 2 - WELD EQ 3: defect weld

0

Variable	Number of Cases	Mean	Standard Deviation	Standard Error
YS yield stress				
GROUP 1	15	428.5333	69.615	17.975
GROUP 2	15	404.1333	29.486	7.613

0

		# Pooled Variance Estimate #			# Separate Variance Estimate #		
F Value	2-tail Prob.	t Value	Degrees of Freedom	2-tail Prob.	t Value	Degrees of Freedom	2-tail Prob.
5.57	.003	1.25	28	.222	1.25	18.87	.227

0

Variable	Number of Cases	Mean	Standard Deviation	Standard Error
UTS ultimate tensile stress				
GROUP 1	15	556.0667	55.386	14.301
GROUP 2	15	537.2000	38.266	9.880

0

		# Pooled Variance Estimate #			# Separate Variance Estimate #		
F Value	2-tail Prob.	t Value	Degrees of Freedom	2-tail Prob.	t Value	Degrees of Freedom	2-tail Prob.
2.09	.179	1.09	28	.287	1.09	24.89	.288

0

APPENDIX 8.4 CONT.

----- T - T E S T -----

GROUP 1 - WELD EQ 2: sound weld
 GROUP 2 - WELD EQ 3: defect weld

Variable	Number of Cases	Mean	Standard Deviation	Standard Error
FS fracture stress				
GROUP 1	15	886.1333	382.521	98.767
GROUP 2	15	554.0000	327.712	84.615

F Value	2-tail Prob.	t Value	Degrees of Freedom	2-tail Prob.	t Value	Degrees of Freedom	2-tail Prob.
1.36	.571	2.55	28	.016	2.55	27.36	.017

Variable	Number of Cases	Mean	Standard Deviation	Standard Error
ELONG percentage elongation				
GROUP 1	15	22.5067	6.346	1.639
GROUP 2	15	15.4867	6.875	1.775

F Value	2-tail Prob.	t Value	Degrees of Freedom	2-tail Prob.	t Value	Degrees of Freedom	2-tail Prob.
1.17	.769	2.91	28	.007	2.91	27.82	.007

----- T - T E S T -----

GROUP 1 - WELD EQ 2: sound weld
 GROUP 2 - WELD EQ 3: defect weld

Variable	Number of Cases	Mean	Standard Deviation	Standard Error
RA percentage reduction in area				
GROUP 1	15	51.7267	17.243	4.452
GROUP 2	15	38.5733	19.411	5.012

F Value	2-tail Prob.	t Value	Degrees of Freedom	2-tail Prob.	t Value	Degrees of Freedom	2-tail Prob.
1.27	.664	1.96	28	.060	1.96	27.62	.060

APPENDIX 8.5 T-TEST FOR PLAIN SPECIMEN VS NOTCH AT WELD

0-----T-----T-----E-----S-----T-----0-----

GROUP 1 - NOTCH EQ 1: plain specimen
 GROUP 2 - NOTCH EQ 2: notch at weld

Variable	Number of Cases	Mean	Standard Deviation	Standard Error

YS yield stress				
GROUP 1	27	427.5556	91.951	17.696
GROUP 2	12	437.7500	34.370	9.922

		Pooled Variance Estimate		Separate Variance Estimate	
F Value	2-tail Prob.	t Value	Degrees of Freedom	t Value	Degrees of Freedom
7.16	.002	-.37	37	.713	36.41
					.618

Variable	Number of Cases	Mean	Standard Deviation	Standard Error

UTS ultimate tensile stress				
GROUP 1	27	540.2593	65.637	12.632
GROUP 2	12	571.1667	37.820	10.918

		Pooled Variance Estimate		Separate Variance Estimate	
F Value	2-tail Prob.	t Value	Degrees of Freedom	t Value	Degrees of Freedom
3.01	.059	-1.52	37	.138	34.22
					.073

APPENDIX 8.5 CONT.

----- T - T E S T -----

GROUP 1 - NOTCH EQ 1: plain specimen
 GROUP 2 - NOTCH EQ 2: notch at weld

Variable	Number of Cases	Mean	Standard Deviation	Standard Error
FS fracture stress				
GROUP 1	27	799.0000	404.800	77.904
GROUP 2	12	666.7500	307.484	88.763

F		t		t		t		
Value	2-tail Prob.	Value	Degrees of Freedom	Value	Degrees of Freedom	Value	2-tail Prob.	
1.73	.340	1.01	37	.320	37	1.12	27.56	.272

Variable	Number of Cases	Mean	Standard Deviation	Standard Error
ELONG percentage elongation				
GROUP 1	27	19.5778	7.133	1.373
GROUP 2	12	19.3583	7.816	2.256

F		t		t		t		
Value	2-tail Prob.	Value	Degrees of Freedom	Value	Degrees of Freedom	Value	2-tail Prob.	
1.20	.669	.09	37	.932	37	.08	19.52	.935

----- T - T E S T -----

GROUP 1 - NOTCH EQ 1: plain specimen
 GROUP 2 - NOTCH EQ 2: notch at weld

Variable	Number of Cases	Mean	Standard Deviation	Standard Error
RA percentage reduction in area				
GROUP 1	27	53.1333	18.559	3.572
GROUP 2	12	36.8750	14.344	4.141

F		t		t		t		
Value	2-tail Prob.	Value	Degrees of Freedom	Value	Degrees of Freedom	Value	2-tail Prob.	
1.67	.373	2.69	37	.011	37	2.97 ✓	27.11	.006

APPENDIX 8.6 T-TEST FOR AIR VS CORROSION

0 - - - - - T - T E S T - - - - -

GROUP 1 - ENVIRON EQ 1: air
 GROUP 2 - ENVIRON EQ 2: corrosion

0

Variable	Number of Cases	Mean	Standard Deviation	Standard Error
YS yield stress				
GROUP 1	13	449.5385	79.252	21.981
GROUP 2	13	420.4615	73.833	20.478

0

		\$ Pooled Variance Estimate \$			\$ Separate Variance Estimate \$		
F Value	2-tail Prob.	t Value	Degrees of Freedom	2-tail Prob.	t Value	Degrees of Freedom	2-tail Prob.
1.15	.810	.97	24	.343	.97	23.88	.343

0

0

0

Variable	Number of Cases	Mean	Standard Deviation	Standard Error
UTS ultimate tensile stress				
GROUP 1	13	569.9231	61.314	17.005
GROUP 2	13	536.3846	51.621	14.317

0

		\$ Pooled Variance Estimate \$			\$ Separate Variance Estimate \$		
F Value	2-tail Prob.	t Value	Degrees of Freedom	2-tail Prob.	t Value	Degrees of Freedom	2-tail Prob.
1.41	.560	1.51	24	.144	1.51	23.32	.145

0

APPENDIX 8.6 CONT.

0- - - - - T - T E S T - - - - -

GROUP 1 - ENVIRON EQ 1: air
 GROUP 2 - ENVIRON EQ 2: corrosion

Variable	Number of Cases	Mean	Standard Deviation	Standard Error
FS fracture stress				
GROUP 1	13	991.0000	273.233	75.781
GROUP 2	13	852.2308	344.970	95.677

F Value	2-tail Prob.	t Value	Degrees of Freedom	2-tail Prob.	t Value	Degrees of Freedom	2-tail Prob.
1.59	.431	1.14	24	.267	1.14	22.80	.267

Variable	Number of Cases	Mean	Standard Deviation	Standard Error
ELONG percentage elongation				
GROUP 1	13	21.8538	7.862	2.180
GROUP 2	13	20.7846	6.805	1.887

F Value	2-tail Prob.	t Value	Degrees of Freedom	2-tail Prob.	t Value	Degrees of Freedom	2-tail Prob.
1.33	.625	.37	24	.714	.37	23.52	.714

0

0- - - - - T - T E S T - - - - -

GROUP 1 - ENVIRON EQ 1: air
 GROUP 2 - ENVIRON EQ 2: corrosion

Variable	Number of Cases	Mean	Standard Deviation	Standard Error
RA percentage reduction in area				
GROUP 1	13	56.4923	17.644	4.894
GROUP 2	13	56.2846	14.486	4.018

F Value	2-tail Prob.	t Value	Degrees of Freedom	2-tail Prob.	t Value	Degrees of Freedom	2-tail Prob.
1.48	.505	.03	24	.974	.03	23.12	.974

APPENDIX 8.7 T-TEST FOR AIR VS HYDROGEN

0- - - - - T - T E S T - - - - -

GROUP 1 - ENVIRON ED 1: air
 GROUP 2 - ENVIRON ED 3: hydrogen

Variable	Number of Cases	Mean	Standard Deviation	Standard Error

YS	yield stress			
GROUP 1	13	449.5385	79.252	21.981
GROUP 2	13	422.0769	84.636	23.474

		* Pooled Variance Estimate *		* Separate Variance Estimate *	
F	2-tail	t	Degrees of	t	Degrees of
Value	Prob.	Value	Freedom	Value	Freedom
1.14	.824	.85	24	.402	23.90
					.402

Variable	Number of Cases	Mean	Standard Deviation	Standard Error

UTS	ultimate tensile stress			
GROUP 1	13	569.9231	61.314	17.005
GROUP 2	13	543.0000	64.801	17.973

		* Pooled Variance Estimate *		* Separate Variance Estimate *	
F	2-tail	t	Degrees of	t	Degrees of
Value	Prob.	Value	Freedom	Value	Freedom
1.12	.851	1.09	24	.287	23.93
					.287

APPENDIX 8.7 CONT.

0- - - - - T - T E S T - - - - -

GROUP 1 - ENVIRON EQ 1: air
 GROUP 2 - ENVIRON EQ 3: hydrogen

Variable	Number of Cases	Mean	Standard Deviation	Standard Error
FS fracture stress				
GROUP 1	13	991.0000	273.233	75.781
GROUP 2	13	431.6923	276.353	76.647

F Value	2-tail Prob.	t Value	Degrees of Freedom	2-tail Prob.	t Value	Degrees of Freedom	2-tail Prob.
1.02	.969	5.19	24	.000	5.19	24.00	.000

Variable	Number of Cases	Mean	Standard Deviation	Standard Error
ELONG percentage elongation				
GROUP 1	13	21.8538	7.862	2.180
GROUP 2	13	15.8923	6.021	1.670

F Value	2-tail Prob.	t Value	Degrees of Freedom	2-tail Prob.	t Value	Degrees of Freedom	2-tail Prob.
1.70	.368	2.17	24	.040	2.17	22.47	.041

0- - - - - T - T E S T - - - - -

GROUP 1 - ENVIRON EQ 1: air
 GROUP 2 - ENVIRON EQ 3: hydrogen

Variable	Number of Cases	Mean	Standard Deviation	Standard Error
RA percentage reduction in area				
GROUP 1	13	56.4923	17.644	4.894
GROUP 2	13	31.6154	12.387	3.436

F Value	2-tail Prob.	t Value	Degrees of Freedom	2-tail Prob.	t Value	Degrees of Freedom	2-tail Prob.
2.03	.235	4.16	24	.000	4.16 ✓	21.52	.000

APPENDIX 8.8 T-TEST FOR PARENT PLATE VS WELD

0- - - - - T - T E S T - - - - -

GROUP 1 - FRACT EQ 0: parent plate
 GROUP 2 - FRACT EQ 1: weld

Variable	Number of Cases	Mean	Standard Deviation	Standard Error
YS yield stress				
GROUP 1	24	428.5417	97.591	19.921
GROUP 2	15	434.1333	32.013	8.266

F Value	2-tail Prob.	t Value	Degrees of Freedom	2-tail Prob.	t Value	Degrees of Freedom	2-tail Prob.
9.29	.000	-.21	37	.832	-.26	30.13	.797 ✓

Variable	Number of Cases	Mean	Standard Deviation	Standard Error
UTS ultimate tensile stress				
GROUP 1	24	541.8750	66.162	13.505
GROUP 2	15	562.4000	47.144	12.172

F Value	2-tail Prob.	t Value	Degrees of Freedom	2-tail Prob.	t Value	Degrees of Freedom	2-tail Prob.
1.97	.191	-1.04	37	.303 ✓	-1.13	36.25	.266

118-Jan-90 modelling the results
 09:38:59 ASTON UNIVERSITY

on SPOCK::

VMS V5.2

Page

APPENDIX 8.8 CONT.

0- - - - - T - T E S T - - - - -

GROUP 1 - FRACT ED 0: parent plate
GROUP 2 - FRACT ED 1: weld

Variable	Number of Cases	Mean	Standard Deviation	Standard Error
FS fracture stress				
GROUP 1	24	847.6667	401.937	82.045
GROUP 2	15	615.3333	296.619	76.587

F Value	2-tail Prob.	t Value	Degrees of Freedom	2-tail Prob.	t Value	Degrees of Freedom	2-tail Prob.
1.84	.241	1.93	37	.061 ✓	2.07	35.84	.046

0

Variable	Number of Cases	Mean	Standard Deviation	Standard Error
ELONG percentage elongation				
GROUP 1	24	21.2750	5.495	1.122
GROUP 2	15	16.6867	8.889	2.295

F Value	2-tail Prob.	t Value	Degrees of Freedom	2-tail Prob.	t Value	Degrees of Freedom	2-tail Prob.
2.62	.039	2.00	37	.053	1.80	20.76	.087 ✓

0

0- - - - - T - T E S T - - - - -

GROUP 1 - FRACT ED 0: parent plate
GROUP 2 - FRACT ED 1: weld

Variable	Number of Cases	Mean	Standard Deviation	Standard Error
RA percentage reduction in area				
GROUP 1	24	56.6500	16.378	3.343
GROUP 2	15	34.5000	13.928	3.596

0

F Value	2-tail Prob.	t Value	Degrees of Freedom	2-tail Prob.	t Value	Degrees of Freedom	2-tail Prob.
1.38	.537	4.34	37	.000 ✓	4.51	33.45	.000

APPENDIX 8.9 ANALYSIS OF VARIANCE (MAIN EFFECTS)

0 *** ANALYSIS OF VARIANCE ***

by YS yield stress
 HEAT heat treatment of the steel
 WELD plain specimen, sound or defective weldm
 NOTCH plain specimen or notched at fusion zone
 ENVIRON air, corrosion or hydrogen environment

Source of Variation	Sum of Squares	DF	Mean Square	F	Sig of F
0Main Effects	151621.047	7	21660.150	8.182	.000
HEAT	104236.033	2	52118.017	19.687	.000
WELD	39578.700	2	19789.350	7.475	.002
NOTCH	32050.240	1	32050.240	12.107	.002
ENVIRON	6942.923	2	3471.462	1.311	.284
0Explained	151621.047	7	21660.150	8.182	.000
0Residual	82067.260	31	2647.331		
0Total	233688.308	38	6149.692		

0 39 cases were processed.
 0 cases (.0 pct) were missing.

by UTS ultimate tensile stress
 HEAT heat treatment of the steel
 WELD plain specimen, sound or defective weldm
 NOTCH plain specimen or notched at fusion zone
 ENVIRON air, corrosion or hydrogen environment

Source of Variation	Sum of Squares	DF	Mean Square	F	Sig of F
0Main Effects	71473.365	7	10210.481	4.929	.001
HEAT	47282.719	2	23641.359	11.414	.000
WELD	8049.652	2	4024.826	1.943	.160
NOTCH	27286.538	1	27286.538	13.173	.001
ENVIRON	8204.923	2	4102.462	1.981	.155
0Explained	71473.365	7	10210.481	4.929	.001
0Residual	64211.558	31	2071.341		
0Total	135684.923	38	3570.656		

0 39 cases were processed.
 0 cases (.0 pct) were missing.

0 Due to empty cells or a singular matrix,

C:\KERM1T>

APPENDIX 8.9 CONT.

*** ANALYSIS OF VARIANCE ***

FS fracture stress
 by HEAT heat treatment of the steel
 WELD plain specimen, sound or defective weldm
 NOTCH plain specimen or notched at fusion zone
 ENVIRON air, corrosion or hydrogen environment

Source of Variation	Sum of Squares	DF	Mean Square	F	Sig of F
OMain Effects	3477931.088	7	496847.298	7.827	.000
HEAT	198241.500	2	99120.750	1.561	.226
WELD	929004.300	2	464502.150	7.317	.002
NOTCH	23617.770	1	23617.770	.372	.546
ENVIRON	2205383.231	2	1102691.615	17.371	.000
OExplained	3477931.088	7	496847.298	7.827	.000
OResidual	1967829.219	31	63478.362		
OTotal	5445760.308	38	143309.482		

39 cases were processed.
 0 cases (.0 pct) were missing.

ELONG percentage elongation
 by HEAT heat treatment of the steel
 WELD plain specimen, sound or defective weldm
 NOTCH plain specimen or notched at fusion zone
 ENVIRON air, corrosion or hydrogen environment

Source of Variation	Sum of Squares	DF	Mean Square	F	Sig of F
OMain Effects	1359.874	7	194.268	9.481	.000
HEAT	690.687	2	345.344	16.854	.000
WELD	406.110	2	203.055	9.910	.000
NOTCH	51.702	1	51.702	2.523	.122
ENVIRON	262.677	2	131.339	6.410	.005
OExplained	1359.874	7	194.268	9.481	.000
OResidual	635.202	31	20.490		
OTotal	1995.076	38	52.502		

39 cases were processed.
 0 cases (.0 pct) were missing.

Due to empty cells or a singular matrix,

*** ANALYSIS OF VARIANCE ***

RA percentage reduction in area
 by HEAT heat treatment of the steel
 WELD plain specimen, sound or defective weldm
 NOTCH plain specimen or notched at fusion zone
 ENVIRON air, corrosion or hydrogen environment

Source of Variation	Sum of Squares	DF	Mean Square	F	Sig of F
OMain Effects	9411.337	7	1344.477	10.412	.000
HEAT	270.140	2	135.070	1.046	.363
WELD	1626.136	2	813.068	6.297	.005
NOTCH	1631.439	1	1631.439	12.634	.001
ENVIRON	5319.060	2	2659.530	20.596	.000
OExplained	9411.337	7	1344.477	10.412	.000
OResidual	4002.946	31	129.127		
OTotal	13414.283	38	353.007		

39 cases were processed.
 0 cases (.0 pct) were missing.

APPENDIX 8.10 ANALYSIS OF VARIANCE (MAIN EFFECTS, 2 AND 3 WAY INTERACTIONS)

*** ANALYSIS OF VARIANCE ***

YS yield stress
 by HEAT heat treatment of the steel
 WELD plain specimen, sound or defective weldm
 ENVIRON air, corrosion or hydrogen environment

Source of Variation	Sum of Squares	DF	Mean Square	F	Sig of F
Main Effects	119570.807	6	19928.468	6.321	.003
HEAT ✓	81359.265	2	40679.633	12.903	.001
WELD	22452.465	2	11226.233	3.561	.061
ENVIRON	6942.923	2	3471.462	1.101	.364
02-Way Interactions	62045.285	12	5170.440	1.640	.202
HEAT WELD ✓	53422.090	4	13355.523	4.236	.023
HEAT ENVIRON	3405.895	4	851.474	.270	.892
WELD ENVIRON	5429.629	4	1357.407	.431	.784
03-Way Interactions	14239.216	8	1779.902	.565	.788
HEAT WELD ENVIRON	14239.216	8	1779.902	.565	.788
0Explained	195855.308	26	7532.896	2.389	.058
0Residual	37833.000	12	3152.750		
0Total	233688.308	38	6149.692		

*** ANALYSIS OF VARIANCE ***

UTS ultimate tensile stress
 by HEAT heat treatment of the steel
 WELD plain specimen, sound or defective weldm
 ENVIRON air, corrosion or hydrogen environment

Source of Variation	Sum of Squares	DF	Mean Square	F	Sig of F
Main Effects	44186.827	6	7364.471	3.125	.044
HEAT ✓	32033.869	2	16016.935	6.797	.011
WELD	2985.336	2	1492.668	.633	.548
ENVIRON	8204.923	2	4102.462	1.741	.217
02-Way Interactions	53660.926	12	4471.744	1.898	.141
HEAT WELD ✓	42260.853	4	10565.213	4.484	.019
HEAT ENVIRON	4554.107	4	1138.527	.483	.748
WELD ENVIRON	6583.574	4	1645.893	.698	.608
03-Way Interactions	9560.671	8	1195.084	.507	.829
HEAT WELD ENVIRON	9560.671	8	1195.084	.507	.829
0Explained	107408.423	26	4131.093	1.753	.154
0Residual	28276.500	12	2356.375		
0Total	135684.923	38	3570.656		

APPENDIX 8.10 CONT.

0 *** ANALYSIS OF VARIANCE ***

by FS fracture stress
 HEAT heat treatment of the steel
 WELD plain specimen, sound or defective weldm
 ENVIRON air, corrosion or hydrogen environment

Source of Variation	Sum of Squares	DF	Mean Square	F	Sig of F
0Main Effects	3454313.319	6	575718.884	12.622	.000
HEAT	231477.069	2	115738.535	2.537	.120
WELD	983803.469	2	491901.735	10.784	.002
ENVIRON	2205383.231	2	1102691.615	24.175	.000
02-Way Interactions	1240160.697	12	103346.725	2.266	.085
HEAT WELD	321944.720	4	80486.180	1.765	.701
HEAT ENVIRON	478682.719	4	119670.680	2.624	.088
WELD ENVIRON	409096.319	4	102274.080	2.242	.125
03-Way Interactions	203941.792	8	25492.724	.559	.792
HEAT WELD ENVIRON	203941.792	8	25492.724	.559	.792
0Explained	4898415.808	26	188400.608	4.131	.007
0Residual	547344.500	12	45612.042		
0Total	5445760.308	38	143309.482		

0 *** ANALYSIS OF VARIANCE ***

by ELONG percentage elongation
 HEAT heat treatment of the steel
 WELD plain specimen, sound or defective weldm
 ENVIRON air, corrosion or hydrogen environment

Source of Variation	Sum of Squares	DF	Mean Square	F	Sig of F
0Main Effects	1308.172	6	218.029	12.491	.000
HEAT	641.601	2	320.800	18.378	.000
WELD	451.648	2	225.824	12.937	.001
ENVIRON	262.677	2	131.339	7.524	.008
02-Way Interactions	426.386	12	35.532	2.036	.116
HEAT WELD	353.393	4	88.348	5.061	.013
HEAT ENVIRON	32.426	4	8.106	.444	.741
WELD ENVIRON	38.349	4	9.587	.549	.703
03-Way Interactions	51.053	8	6.382	.366	.920
HEAT WELD ENVIRON	51.053	8	6.382	.366	.920
0Explained	1785.611	26	68.677	3.934	.008
0Residual	209.465	12	17.455		
0Total	1995.076	38	52.502		

0 *** ANALYSIS OF VARIANCE ***

by RA percentage reduction in area
 HEAT heat treatment of the steel
 WELD plain specimen, sound or defective weldm
 ENVIRON air, corrosion or hydrogen environment

Source of Variation	Sum of Squares	DF	Mean Square	F	Sig of F
0Main Effects	7779.898	6	1296.650	4.555	.012
HEAT	8.214	2	4.107	.014	.986
WELD ✓	2456.678	2	1228.339	4.315	.039
ENVIRON ✓	5319.060	2	2659.530	9.343	.004
02-Way Interactions	1916.693	12	159.724	.561	.835
HEAT WELD	1253.443	4	313.361	1.101	.400
HEAT ENVIRON	421.495	4	105.374	.370	.825
WELD ENVIRON	243.020	4	60.755	.213	.926
03-Way Interactions	301.717	8	37.715	.132	.996
HEAT WELD ENVIRON	301.717	8	37.715	.132	.996
0Explained	9998.308	26	384.550	1.351	.299
0Residual	3415.975	12	284.665		
0Total	13414.283	38	353.007		

APPENDIX 8.11 REGRESSION MODELLING (PARENT PLATE)

Variable(s) Entered on Step Number
 2.. HEATWELD

0
 Multiple R .75483
 R Square .56976
 Adjusted R Square .52879
 Standard Error 66.99128

Analysis of Variance

	DF	Sum of Squares	Mean Square
Regression	2	124807.48611	62403.74306
Residual	21	94244.47222	4487.83201

F = 13.90510 Signif F = .0001

0
 ----- Variables in the Equation -----

Variable	B	SE B	Beta	T	Sig T
HEAT	154.305556	29.540379	.781932	5.224	.0000
HEATWELD	-96.083333	43.242687	-.332613	-2.222	.0374
(Constant)	344.111111	22.330428		15.410	.0000

0
 Variable(s) Entered on Step Number
 1.. HEAT heat treatment of the steel

0
 Multiple R .70809
 R Square .50140
 Adjusted R Square .47873
 Standard Error 47.76819

Analysis of Variance

	DF	Sum of Squares	Mean Square
Regression	1	50481.02500	50481.02500
Residual	22	50199.60000	2281.80000

F = 22.12333 Signif F = .0001

0
 ----- Variables in the Equation -----

Variable	B	SE B	Beta	T	Sig T
HEAT	94.733333	20.140837	.708094	4.704	.0001
(Constant)	482.666667	15.922730		30.313	.0000

118-Jan-90 modelling the results

Variable(s) Entered on Step Number
 2.. HEAT heat treatment of the steel

0
 Multiple R .78029
 R Square .60885
 Adjusted R Square .57160
 Standard Error 263.07669

Analysis of Variance

	DF	Sum of Squares	Mean Square
Regression	2	2262337.04444	1131168.52222
Residual	21	1453396.28889	69209.34709

F = 16.34416 Signif F = .0001

0
 ----- Variables in the Equation -----

Variable	B	SE B	Beta	T	Sig T
ENVIRON	-583.750000	113.915550	-.699365	-5.124	.0000
HEAT	281.244444	110.922874	.346037	2.535	.0192
(Constant)	866.472222	95.560394		9.067	.0000

APPENDIX 8.11 CONT.

Variable(s) Entered on Step Number
 1.. ENVIRON air, corrosion or hydrogen environment

0
 Multiple R .40914
 R Square .16739
 Adjusted R Square .12955
 Standard Error 5.12673

Analysis of Variance

	DF	Sum of Squares	Mean Square
Regression	1	116.25187	116.25187
Residual	22	578.23313	26.28332

F = 4.42303 Signif F = .0471

0
 ----- Variables in the Equation -----

Variable	B	SE B	Beta	T	Sig T
ENVIRON	-4.668750	2.219938	-.409137	-2.103	.0471
(Constant)	22.831250	1.281682		17.814	.0000

 118-Jan-90 modelling the results

3.. HEWELENU

0
 Multiple R .94388
 R Square .89090
 Adjusted R Square .87454
 Standard Error 5.80123

Analysis of Variance

	DF	Sum of Squares	Mean Square
Regression	3	5496.53563	1832.17854
Residual	20	673.08437	33.65422

F = 54.44127 Signif F = .0000

0
 ----- Variables in the Equation -----

Variable	B	SE B	Beta	T	Sig T
ENVIRON	-38.431250	3.649858	-1.129938	-10.530	.0000
HEATENU	16.950000	4.430759	.429335	3.826	.0011
HEWELENU	-19.250000	6.485967	-.239916	-2.968	.0076
(Constant)	66.731250	1.450306		46.012	.0000

 118-Jan-90 modelling the results

APPENDIX 8.12 REGRESSION MODELLING (WELD)

Variable(s) Entered on Step Number 2.. HEAT heat treatment of the steel
 Multiple R .82009
 R Square .67235
 Adjusted R Square .61797
 Standard Error 19.78676

Analysis of Variance

	DF	Sum of Squares	Mean Square
Regression	2	9649.54286	4824.77143
Residual	12	4698.19048	391.51667

F = 12.32331 Signif F = .0012

Variable	B	SE B	Beta	T	Sig T
WELD	-48.571429	10.576468	-.769379	-4.592	.0006
HEAT	27.761905	10.576468	.439753	2.625	.0222
(Constant)	445.619048	9.654950		46.258	.0000

Variable(s) Entered on Step Number 1.. HEWELENV

Multiple R .57738
 R Square .33878
 Adjusted R Square .23407
 Standard Error 41.25907

Analysis of Variance

	DF	Sum of Squares	Mean Square
Regression	1	8985.60000	8985.60000
Residual	12	22120.00000	1702.30769

F = 5.27848 Signif F = .0388

Variable	B	SE B	Beta	T	Sig T
HEWELENV	-72.000000	31.338484	-.537384	-2.297	.0388
(Constant)	572.000000	11.443196		49.986	.0000

Variable(s) Entered on Step Number 3.. WELDENV

Multiple R .91746
 R Square .84173
 Adjusted R Square .79857
 Standard Error 133.12525

Analysis of Variance

	DF	Sum of Squares	Mean Square
Regression	3	1036815.66667	345605.22222
Residual	11	194945.66667	17722.33333

F = 19.50111 Signif F = .0001

Variable	B	SE B	Beta	T	Sig T
WELD	-516.500000	85.931982	-.882995	-6.011	.0001
ENVIRON	-590.500000	115.287852	-.971395	-5.122	.0003
WELDENV	417.833333	148.838559	.583237	2.807	.0171
(Constant)	1038.500000	66.562627		15.602	.0000

APPENDIX 8.12 CONT.

0
 Multiple R .98032
 R Square .76103
 Adjusted R Square .93937
 Standard Error 2.18874

Analysis of Variance

	DF	Sum of Squares	Mean Square
Regression	5	1063.14206	212.62841
Residual	9	43.11528	4.79059

F = 44.38463 Signif F = .0000

0
 ----- Variables in the Equation -----
 0Variable B SE B Beta T Sig T

WELD	-12.455556	1.504060	-.710536	-0.781	.0000
ENVIRON	-10.250000	1.875505	-.562646	-5.408	.0004
NDTCH	11.441667	1.671678	.532926	6.844	.0001
HEAT	6.616667	1.263670	.377453	5.236	.0005
WELDENV	6.016667	2.447087	.280242	2.459	.0362
(Constant)	<u>13.250000</u>	2.278114		5.816	.0003

4.. HEWELENV

0
 Multiple R .97802
 R Square .95653
 Adjusted R Square .93914
 Standard Error 3.43600

Analysis of Variance

	DF	Sum of Squares	Mean Square
Regression	4	2597.77917	649.44479
Residual	10	118.06083	11.80608

F = 55.00933 Signif F = .0000

0
 ----- Variables in the Equation -----
 0Variable B SE B Beta T Sig T

WELD	-25.391667	2.217927	-.924465	-11.448	.0000
ENVIRON	-28.025000	2.975662	-.981822	-9.418	.0000
WELDENV	30.341667	4.756924	.901972	6.378	.0001
HEWELENV	-15.500000	4.208271	-.391580	-3.683	.0042
(Constant)	<u>53.075000</u>	1.717999		32.058	.0000